

Deciphering the Roles of Nuclear Envelope Proteins Associated with Emery-Dreifuss
Muscular Dystrophy in the Heart

Qi Jin

Submitted in partial fulfillment of the
requirements for the degree of
Doctor of Philosophy
in the Graduate School of Arts and Sciences

COLUMBIA UNIVERSITY

2024

ABSTRACT

Deciphering the Roles of Nuclear Envelope Proteins Associated with Emery-Dreifuss Muscular Dystrophy in the Heart

Qi Jin

Mutations in the gene encoding the nuclear lamina protein lamin A/C (*LMNA*) and the associated integral inner nuclear membrane protein emerin (*EMD*) give rise to similar disease phenotypes and are both classified as Emery-Dreifuss muscular dystrophy (EDMD). However, the connection between the function of these nuclear envelope proteins and disease phenotype remains elusive. Given the consistent manifestation of dilated cardiomyopathy in EDMD, my investigation focused on deciphering the roles of these nuclear envelope proteins in the heart. To better understand their functions, I generated a set of isogenic human induced pluripotent stem cell (iPSC) lines with either *LMNA* mutation causing lamin A/C haploinsufficiency or *EMD* mutation causing emerin deficiency. I differentiated these iPSCs into cardiomyocytes (iPSC-CMs) and obtained their RNA transcript and protein expression profiles. I found that both mutant lines exhibited significant overlap in transcriptome and proteome changes. Analyzing alterations at both RNA and protein levels shed light on the potential functional roles of lamin A/C and emerin in cardiomyocytes and pathogenic mechanisms. To better understand the cardiac defects caused by loss of lamin A/C, I generated mice lines with tissue-specific and temporally regulated knockout of *Lmna* in the heart. The mutant mice experienced lethality due to heart failure, regardless of whether *Lmna* was knocked out at the embryonic or mature adult heart. This demonstrates that lamin A/C has a vital role in the normal function of cardiomyocytes.

Table of Contents

List of tables and Figures	iv
Acknowledgements	vi
Chapter 1: Introduction	1
The nuclear envelope	1
Overview	1
Diverse roles of the nuclear lamina	4
Remarks.....	9
Nuclear lamina and disease	9
Clinical phenotypes converge on two genes encoding nuclear envelope proteins.....	9
Laminopathies.....	11
Cardiac features caused by mutations in <i>LMNA</i> and <i>EMD</i>	14
The basic biology of lamin A/C	17
Expression	17
Genetics, splicing, and processing	18
Structure.....	18
Function	19
Post-translational modifications	21
The basic biology of emerin	22
Genetics, structure, and localization.....	22
Function	23
Post-translational modification.....	25
How do alterations in A-type lamins and emerin cause cardiomyopathy?	26
The hypothesis of lamin A/C.....	26
The mystery of emerin	28
Conclusions and research motivation.....	29
Chapter 2: Investigating the Role of Emerin and Lamin A/C in Human Cardiac Cell Culture Model	32
Introduction	32
iPSCs and disease modeling	32
iPSC studies of cardiolaminopathies	33
Motivation	35
Results	36
Production of isogenic lines	36
Differentiation into cardiomyocyte and characterization	42
Gene ontology analysis of DEGs shows common affected pathways between mutants	45
Proteomic analysis identifies significant alterations in proteins related to metabolism and splicing in mutant iPSC-CMs	53
Metabolic changes in mutant iPSC-CMs	58
Discussion	63
Upregulated alternative fate genes related to the nervous system	63

Downregulation of lipid metabolism genes and liver, small intestine associated genes and upregulation of metabolic proteins.....	65
Reduced splicing and nuclear factors.....	67
Nuclear lamina and metabolism.....	69
Multi-omic loss of <i>LDHB</i> and reduction of lactate.....	72
Overlapping effects of lamin A/C haploinsufficiency and emerin deficiency in iPSC-CMs.....	74
Weakness.....	74
Chapter 3: Investigating the Requirement of Lamin A/C in Mature Striated Muscle	75
Introduction.....	75
Mouse models of cardiolaminopathies.....	75
<i>EMD</i> knockout mouse model.....	78
Mouse models of other nuclear lamina proteins.....	78
Gap in understanding.....	79
Mouse cardiomyogenesis.....	80
Results.....	81
Lamin A/C knockout in striated muscle highlights heart.....	81
Induction of Lamin A/C knockdown in adult cardiac muscle causes immediate fibrotic change and death 3 weeks post induction.....	86
Discussion.....	89
Disruption of <i>Lmna</i> expression is detrimental to cardiomyocytes.....	89
Potential long half-life of lamin A/C.....	91
Chapter 4: Discussions and Future Directions.....	92
Cardiomyocytes require the expression of A-type lamins for cardiac function.....	92
Long lived lamins and implications.....	93
New understanding of lamin functions.....	95
Alterations in metabolism are a possible underlying feature of cardiolaminopathy.....	97
The metabolic hypothesis of laminopathy and emerinopathy.....	99
Overlapping effects of lamin A/C haploinsufficiency and emerin deficiency.....	102
How does emerin loss have the same cellular effects at lamin A/C haploinsufficiency?.....	103
Final Word.....	104
Chapter 5: Material and Methods.....	105
Basic methods.....	105
Immunofluorescence staining and microscopy.....	105
Immunoblotting.....	105
Mice.....	106
Mouse husbandry.....	106
Histology.....	107
IPSCs.....	107
IPSC maintenance.....	107
CRISPR.....	107
Cardiomyocyte differentiation.....	109
Proximity ligation assay.....	110
RNA sequencing.....	111
Proteomic analysis.....	111
Metabolomic Analysis.....	112

References	113
Appendix A	136
Appendix B	161
Appendix C	204

List of tables and Figures

Figure 1.1: an overview of the cell, nuclear envelope, and the nuclear lamina.

Figure 1.2: 12 years of discovery and identification of diseases caused by mutations in *LMNA* and other associated nuclear lamina proteins.

Figure 1.3: laminopathies of the straited muscles always affects the heart.

Figure 2.1: CRISPR strategy and resultant alleles generated for *LMNA*.

Figure 2.2: CRISPR strategy and resultant alleles generated for *EMD*.

Figure 2.3: Immunofluorescence validation of CRISPR mutants showing loss of target protein in emerin but inconclusive of lamin A/C.

Figure 2.4: Differentiation of WT, *LMNA*^{-/+}, and *EMD*^{-/-} iPSC into cardiomyocytes and validation of lamin A/C haploinsufficiency and emerin deficiency.

Figure 2.5 heterochromatin distribution in WT, *LMNA*^{-/+} and *EMD*^{-/-} iPSC-CM.

Figure 2.6: Volcano plots of differential gene expression of mutant iPSC-CMs compared to control.

Figure 2.7 Gene Ontology (GO) enrichment analysis of upregulated DEGs in mutants.

Figure 2.8 Gene Ontology (GO) enrichment analysis of downregulated DEGs in mutants.

Figure 2.9: IPA analysis of DEGs identify significant downregulation in major metabolic pathways.

Figure 2.10: Volcano plots of differential protein expression of mutant iPSC-CMs compared to control.

Figure 2.11: Gene Ontology (GO) enrichment analysis of upregulated DEPs in mutants.

Figure 2.12: Gene Ontology (GO) enrichment analysis of downregulated DEPs in mutants.

Figure 2.13: Metabolomic analysis of *LMNA*^{-/+} and *EMD*^{-/-} compared to WT shows similarities.

Figure 2.14: Metabolite enrichment analysis for metabolites with significant differential abundance between mutant and wildtype.

Figure 2.15 Lactate reduction in mutants and LDHB reduction.

Figure 3.1: MCK-Cre; *Lmna*^{flox/flox} has normal development but deteriorates rapidly and dies 3-4 weeks postnatal.

Figure 3.2: MCK-Cre; *Lmna*^{flox/flox} heart exhibit ventricular dilation and dystrophic cardiac myocytes.

Figure 3.3: increased interstitial fibrosis in MCK-Cre; *Lmna*^{flox/flox} mice.

Figure 3.4: MCK-Cre; *Lmna*^{flox/flox} heart exhibit no differences in skeletal muscle fiber morphology.

Figure 3.5: Inconclusive reduction in lamin A/C protein in skeletal and cardiac muscle.

Figure 3.6: Induction of cardiomyocyte specific knockout of *Lmna* in adult mice lead to lethality.

Figure 3.7: Heart of MHC-MCM; *Lmna*^{flox/flox} mice treated with tamoxifen exhibit ventricular dilation and dystrophic cardiac myocytes.

Figure 3.8: Increased interstitial fibrosis in MHC-MCM; *Lmna*^{flox/flox} mice treated with tamoxifen.

Figure 5.1: Timeline of protocol for differentiation of iPSCs to cardiomyocytes.

Table 5.1: List of antibodies

Table 5.2: List of mouse lines.

Table 5.3: sgRNA sequences for CRISPR.

Table 5.4: PCR and sequencing primers for confirmation of CRISPR edits.

Table AA: Differentially expressed RNA transcripts.

Table AB: Differentially expressed proteins.

Table AC: Differentially abundant metabolites.

Acknowledgements

I would like to express my deepest gratitude to my advisor, Dr. Howard Worman, for giving me the opportunity to learn and grow in his lab. I am deeply grateful for his unwavering support, endless patience, and constant availability throughout this journey. I also want to express my heartfelt thanks to the members of the Worman lab, with a special mention to Dr. Ji-Yeon Shin. Since my first day, Dr. Shin has gone above and beyond to help and guide me, becoming like a second mentor to me. I'm also incredibly grateful to Dr. Wei Wu for her valuable assistance whenever I faced challenges, and those water cooler discussions.

I am incredibly appreciative to Dr. Barry Fine, Dr. Gregg Gundersen, and Dr. Masayuki Yawaza for their valuable contributions on my thesis committee. Their expertise, guidance, and thoughtful feedback throughout the committee meetings have been instrumental. I am incredibly grateful for the time and effort they invested in my committee meetings, particularly notable was Dr. Yawaza, who attended one meeting past midnight from the other side of the world. I consider myself incredibly fortunate to have had the privilege of being guided by such distinguished scientists.

To my program director, Dr. Ron Liem, and program coordinator, Zaia Sivo, both of whom I can't thank enough for their unwavering support during this challenging and rewarding marathon of a graduate school journey. Sometimes I can't believe I am so lucky to be in a program with such amazing and supportive administrators.

Thanks to all my past scientific mentors and colleagues for their contributions in shaping me to be the scientist I am today. I promise to pay it forward.

Last but not least, shout out to my family and friends near and far, and all the wonderful people I have crossed paths with while on this journey for all their positive influences on me.

Chapter 1: Introduction

The nuclear envelope

Overview

In the eukaryotic cell, an intracellular compartment called the nucleus encloses the genomic DNA and separates it from the parts and processes of the rest of the cell. Two lipid bilayer membranes define its boundaries, together termed the nuclear envelope (Figure 1.1). The inward-facing lipid bilayer of the nuclear envelope, the inner nuclear membrane (INM), faces the contents of the nucleus, including DNA and various proteins in the nucleoplasm. The outer lipid bilayer of the nuclear envelope, known as the outer nuclear membrane (ONM), radiates beyond the nucleus and forms the endoplasmic reticulum (ER). There is space between the INM and ONM, called the perinuclear space, which is continuous with the ER lumen. Spanning across the perinuclear space and through the INM and ONM are pores formed by a multi-component protein complex called nuclear pore complex (NPC). The NPCs serve as a gateway between the nucleus and cytoplasm, allowing specific soluble molecules to pass through. Inside the nucleus and adjacent to the nuclear envelope, there exists a concentrated network of proteins lining the nucleoplasmic face of the INM known as the nuclear lamina (Figure 1.1). The nuclear lamina is comprised mainly of nuclear lamins, which form the interlacing protein meshwork and provide structural support for the otherwise flimsy lipid membranes of the nuclear envelope (Gerace et al., 1978).

Nuclear lamins are type V intermediate filament proteins, categorized as A-type or B-type (Fisher et al., 1986; McKeon et al., 1986). A-type lamins predominantly comprise lamin A and C, which are alternatively spliced products of the gene *LMNA* (Lin and Worman, 1993). B-type comprises lamin B1 and B2, encoded by *LMNB1* and *LMNB2*, respectively (Biamonti et al., 1992; Lin and Worman, 1995). These nuclear intermediate filaments form a fibrous meshwork of

atypical 3.5-nm diameter filaments in the nucleus along the inner nuclear membrane (Turgay et al., 2017). Some studies have suggested nuclear lamins are involved in additional structures in the nuclear interior (Hozák et al., 1995; Kolb et al., 2011; Moir et al., 2000).

The nuclear lamins interact with a set of integral inner nuclear membrane proteins. Roles have been attributed to these proteins, such as chromatin organization, regulation of gene expression, and mediation of signaling pathways into the nucleus. There are nearly 100 integral inner nuclear membrane proteins, many of which are largely uncharacterized (Dreger et al., 2001; Schirmer et al., 2003). The first identified was lamin B receptor (LBR) (Worman et al., 1990; Worman et al., 1988). Other integral inner nuclear membranes include those of the LEM domain family, named after LAP2, Emerin, and Man1 (Lin et al., 2000). Among their various functions, they bind to nuclear lamins and mediate their association with the inner nuclear membrane. On the other hand, the peripheral nuclear lamin network is required to facilitate the localization and retention of inner nuclear membrane proteins (D'Angelo and Hetzer, 2006; Soullam and Worman, 1995).

In addition to the proteins of the nuclear lamina aiding the localization of one another, the various functions of the nuclear lamina depend on the network of rightly associated interactions between its component proteins. Together, they act as a scaffold and are involved in most, if not all, the processes in the nuclei. It can be considered a whole organelle-encompassing protein complex that facilitates functions in mechanical support, chromatin organization, cell division, development, and differentiation. It is important to view the nuclear envelope as a whole, as it is difficult to parse out the individual contributions of each other component, as mutations in encoding a number of them have been shown to cause human disorders (Worman and Bonne, 2007).

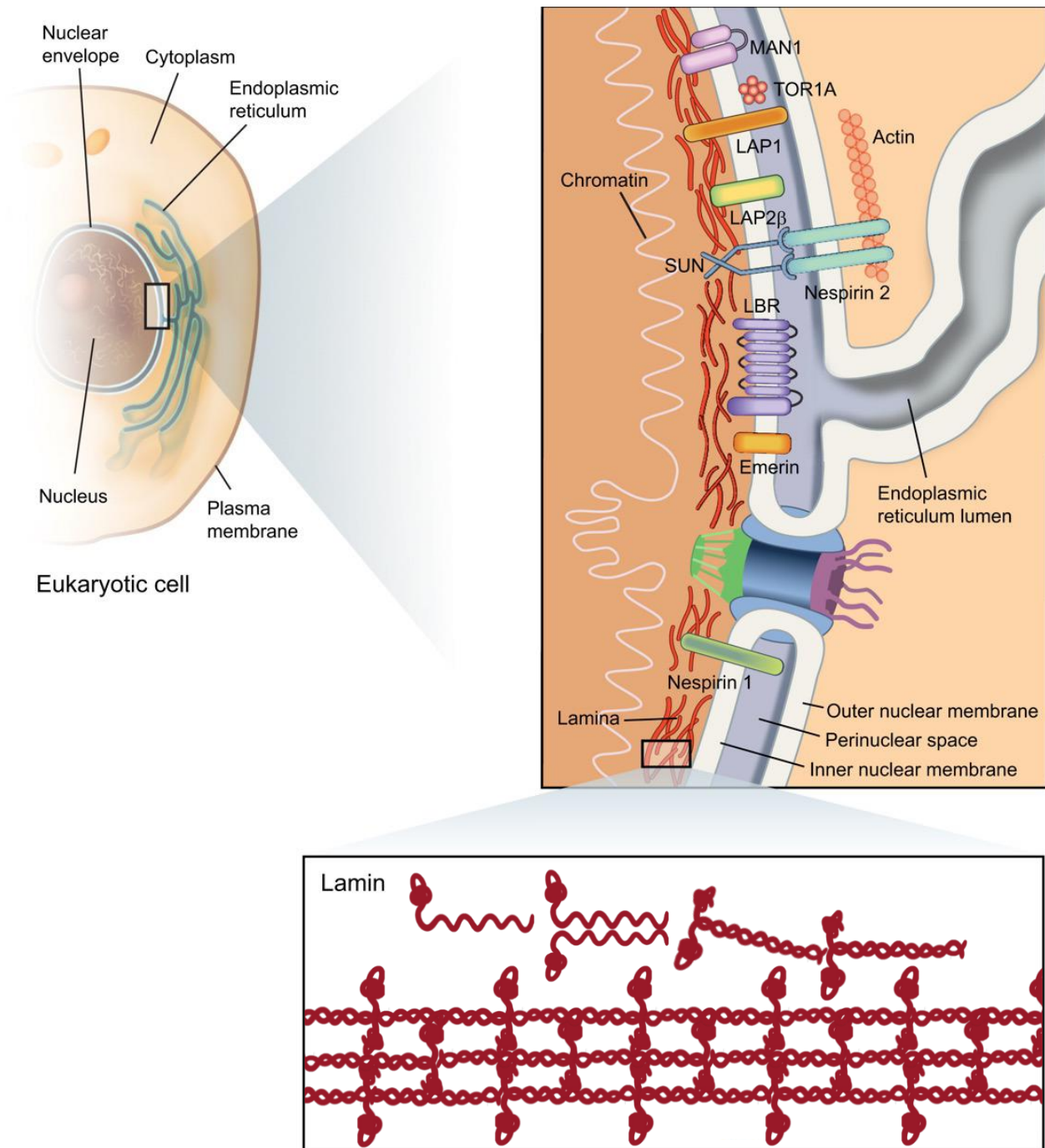


Figure 1.1: an overview of the cell, nuclear envelope, and the nuclear lamina. Inside every eukaryotic cell is the nucleus, the cell's command center. The nuclear envelope separates the contents of the nucleus from the rest of the cell. It comprises the inner and outer nuclear membranes, nuclear pore complexes that span both layers, and the nuclear lamina along the inner nuclear membrane. The endoplasmic reticulum membranes are extensions of the nuclear membranes and share a continuous luminal space. The nuclear lamina is a meshwork of intermediate filaments called nuclear lamins. Each lamina fiber is composed of many individual lamin proteins. The lamina is associated with a group of integral proteins of the inner nuclear

membrane; they include MAN1, lamina-associated polypeptide-1 (LAP1), the SUN protein, lamina-associated polypeptide-2 β (LAP2 β), lamin B receptor (LBR), emerin, and a nesprin-1 isoform. The SUN proteins bind to the outer nuclear membrane proteins called nesprins. TorsinA (Tor1A) is a resident of the perinuclear space. Adapted from Dauer and Worman 2009.

Diverse roles of the nuclear lamina

Nuclear architecture and mechanotransduction

In 1974, Aaronson and Blobel removed the nuclear membranes and found a study layer still holding the nuclear contents and the NPCs in place, which was primarily the result of the structural stabilizing properties of the nuclear lamina (Aaronson and Blobel, 1974). The nuclear lamina functions as a scaffold that supports the organization and the spatial arrangement of the components of the nucleus. Nuclear lamins, the main constituent of the nuclear lamina, have been found to interact with the components of the nuclear pore complex, which in turn plays a role in their incorporation and spacing in the nuclear envelope (Al-Haboubi et al., 2011; Goldberg et al., 1995; Osouda et al., 2005; Smythe et al., 2000).

The nuclear lamina has a crucial role in maintaining the architecture of the nucleus. A-type lamins are essential contributors to the mechanical stiffness of the nucleus as their absence resulted in the formation of irregularly shaped nuclei and significantly reduced nuclear stiffness (Lammerding et al., 2004). Conversely, lamin B1 does not play a role in nuclear stiffness, but its absence is associated with the presence of protruding structures of the nucleus called nuclear blebs, indicating its involvement in preserving nuclear integrity (Lammerding et al., 2006).

While providing structural support for the nucleus, the nuclear lamina also transmits forces. Force acting on the cell is transferred through the cytoskeleton to the nuclear lamina via the Linker of Nucleoskeleton and Cytoskeleton (LINC) complex, made up of nesprins and SUN domain proteins (Crisp et al., 2006). Nesprins are integral ONM proteins that connect to the

various components of the cytoskeleton on the cytoplasmic side of the nuclear envelope and connect to SUN domain proteins on the luminal side (Crisp et al., 2006; Haque et al., 2006; Padmakumar et al., 2005). At the same time, SUN domain proteins span the INM bridging the connection between Nesprins and the nuclear lamina (Haque et al., 2006; Padmakumar et al., 2005).

The rigidity of the nucleus is not a constant and is highly regulated. The expression level of A-type lamins is different in tissues of different rigidity (Swift et al., 2013). Furthermore, varying the softness of the matrix where a cell grows alters the levels of A-type lamins, while the B-type lamins are unaffected (Swift et al., 2013). Furthermore, the dynamic regulation of nuclear lamina stiffness through alterations of the levels of A-type lamins is also observed in migrating cells (Harada et al., 2014).

DNA replication and cell division

In addition to its presence on the inner aspect of the inner nuclear membranes, a fraction of nuclear lamins is present in the nuclear interior, where they interact with DNA replication complexes (Moir et al., 1994; Shumaker et al., 2008). Evidence in *Xenopus* supports the idea that soluble nuclear lamins are required for DNA replication, although this requirement has not been tested in mammalian models (Lopez-Soler et al., 2001).

At the start of mitosis, the nuclear lamina, along with the nuclear membrane and the NPCs, are disassembled to allow the condensed chromatin to engage with the microtubules of the mitotic spindle. This is initiated by the hyperphosphorylation of nuclear lamins, which leads to the disassembly of the nuclear lamina, which is critical for nuclear envelope breakdown (Gerace and Blobel, 1980; Heald and McKeon, 1990; Peter et al., 1990). At the end of mitosis, the components of the nuclear envelope and the nuclear membrane are reassembled around the segregated chromosomes. Dephosphorylation of the mitotic sites on lamins is required for the reassembly of the nuclear lamina (Thompson et al., 1997; Vivante et al., 2021).

Chromatin organization, transcription control, and differentiation

The dense transcriptionally silenced heterochromatin is mainly localized at the nuclear periphery. Regions of the heterochromatin that interact with the nuclear lamina are termed Lamina-Associated Domains or LADs (van Steensel and Belmont, 2017). These interactions aid in the 3D organization of chromatin and are associated with gene repression (van Steensel and Belmont, 2017). LADs have been mapped in various model organisms and have been reported to cover more than one-third of the mouse and human genomes (van Steensel and Belmont, 2017).

During the early embryonic development of mammals, LBR, a protein linked to B-type lamins, plays a vital role in preserving the peripheral location of heterochromatin (Solovei et al., 2013). LBR binds to heterochromatin protein 1 α (HP1 α), which interacts with the histone modification H3K9me_{2/3} that defines the heterochromatin (Guelen et al., 2008; Wen et al., 2009; Ye and Worman, 1996). In addition to LBR, which plays a crucial role in early development, various NET proteins expressed specifically in different tissues have been demonstrated to anchor specific loci or entire chromosomes to the nuclear envelope, particularly in differentiated mammalian cells (Robson et al., 2016; Zuleger et al., 2013).

These interactions have a net role in organizing the chromatin (Sullivan et al., 1999). The interaction between A-type lamins and LADs has a special stabilizing effect that reduces the mobility of chromatin (De Vos et al., 2010). Loss of the *Lmnb1* gene in mouse embryonic fibroblasts leads to the translocation of chromosome 18 to the interior of the nucleus (Malhas et al., 2007). More dramatic effects were observed in cells lacking both A-type lamins and LBR, where heterochromatin collected at the center of the nucleus as opposed to the periphery (Solovei et al., 2009; Solovei et al., 2013). While chromatin organization can be drastically altered by manipulating lamins, it is not clear if that is a direct effect of nuclear lamins on

chromatin or if the effect is a consequence of destabilized nuclear lamina caused by loss of lamins.

On top of the role of lamin A/C in the positioning of chromatin, it can also regulate gene expression through interactions with transcriptional factors. Several transcription factors have been shown to be sequestered by lamin A/C, such as c-Fos and sterol regulatory element-binding protein-1 (SREBP1) (Capanni et al., 2005; Ivorra et al., 2006). Further studies have shown nuclear lamins have a broad effect on gene expression via RNA polymerase II-dependent transcription (Kumaran et al., 2002; Spann et al., 2002). RNA-seq revealed that the absence of all lamins not only increases the overall transcription within LADs but also modifies the expression of genes located in the nucleoplasm (Kim et al., 2011; Ulianov et al., 2019; Zheng et al., 2018). INM proteins are also found to interact with transcription factors. MAN1 and its interaction with Smad transcription factors that have the capacity to influence transforming growth factor- β (TGF β), bone morphogenic protein (BMP), and activin signaling (Bourgeois et al., 2013; Hellemans et al., 2004; Lin et al., 2005).

During differentiation, the nuclear lamina's interaction with chromatin and transcription factors works in concert to make large-scale gene expression changes. The transition from an undifferentiated or pluripotent state towards a distinct cell lineage is associated with a higher compaction of chromatin at the nuclear periphery (Ahmed et al., 2010; Meister et al., 2011). This increased compaction is associated with increased heterochromatin marker H3K9me3, which, as previously mentioned associated with the nuclear lamina via protein linkers such as HP1 α (Ugarte et al., 2015; Zhu et al., 2013). The nuclear lamina may have a more important role in differentiated cell types than in undifferentiated ones (Gigante et al., 2017; Kim et al., 2011; Robson et al., 2016). Loss of B-type lamin in *Drosophila* led to the loss of heterochromatin and expression of alternative fate genes suggesting they are important for their differentiated status (Chen et al., 2014).

DNA repair and apoptosis

Studies have shown the nuclear lamina's association with DNA damage repair. Many components responsible for base excision repair were found to be reduced in Lamin A/C knockout cells (Maynard et al., 2019). Lamin A/C promotes base excision repair and the restart of stalled replication forks, a prerequisite of DNA damage repair via homologous recombination pathway (Maynard et al., 2019; Singh et al., 2013). Lamin B1 acetylation was recently shown to negatively regulate canonical nonhomologous end-joining by impairing the recruitment of 53BP1 to damaged DNA (Murray-Nerger et al., 2021). Proximity to the nuclear lamina can influence the choice between nonhomologous end joining (NHEJ) or homologous recombination (HR) for repairing double-stranded DNA breaks (DSBs) in a yet-to-be fully understood mechanism (Lemaître et al., 2014).

The nuclear lamina is a target of apoptotic processes (Lazebnik et al., 1995). In contrast to the phosphorylation-induced disassembly during mitosis, the nuclear lamina is degraded by proteolytic cleavage, and both the lamins and the nuclear lamin-associated membrane proteins are targeted (Lindenboim et al., 2020). This proteolytic activity is performed by members of the caspase-protein family who cleave the lamins after aspartic acid (Asp) residues (Lindenboim et al., 2020). The expression of uncleavable A-type lamins inhibited apoptosis to a large extent and delayed the eventual fragmentation of genomic DNA (Rao et al., 1996). Other components of the nuclear lamina, such as LBR and emerin, are also targeted by caspases (Columbaro et al., 2001; Duband-Goulet et al., 1998). In addition to being the target of apoptotic processes, nuclear lamins participate in apoptotic signaling by serving as a platform for apoptotic complexes (Lindenboim et al., 2020).

Remarks

The nuclear lamina is intricately involved in processes from the birth of a new cell through its involvement in DNA replication and mitosis, to the death of the cell in apoptosis, and seemingly everything in between. The diverse functions of the nuclear lamina are interconnected and interdependent. While multiple studies cited above found various effects by eliminating nuclear lamins, the deleterious effects cannot be isolated to the lamins as it is the foundational scaffold of nuclear lamina that retains many INM proteins, many of which are unknown. The breadth of nuclear lamina functions and the lack of knowledge of the specific functions of the protein members are huge obstacles when it comes to an understanding and dissecting the molecular mechanisms of diseases associated with the nuclear lamina.

Nuclear lamina and disease

Clinical phenotypes converge on two genes encoding nuclear envelope proteins.

Muscular dystrophies are a group of diseases characterized by loss of muscle strength and other muscle-related symptoms (Emery, 2002). There are various types of muscular dystrophies distinguished by clinical factors such as the age of onset, distribution of muscles affected, severity, inheritance pattern, and more. Muscular dystrophies include nearly 30 different genetic diseases. Before scientists understood genetics and pathologies of the mechanisms of various muscular dystrophies, they were identified and classified by their clinical presentation.

In 1961, Dreifuss and Hogan described a large family with an X-linked form of muscular dystrophy that they considered to be a mild form of Duchenne muscular dystrophy (Dreifuss and Hogan, 1961). This family was subsequently reevaluated by Emery and Dreifuss, who recognized the presence of clinical phenotypes, which distinguishes the case from other

muscular dystrophy classifications at the time (Emery and Dreifuss, 1966). They characterized the novel X-linked muscle dystrophy with the clinical triad of 1) early weakness in the muscles of the shoulders, upper arms, and calves (scapulohumeroperoneal distribution), 2) early tendon contractures localized in the elbows, heels, and neck, and 3) dilated cardiomyopathy with conduction defects. Céstan and LeJonne at l'Hôpital de la Salpêtrière in Paris may have described this phenotype over half a century earlier (Cestan and Lejonne, 1902).

It wasn't long before other clinicians began to describe additional cases of X-linked muscular dystrophy fitting the clinical triad Emery and Dreifuss described. In 1979, Rowland and colleagues (Rowland et al., 1979) at Columbia University coined the term “Emery-Dreifuss type muscular dystrophy” (EDMD). While the originally described cases and many subsequently identified cases of EDMD were X-linked, clinicians began to describe cases of EDMD with an autosomal-dominant pattern of inheritance (Galassi et al., 1986; Miller et al., 1985). Additional cases of autosomal dominant (AD) EDMD were being described, and thus the classification of EDMD is subdivided into X-linked EDMD and AD-EDMD. In 1994 the genetic cause was identified for X-linked EDMD; the protein was named emerin after the disease's namesake (Bione et al., 1994). Subsequently, emerin was shown to be an integral protein of the inner nuclear membrane (Manilal et al., 1996; Nagano et al., 1996). Later in the decade, autosomal dominant EDMD was found to be caused by mutations in *LMNA* encoding lamin A/C (Bonne et al., 1999). Lamin A/C and emerin were then shown to interact with each other at the inner nuclear membrane (Sullivan et al, 1999; Clements et al., 2000).

The prevalence of X-linked EDMD has been estimated from as low as 0.13:100,000 to as high as 1:100,000 (Helbling-Leclerc et al., 2002; Norwood et al., 2009). X-linked EDMD caused by a mutation in *EMD* accounts for approximately 8% of the total cases of EDMD (Bonne and Quijano-Roy, 2013). More than half of EDMD cases cannot be attributed to *LMNA* or *EMD* mutations and lacks a molecular diagnosis, aside from *FHL1*, which accounts for

approximately 1% of EDMD cases, which are atypical in that they have hypertrophic rather than dilated cardiomyopathy (Gueneau et al., 2009). AD-EDMD caused by mutations in *LMNA* contributes to about 28% of the cases (Kovalchuk et al., 2021). However, since the association of *LMNA* and EDMD, *LMNA* mutations have been implicated in several other human diseases.

Laminopathies

While AD-EDMD is linked to mutations in *LMNA*, mutations in *LMNA* additionally cause a large family of diseases affecting various tissue types, moving the understanding far from the "one gene-one disease" idea. Laminopathies refer to the group of diseases caused by mutations in genes encoding proteins that make up the nuclear lamina and are dominated by mutations in *LMNA* specifically (Figure 1.2). To date, over 498 mutations in *LMNA* have been documented, linked to over 15 distinct phenotypes (Craστο et al., 2020). Laminopathies resulting from *LMNA* gene mutations fall under ten different clinical syndromes and can be categorized into groups affecting striated muscle, adipose tissue, peripheral nerve systems, or multiple systems with features of accelerated aging (Dauer and Worman, 2009).

Soon after mutations in *LMNA* were shown to cause AD-EDMD, they were linked to dilated cardiomyopathy 1A, and limb-girdle muscular dystrophy 1B (Fatkin et al., 1999; Muchir et al., 2000). Dilated cardiomyopathy with conduction abnormalities overlaps between these two diseases as well as EDMD; as their name suggests, one has minimal to no skeletal muscle involvement, while the other presents a distinct pattern of skeletal muscle involvement.

LMNA mutations have also been linked to Dunnigan-type familial partial lipodystrophy (Cao and Hegele, 2000; Shackleton et al., 2000; Speckman et al., 2000). Patients with this autosomal dominant disorder experience gradual loss of subcutaneous adipose tissue in the extremities, accompanied by fat accumulation in the face and neck. Insulin resistance is observed in almost all affected individuals, and a considerable number develop diabetes mellitus. Rare cases of subjects with a heterozygous missense mutation in *LMNA* exhibiting

predominantly metabolic defects (Caux et al., 2003; Young et al., 2005a). Few rare cases of lipodystrophy in subjects with muscular dystrophy and cardiomyopathy have been reported (Garg et al., 2002; van der Kooi et al., 2002).

Defects in peripheral nerves were associated with *LMNA* when a homozygous missense mutation was reported to cause autosomal recessive Charcot-Marie-Tooth type 2B1, a peripheral neuropathy (De Sandre-Giovannoli et al., 2002). Additionally, some muscular dystrophy patients with *LMNA* mutations also exhibit peripheral neuropathy, including a mutation that leads to haploinsufficiency of A-type lamins (Benedetti et al., 2005; Goizet et al., 2004; Walter et al., 2005). The expression of neurogenic and myogenic phenotypes in these cases associated with *LMNA* mutations adds another layer of phenotypic complexity to *LMNA*.

Mutations in *LMNA* also cause dramatic phenotypes affecting multiple tissues, such as in Hutchinson-Gilford progeria syndrome (De Sandre-Giovannoli et al., 2003; Eriksson et al., 2003). Subjects affected by this multi-system disorder exhibit symptoms associated with premature aging, often resulting in death from cardiovascular disease in the second decade of life (DeBusk, 1972). This disease is caused by particular mutations in *LMNA* that lead to defective processing of the lamin A precursor protein, prelamin A (De Sandre-Giovannoli et al., 2003; Eriksson et al., 2003). Furthermore, *LMNA* mutations have also been associated with patients with accelerated aging phenotypes under the diagnosis of atypical Werner syndrome (Chen et al., 2003). These disorders with accelerated aging phenotypes are together known as progeroid laminopathies (Marcelot et al., 2021)

The autosomal recessive disorder mandibulofacial dysplasia, which is characterized by clinical features including postnatal growth retardation, craniofacial abnormalities, skeletal malformations, and mottled cutaneous pigmentation and is caused by a specific homozygous missense *LMNA* mutation (Novelli et al., 2002). Another rare disorder caused by *LMNA* is restrictive dermopathy, a neonatal, lethal syndrome with severe intrauterine growth retardation,

congenital contractures, and tense skin (Navarro et al., 2004). These disorders have overlapping features with Hutchinson-Gilford progeria syndrome. Mutations in *ZMPSTE24*, a enzyme involved in processing of lamin A precursor (described later), had been found to cause mandibuloacral dysplasia, a severe form of progeria, and restrictive dermopathy as well (Agarwal et al., 2003; Moulson et al., 2005; Shackleton et al., 2005).

Laminopathies also include diseases caused by mutations in genes coding other proteins of the nuclear envelope, such as B-type lamins, and nuclear envelope proteins, such as emerin, MAN1, LBR, and nesprins (Worman and Bonne, 2007). *LMNB1* duplications can cause leukodystrophy, characterized by widespread myelin loss in the central nervous system (Coffeen et al., 2000; Molloy et al., 2012; Padiath et al., 2006; Schwankhaus et al., 1994). *LMNB1* missense mutations have been associated with syndromic microcephaly (Cristofoli et al., 2020). *LMNB2* variants were found to correlate with increased susceptibility of acquired Barraquer-Simons syndrome, a mostly sporadic acquired form of progressive lipodystrophy (Hegele et al., 2006). As previously noted, X-EDMD is due to mutations in the *EMD* gene encoding the integral inner membrane protein emerin. Heterozygous mutations in *LBR* cause Pelger-Huet anomaly, which only affects the nuclear shape of blood neutrophils, while homozygous mutations of *LBR* lead to HEM/Greenberg skeletal dysplasia and is generally lethal *in utero* (Waterham et al., 2003). MAN1 has been linked to disorders characterized by increased bone density (Hellemans et al., 2004). More recently, a mutation in the gene encoding lamina-associated polypeptide 1 (LAP1) was found in a Turkish family with an autosomal recessive limb-girdle muscular dystrophy with joint contractures (Kayman-Kurekci et al., 2014).

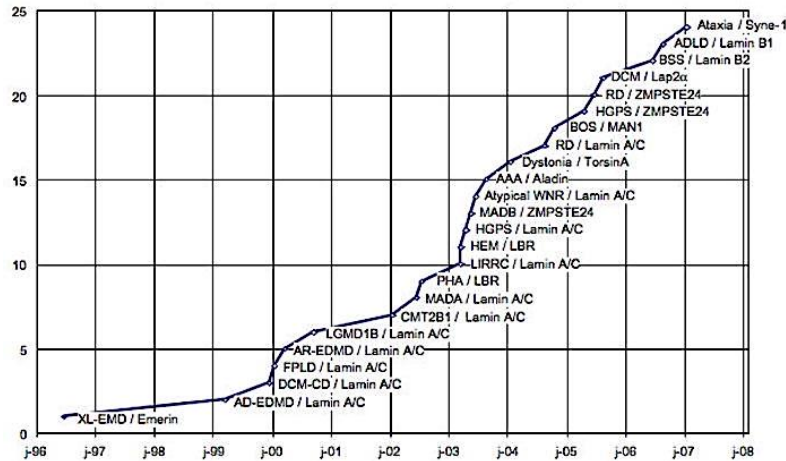


Figure 1.2: 12 years of discovery and identification of diseases caused by mutations in *LMNA* and other associated nuclear lamina proteins. Year of discovery on the x-axis vs. number of diseases on the y-axis. Emerin is mutated in X-linked EDMD, and it was identified as a nuclear envelope protein in 1996. *LMNA* mutations were reported to cause AD-EDMD in 1999. Dilated cardiomyopathy, Dunnigan-type familial partial lipodystrophy, autosomal recessive EDMD, and limb-girdle muscular dystrophy type 1B were all linked to mutations in *LMNA* in 2000. Charcot-Marie-Tooth disorder type 2B1 and mandibulacral dysplasia were linked to mutations in *LMNA* in 2002, while mutations in LBR were reported to cause Pelger-Huet anomaly. Lipoatrophy with diabetes, hepatic steatosis, hypertrophic cardiomyopathy and leukomelanodermic papules (LIRRC), Hutchinson-Gilford progeria syndrome, and atypical Werner syndrome were linked to *LMNA* mutations in 2003, while LBR mutations were linked to HEM/Greenberg dysplasia, *ZMPSTE24* linked to mandibulacral dysplasia, and gene encoding Aladin linked to triple A syndrome. Restrictive dermopathy was linked to *LMNA* mutations in 2004, while DYT1 dystonia caused by mutations in *torsinA* and Bushke-Ollendroff was linked to gene coding for *MAN1*. A progeria syndrome and restrictive dermopathy were linked to mutations in *ZMPSTE24* in 2005, while *Lap2α* polymorphisms were associated with patients were dilated cardiomyopathy. *LMNB1* was reported to cause adult-onset autosomal dominant leukodystrophy and *LMNB2* was associated with Barraquer-Simons syndrome in 2006. In 2007, mutations in *SYNE1* were linked to cerebellar ataxia. Figure reproduced from Worman and Bonne 2007.

Cardiac features caused by mutations in *LMNA* and *EMD*

The diseases affecting striated muscles caused by *LMNA* mutations are classified based on the presence and pattern of skeletal muscle involvement, while cardiac features are invariant (Figure 1.3). More in-depth analysis showed that the same *LMNA* mutation could cause the clinical diagnosis of AD-EDMD, limb-girdle muscular dystrophy 1B, and dilated cardiomyopathy 1A, even within the same family (Bonne et al., 2000; Brodsky et al., 2000). Likely the diverse biological processes A-type lamins participate in as a crucial part of the nuclear lamina makes it

susceptible to influences of various genetic and environmental modifiers. Therefore, the striated muscle disorders caused by *LMNA* mutations can be viewed as dilated cardiomyopathy with variable skeletal muscle involvement. The cardiomyopathy caused by mutations in *LMNA* is sometimes referred to as cardiolaminopathy.

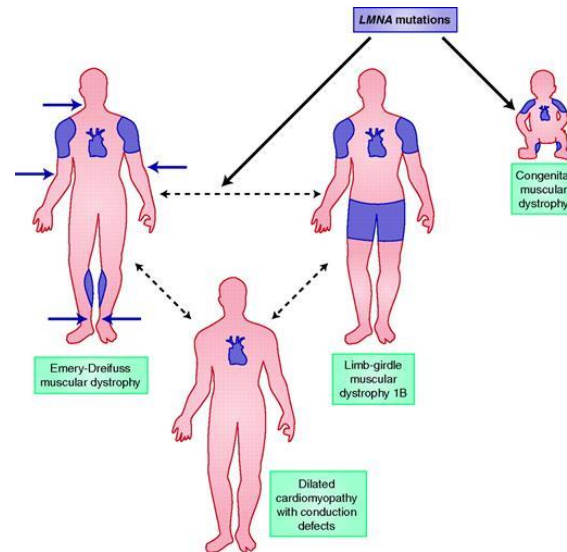


Figure 1.3: laminopathies of the striated muscles always affects the heart. Clinically defined laminopathies affecting the striated muscles (Emery-Dreifuss muscular dystrophy, dilated cardiomyopathy with conduction defects, limb-girdle muscular dystrophy 1B, and congenital muscular dystrophy) are shown with affected striated muscle groups shown in purple. Solid purple arrows indicate areas of joint contracture. *LMNA* mutation can cause any of the three adult onset laminopathies as they are considered as cardiomyopathy with a spectrum of skeletal muscular dystrophy. Reproduced from Lu et al. 2011.

Cardiolaminopathy is characterized by dilated cardiomyopathy and conduction-system disease, which can result in heart failure or sudden death (Bonne et al., 1999; Fatkin et al., 1999). In a detailed analysis of patients, atrioventricular block, atrial arrhythmias, ventricular arrhythmias, left ventricular systolic dysfunction, and end-stage heart failure had variant incidence but high incidence of progression (Kumar et al., 2016). By age 60, 55% of cardiomyopathy patients with *LMNA* mutation die of cardiovascular death or receive a heart transplant, whereas the rate is 11% for cardiomyopathy patients without *LMNA* mutation (Taylor et al., 2003). The development of malignant ventricular arrhythmias was significantly associated

with male sex, non-missense mutations in *LMNA* (Hasselberg et al., 2014; Kumar et al., 2016; Nishiuchi et al., 2017; van Rijsingen et al., 2012).

Conduction system disease and/or arrhythmias almost always occur prior to or in association with the evolution of dilated cardiomyopathy and commonly before the development of heart failure caused by *LMNA* or *EMD* mutations (Crasto et al., 2020). Bradyarrhythmias and supraventricular tachyarrhythmias often preceded the development of dilated cardiomyopathy by decades (Crasto et al., 2020). Conduction system involvement usually starts with the disease of the sinus node and/or atrioventricular node that can manifest as sinus bradycardia, sinus node arrest with junctional rhythms, or heart block (Boriani et al., 2018).

LMNA is the second most commonly mutated gene causing familial cardiomyopathy, accounting for ~6-8% of the cases of idiopathic dilated cardiomyopathy and up to 33% of dilated cardiomyopathy with conduction system disease (Arbustini et al., 2002; Hershberger and Siegfried, 2011; McNally and Mestroni, 2017). Most other causative genes of dilated cardiomyopathy encode proteins of the sarcomere or closely associated proteins that are involved in the generation and transmission of contractile force in the cardiomyocyte, such as *TTN*, *MYH7*, and *TNNT2*. In contrast, A-type lamins have a less direct association with contractile machinery. Furthermore, in an analysis of a large genome bank cohort, *LMNA* variants that are missense mutants not classified as pathogenic were found to be significantly associated with atrial fibrillation, bradyarrhythmias, ventricular arrhythmias, dilated cardiomyopathy, and heart failure (Lazarte et al., 2022).

Detailed analysis of a small cohort of patients with *EMD* mutation suggests there is also a spectrum of variable phenotypic expression ranging from EDMD to cardiomyopathy only and lacking contractures and muscle weakness (Ishikawa et al., 2020). The spectrum of disease features caused by emerin mutation is sometimes known as emerinopathy. Features of cardiac emerinopathy have not been characterized on a large scale; smaller studies have found

atrioventricular block occurred earlier in patients with emerinopathy (usually in the second or third decade of life), while its occurrence in cardiolaminopathy was more spread over the decades (Astejada et al., 2007; Ishikawa et al., 2020).

It is unclear why dilated cardiomyopathy with conduction disease is the most common phenotype of mutations in *LMNA* and *EMD*. Further study into both proteins and their functional overlap may elucidate pathways essential to uncovering the mechanism behind their cardiac phenotype. In the next section, I will focus on specific features of each protein.

The basic biology of lamin A/C

Expression

Early studies on differential A-type lamin expression using an antibody against a protein named statin showed that it is absent in proliferating cells and highly expressed in non-proliferating senescent cells (Wang, 1985). Studies have confirmed the lack of lamin A/C in pluripotent cells (Constantinescu et al., 2006; Lebel et al., 1987; Stewart and Burke, 1987). During mouse embryogenesis, lamin A/C starts to be expressed on days 10 to 12 in the embryo (Dittmer and Misteli, 2011). The temporally regulated expression of A-type lamins in differentiation supports the idea that they facilitate cell differentiation (Butin-Israeli et al., 2012; Worman and Bonne, 2007). However, it is controversial as lamin A/C has been reported to be expressed in various mouse embryonic stem cells and in developing blastocysts, albeit at very low levels (Eckersley-Maslin et al., 2013). Furthermore, the link between A-type lamins and proliferation cannot be considered a universal rule as rapidly proliferating cancer cells do express A-type lamins at varying levels (Broers and Ramaekers, 2014). On the other hand, B-type lamins are expressed in most cell types independent of their differentiation states (Stewart and Burke, 1987). A-type lamin expression also varies with matrix stiffness. In a survey of

proteomes across tissues, Lamin A was found to increase 30-fold from soft to stiff tissue, while B-type lamins varied less than 3-fold (Swift et al., 2013)

Genetics, splicing, and processing

Lamin A and lamin C are the most common isoforms coded by the gene *LMNA* at chromosome 1q21.2-q21.3 (Wydner et al., 1996). *LMNA* consists of 12 exons that produce the transcripts for prelamin A and lamin C (Lin and Worman, 1993). Lamin C and prelamin A share identical sequences in their first 566 amino acids, which are encoded by exons 1-10. The differences between them lie in their carboxyl-terminal region. Lamin C ends with exon ten sequences and includes six unique amino acids at the carboxyl terminus. On the other hand, prelamin A contains 98 unique amino acids encoded by exons 11-12. The last four amino acids of prelamin A (CSIM) play a crucial role in protein farnesylation, methylation, and endoproteolytic processing, leading to the conversion of prelamin A to mature lamin A (Sinensky et al., 1994). The steps will be reviewed later. The multistep processing is highly efficient, resulting in minimal detection of prelamin A in normal cells. Perturbation in the processing of prelamin A can cause a dramatic phenotype, as mentioned above regarding Hutchinson-Gilford progeria syndrome. However, lamin A itself appears to be dispensable in mice (Fong et al., 2006).

Structure

The structure of A-type lamins consists of a central α -helical coiled-coil "rod" domain, flanked by a nonhelical N-terminal "head" domain and C-terminal "tail" domain. The central rod domain consists of four sub-helical regions, known as coil 1A, 1B, 2A, and 2B. These coils are separated by three short linker segments: L1, L12, and L2, with L12 being the most flexible among them (Parry et al., 1986). The head domain appears to be unstructured, while the tail contains a structural motif similar to an immunoglobulin fold (Dhe-Paganon et al., 2002; Krimm

et al., 2002). Between the end of the rod domain and the tail domain is the nuclear localization signal (Loewinger and McKeon, 1988).

To form the meshwork at the nuclear periphery, A-type lamins first assemble into coiled dimers through parallel interactions via their rod domain. These dimers associate longitudinally in a head-to-tail manner to form protofilaments. These polymers then assemble laterally in an antiparallel manner into filaments (Gruenbaum and Foisner, 2015). *In vitro*, human lamin A has been shown to form higher-order para-crystal structures. However, *in vivo*, the best evidence suggests that lamins form 3.5 nm thick filaments consist of tetramers (Turgay et al., 2017; Turgay and Medalia, 2017). The organization of these filaments into lamin networks *in vivo* is unknown.

In addition to the stable networks near the inner nuclear membrane, lamins are also distributed throughout the nucleoplasm (Gerace and Huber, 2012; Kolb et al., 2011). Nucleoplasmic A-type lamins have higher mobility and are more soluble than their peripheral counterparts (Dittmer and Misteli, 2011). Even less is known about the functions of nucleoplasmic lamins; they have been associated the intranuclear structures such as nuclear speckles and the nucleoplasmic reticulum (Dittmer and Misteli, 2011; Kumaran et al., 2002).

Function

In addition to forming filaments through homotypic interactions, A-type lamins have been reported to bind to many partners. The additional functions of A-type lamins can be viewed through some of these well-studied binding partners. As previously mentioned, A-type lamins interact with other components of the nucleoskeleton, such as B-type lamins, the LINC complex SUNs, and NPCs. Furthermore, lamins are important for the incorporation and spacing of nuclear pores (Al-Haboubi et al., 2011; Goldberg et al., 1995; Osouda et al., 2005; Smythe et al., 2000).

Lamin A/C interacts with a group of inner nuclear membrane proteins called LEM proteins. Emerin, LAP2, and MAN1 all contain the LEM domain, which interacts with the barrier to autointegration factor (BAF), a DNA binding factor responsible for recruiting chromatin to the nuclear periphery (Cai et al., 2001; Furukawa, 1999; Lee et al., 2001; Mansharamani and Wilson, 2005). In addition to their indirect interaction with chromatin through the LEM proteins, they have been shown to directly interact with chromatin and DNA (Cai et al., 2001; Stierlé et al., 2003; Taniura et al., 1995).

Many studies link lamins with signal transduction pathways, including retinoblastoma Rb/E2F, Wnt/ β -catenin, TGF β /SMAD, and MAP kinase pathways (Dittmer and Misteli, 2011). Lamins are thought to regulate these signaling pathways by binding and sequestering proteins within these cascades, as is the case with c-Fos, pRb, and SMADs (Dittmer and Misteli, 2011). Phosphorylation of ERK1/2 causes it to translocate into the nucleus, where it phosphorylates c-Fos. This leads to c-Fos being released from the nuclear lamina and activating transcription (González et al., 2008). Through a similar mechanism, upstream signaling cascades can release Rb from its interaction with lamin A/C, leading to its phosphorylation and promoting E2F activation (Rodríguez et al., 2010). While the sequestration of pRb prevents its degradation by the proteasome (Johnson et al., 2004). Furthermore, the sequestration of SMADs by A-type lamins can negatively regulate TGF β signaling (Van Berlo et al., 2005).

Part of the function of lamin A/C is conferred by the binding of transcription factors. Its binding to SREBP1 may partly explain the pathogenic mechanism of Dunnigan-type familial partial lipodystrophy (Lloyd et al., 2002). SREBP1 is an important regulator of lipid metabolism that stimulates the expression of various lipid metabolism genes such as fatty acid synthase (FAS), acetyl-CoA carboxylase, and lipoprotein lipase. (Im et al., 2009). It has been suggested that prelamin A interacts with SREBP1 (Capanni et al., 2005). In addition to interacting with transcription factors, the C-terminal immunoglobulin-like domain of lamin A/C directly interacts

with the PCNA replication factor, which plays an important role in DNA replication (Cobb et al., 2016; Shumaker et al., 2008).

Post-translational modifications

As mentioned earlier, lamin A is synthesized in its precursor form, prelamin A, and is post-translationally modified and processed to become the mature form. The processing steps occur as follows: protein farnesyltransferase catalyzes farnesylation at the cysteine of the C-terminal CAAX motif (Beck et al., 1990). Second, either Ras-converting enzyme 1 (RCE1) or zinc metallopeptidase STE24 homolog (ZMPSTE24) catalyzes the proteolytic cleavage of the -AAX. Third, isoprenylcysteine carboxyl methyltransferase (ICMT) catalyzes the methylation of the farnesylated cysteine. Then lastly, ZMPSTE24 catalyzes an additional cleavage to remove the last 15 amino acids to generate mature lamin A. Lamin C does not undergo these processing steps because it lacks a CAAX motif. This process is affected by the G608G mutation that causes HGPS. The mutations cause alternative splicing that removes the part of the mRNA that codes for the ZMPSTE24 cleavage site, resulting in a truncated prelamin A that retains its farnesylated and carboxymethylated cysteine residue, called progerin (Rusiñol and Sinensky, 2006; Young et al., 2005b).

Lamin phosphorylation is known to promote disassembly and protein turnover (Bertacchini et al., 2013; Goldman et al., 2002). Phosphorylation by kinases, including PKC1 and CDK1, impedes the assembly of head-to-tail polymers and is required for lamin depolymerization during mitosis (Peter et al., 1991; Peter et al., 1990). A-type lamins are also phosphorylated in interphase that alters their distribution within the nucleus, suggesting dynamic regulation of lamins has functions outside of mitosis (Kochin et al., 2014). A recent study shows phosphorylated lamin A at the interior of the nucleus binds to enhancer regions on genomic DNA (Ikegami et al., 2020). Despite what is known, there is limited knowledge regarding the impact of interphase lamin phosphorylation.

A-type lamins have been found to be SUMOylated (Zhang and Sarge, 2008). SUMOylation is capable of modifying nuclear processes such as nuclear import/export, transcription, apoptosis, cell cycle regulation, and protein stability (Geiss-Friedlander and Melchior, 2007). Many of the enzymes that add or remove SUMO are localized at the nucleus (Wilkinson and Henley, 2010). Not much is known about the effect of SUMOylation on lamin A/C. However, many mutations associated with cardiomyopathy are predicted to directly or indirectly block sumoylation (Simon and Wilson, 2013).

A-type lamins have also been reported to be modified by O-GlcNAcylation, acetylation, and ubiquitylation (Simon and Wilson, 2013). The effect and regulation of many of the post-translational modifications of A-type lamin are a mystery. Further research is necessary to determine if they are important in understanding the pathobiology of mutations in *LMNA*.

The basic biology of emerin

Genetics, structure, and localization

Named after Alan Emery, emerin is a ubiquitously expressed type II integral membrane protein of the inner nuclear membrane. It is encoded by the *EMD* gene, previously known as *STA*, on the X chromosome (Bione et al., 1994). The gene consists of six exons encoding 254 amino acid proteins with a 220 amino acid N-terminal nucleoplasmic domain, a 23 amino acid C-terminal transmembrane domain, and an 11 amino acid luminal domain in the perinuclear space. It contains a LEM domain, mostly found in the nucleoplasmic side of inner nuclear membrane proteins, including MAN1, LAP2, and LEMD3. The LEM domain comprises 40 amino acids at emerin's N terminal and forms a helix-loop-helix fold which is essential for binding BAF. Through BAF, emerin and other LEM domain proteins bind to chromatin and tether it to the nuclear envelope. BAF binding is the only known role of the LEM domain. Between the LEM

domain and the transmembrane domain is an unstructured region that is implicated in lamin binding and nuclear localization.

Newly synthesized emerin in the cytoplasm appears to be inserted into the ER membrane post-translationally (Ellis et al., 1998). It freely diffuses between the ER, outer and inner nuclear membrane and through membrane associated with NPCs, which is a diffusion barrier for bigger membrane proteins (Ostlund et al., 1999). Once at the inner nuclear membrane, emerin binds to A-type lamins which retain and concentrates emerin. In cells lacking A-type lamins, emerin is not retained in the inner nuclear membrane but localized diffusely throughout the ER (Sullivan et al., 1999). Its diffusional mobility in the inner nuclear membrane is also decreased in cells lacking A-type lamins (Ostlund et al., 2006).

Function

The biological function of emerin is a mystery. However, many of its functions are inferred from the function of its interacting proteins. Despite that, the physiological consequence of these protein interactions with emerin is unclear.

Nuclear structure

Emerin null cells exhibit increased nuclear fragility, much like lamin A/C-deficient cells (Rowat et al., 2006). Emerin directly interacts with nuclear lamins, nesprins, and SUN-domain proteins of the LINC complex (Haque et al., 2010; Lee et al., 2001; Wheeler et al., 2007). Emerin binds to multiple actin-binding proteins, and *in vitro*, emerin binds and caps actin filaments providing a stabilizing effect (Holaska et al., 2004; Holaska and Wilson, 2007). Therefore emerin may play a role in anchoring nuclear actin, which provides structural support to the nucleus (Koch and Holaska, 2014). However, the physiological significance of the emerin-actin associations remains speculative.

Chromatin architecture

Cells lacking emerin have less heterochromatin implicating it in chromatin repression (Meaburn et al., 2007; Ognibene et al., 1999). How emerin modulates chromatin is unclear. However, it is known to bind to two proteins that associate with DNA or chromatin, BAF and HDAC3. As mentioned, the LEM domain of emerin facilitates its binding to BAF. BAF binds to the phosphate backbone of DNA in a nonspecific manner and has been implicated in many pathways, including mitosis, nuclear assembly, viral infection, DNA damage response, and chromatin and gene regulation (Margalit et al., 2007; Segura-Totten et al., 2002). Emerin directly binds with HDAC3, and certain EDMD-causing mutations disrupt this interaction. (Demmerle et al., 2012)

Transcription

Like lamin A/C, emerin binds to several transcriptional regulators and alters their dynamics and availability. In addition to binding with BAF, emerin also binds to GCL, a transcriptional repressor, which competes with BAF for binding to emerin (Holaska et al., 2003). Emerin binds to another transcription repressor called Btf, or BCLAF1, which has been shown to be associated with various processes such as DNA damage response, splicing, and processing of pre-mRNA (Haraguchi et al., 2004; Yu et al., 2022). Rare EDMD-causing mutations in *EMD* that produce mutated emerin have been found to affect the binding of GCL and Btf (Haraguchi et al., 2004). Lmo7 binding is also disrupted by a specific EDMD causing mutation in *EMD* (Holaska et al., 2006). Lmo7 is a shuttling transcription activator that is inhibited by emerin binding (Holaska et al., 2006). Additionally, emerin directly binds β -catenin, an important transcription coactivator, sequesters and inhibits its downstream effect (Markiewicz et al., 2006). Emerin also has been found to bind to the splicing factor YT521-B (Wilkinson et al., 2003). The physiological consequences of emerin binding to these transcription and splicing factors is however unknown.

Signaling

In emerin-null mouse myogenic progenitors, many signaling pathways are altered, including Wnt, TGF β , Notch, and IGF pathways (Koch and Holaska, 2012). Additionally, JNK, MAPK, NF- κ B, and integrin signaling pathways are also disrupted from loss of emerin in humans and mice (Koch and Holaska, 2014). How loss of emerin leads to altered signaling pathways is an open question.

Post-translational modification

Emerin contains around 40 phosphorylation sites (Koch and Holaska, 2014). Like lamins, emerin is phosphorylated during mitosis to promote nuclear disassembly (Ellis et al., 1998). During interphase, phosphorylation of emerin by various kinases such as Src, PKA, GSK3 β , PKC δ , and ERK2/MAPK, with the functional consequence of phosphorylation poorly understood. Mutation of certain phosphorylation sites decreases emerin binding to BAF (Tiffet et al., 2009). Furthermore, interaction of emerin with actin appears to be modulated by phosphorylation (Lattanzi et al., 2003). More work needs to be done to understand emerin phosphorylation as the physiological consequences are unknown.

Emerin is also a target of O-GlcNAcylation (Berk et al., 2013). O-GlcNAcylation is a nutrient and stress sensor and can affect transcription, epigenetic regulation, and cell signaling (Hart et al., 2011; Ranuncolo et al., 2012; Sakabe et al., 2010; Zachara et al., 2011; Zachara et al., 2004). It has been shown to modulate binding with emerin interactors such as BAF and lamins (Berk et al., 2013). However the biological significance is unknown.

How do alterations in A-type lamins and emerin cause cardiomyopathy?

The hypothesis of lamin A/C

Various mutations in *LMNA* cause striated muscle diseases. Missense mutations are predicted to have a dominant negative mechanism, while haploinsufficiency likely explains other mutations of *LMNA*. Attempts have been made to correlate the location of the various missense mutations and types of laminopathy (Hegele, 2005). Missense mutations that affect skeletal muscles and/or the heart are spread throughout the gene (Tesson et al., 2014). While diseases primarily affecting the peripheral nerves, bones, and metabolism or causing premature aging tend to be associated with specific regions of the gene (Eriksson et al., 2003; Novelli et al., 2002; Speckman et al., 2000). The vast majority of mutations causing Dunnigan-type familial partial lipodystrophy cause amino acid substitutions in the immunoglobulin-like fold motif of lamin A/C and their structural consequences have been examined. The lipodystrophy-causing mutations lead to amino acid substitutions that change the charge of the fold's surface, whereas muscle disease-causing missense mutations changing amino acids in the fold disrupt its overall three-dimensional structure (Dhe-Paganon et al., 2002; Krimm et al., 2002).

How mutation in a gene encoding a ubiquitously expressed protein in differentiated tissues results in tissue-selective phenotypes is not clear. Answering this question requires a better understanding of the functional roles of lamin A/C. Based on current knowledge, two mutually nonexclusive prevalent hypotheses have been widely proposed to explain the tissue specificity of phenotypes resulting from mutations in lamin A/C. The two hypotheses are: 1) The "mechanical hypothesis" proposes that disruption in the nuclear lamina leads to nuclear fragility and sensitivity to mechanical stress. This helps to explain the susceptibility of striated muscles to mutations in *LMNA*. 2) The "gene expression hypothesis" proposes that interaction between the chromatin, gene regulatory factors, and nuclear lamina are disrupted in cells with *LMNA* mutation, which leads to aberrant gene expression that may affect certain tissues more than

others. These two hypotheses are not mutually exclusive and other possible pathogenic mechanisms have not been excluded.

Many lines of evidence are used to support the mechanical hypothesis. Knockout studies in various cell types have established lamin A/C as important in maintaining nuclear shape, stability, and stiffness (Stiekema et al., 2020). Loss of nuclear integrity can lead to nuclear rupture under high mechanical stress (Earle et al., 2020). Nuclear envelope breakage results in the uncontrolled exchange of cytoplasmic and nuclear content and can lead to DNA damage, which is exacerbated by defective DNA repair caused by mutant lamin A/C (Earle et al., 2020; Shah et al., 2021a). One study has shown that knocking out SUN1 can partially rescue phenotypes associated with a lack of lamin A/C in the heart (Chai et al., 2021). Knocking out Sun1 has the effect of uncoupling the connection between lamin A/C and the cytoplasmic microtubule cytoskeletal network via the LINC complex. Although there was no increase in DNA damage detected, the study shows that alterations in mechanical force transduced from the cell to the nuclear lamina may be part of the mechanism behind the loss of lamin A/C in the heart (Chai et al., 2021).

The gene expression hypothesis is supported by the numerous observation that loss of lamin A/C alters gene expression (Puckelwartz et al., 2011). Alteration of gene expression can occur through the disruption of chromatin organization. Many studies have made the observation that heterochromatin is altered in *LMNA* mutant cells. As a result, gene silencing mediated by heterochromatin can become disturbed, leading to aberrant gene expression. Two studies using human iPSC-CMs with *LMNA* mutations from patients with cardiomyopathy found upregulation of genes associated with the nervous system (Bertero et al., 2019; Shah et al., 2021b). Among those genes of the nervous system are ion channels, which may explain the conduction defects seen in cardiolaminopathies (Bertero et al., 2019; Shah et al., 2021b).

Gene expression can also be caused by the misregulation of transcriptional regulators and signal transduction pathways in lamin A/C mutant cells. Lamin A/C has been shown to regulate key transcriptional regulators through sequestration and regulating their activation and availability. Many studies have associated lamins with the regulation of major signaling cascades pathways such as MAPK/ERK, TGF β , and Wnt/ β -catenin. Mouse models of dilated cardiomyopathy caused by *Lmna* mutation have activated MAPK signaling, and specific inhibitors were able to prevent or delay the development of cardiomyopathy (Muchir and Worman, 2016). Furthermore, downstream effects of activation of the ERK pathway have been shown to upregulate *Dusp4* and the mTOR pathway (Choi et al., 2012; Ramos et al., 2012). There are additional cardiac-specific pathways altered in *LMNA* mutants to be discovered. A recent study using *LMNA* haploinsufficient iPSC-cardiomyocytes found upregulation of genes in the PDGF pathway (Lee et al., 2019).

The mystery of emerin

In contrast to *LMNA*, mutations in *EMD* only cause only striated muscle disease. However, the tissue specificity of its loss of function phenotype is still a question as it is a ubiquitously expressed protein. The mechanical hypothesis and chromatin hypothesis used to explain the tissue-specific of phenotypes from *LMNA* mutations can also apply to emerin.

The vast majority of mutations are nonsense, missense, and frameshift that result in the absence of protein expression (Yates et al., 1999). Only a few known mutations lead to the expression of modified emerin (Manilal et al., 1996; Nagano et al., 1996; Yates et al., 1999). Emerin-deficient cells exhibit abnormal nuclear shape and impaired mechanotransduction, similar to cells without A-type lamins (Lammerding et al., 2005). This hypothesis has not been thoroughly tested in the heart, as *Emd* null mice do not exhibit disease phenotype (Melcon et al., 2006; Ozawa et al., 2006).

Emerin also may affect gene expression in different ways compared to A-type lamins. Through its specific interaction with BAF, emerin interacts with chromatin, the effect of which has yet to be thoroughly investigated (Koch and Holaska, 2014). Additionally, emerin has been found to bind to a number of transcription regulators, including GCL, Btf, and Lmo7, all have the potential to aberrantly alter gene expression in emerin-deficient cells. In particular, Lmo7 is an emerin effector that is also highly expressed in striated muscle and regulates the transcription of many genes relevant to the muscle (Holaska et al., 2006).

Conclusions and research motivation

The nuclear envelope and lamina proteins participate in many biological processes, many of which are still yet to be elucidated and characterized. Mutations in two genes, *LMNA* and *EMD*, that encode for proteins associated with the nuclear envelope were found to be associated with human disease. The pathobiology and mechanism of the disease are currently unknown. Additionally, studying *LMNA*-associated dilated cardiomyopathy and *EMD*-associated dilated cardiomyopathy has been challenging as genotypes do not result in a straightforward cellular phenotype that can be linked to disease. While the function of emerin is still unknown, the function of lamin A/C is obscured by its involvement in many diseases affecting different tissues. The tissue specificity of laminopathies has led to the mechanical hypothesis and the gene expression hypothesis, two mutually non-exclusive perspectives to begin to answer the question of how these nuclear envelope proteins cause disease with tissue specificity.

Studies conducted so far have described lamin A/C to be involved in diverse biological processes that span from a structural role in the nucleus to the regulation of response to mechanical stress and gene expression. However, none of those is *per se* able to fully justify the functional and clinical phenotypes. Further research is required to investigate the tissue-

specific role of the nuclear lamina, particularly in cardiomyocytes, which are arguably the most significant cell type in terms of laminopathies.

This study aims to improve understanding of the essential biological role of the nuclear lamina envelope A-type lamins and emerin. *EMD* mutations as well as many mutations in *LMNA* cause clinically identical dilated cardiomyopathy with conduction system disease. The encoding proteins lamin A/C and emerin also physically interact on the nuclear envelope. Therefore, I hypothesize that these two proteins have functional overlap in cardiomyocytes, and their interaction is critical in cardiomyocytes. So far, no studies have investigated the functional overlap of emerin and lamin A/C in cardiomyocytes. I will begin with an unbiased, comprehensive analysis of the gene expression and protein level changes in cardiomyocytes with disruptions in lamin A/C or disruption in emerin. The objective is to find the functional overlap between disruptions in lamin A/C and emerin in order to understand their role in cardiomyocytes and furthermore, how they can cause disease.

Additionally, it would be valuable to know if loss of lamin A/C in mature cardiomyocytes is sufficient to disrupt cardiac function. Previous mouse studies with germline knockout of lamin A/C noted cardiac defects as the likely cause of death. Lamin A/C has been implicated in cell differentiation and providing mechanical strength to cells. It is unknown if loss of lamin A/C was detrimental to cardiomyocyte differentiation, maturation, or mature heart function. I will generate mice lines with conditional knockout of *Lmna* in cardiomyocytes at the embryonic level and mature adult level. By characterizing these mice, I will be able to determine if disruption of lamin A/C is detrimental to mature cardiomyocytes and further narrow down the specific cardiac requirement of lamin A/C.

This work aims to contribute to understanding the functions of these EDMD-associated nuclear envelope proteins in cardiomyocytes and improve understanding of how mutations in their genes cause the phenotype of dilated cardiomyopathy with conduction disease.

Knowledge gained from this study will be informative in further studies in the pathobiology and mechanisms of cardiomyopathy associated with disruptions in A-type lamins and emerin.

Chapter 2: Investigating the Role of Emerin and Lamin A/C in Human Cardiac Cell Culture Model

Introduction

iPSCs and disease modeling

Although commonly used animal models such as mice have provided valuable insight into human disease (see chapter 3), species differences can obscure the recapitulation of human diseases. In 2006, a significant breakthrough was made with the discovery that cells with a gene expression profile and pluripotent potential similar to the ethically controversial embryonic stem cells can be generated from mouse somatic cells by using four transcription factors (Takahashi and Yamanaka, 2006). The four transcription factors OCT4, SOX2, KLF4, and MYC were termed “Yamanaka factors” and the cells they generated were termed induced pluripotent stem cells or iPSCs (Takahashi and Yamanaka, 2006). One year later, two independent groups reported generating and characterizing human iPSCs made from fibroblasts (Takahashi et al., 2007; Yu et al., 2007). The human origin, easy accessibility, and the ability to expand and give rise to almost any cell type led to a new era of disease modeling, drug discovery, and regenerative medicine. Furthermore, concurrent advancements in gene editing technologies, such as CRISPR-Cas9 technology, are enabling rapid development of genetically defined human iPSC disease models.

Lack of expandable sources of cells from patients, especially the difficult-to-access cells of specialized organs such as the brain and heart, has been a major obstacle in disease modeling. The arrival of iPSC solves that limitation allowing human diseases, particularly genetic disorders, to be modeled using iPSCs derived from accessible cell types such as skin fibroblasts and blood cells. From their ability for self-renewal and potential to differentiate, large quantities of disease-relevant and patient-specific cells can be produced. Early disease

modeling studies using iPSCs derived from patients used iPSCs derived from healthy individuals as controls, which introduces confounds such as different genetic backgrounds and line-to-line variations. With the rapidly developing genome editing technologies, genetic changes can be introduced in a site-specific manner, enabling the generation of isogenic iPSC lines with the introduced mutation as the sole variable. This is particularly useful in modeling diseases with many unknown genetic modifiers. iPSC-CMs has been used to study the nuclear lamina proteins that when altered cause EDMD.

Disease modeling using iPSCs is extensively employed to investigate monogenic disorders, particularly those characterized by early onset. This method is particularly well-suited for such disorders due to the ease of generating iPSCs from patient samples and differentiating them into disease-relevant cell types like neurons and cardiomyocytes. Moreover, the relatively immature state of iPSC-derived cells offers a better chance of recapitulating the early molecular changes that may be relevant to the disease.

iPSC studies of cardiomyopathies

iPSC offers a great opportunity to study cardiomyopathy mutations, thereby eliminating the species differences when it comes to mouse models and raising hopes to model cardiomyopathy caused by *EMD* mutations. Sadly, there is only one published study of iPSC-CMs with *EMD* mutation; the only finding from the study was differences in the decay of nuclear calcium transients (Shimajima et al., 2017). Several studies have generated iPSC lines from human patients with LMNA mutations. Initial studies relied on the characterization of stressed-induced phenotypes such as nuclear morphology and electrophysiological properties.

The earliest study using iPSC reprogrammed from patient cells to study cardiomyopathy was published in 2012 (Siu et al., 2012). The patient has a missense mutation R225X that resulted in haploinsufficiency of A-type lamins. After successfully differentiating the patient-derived iPSC and control iPSC derived from a healthy donor into

cardiomyocytes, there were no differences in electrophysiological properties or nuclear morphology. However, after inducing stress with electrical stimulation, *LMNA* mutants had a dramatic increase in aberrant nuclear morphology and increased apoptosis. Additionally, the increased apoptosis in mutant iPSC-CMs could be attenuated by therapeutic blockage of ERK1/2 pathway. The same group in a later study examined patients with the *LMNA* Q354X, T518fs, and the previously studied R225X mutations (Lee et al., 2017). They continued to evaluate the phenotype of the mutant iPSC-CMs using electrical stimulation-induced aberrant nuclear morphology and apoptosis, with the additional characterization of calcium-dependent excitation-contraction coupling, which was defective in the mutants (Lee et al., 2017). Shah *et al.* generated a human iPSC line with p.S143P *LMNA* mutation from patients exhibiting dilated cardiomyopathy (Shah et al., 2019). The mutant iPSC-CMs were similar to control until exposure to hypoxic conditions induced various phenotypes such as sarcomere disorganization and various heat shock factors. Furthermore, repeat exposures to hypoxic conditions led to the mutant having sustained reduced contraction rates (Shah et al., 2019).

Most later studies relied on transcriptomics data and made conclusions that supported the hypothesis that altered chromatin organization may underlie disease. Salvarani and colleagues investigated the *LMNA* p.K219T variant from a patient with severe dilated cardiomyopathy (Salvarani et al., 2019). Initial electrophysiological characterization led the authors to investigate sodium currents specifically, finding a reduction of current density in mutant iPSC-CMs. In search of a mechanism, they found a reduction of sodium channel SCN5A which they concluded was due to altered chromatin dynamics that led to faulty repression of the channel's expression (Salvarani et al., 2019). Bertero and colleagues generated iPSCs from a patient with the *LMNA* pR225X mutation (Bertero et al., 2019). They used Hi-C and RNA sequencing to analyze 3D chromatin organization and gene expression. They found significant changes in chromatin compartmentalization due to altered chromatin dynamics during

differentiation. One of the consequences was the upregulation of neuronal-lineage-associated genes, including neuronal calcium channel *CACNA1A*, which they found contributed to some of the electrophysiological abnormalities in the *LMNA*-haploinsufficient iPSC-CMs (Bertero et al., 2019). Notably, this was the first iPSC study on *Lmna* that used an isogenic control generated by reversing the patient cell mutation using CRISPR/CAS9 editing.

Lee and colleagues generated an iPSC mutant line from a patient with the *LMNA* p.K117fs mutation, which results in haploinsufficiency of lamin A/C (Lee et al., 2019). Electrophysiological studies of spontaneous action potential and calcium imaging showed that the mutant iPSC-CMs had phenotypes characteristic of arrhythmia. Transcriptomic analysis identified upregulation of components of the PDGF pathway in mutant iPSC-CMs compared to isogenic control. Inhibition of PDGF signaling eliminated the arrhythmic phenotypes in mutants (Lee et al., 2019). Shah and colleagues conducted the most recent and comprehensive study yet of cardiomyopathy with iPSCs (Shah et al., 2021b). They introduced two pathogenic mutations of *LMNA* into human iPSCs and differentiated them into cardiomyocytes, hepatocytes and adipocytes. They found cardiomyocyte-specific loss of lamina-bound chromatin that resulted in aberrant expression of non-cardiac genes. Neuronal genes were overrepresented in agreement with a previous study by Bertero and colleagues (Shah et al., 2021b).

Motivation

The large breadth of nuclear lamina functions and even the diverse effects of *LMNA* mutations present difficulty in understanding the basic importance of nuclear lamina proteins in cardiomyocytes. Previous studies investigating iPSC-CMs with pathogenic *LMNA* mutations found phenotypes that can be associated with dilated cardiomyopathies, such as arrhythmia, on the single-cell level. Only more recent studies unbiased look at large-scale global changes in the transcriptome. Despite the recent studies using isogenic lines in order to pinpoint specific differences in *LMNA* mutants, very few clearly pathogenic mechanisms were identified.

The studies outlined above were motivated by the search for pathogenic mechanisms by using iPSCs derived from patients or introducing mutations from patients into cultured cells. However, it can be difficult to infer pathogenic mechanisms when there is still a large mystery of the normal functional requirement of nuclear lamina proteins in cardiomyocytes. Furthermore, iPSC studies still need to comprehensively examine the effects of emerin deficiency, likely due to the relative rarity of X-EDMD patients compared to those with AD-EDMD. Humans with *EMD* mutations generally have a complete loss of emerin protein and show invariant phenotypes in the heart, hence it provides a great opportunity to investigate the basic requirement of nuclear envelope proteins in cardiomyocytes.

I postulate that cardiomyocytes require a robustly intact nuclear lamina, which when weakened by loss of emerin or lamin A/C haploinsufficiency, make the cells susceptible to damage or altered cell signaling. To pinpoint the intersection of the roles of emerin and the role of lamin A/C in cardiomyocytes, I generated a panel of isogenic lines in order to identify the common and differential effects of those two mutations. I then conducted an unbiased survey of all the processes affected by each respective mutation. I anticipated a significant overlap in gene and protein expression changes between the mutants that will aid in the additional understanding of the basic roles of these two nuclear lamina proteins in cardiomyocytes.

Results

Production of isogenic lines

iPS-DF19-9-11T was chosen to be the wildtype line and the background for the CRISPR mutants. This line is used as the standard wildtype (WT) for the study. I chose this line because of its widespread usage, male sex (X-EDMD only occurs in men and boys), and the method of

its generation, which made use of non-integrating episomal vectors, thereby eliminating any genomic integration (Yu et al., 2009).

To generate deletion of an *LMNA* allele, I targeted *LMNA* exon 3 with a multi-guide strategy (Figure 2.1A). Multi-guide strategy for CRISPR-mediated genome editing makes use of guide RNAs at close genomic proximity so that synergistic genome edits at each guide target site will create large deletions and more effective knockout allele generation. Direct delivery via electroporation was used to introduce the Cas9-sgRNA ribonucleoprotein complex into the iPSC cell. Subsequently, CRISPR clones were isolated and validated by Sanger DNA sequencing. Multiple CRISPR clones were generated, and two notable lines are shown (Figure 2.1B). One line with homozygous deletion of 134 bp was isolated (*LMNA c.368_502del*). A second line with a heterozygous deletion of 62 bp was also isolated. I decided to analyze the heterozygous deletion line for this study because many AD-EDMD mutations result in haploinsufficiency of lamin A/C.

To generate deletion in the *EMD* allele, I targeted *EMD* exon 2 with a multi-guide strategy (Figure 2.2A). A line with 92-bp deletion was isolated that was initially expected to be a knockout (Figure 2.2B). However, later analysis uncovered that this allele led to the production of emerlin mRNA without exon 2 (Figure 2.2C). A smaller emerlin protein, likely one without the exon 2 region, that can be detected by a subset of emerlin antibodies (Figure 2.2D). This line with exon 2 deletion allele can be useful for future studies as exon 2 was identified as a mutation hot spot in patients with EDMD (Brown et al., 2011). I took a different strategy and used a single guide (sgRNA 2) to make the CRISPR edit and generate an *EMD* deletion. A line with 1-bp deletion (*EMD c.130del*) was isolated (Figure 2.2E).

Immunoblot and immunofluorescence microscopy confirmed *EMD c.130del* was an effective emerlin knockout and will be known as *EMD^{ly}* from here onwards (Figure 2.3A). *LMNA* deletion could not be validated at the iPSC level. Conflicting reports exist on if lamin A/C is

expressed in pluripotent cells (Constantinescu et al., 2006; Eckersley-Maslin et al., 2013). Confocal immunofluorescence microscopy picks up a signal at the nucleus (Figure 2.3A). Similar signal at the nucleus can also be seen in the *LMNA* homozygous deletion (data not shown). However, widefield immunofluorescence microscopy shows heterogeneous laminin A/C expression in the WT iPSC population (Figure 2.3B). *LMNA c.368_502del* was later confirmed to be a heterozygous *LMNA* line after differentiation and will be referred to as *LMNA*^{-/+} (Figure 2.4B,C).

Whole genome sequencing was performed on a set of isogenic lines WT, *LMNA*^{-/+}, and *EMD*^{-y} to confirm the lack of genome irregularities and CRISPR off-target effects.

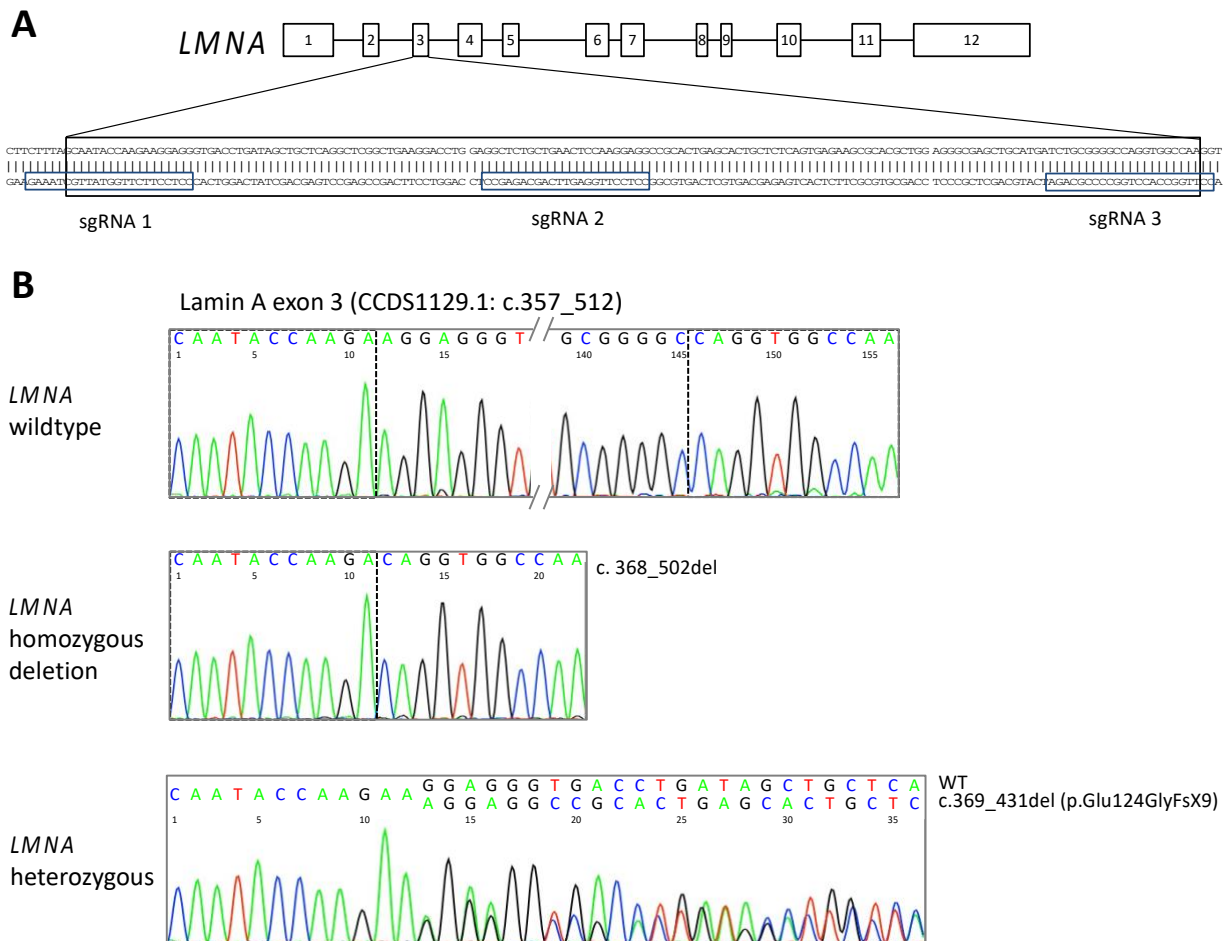


Figure 2.1: CRISPR strategy and resultant alleles generated for *LMNA*. A) *LMNA* gene structure showing 12 exons with sequence from exon 3 and sgRNA target sequence highlighted. B) Chromatographs from Sanger sequencing of exon 3 in wildtype (top), *LMNA* homozygous deletion line (middle), and *LMNA* heterozygous deletion line candidate (bottom).

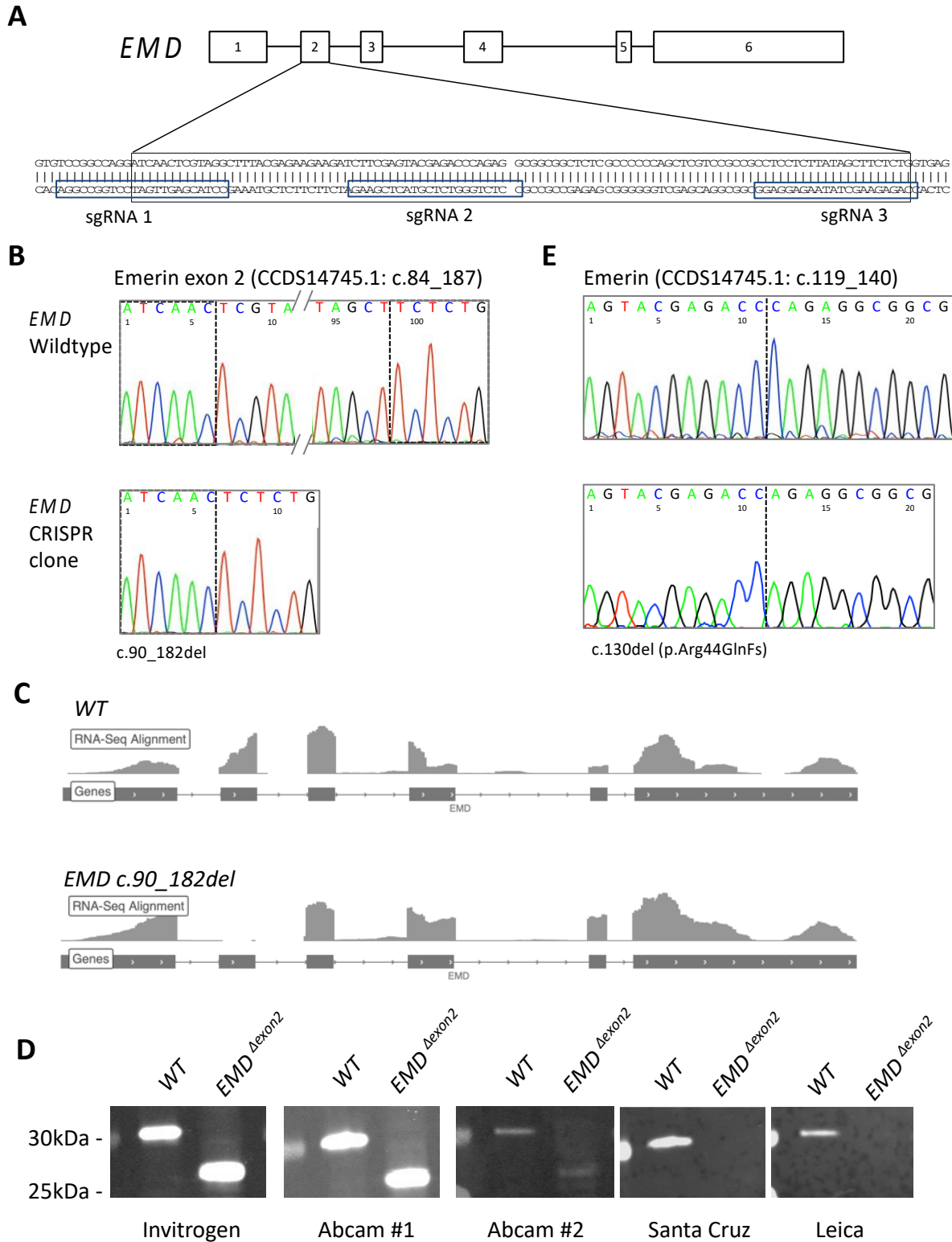


Figure 2.2: CRISPR strategy and resultant alleles generated for *EMD*. A) *EMD* gene structure showing 6 exons with sequence from exon 2 and sgRNA target sequence highlighted. B) Relevant regions of chromatographs from Sanger sequencing of exon 2 in wildtype (top),

EMD knockout candidate from multi-guide CRISPR (bottom). C) RNA sequencing reads alignment to *EMD* reveals multi-guide strategy generated RNA without exon2. D) The RNA generated produce stable protein that can be detected by select subset of commercial antibodies. E) relevant region of exon2 in wildtype (top), *EMD* knockout candidate from single-guide CRISPR (bottom).

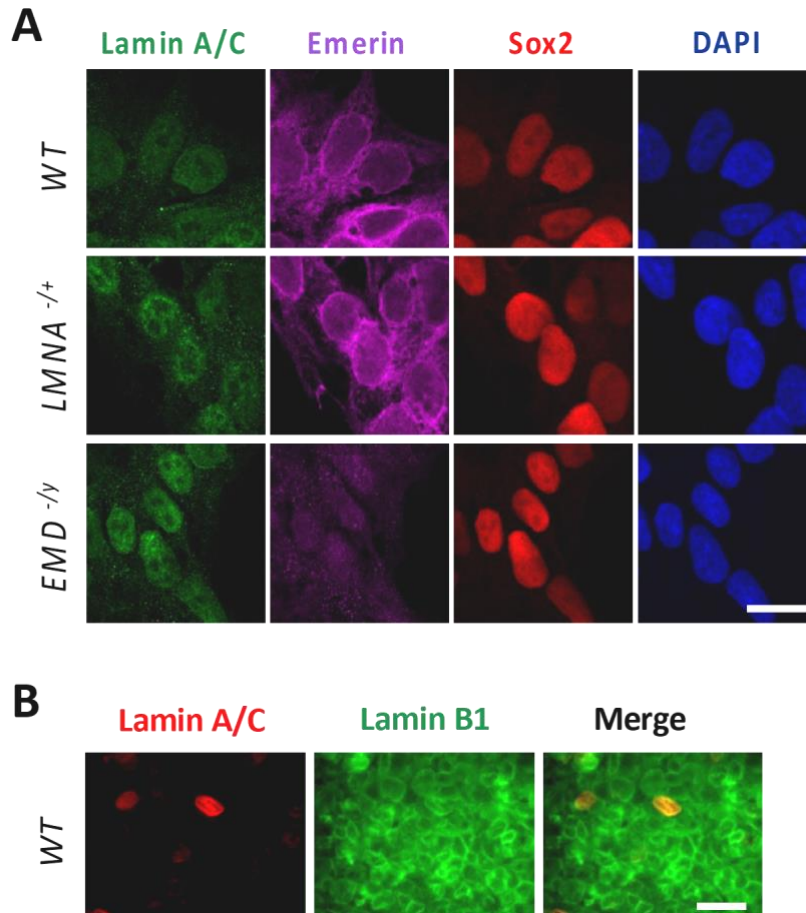


Figure 2.3: Immunofluorescence microscopic validation of CRISPR mutants showing loss of target protein in emerlin but inconclusive results for lamin A/C. A) Immunofluorescence micrographs of an isogenic panel of CRISPR lines showing effective knockout of emerlin in the *EMD*^{-/-} line, *LMNA*^{-/-} is inconclusive, co-stained with iPSC pluripotency marker SOX2, scale bar 20 μ M. B) Widefield images of WT line showing sporadic expression of lamin A/C in iPSC co-stained with an antibody against lamin B1, scale bar 50 μ M.

Differentiation into cardiomyocyte and characterization

The panel of 3 isogenic iPSC lines was differentiated into cardiomyocytes using a growth factor and serum-free differentiation protocol, purified with glucose starvation, and matured with lipid-rich maturation medium (Feyen et al., 2020; Lian et al., 2013; Sharma et al., 2015). This differentiation protocol was able to generate high purity iPSC-cardiomyocytes (iPSC-CMs) in all 3 genotypes with over 90% of total cells positive for cardiac troponin (cTnT) (Figure 2.4A). Immunoblot and immunofluorescence analysis confirmed that *LMNA*^{-/+} iPSC-CMs had a reduction of lamin A/C, and *EMD*^{-/-} CMs had no detectable emerin (Figure 2.4B,C). To test the direct effect of lamin A/C haploinsufficiency, I measured the interaction between emerin and lamin A/C using proximity ligation assay. The proximity of the lamin A/C and emerin epitope will result in a punctate fluorescent signal, and the number of the signals is a quantitative readout of the relative degree of interaction between the two proteins probed. Proximity ligation assay showed that the lamin A/C-emerin interaction was dramatically reduced in lamin A/C-haploinsufficient and absent in emerin-deficient iPSC-CMs (Figure 2.4D).

EDMD mutant cells have altered heterochromatin organization (Park et al., 2009). Therefore, I stained for the heterochromatin marker H3K9me3 to visualize by fluorescence microscopy any alterations to heterochromatin in the panel of iPSC-CMs (Figure 2.5). No major changes in the distribution of H3K9me3 was observed in lamin A/C haploinsufficient and emerin deficient iPSC-CMs compared to wildtype, though small changes could not be ruled out. Previous studies have also failed to observe heterochromatin alteration in other cell types with mutations in lamin A/C (Chaturvedi and Parnaik, 2010).

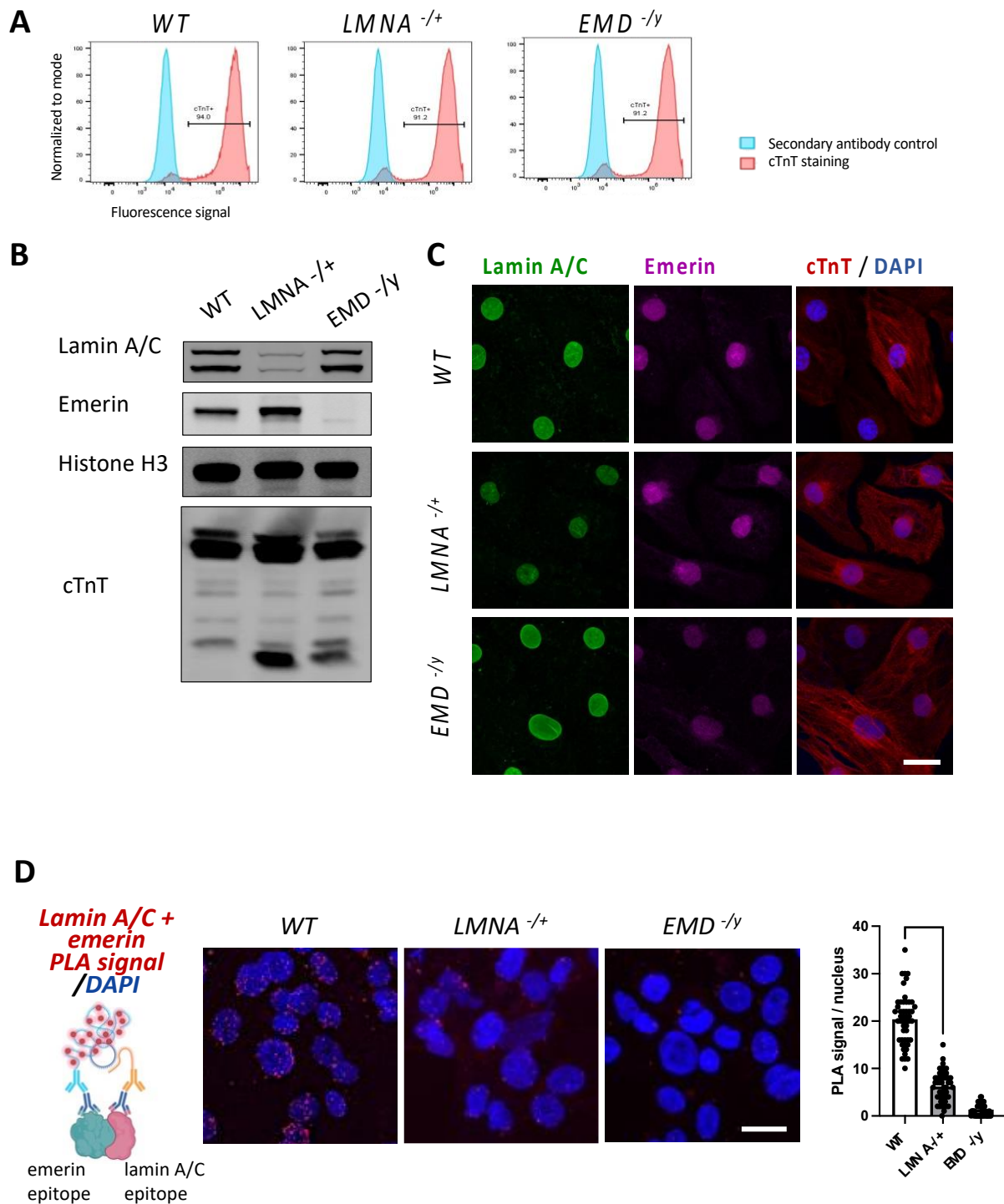


Figure 2.4: Differentiation of WT, *LMNA*^{+/-}, and *EMD*^{-/y} iPSC into cardiomyocytes and validation of lamin A/C haploinsufficiency and emerin deficiency. A) Flow cytometry analysis was performed on the pool of differentiated iPSC-CMs for the presence of cardiomyocyte marker cardiac troponin (cTnT). Red history represents the pool of cells that were stained with a cTnT antibody and a fluorescent secondary antibody. Blue history represents the staining control, where the pool of cells was incubated with only a secondary

antibody. B) Immunoblot of isogenic panel of iPSC-CMs. cTnT as the cardiomyocyte marker and histone H3 was used as a loading control. C) Immunofluorescence micrographs of an isogenic panel of iPSC. *LMNA*^{-/+} iPSC-CMs has lower lamin A/C fluorescent signal compared to WT and *EMD*^{-/-}. while *EMD*^{-/-} had no marine signal, cTnT as cardiomyocyte marker, scale bar 20 μ M. D) Measurement of lamin A/C-emerin interaction via proximity ligation assay (PLA). Schematic (left) shows the experimental design of the PLA assay. Emerin and lamin A/C antibody binding at their respective epitope are bound by PLA secondary antibody probe conjugated to an oligonucleotide. The proximity of the probes will lead to hybridization and amplification of the probe oligonucleotide, which is bound by fluorescent dye and will emit distinct punctate red fluorescence at each interaction site. Confocal images (middle) displaying red fluorescence across the nucleus (stained with DAPI) in WT. *LMNA*^{-/+} and *EMD*^{-/-} exhibit fewer PLA signals. Quantification of puncta per nucleus revealed a significant difference ($P < 0.0001$ for WT vs *LMNA*^{-/+}) by a student t-test (right); each symbol in the graph represents a single nucleus ($n = 50$ for each group).

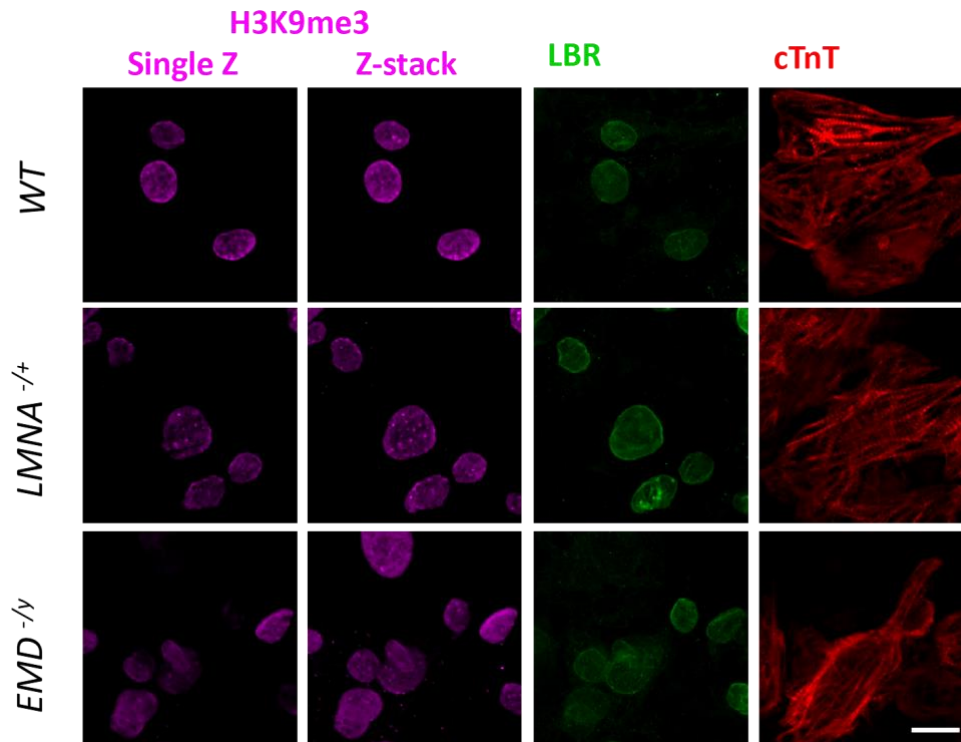


Figure 2.5 Heterochromatin distribution in WT, *LMNA*^{-/+} and *EMD*^{-/-} iPSC-CMs.

Representative confocal images of WT and mutant iPSC-CMs stained with H3K9me3, LBR, and cTnT. Scale bar 20 μ M.

Gene ontology analysis of DEGs shows common affected pathways between mutants

RNA was isolated from WT, *LMNA*^{-/+}, and *EMD*^{-/-} iPSC-CMs at day 30 of differentiation (confirmed >90% TNNT2+; n=6), sequenced, and analyzed for differentiation expression. Compared to WT control, *LMNA*^{-/+} iPSC-cardiomyocytes had 1,524 significant differentially-expressed genes (DEGs) while *EMD*^{-/-} had 1,203 significant DEGs (FDR <0.00005; |log₂FC vs WT| >1). Out of the total DEGs from each comparison, 571 were up in *LMNA*^{-/+} vs WT, and 953 were down (Figure 2.6A). In *EMD*^{-/-} vs WT, 312 were up, and 891 were down (Figure 2.6B).

Next, I performed Gene Ontology (GO) enrichment analysis to determine whether the DEGs between each comparison were enriched for certain biological pathways, cellular components, and molecular functions. In addition to analyzing each mutant comparison to wildtype control, I also performed enrichment analysis on the set of DEGs that are shared between both mutants in order to determine to certain enriched categories would stand out in the common set. The top 10 GO terms with significant enrichment (FDR<0.05) in each category are shown for each comparison.

DEGs upregulated in *LMNA*^{-/+} compared to control iPSC-CMs were significantly enriched for terms associated with mitosis in terms of biological processes, chromosomes in terms of cellular components, and ion channels in terms of molecular functions (Figure 2.7A). Upregulated DEGs in *EMD*^{-/-} compared to WT were enriched in different terms, in terms of biological processes, terms associated with development, morphogenesis especially related to the nervous system were enriched. By extension, nervous system-related cellular components were enriched. While molecular functions terms associated with transcription are enriched (Figure 2.7B). The 67 DEGs that are shared between the mutants were also analyzed for GO enrichment. This comparison showed enrichment for biological processes related to the nervous system, and cellular components were also enriched for many nervous system-related compartments as well as ion channels; the few significant categories of molecular functions that

were enriched in the shared upregulated DEGs are related to transcription (Figure 2.7C). The significant upregulation of genes associated with the nervous system and development might at first appear odd in the context of iPSC-CMs. However, it validates a previous study that also found upregulation of neurodevelopment genes in a different line of lamin A/C haploinsufficient iPSC-CMs (see discussion) (Shah et al., 2021b). Furthermore, the overlap of upregulated DEGs enriched in the nervous system and development in emerin-deficient iPSC-CM highlights the similarities between the disruption of the two genes.

Downregulated DEGs of *LMNA*^{-/+} compared to WT were enriched for broad biological processes related to homeostasis, with specific terms such as digestion and lipid transport and localization (Figure 2.8A). Downregulated genes were associated with brush border cellular components and transporter biological functions. Downregulated DEGs of *EMD*^{-/-} vs. WT were enriched for biological processes such as digestion and lipoprotein (Figure 2.8B). Additionally, enrichment was also found in brush border cellular components and transporter molecular functions. Unsurprisingly, when the common DEGs between both mutants were analyzed, many of the common GO terms in the separate analysis also appeared. In terms of biological processes, digestion was the most significant. Brush border and transporter terms were enriched in cellular components and molecular function. To make sense of the downregulated gene, I performed transcription factor enrichment analysis using ChEA3. Many of the downregulated genes were predicted to be regulated by transcription factors associated with hepatocytes and intestinal cells, such as ISX, CDX1, and HNF4A (Figure 2.8C).

To confirm the analysis, I obtained an independent analysis of the transcriptomics gene data set analyzed using Ingenuity Pathway Analysis (IPA). While input for gene set enrichment analysis is a simple unordered and unstructured collection of genes, IPA analysis takes into account the direction and order of gene differences. Common altered pathways in both mutants, when compared to WT, include LXR/RXR/FXR pathways which are nuclear receptors

associated with hepatocytes and/or enterocytes (Figure 2.9 A,B). The top upstream regulators were determined to be HNF4A, in agreement with previous independent analysis (Figure 2.9C). Therefore, it downregulated genes in appears lamin A/C haploinsufficient iPSC-CMs and emerin deficient iPSC-CMs are highly enriched in genes highly associated with intestinal and liver cells, with the additional theme of nutrient and lipid transport.

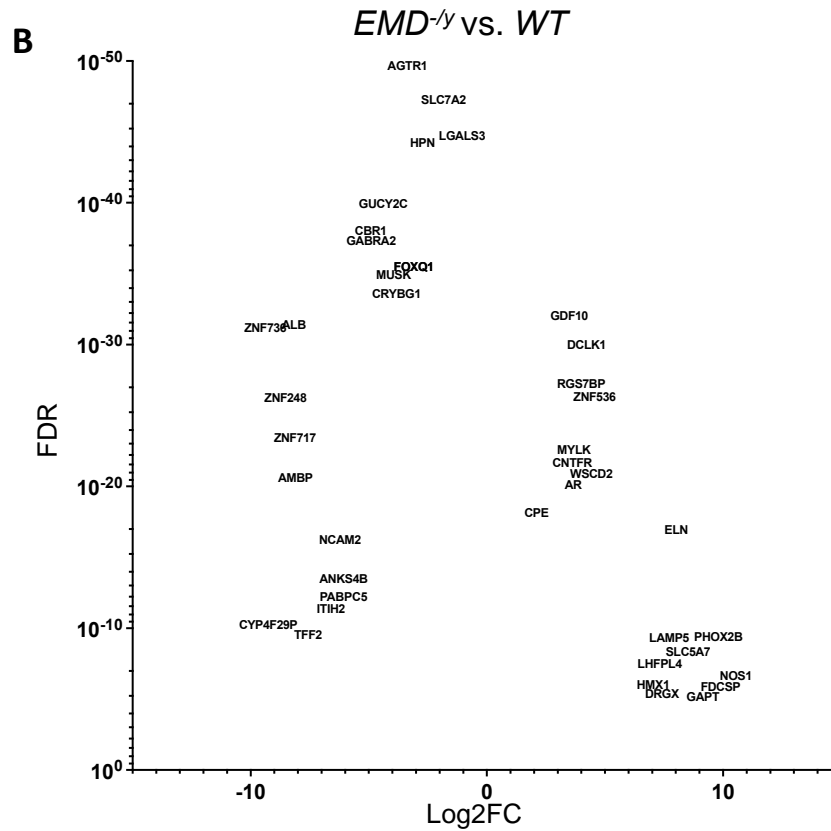
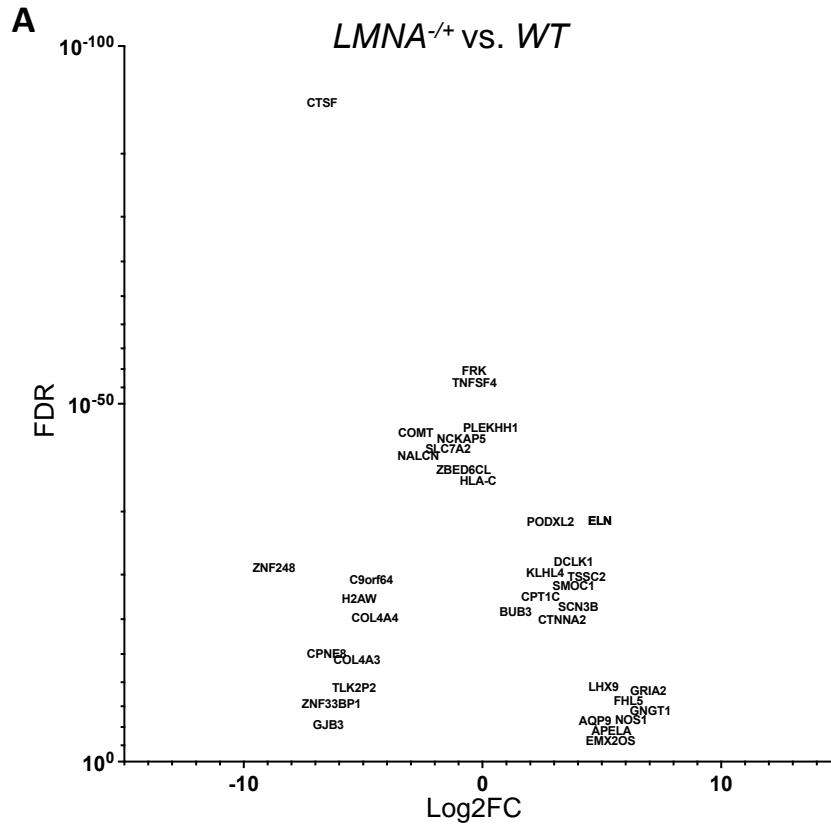


Figure 2.6: Volcano plots of differential gene expression of mutant iPSC-CMs compared to control. The average log₂ fold change (Log₂FC) of *LMNA*^{-/+} iPSC-CMs (A) and *EMD*^{-/-} iPSC-CMs (B) when compared to wildtype control iPSC-CMs, is plotted against the false discovery rate (FDR). 0.0005 was used as the cut-off for the FDR; genes represented by grey points fell short of the FDR cutoff. A log₂FC of greater than 1 or less than -1 was used to select differentially expressed genes (DEGs) for further analysis. Red points represent genes that have a log₂FC > 1, and blue points represent genes that have a log₂FC < -1. Top 10 DEGs in terms of FDR and/or Log₂FC for both downregulated and upregulated groups are labeled.

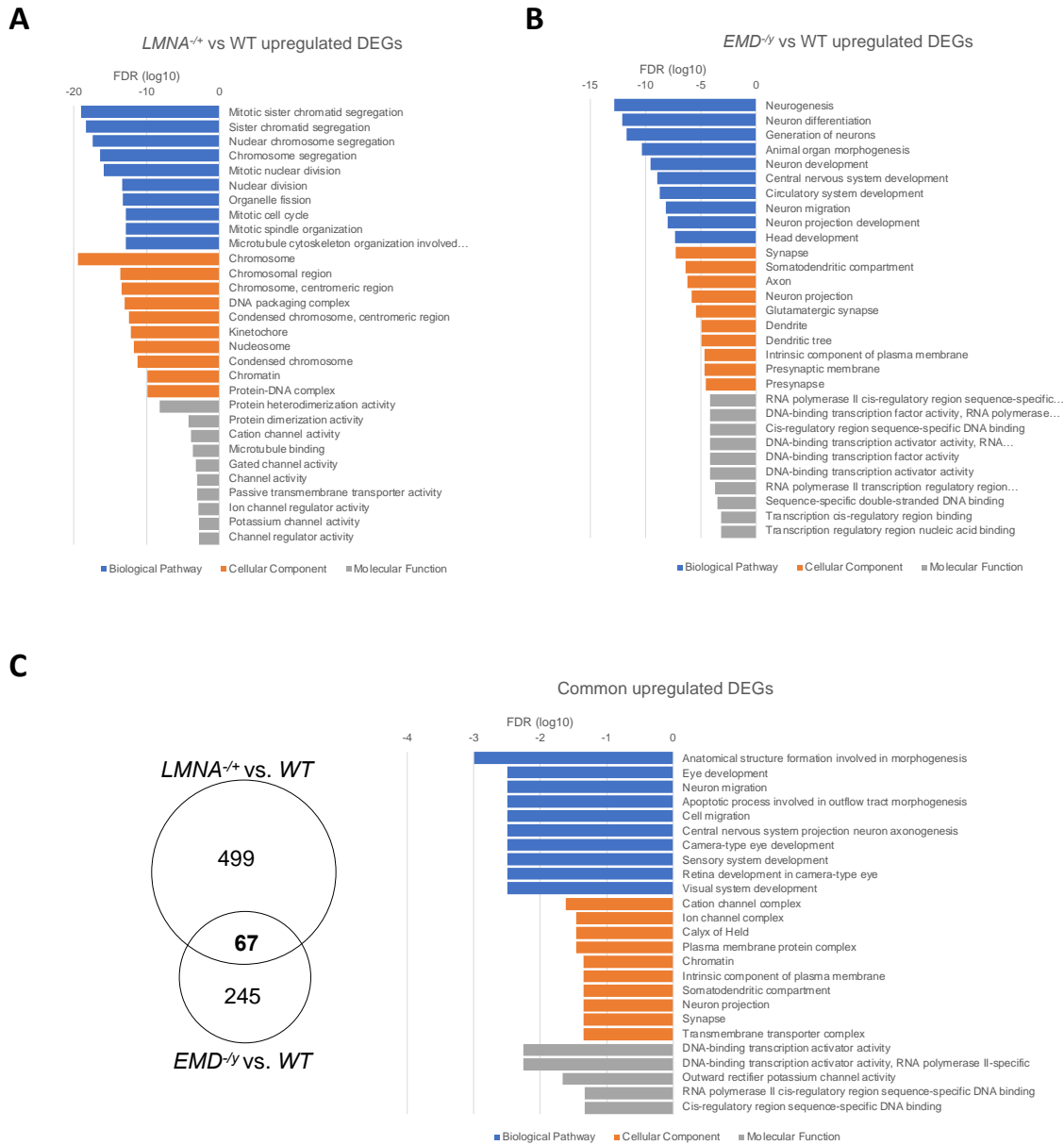


Figure 2.7 Gene Ontology (GO) enrichment analysis of upregulated DEGs in mutants. Top 10 significant (FDR<0.05) biological processes (blue), cellular components (orange), and molecular functions (grey) for (A) 566 upregulated DEGs in *LMNA*^{-/-} vs. WT, (B) 312 upregulated DEGs in *EMD*^{-/-} vs. WT, and (C) 67 upregulated DEGs shared between both mutants.

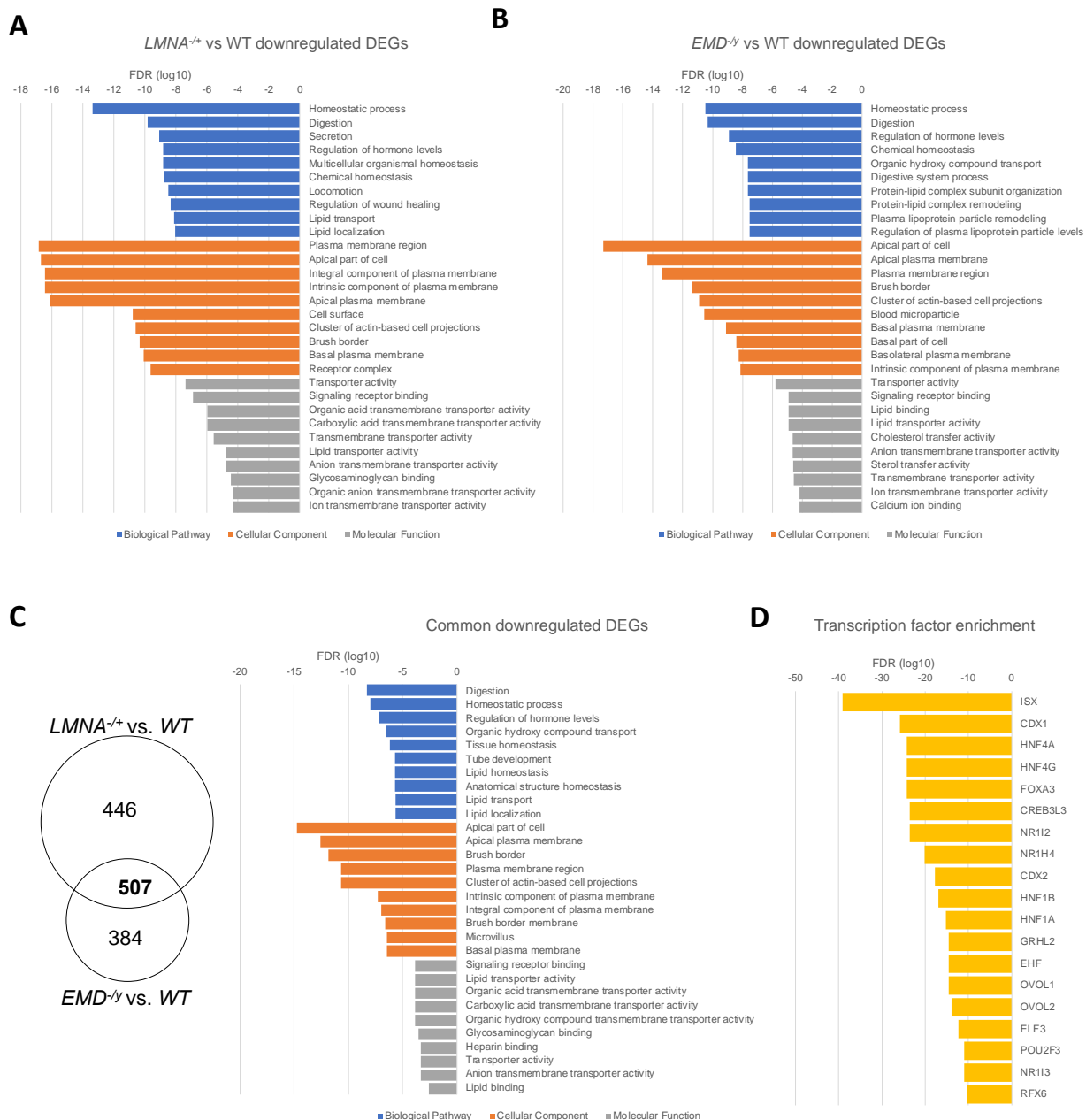


Figure 2.8 Gene Ontology (GO) enrichment analysis of downregulated DEGs in mutants. Top 10 significant (FDR<0.05) biological processes (blue), cellular components (orange), and molecular functions (grey) for (A) 952 downregulated DEGs in *LMNA*^{-/-} vs. WT, (B) 891 downregulated DEGs in *EMD*^{-/-} vs. WT, and (C) 507 downregulated DEGs shared between both mutants. (D) Transcription factor enrichment analysis result showing the top 10 predicted transcription factors of the shared 507 downregulated DEGs.

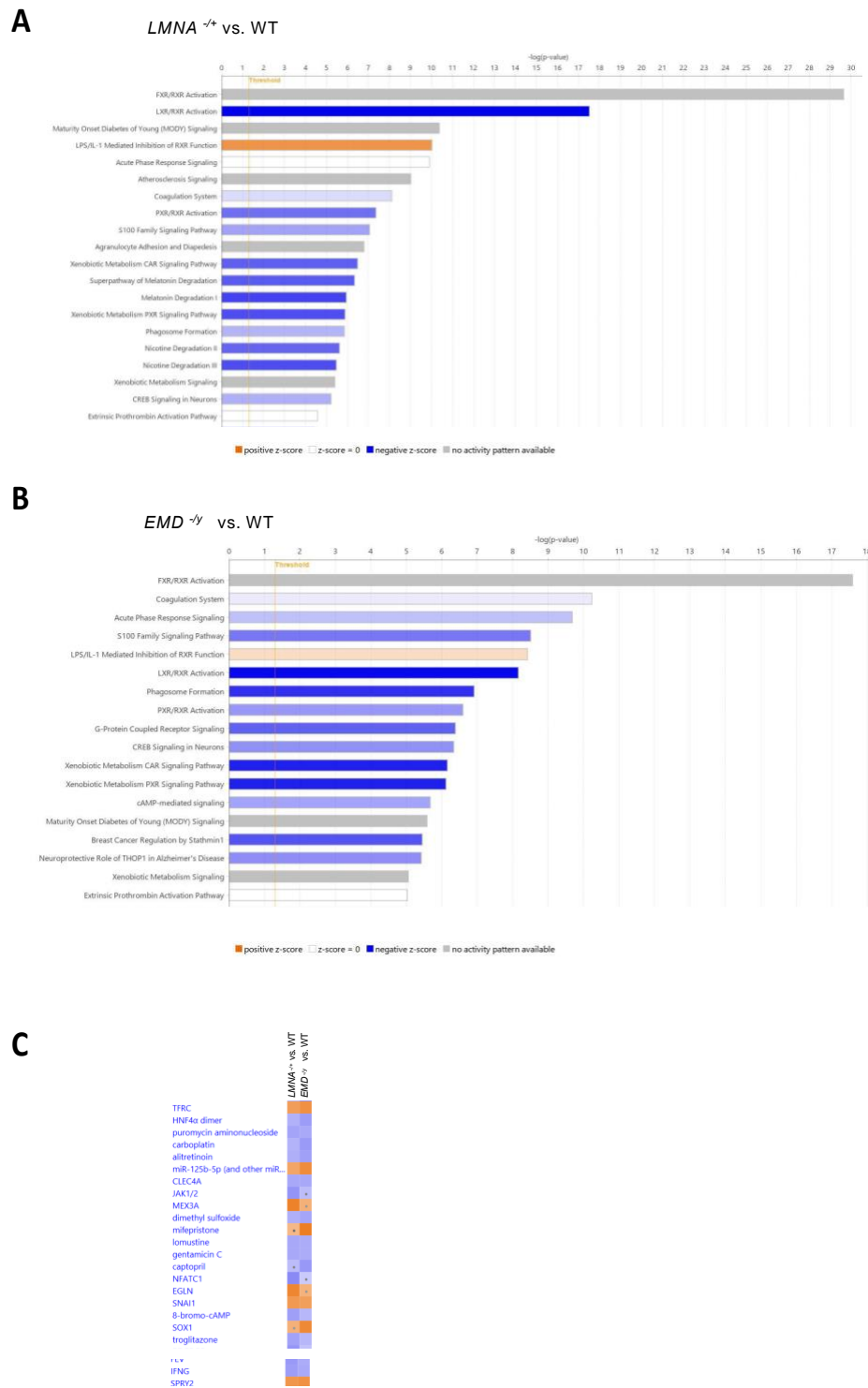


Figure 2.9: IPA analysis of DEGs identify significant downregulation in major metabolic pathways. Top 20 enriched pathways for *LMNA*^{-/-} vs. WT (A) and *EMD*^{-/-} vs. WT (B). The color

of the bar represents the z-score, a statistical measure used to assess the activation or inhibition of biological pathways based on gene expression data. Shades of blue indicate inhibition of the pathway, and shades of orange indicate activation. Grey indicates the analysis was unable to determine activation or inhibition, despite many components being enriched. (C) Top 20 upstream regulators shared between two mutants when compared to WT. Blue indicates an inhibitory effect of the pathways controlled by the indicated upstream regulator, while orange indicates an activating effect.

Proteomic analysis identifies significant alterations in proteins related to metabolism and splicing in mutant iPSC-CMs

To obtain further information on the differences between *LMNA*^{-/+} and *EMD*^{ly} iPSC-CMs when compared to WT, I performed proteomic analysis to get a better understanding of the differences. Three replicate differentiations (cTNT>85%) of each genotype were harvested and used for proteomic analysis. When compared to WT, *LMNA*^{-/+} iPSC-CMs have 803 differentially expressed proteins (DEPs) with 379 upregulated and 424 downregulated, and *EMD*^{ly} iPSC-CMs has a total of 1,861 DEPs with 738 proteins up and 1,123 down (FDR < 0.05; |log₂FC vs. WT| <0.58) (Figure 3.10).

GO enrichment analysis was performed for up and down-regulated DEPs. DEPs upregulated in *LMNA*^{-/+}, when compared to WT, were highly enriched in multiple biological processes associated with cellular respiration (Figure 2.11A). By extension, cellular components were enriched in mitochondrial components and the ER. Furthermore, molecular functions were associated with activity related to mitochondrial cellular respiration, such as electron transfer and cytochrome-c oxidase. DEPs upregulated in *EMD*^{ly} compared to WT were enriched in biological processes associated with protein transport and localization (Figure 2.11B). Cellular components were encircled for mitochondria and ER components. The molecular functions were enriched for nucleotide binding. The two mutants shared 288 upregulated DEPs. The common DEPs were enriched for lipid and general metabolism, mitochondrial organization, and protein transport (Figure 2.11C). Cellular components were enriched for ER and mitochondrial

membranes. There was slight significant enrichment in molecular functions. In summary, the lamin A/C-haploinsufficient iPSC-CMs and emerin-deficient iPSC-CMs had upregulated proteins that are associated with metabolism, specifically lipid metabolism and cellular respiration. Many of the proteins are associated with the ER or mitochondrial membranes.

DEPs downregulated in *LMNA*^{-/+} iPSC-CMs, when compared to WT, were highly enriched in RNA splicing and chromatin organization biological processes, spliceosome cellular functions, and DNA/RNA binding molecular functions (Figure 2.12A). DEPs downregulated in *EMD*^{-/-} iPSC-CMs, when compared to WT, were also highly enriched in RNA splicing biological processes (Figure 2.12B). Cellular functions were enriched for mitochondrial, ribosome, and spliceosome. The molecular functions were enriched in RNA and chromatin binding. The two mutants shared 246 downregulated DEPs, and the set was enriched for RNA splicing biological processes, spliceosome cellular components, and chromatin binding molecular functions (Figure 2.12C). In summary, proteins associated with RNA splicing were down in both lamin A/C haploinsufficient iPSC-CMs and emerin deficient iPSC-CMs when compared to WT iPSC-CMs. Emerin deficient iPSC-CMs had additional downregulated proteins associated with ribosomes.

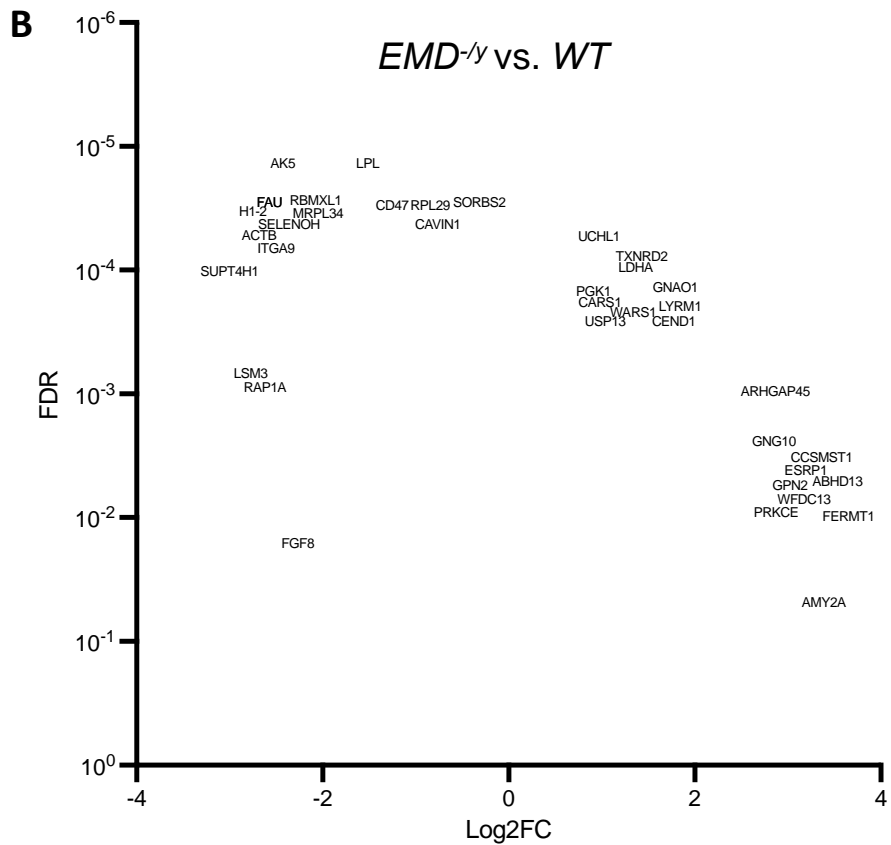
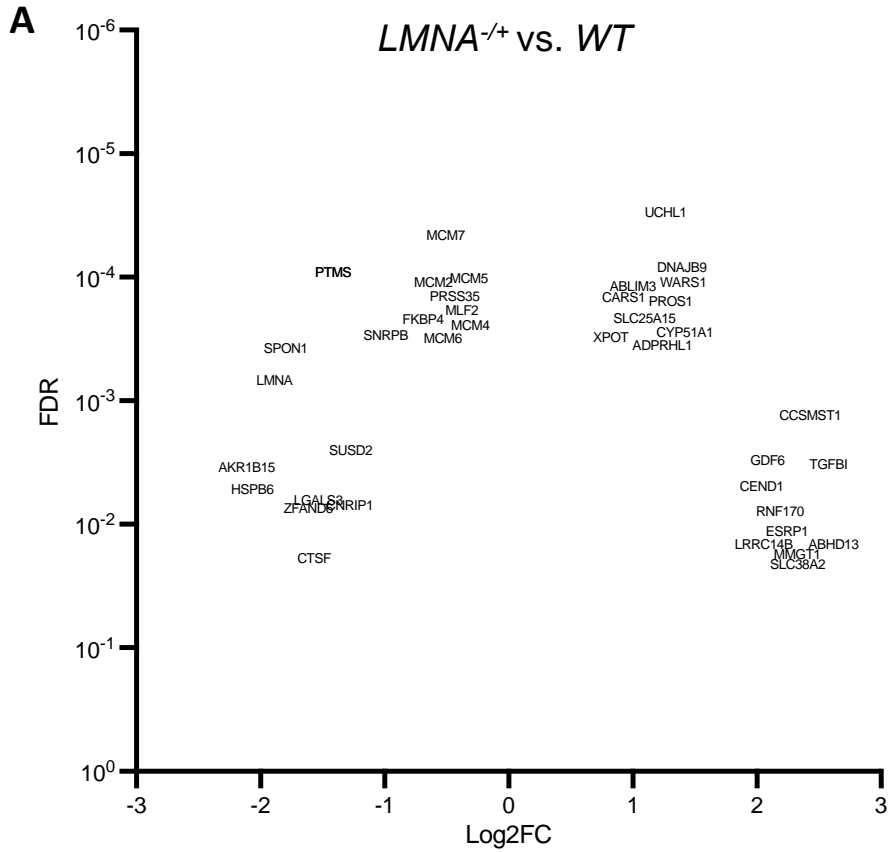


Figure 2.10: Volcano plots of differential protein expression of mutant iPSC-CMs compared to control. The average log2 fold change (Log2FC) of *LMNA*^{+/-} iPSC-CMs (A) and *EMD*^{-/-} iPSC-CMs (B) when compared to wildtype control iPSC-CMs, is plotted against the false discovery rate (FDR). 0.05 was used as the cut-off for the FDR; genes represented by grey points fell short of the FDR cutoff. A log2FC of greater than 0.58 or less than -0.58 was used to select differentially expressed proteins (DEPs) for further analysis. Red points represent genes that have a log2FC>0.58, and blue points represent genes that have a log2FC<-0.58. Top 10 DEPs in terms of FDR and Log2FC for both downregulated and upregulated groups are labeled.

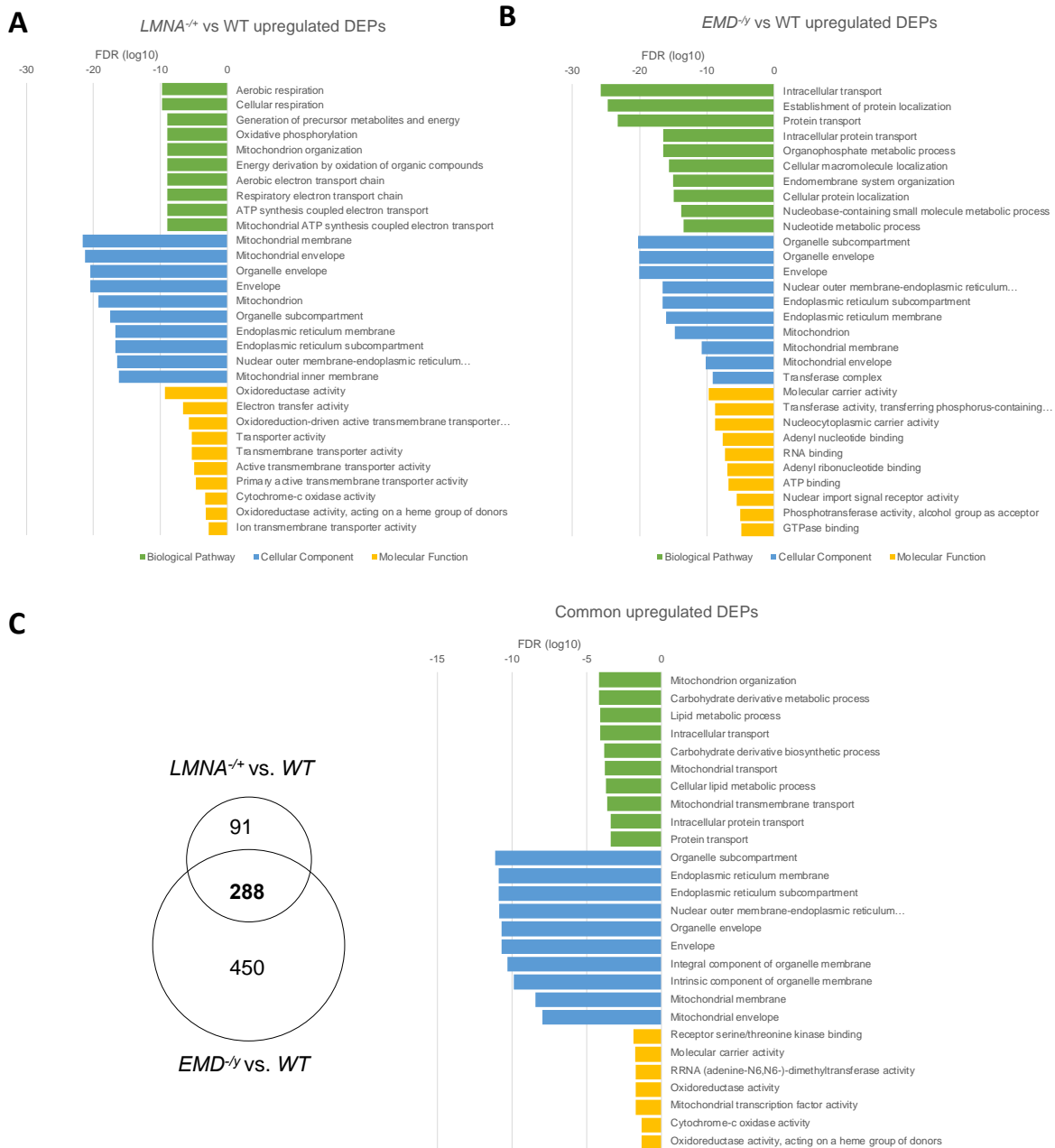


Figure 2.11: Gene Ontology (GO) enrichment analysis of upregulated DEPs in mutants. Top 10 significant (FDR<0.05) biological processes (green), cellular components (blue), and molecular functions (yellow) for (A) 379 upregulated DEPs in *LMNA*^{-/+} vs. WT, (B) 738 upregulated DEGs in *EMD*^{-/-} vs. WT, and (C) 288 upregulated DEGs shared between both mutants.

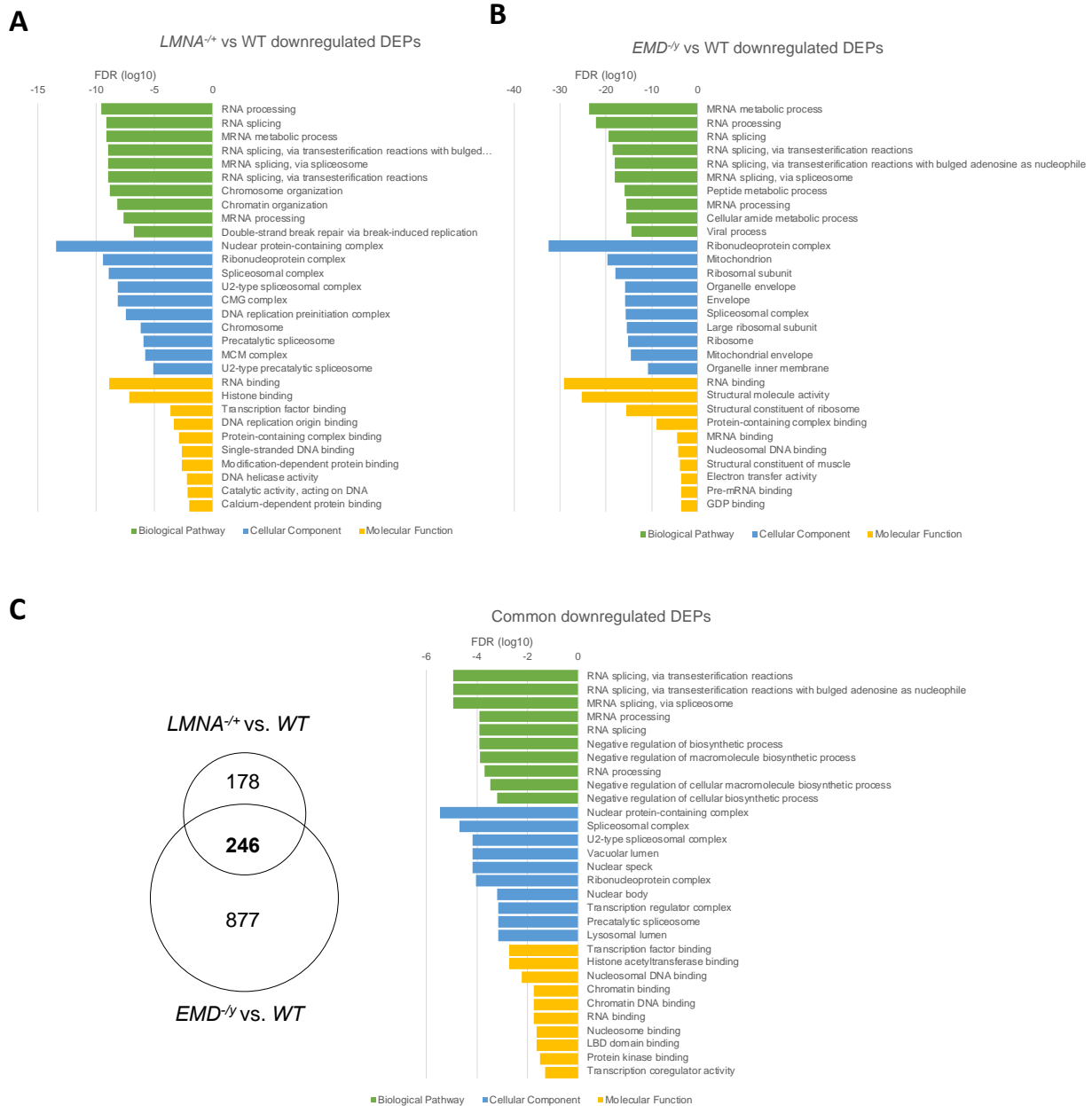


Figure 2.12: Gene Ontology (GO) enrichment analysis of downregulated DEPs in mutants. Top 10 significant (FDR<0.05) biological processes (green), cellular components (blue), and molecular functions (yellow) for (A) 424 upregulated DEPs in *LMNA*^{-/+} vs. WT, (B) 1123 upregulated DEGs in *EMD*^{-/-} vs. WT, and (C) 246 upregulated DEGs shared between both mutants.

Metabolic changes in mutant iPSC-CMs

Downregulated genes and upregulated proteins in both mutants were significantly enriched for terms that fall under the broad theme of metabolism. Therefore, I hypothesize that there would be common metabolic differences between lamin A/C haploinsufficient iPSC-CMs and emerin deficient iPSC-CMs when compared to WT iPSC-CMs. WT, *LMNA*^{+/-}, and *EMD*^{-/-} iPSC-CMs (>85% cTnT+) were harvested 30 days after the start of differentiation for untargeted metabolomic analysis. 337 metabolites were identified and differentially determined (Figure 2.13A). Hierarchical clustering shows the two mutants clustered together. Thirty metabolites were different between *LMNA*^{+/-} and WT iPSC-CMs (log₂FC 0.5, FDR<0.05) with 12 down and 18 up (Figure 2.13B). Sixty-five metabolites were found to be different between *EMD*^{-/-} and WT iPSC-CMs, with 24 down and 41 up (Figure 2.13C). Metabolite enrichment analysis was performed with the sets of significantly up and down metabolites in each comparison. Metabolites that were significantly different between *EMD*^{-/-} iPSC-CMs and WT iPSC-CMs were enriched in pathways including gluconeogenesis, galactose metabolism, glycolysis, Warburg effect, glycerolipid and sphingolipid metabolism (FDR>0.05) (Figure 2.14A). The set of metabolites that were significantly different between *LMNA*^{+/-} and WT was too small to obtain significance, however, metabolites in the categories of linoleic acid metabolism, mitochondrial electron transport chain, Warburg effect, and glycerolipid metabolism are more enriched (Figure 2.14B).

The two mutants shared 19 common differentially abundant metabolites when compared to WT, with 4 up and 15 down. One of the most significantly reduced metabolites in both mutant iPSC-CMs is lactate. Lactate, also known by its conjugate acid lactic acid, is a metabolite constantly produced from pyruvate by the enzyme lactate dehydrogenase (LDH) (Figure 2.14A). This reaction is known as anaerobic respiration, or fermentation, and it forms an important means of regenerating NAD⁺, enabling the continuation of glycolysis. Pyruvate is an

intermediate in many central metabolic processes. It is made from glucose via glycolysis, or converted to carbohydrates via gluconeogenesis, or converted to fatty acids in a reaction with acetyl-CoA. Furthermore, it is the main input for the Krebs cycle (TCA cycle).

LDH exists in 5 isoforms, and all are translational products of the *LDHA* and *LDHB* genes (Read et al., 2001). Each isoform of LDH is made up of 4 subunits of varying numbers of the A or B subunits. LDH-1 is a tetramer of all B subunits and is the most abundant in the heart. A review of transcriptomic and proteomic data shows both lamin A/C haploinsufficient and emerin deficient iPSC-CMs had down significantly lower LDHB RNA and protein (Figure 2.14B). However, the reduction in *LMNA*^{-/+} iPSC-CMs did not pass the log₂FC cutoff to be included as a DEG and the protein reduction seen in *EMD*^{-/-} iPSC-CMs did not pass the log₂FC threshold to be included as a DEP. Immunoblot shows indeed LDHB is significantly reduced in both mutants (Figure 2.14C).

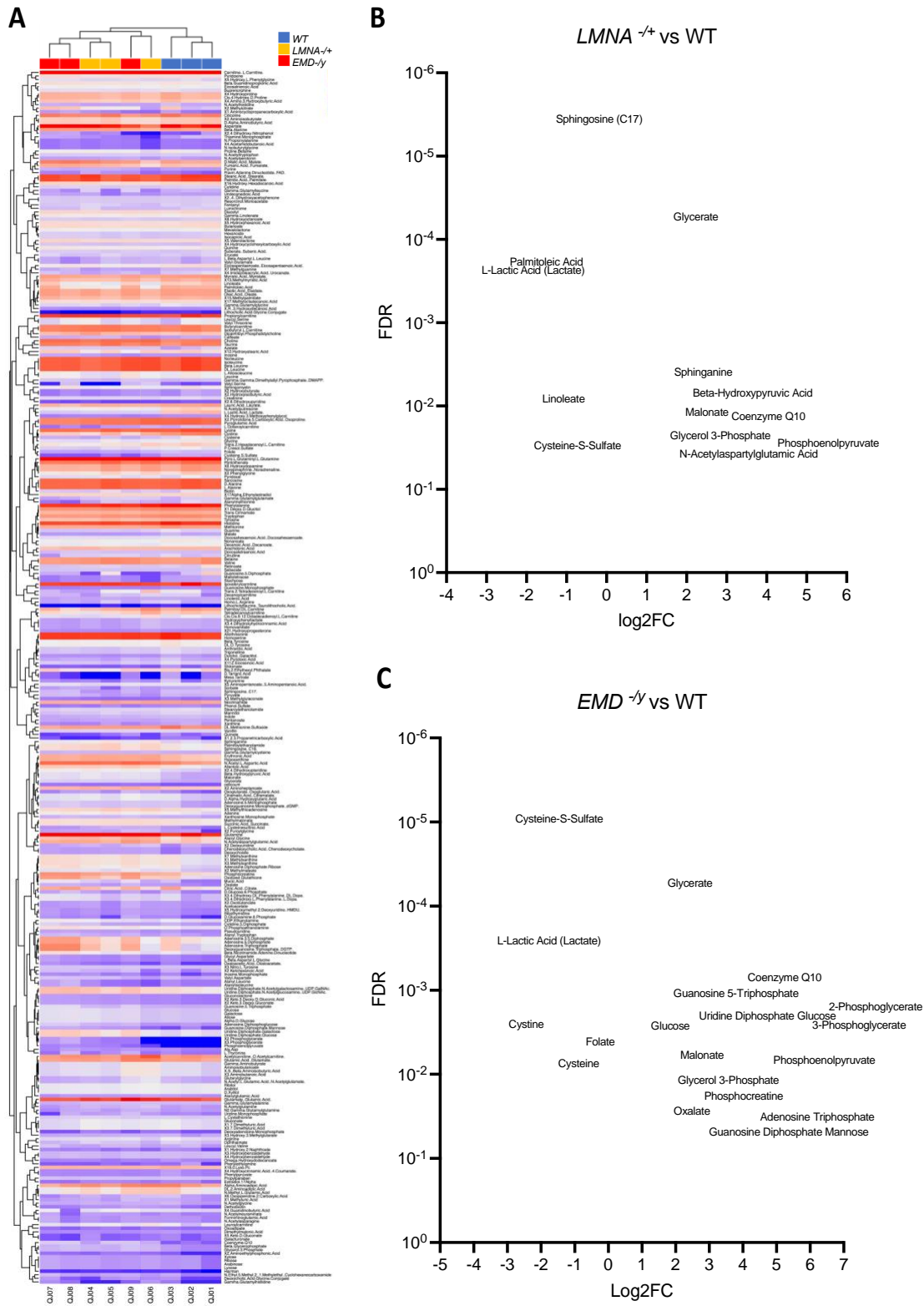


Figure 2.13: Metabolomic analysis of *LMNA*^{-/-} and *EMD*^{-/-} iPSC-CMs compared to WT shows similarities. A) Hierarchical clustering of each samples for the each of the 3 genotypes

(n=3) based on the levels of 337 metabolites measured. Volcano plots depict the log₂ fold change of metabolite abundance between (B) *LMNA*^{+/-} vs. WT, and (C) *EMD*^{-/-} vs WT, against FDR. Metabolites with significant differential abundance (FDR<0.05) in each mutant when compared to WT are represent by red if they are higher in mutant (log₂FC>0.5, and blue if they are lower in mutant (log₂FC<-0.5). Select metabolites are labeled.

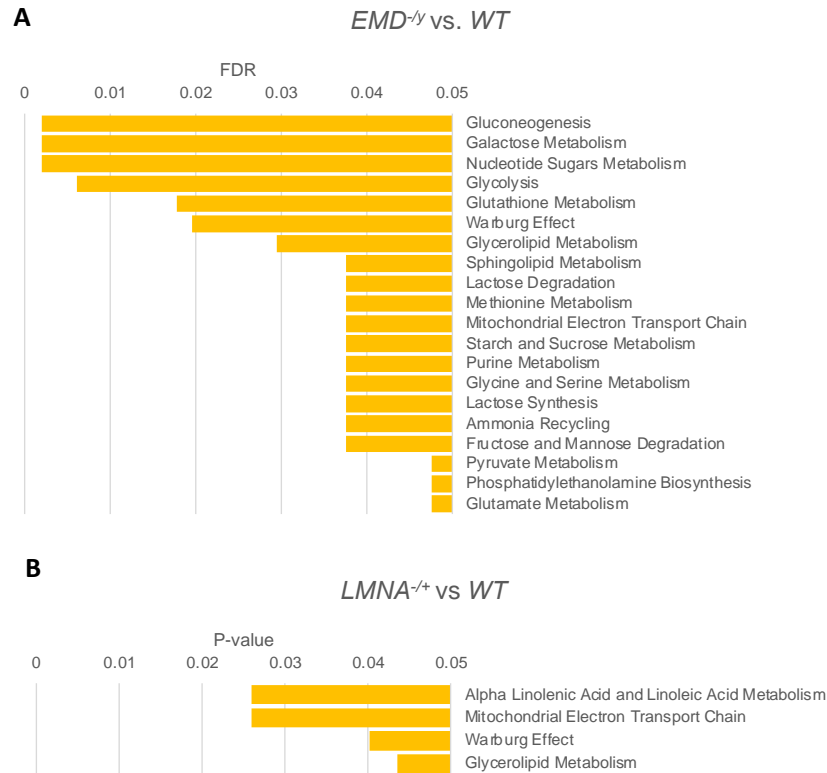


Figure 2.14: Metabolite enrichment analysis for metabolites with significant differential abundance between mutant and wildtype. A) Top 20 enriched pathways in *EMD*^{-/-} vs WT (FDR<0.05). B) Enriched pathways in *LMNA*^{+/-} vs WT, no pathways showed significant enrichment (FDR <0.05) due to small sets of metabolites with differential abundance available, figure instead shows top 4 pathways with a more lenient cutoff (P<0.05).

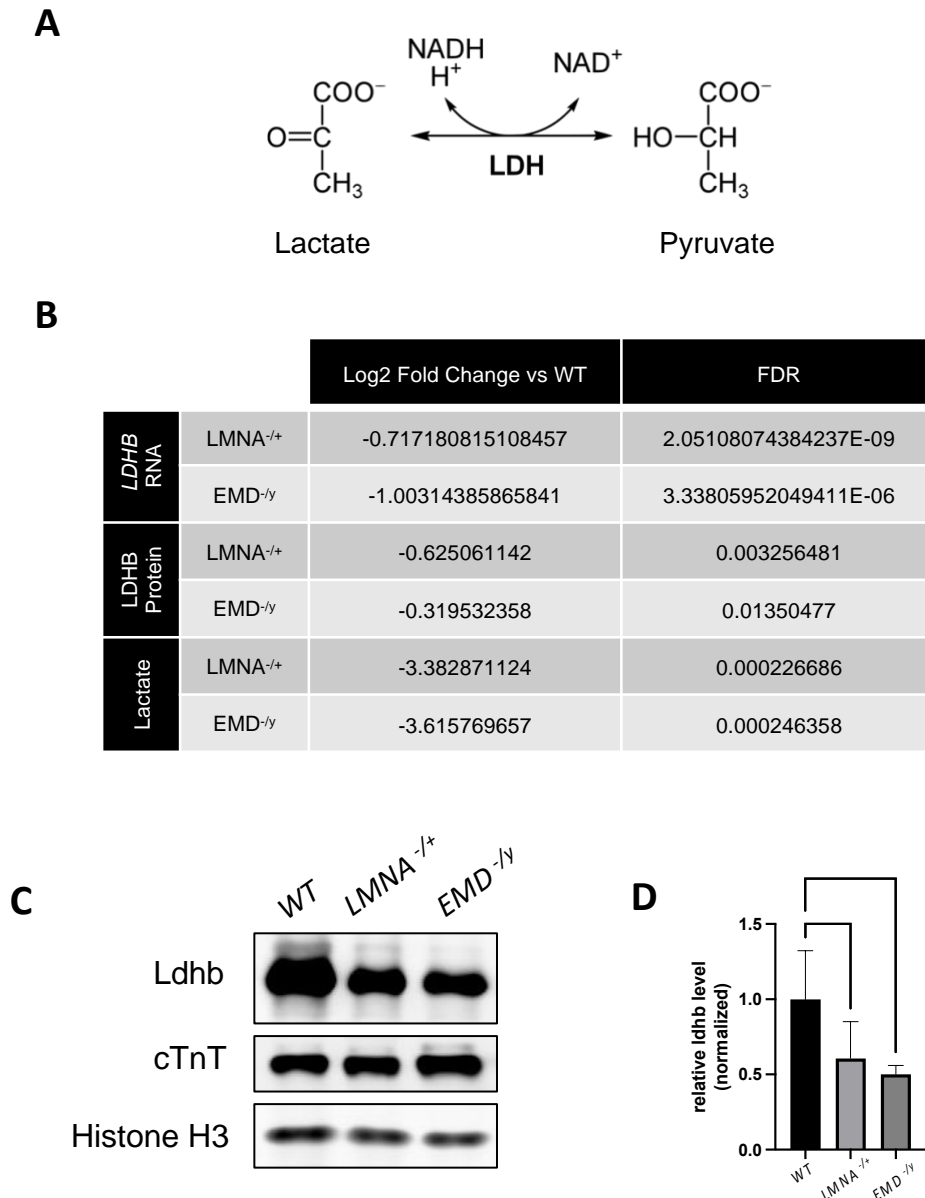


Figure 2.15: Lactate reduction in mutants and LDHB reduction. A) Illustration of the enzymatic interconversion of lactate and pyruvate, facilitated by lactate dehydrogenase (LDH) enzymatic activity. B) Log2 fold change vs. WT and False Discovery Rate (FDR) values for *LMNA*^{-/+} and *EMD*^{-/-}, derived from transcriptomics, proteomics, and metabolomics analyses. The data demonstrate a significant reduction in *LDHB* RNA, LDHB protein, and lactate levels. C) Immunoblot validating reduction of LDHB in *LMNA*^{-/+} and *EMD*^{-/-} iPSC-CMs. D) Quantification of LDHB immunoblot band intensities, with n=5 replicates. Statistical analysis conducted using a one-way ANOVA multiple comparisons test (*P < 0.05).

Discussion

Upregulated alternative fate genes related to the nervous system

In the study published in May 2021, Shah and colleagues generated two *LMNA* iPSC lines each with a patient-based mutation and found disruption in lamina-chromatin interaction and de-repression of alternative fate genes (Shah et al., 2021b). The missense mutation from patients they introduced into a control iPSC line resulted in lamin A/C haploinsufficiency. Like this study, they differentiated the iPSCs into cardiomyocytes and performed transcriptomics analysis and gene enrichment analysis. They also found genes associated with nervous system development as the top category of enriched genes (Shah et al., 2021b). Specifically, they found significant enrichment in GO biological processes including “neurogenesis”, “neuron differentiation”, “nervous system development”, and “eye development”. which all were among the top 10 enriched biological processes in the mutants of this study as well (Shah et al., 2021b). Additional consensus came from the 2019 study by Bertero and colleagues (Bertero et al., 2019). While they did not find nervous system related genes in the top GO enrichment biological process of upregulated DEGs, they noted the upregulation of a neuron specific calcium channel *CACNA1A* (Bertero et al., 2019). I did not find upregulation of *CACNA1A* in *LMNA*^{-/+} iPSC-CMs but, I found significant upregulation of another subunit of the same channel *CACNA1E* ($\log_2FC_{vsWT} = 1.62$, $FDR = 3.9E-10$).

Bertero and colleagues also studied chromosome topology with Hi-C in their mutant and control (Bertero et al., 2019). They found that chromosome compartments that were specifically dysregulated in lamin A/C haploinsufficient iPSC-CMs were highly enriched for GO biological processes related to nervous system development. Shah and colleagues performed CHIP-seq to identify chromatin regions associated with the nuclear periphery, and they found that neuronal genes had the biggest difference in nuclear periphery occupancy between control and lamin A/C haploinsufficient iPSC-CMs. The loss of peripheral occupancy correlated with an

upregulation in those genes. These two studies used different methods to arrive at the conclusion that there is major displacement of neuronal genes in *LMNA*-haploinsufficient iPSC-CMs. This is likely the mechanism behind the observation of upregulated neuronal genes in this study.

While the studies from Shah *et al.* and Bertero *et al.* only examined *LMNA* mutants, I also looked at *EMD*^{-/-} iPSC-CMs and found similar downregulation of nervous system related genes (Bertero *et al.*, 2019; Shah *et al.*, 2021b). Therefore, it is likely that the same specific chromatin compartment changes that occurred to *LMNA* haploinsufficient iPSC-CMs also occurred in *EMD*^{-/-} iPSC-CMs. While emerin interaction directly with lamin A/C and may affect chromatin changes through that interaction, it also known interacts with chromatin via BAF. Since *LMNA*^{-/+} iPSC-CMs had significantly decreased interaction between emerin and lamin A/C, I speculate that the upregulation of neuronal specific genes in emerin deficient iPSC-CMs is a result of disrupted interaction between emerin and lamin A/C. It is possible that emerin and lamin A/C synergistically interact with chromatin and that synergy can be disrupted by either lamin A/C haploinsufficiency or emerin deficiency. This emerin and lamin A/C interaction may be especially important in maintaining chromatin organization in cardiomyocytes, or cardiomyocytes are extra sensitive to the effect of the loss of chromatin organization and aberrant gene expression.

Misregulation of ion channels may contribute to the development of conduction disease that is known to precede dilated cardiomyopathy in cardiomyopathy cases. One possibility is that the downregulation of a specific cardiac sodium channel is associated with arrhythmogenic conduction defects (Salvarani *et al.*, 2019), while the previously mentioned studies suggest aberrant upregulation of neuronal specific ion channels is to blame (Bertero *et al.*, 2019; Shah *et al.*, 2021b). Among the significantly upregulated genes shared between both *Lmna*^{-/+} and *EMD*^{-/-}

iPSC-CMs are multiple neuronal associated ion channels including 3 potassium channel subunits (*KCNA2*, *KCNK2*, and *KCNQ2*) in addition to the previously mentioned *CACNA1E*.

Downregulation of lipid metabolism genes and liver, small intestine associated genes and upregulation of metabolic proteins.

It is harder to explain the enrichment analysis of downregulated genes in both *Lmna*^{-/+} and *EMD*^{-y} iPSC-CMs. The enrichment in terms associated with digestion and lipid-related biological processes, intestine related cellular components, and transported-related molecular functions suggests an overall downregulation of a group of genes expressed in the gastrointestinal system. Indeed, transcription factor enrichment analysis and IPA upstream analysis both identified transcription factors that are master regulators of genes expressed in the gastrointestinal system. One factor is HNF4A, a nuclear receptor that drives the brush border gene program in the intestines (Chen et al., 2021). *HNF4A* mutations cause a group of familial diabetes called maturity onset diabetes of the young (MODY), one of the top 10 significantly enriched IPA pathways (Chandran et al., 2020).

FXR/RXR, LXR/RXR, PXR/RXR activation pathways are overrepresented in IPA pathway analysis for both *Lmna*^{-/+} and *EMD*^{-y} iPSC-CMs compared to WT. The action of these pathways separately, and together through cross talk, controls many metabolic processes including glucose, lipid, cholesterol homeostasis (Chawla et al., 2001). These are a family of nuclear receptors that are integrators of hormonal and nutritional signals that responds by mediating changes to metabolic pathways. Liver X receptors (LXR), farnesoid X receptors (FXR), and pregnane X receptor (PXR) form heterodimers with retinoid X receptor (RXR) (Chawla et al., 2001; Keller et al., 1993). Lamin A regulates nuclear translocation of retinoic acid receptor (RAR), which heterodimerizes with RXR in the absence of their retinoid ligand and bind

the hormone responsive elements known as retinoic acid response elements (RAREs) (Swift et al., 2013). Interestingly, The *LMNA* promoter has RAREs and its expression is regulated by retinoic acids which suggests an intimate relationship between A-type lamins and retinoic acid signaling (Lebel et al., 1987; Okumura et al., 2000; Pellegrini et al., 2015; Swift et al., 2013). The interaction between the nuclear lamina and nuclear receptors is a worthy topic to investigate in the future. Retinoic acid is already being used to modulate *LMNA* expression in cellular models of laminopathies (Pellegrini et al., 2015). I speculate that the misregulation of these nuclear receptors leads to changes in the metabolic genes enriched in the DEGs, and lamin A/C and emerin may have a specific role in their regulation.

Metabolic phenotypes such as lipodystrophy and diabetes are features of certain laminopathies. MAD patients, in addition to many morphological syndromes, have clinical features of metabolic syndrome such as insulin resistance, glucose intolerance, diabetes Mellitus, and hypertriglyceridemia. Dunnigan familial partial lipodystrophy and atypical Werner syndrome also have metabolic defects associated with lipodystrophic phenotypes. There are potential links between nuclear lamina and metabolism. Conditional deletion of *Lmna* in mice liver caused steatosis and increased susceptibility to steatohepatitis.(Kwan et al., 2017). LBR is essential for cholesterol synthesis (Tsai et al., 2016). LAP1 and LAP2 disruption has been associated with altered lipid metabolism in liver (Brady et al., 2018; Shin et al., 2019). Many lipid metabolic processes are localized to the ER, and both mutants in this study had enrichment in proteins associated with the ER (Fu et al., 2012). It is unknown if the altered metabolism phenotype is a major contributor to cardiolaminopathies.

Alteration in metabolism may be a common feature between laminopathies with metabolic defects, and haploinsufficient cardiac laminopathy. The heart is a major metabolic organ and many genes associated with many of the primary metabolic organs such as liver, intestines and adipose tissues are also expressed and functionally relevant in the heart.

Examples include microsomal triglyceride transfer protein (MTTP), apolipoproteins A and B (ApoA, ApoB), lipoprotein lipase (LPL), and fatty acid synthase (FASN) (Abdalla et al., 2011; Boren et al., 1998; Klevstig et al., 2019; Nielsen et al., 1998; Yagyu et al., 2003; Zhang et al., 2023). However, these proteins are annotated in categories associated with primary metabolic organs and not cardiomyocytes, therefore it is likely the main reason that terms associated with gastrointestinal system show up in GO analysis.

There is no known association between emerin and metabolic pathways. This study finds that emerin deficient cardiomyocytes have alterations in metabolic pathways on the RNA and protein level. Furthermore, it is an overlapping feature with lamin A/C haploinsufficient cardiomyocytes. My finding suggests that further investigation of the metabolic differences in lamin A/C haploinsufficient and emerin deficient cardiomyocytes is warranted.

Reduced splicing and nuclear factors

The reduction of many proteins associated with RNA splicing in both lamin A/C haploinsufficient and emerin deficient iPSC-CMs is particularly notable. For most eukaryotic genes, the initial transcribed RNA must be processed before it becomes a mature mRNA that can be translated by the ribosome. One of the steps in the processing is RNA splicing. The spliceosome, a complex of small ribonucleoproteins (snRNPS) catalyzes a series of reactions that removes the introns and splice back together the exons. Splicing occurs in the nucleus during or immediately after transcription, and like transcription, is spatially regulated in the nucleus. The nucleoplasm contains morphological and function sub-compartments associated with various nuclear activities.

Nuclear speckles, also called interchromatin granule clusters or splicing factor compartments, were discovered to be sites where splicing factors concentrate (Spector et al.,

1991; Spector et al., 1983). These subcompartments are interspersed in the nucleoplasm forming 20-50 spots in the human interphase nucleus (Galganski et al., 2017). Nuclear speckles are membrane-less compartments that are highly dynamic structures while remaining distinct from the rest of the nucleoplasm through phase separation (Phair and Misteli, 2000; Saitoh et al., 2004). They are not thought to be the regions where splicing occurs, but rather a location storage and assembly of splicing factors. Sites of RNA polymerase II transcription occur in close proximity to the nuclear speckles and inhibition of transcription leads to accumulations of proteins and associated enlargement of nuclear speckles, which returns to normal size upon removal of the block (Galganski et al., 2017).

Nuclear lamins such as lamin B1 is primarily at the nuclear periphery and associates with heterochromatin, A-type lamins are additionally also localized in the nucleoplasm, where it interacts with the transcriptionally active euchromatin (Gesson et al., 2016). This soluble pool of lamin A/C in the nucleoplasm interacts with a non-membrane-bound LAP2 isoform, LAP2alpha (Dechat et al., 2010). Selective deletion of the LAP2alpha isoform leads to loss of nucleoplasmic lamin A/C, and causes various tissue specific phenotypes that includes delayed skeletal muscle differentiation and impaired heart function (Gotic et al., 2010a; Gotic et al., 2010b; Naetar et al., 2008). Nucleoplasmic lamins are thought to provide structural support for many functions of the nuclear interior (Hozák et al., 1995). A-type lamins have been observed to colocalize with nuclear speckles (Jagatheesan et al., 1999; Kumaran et al., 2002).

Emerin has been shown to be associated with proteins that has roles in splicing (Holaska and Wilson, 2007). *In vitro*, it interacts with the splicing associated factor YT521-B (Wilkinson et al., 2003). Rare EDMD-causing mutations in *EMD* generating amino acid substitutions affect emerin binding to BCLAF1, which is involved in multiple biological processes including splicing (Haraguchi et al., 2004). Not much more is known regarding the links between emerin and RNA splicing.

Disruption in RNA splicing has been implicated in human disease pathogenesis. In myotonic dystrophy type 1, abnormal expansion of CTG repeats in the *DMPK* gene leads to trapping of proteins that results in misregulation of alternative splicing (Thomas et al., 2017). One of the trapped proteins is MBNL1, a regulator of alternative splicing (Wang et al., 2012). Disruption in specific splicing regulators can cause defects in the heart. Dilated cardiomyopathy can be induced by ablation of the splicing factor SC35 in heart tissues (Ding et al., 2004). Mutations in the splicing regulator RBM20 has been identified as the cause of 2-3% of sporadic and familial dilated cardiomyopathy cases (Kayvanpour et al., 2017; Li et al., 2010; Refaat et al., 2012). It has been identified as a regulator of *TTN* splicing (Guo et al., 2012). *TTN* has 364 exons, the most exons in a single gene for mammals, and it codes for titin, a sarcomeric structural protein (Gigli et al., 2016). *TTN* undergoes extensive alternative splicing to encode for different isoforms, and the variable isoform expression have been relevant in cardiac diseases (Gigli et al., 2016).

The functional consequence of the observed reduction of splicing related proteins in lamin A/C haploinsufficient and emerin deficient iPSC-CMs is unknown. Given the relationship between splicing and striated muscle disorders, and the potential interaction of lamin A/C and regulators of splicing in the nucleoplasm, dysregulation of splicing in cardiomyopathy models is worth investigating.

Nuclear lamina and metabolism

Proteomic and metabolomic data suggests lamin A/C haploinsufficient iPSC-CMs and emerin deficient iPSC-CMs have major alterations in metabolic pathways such as glycolysis and fatty acid metabolism (Figure 2.16). The heart is one of the highest energy-consuming organs of the body. In adult fasting mammals, 60-80% of cardiac energy metabolism depends on fatty acid oxidation, and the remaining is supplied by glucose, lactate, and ketones (Neely et al., 1972). The heart's energy substrate preferences changes throughout life as well as under physiological and pathological stress. This metabolic flexibility gives the heart adaptability

across environmental conditions. The heart energy source shifts during development as well. The fetal heart functions in a low oxygen environment and mainly use glucose and lactate for ATP generation. After birth, increased cardiac work load, higher blood oxygen levels, and circulating fatty acid from milk drives the metabolic shift towards fatty acid oxidation while lactate oxidation and glycolysis decrease significantly.

The heart is often referred as an omnivore, in the sense that it will use any substrate available for energy (Ritterhoff and Tian, 2017). This metabolic flexibility allows the heart to maintain its output amid variations in nutrient availability. For example, loss of lipoprotein lipase led to increase glucose metabolism in mouse hearts (Augustus et al., 2006). During stress conditions such as ischemia and hypertrophy, the heart increases consumption of glucose (Sambandam et al., 2002; Stanley et al., 1997). Additionally, while lactate is traditionally thought of as a by-product in ischemic and hypoxic tissues, it may represent an important fuel for cardiomyocytes during exercise or stress (Dong et al., 2021b). In hearts of diabetic rats, the rate of lactate efflux was greater than lactate uptake (Chatham et al. 2001). Decreased lactate uptake might be related to the increased cytosolic NADH/NAD⁺ ratio in the diabetic state (Chatham et al., 1999; Puckett and Reddy, 1979).

A subset of laminopathies have dominant metabolic features. Lipodystrophy is a common phenotype across Dunnigan-type familial partial lipodystrophy, Hutchinson-Gilford progeria syndrome, manibuloacral dysplasia, and atypical Werner syndrome (Guillín-Amarelle et al., 2018). In these laminopathies, lipodystrophy is characterized by systemic or partial fat atrophy, and often accompanying lipodystrophy is insulin resistance, diabetes mellitus, dyslipidemia, and fatty liver (Guillín-Amarelle et al., 2018). Furthermore, *LMNB1* duplications causes adult-onset demyelinating leukodystrophy, where reduced lipid synthesis leads to decrease myelin synthesis (Padiath and Fu, 2010). Polymorphisms in *LMNB2* encoding lamin B2 is also associated with predisposition to acquired partial lipodystrophy (Hegele et al., 2006).

Non-pathogenic *LMNA* alleles have been found to be associated with dyslipidemia and insulin resistance (Murase et al., 2002). It is suggested that the association between *LMNA* mutations and metabolic syndrome signifies that metabolic alterations represent a mild form of laminopathy (Dutour et al., 2011). Common *LMNA* variations have been found to be associated with a higher prevalence of type 2 diabetes (Wegner et al., 2007). In skeletal muscle, Dunnigan's familial partial lipodystrophy and limb girdle muscular dystrophy type 1b patients with *LMNA* mutations showed imbalance between lipid oxidation and oxidative glucose metabolism (Boschmann et al., 2010). The NAD⁺ salvage pathway was altered in the hearts of mouse and humans carrying cardiomyopathy-causing *LMNA* mutation, and supplementation of nicotinamide riboside, a natural NAD⁺ precursor, led to an improvement in the cardiac phenotype of *Lmna* mutant mice (Vignier et al., 2018). As the heart is such a metabolically demanding organ, if lamin A/C can affect metabolism in other affected cell types, it is very likely it can affect the metabolism of cardiomyocytes.

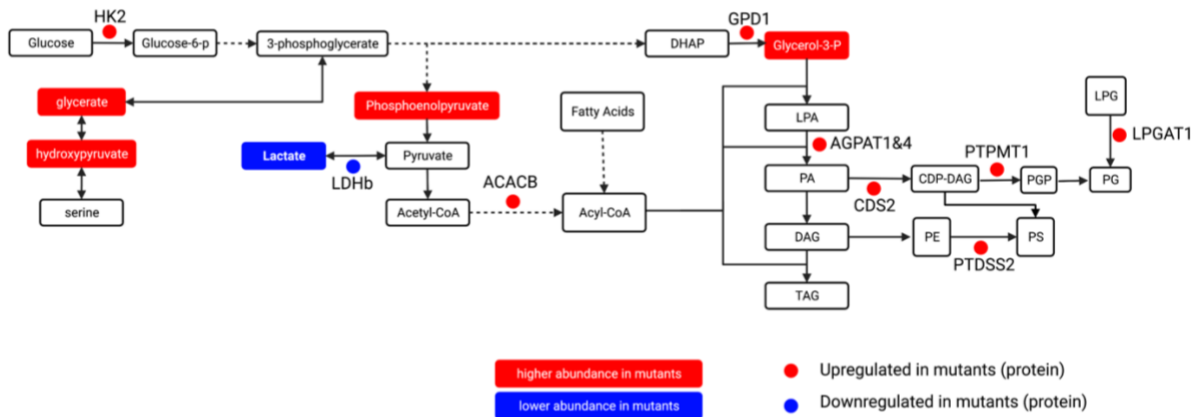


Figure 2.16: Major metabolic processes altered in iPSC-CMs with mutations associated with EDMD. Lamin A/C haploinsufficient and emerin deficient iPSC-CMs share many DEPs when compared to WT iPSC-CMs. Many of their overlapping DEPs are enzymes that participate in key metabolic processes. Furthermore, the two mutants share common changes in metabolite abundance. Simplified metabolic processes are shown; all labeled enzymes are either significantly upregulated (red dot) or downregulated (blue dot) in both mutants when compared to wildtype on the protein level. Select relevant metabolites with either significantly

higher abundance (red box) or lower abundance (blue box) in both mutants when compared to WT are highlighted.

Multi-omic loss of *LDHB* and reduction of lactate

LDHB is one of the few genes where its transcripts are significantly changed in both *LMNA*^{-/+} and *EMD*^{-/-} iPSC-CMs compared to WT iPSC-CMs. Its protein product is changed significantly in both mutants compared to WT as well. Furthermore, the product of its enzymatic reaction, lactate, is also significantly different in when both mutants are compared to WT. In a 2015 published study analyzing lamin A/C chromatin binding, the authors performed chromatin immunoprecipitation using on chromatin from HeLa cells and targeted lamin A/C for immunoprecipitation (Lund et al., 2015). They found lamin A/C associated with roughly ¼ of the genome in HeLa cells, one of the genes in a lamin A/C associated chromatin domain they used as an example was *LDHB* (Lund et al., 2015). Therefore, while a protein-protein interaction may cause alterations in *LDHB*, it is likely that loss of it began at the transcript level.

LHD catalyzes the interconversion of pyruvate and lactate, however only lactate reduction is detected my metabolomics data. A direct consequence of the reduction of lactate would be an increase in pyruvate. Since pyruvate is a central metabolite in many metabolic processes, it is difficult to deduce the cause and effect of the observed lower lactate levels. Increases in phosphoenolpyruvate, glycerate, and glycerol-3-phosphate were detected in both lamin A/C haploinsufficient iPSC-CMs and emerin deficient iPSC-CMs, which are all downstream metabolites of biochemical processes requiring pyruvate.

An enrichment in gluconeogenesis was observed in emerin deficient iPSC-CMs when compared to WT, with metabolites associated with this pathway at higher concentrations in the mutant. These cells were maintained in a maturation medium with low glucose and high lipids. Therefore, gluconeogenesis may have been upregulated to compensate for the lack of alternative energy sources.

The lower LDHB levels and reduced lactate can have many effects. Primarily there will be a reduction in energy production. The conversion of pyruvate to lactate by LDH is a crucial step in anaerobic glycolysis. While the heart mostly relies on aerobic metabolism, during high workload or stress, or under hypoxic conditions, the heart will rely on anaerobic glycolysis. A study of EDMD patient iPSC-CMs with *LMNA* mutation found them to be more susceptible to hypoxia-induced stress than WT (Shah et al., 2019). In certain pathological conditions, such as heart failure or myocardial infarction, there can be a shift towards increased reliance on anaerobic glycolysis due to impaired oxygen delivery or mitochondrial dysfunction (Dong et al., 2021a).

LDH plays a role in maintaining cellular redox balance by participating in the NADH/NAD⁺ shuttle system (Keith Chenault and Whitesides, 1989). The conversion of lactate to pyruvate by LDH involves the transfer of hydrogen ions and electrons. Reduced LDH levels can disrupt this redox balance and impair cellular metabolism, potentially leading to oxidative stress and cellular dysfunction (Lin et al., 2022).

Reduced lactate can have physiological consequences beyond its role as an energy source. Lactate can influence the generation and scavenging of reactive oxygen species (ROS), contributing to the regulation of oxidative stress in cells (Tauffenberger et al., 2019). Lactate can enhance the activity of antioxidant enzymes, such as superoxide dismutase (SOD) and catalase, which help neutralize ROS (Gabriel-Costa et al., 2015). Its role in modulating responses to oxidative stress highlights its importance in maintaining cellular redox balance and protecting against oxidative damage.

Overlapping effects of lamin A/C haploinsufficiency and emerin deficiency in iPSC-CMs

The original hypothesis of this study was that lamin A/C haploinsufficient iPSC-CMs and emerin deficient iPSC-CMs will exhibit similar biological differences. Although originally patients with *LMNA* mutation and *EMD* mutation were thought to have the same disease, the discovery of laminopathies and the variable phenotypic expression of the same mutation complicated that idea. Here I showed that on the same genetic background in human iPSC-CM model that the two mutations do have the same biological effect in the aberrant upregulation of nervous system and developmental genes, dysregulation of metabolic genes and proteins, reduction of splicing proteins, and a reduction of lactate.

Weakness

Although hiPSC-CMs has advantageous over existing animal models, batch-to-batch variation in differentiation cannot always be fully controlled. While replicates can take account of the variation that arrives with different batches of differentiation, the ideal validation would be confirmation the results in a set of isogenic lines with a different genetic background. The study presented in this chapter is exploratory and lacked functional validation. Human iPSC-CMs have an immature phenotype compared to adult cardiomyocytes, hence they can be only thought of as a human cardiomyocyte-like biological system and not true replication of human tissue or a disease state. iPSC-CMs are cultured in a simplified *in vitro* environment that lacks the complexity and cues present in the native cardiac tissue microenvironment, and by extension shows limited disease specific phenotypes. Caution must therefore be taken in translating any findings from lamin A/C haploinsufficient and emerin deficient iPSC-CMs to disease.

Chapter 3: Investigating the Requirement of Lamin A/C in Mature Striated Muscle

Introduction

Mouse models of cardiolaminopathies

As previously stated, a large set of mutations in *LMNA* have been shown to cause disease with a range of phenotypes and tissues affected. In virtually all the laminopathies (except Charcot-Marie-Tooth syndrome type 2 and anecdotal cases of compound heterozygous EDMD), the patients retain one normal *LMNA* allele (De Sandre-Giovannoli et al., 2002; Raffaele Di Barletta et al., 2000). However, most of the mouse models used to understand laminopathies are homozygous *Lmna* mutants. A homozygous *LMNA* nonsense mutation has been reported in a newborn that resulted in the complete loss of A-type lamins, and the resulting phenotype was lethal (van Engelen et al., 2005).

The first *Lmna* mutant mouse model was a deletion of exon 8 to 11, resulting in the knockout of both lamin A and C (Sullivan et al., 1999). These homozygous mice develop to term with no overt abnormalities; however, postnatal growth is severely retarded, and they die at around 4 to 8 weeks (Sullivan et al., 1999). Other notable phenotypes include reduced stores of white fat and cardiac arrhythmia (Sullivan et al., 1999). Despite the wide use of this mouse model, it was later discovered that the deletion allele still enabled the expression of a truncated prelamin A protein of 54 kDa, which was encoded by exons 1-7 and 12 (Jahn et al. 2012; Kim et al, 2023). Wolf et al. suggested that the truncated prelamin A likely acts in a dominant negative fashion because heterozygous mice have apoptotic cell death of cells of the atrial ventricular node and enhanced induced arrhythmogenicity, albeit with normal left ventricular function, 4 weeks after birth (Wolf et al., 2008). While this model was informative, the potential dominant negative mechanism complicates the understanding of the role of lamin A/C.

Another *Lmna* germline knockout mouse line was created using gene trap (GT) technology, where a reporter containing gene trap cassette was introduced into the upstream sequence of exon 2 (Kubben et al., 2011). However, this line allows the expression of the N-terminal 118 amino acids as a fusion with the reporter protein. The reporter was detected as early as embryonic day 11 in organs including the heart and liver (Kubben et al., 2011). The *Lmna*^{GT^{-/-}} mice develop to term with no overt abnormalities, however severe growth delay occurs starting at 7 days postnatal and they die 16-19 days after birth (Kubben et al., 2011). No notable phenotype was observed in the heterozygous mice (Kubben et al., 2011). Hearts of the *Lmna*^{GT^{-/-}} mice were hypertrophic, which worsened with age, with no signs of fibrosis. However, the hearts did not show enlarged cardiac chambers or thinning of cardiac walls. Skeletal muscles were hypotrophic but were not disorganized or dystrophic. The mice were hypoglycemic and increasingly catabolic compared to WT. The cardiac and skeletal muscle phenotypes did not recapitulate human AD-EDMD.

Subsequently, a mouse line with conditional deletion *Lmna* allele using Cre-lox technology was generated, with loxP sites flanking exon 2 (Kim and Zheng, 2013). The co-expression of globally expressed Cre resulted in a germline deletion of *Lmna*. Similar to the *Lmna*^{GT^{-/-}} mice, homozygous knockout of *Lmna* in this line, induced by crossing to a generalized Cre expressing line, were normal at birth, then exhibited severe postnatal defects, then die at 16-18 days after birth (Kim and Zheng, 2013). Their defects include growth retardation and skeletal muscle defect that was originally noted (Kim and Zheng, 2013). Another conditional mutant mouse with exons 10 and 11 of *Lmna* flanked by loxP sites dies at approximately 2-3 weeks of age after generalized deletion of the gene (Wang et al., 2015).

Several mouse models have been generated with missense mutations of *Lmna* found in human patients. Few notable ones are described here. *LMNA* with H222P mutation causes AD-EDMD in humans. Mice homozygous in the corresponding *Lmna* mutation develop with skeletal

and cardiac phenotypes mimicking the human disease (Arimura et al., 2005). These mice develop progressive ventricular dilatation, thinning of the ventricular walls, and heart failure, as well as skeletal muscular dystrophy (Arimura et al., 2005). Male mice develop symptoms earlier than female mice with male *Lmna*^{H222P/H222P} mice dying between 4 and 9 months and female littermates dying between 7 and 13 months of age. The differences between the sexes were shown to depend on sex hormone levels; knocking down androgen receptors improved the survival of males, while testosterone worsened the phenotype of females (Arimura et al., 2013). The *LMNA* N195K mutation causes dilated cardiomyopathy with severe arrhythmia in humans. Mice homozygous for the missense mutation are born normal and began to fall behind WT in weight gain starting at 4 weeks but are otherwise apparently healthy until a rapid decline and death at 12-14 weeks after birth (Mounkes et al., 2005). Homozygous males die before females. Cardiac chamber dilatation, along with thinning of the ventricular walls is observed, but there is no skeletal muscle phenotypes (Mounkes et al., 2005). Episodes of severe bradycardia and conduction defects were present, which may have caused death (Mounkes et al., 2005). Another notable model is mice expressing a lamin A/C variant with an internal single amino acid deletion (*Lmna*^{ΔK32/ΔK32}), found in severe EDMD or congenital muscular dystrophy patients. Homozygous mice with the variant have growth retardation and cardiac defects and do not survive past three weeks of age (Bertrand et al., 2012). In this model, severe metabolic deficiencies were noted and attributed to the repression of SREBF-1 (Bertrand et al., 2012). While H222P and N195K heterozygous mice were comparable to their WT siblings, *Lmna*ΔK32 heterozygous mice progressively developed dilated cardiomyopathy and died between 35 to 70 weeks of age (Arimura et al., 2005; Bertrand et al., 2012; Mounkes et al., 2005).

In addition to knockout or missense mutation models, mouse models that partially alter features of A-type lamins offer more clues. To model progeria, mice that express a non-farnesylated prelamin A only were generated (Davies et al., 2010). These mice exhibited dilated

left ventricles, decreased left ventricular ejection fraction and mild to moderate cardiac fibrosis (Davies et al., 2010). Mice engineered to exclusively express mature lamin A exhibited a normal, healthy state without any observable phenotype (Coffinier et al., 2010). Analysis of fibroblasts derived from these mice showed nuclear blebbing but nuclear stiffness was comparable to WT (Coffinier et al., 2010). On the other hand, mice that only express lamin C were also comparable with WT (Fong et al., 2006). Cultured primary fibroblast from these mice only had the notable difference of increased nuclear strain in response to mechanical stress (Fong et al., 2006).

EMD knockout mouse model

Emerin mutant mice were generated through the deletion of most of exon 6 of *Emd*, which encodes for the transmembrane domain of Emerin protein. These emerin-deficient mice had normal lifespan and body weight and showed no pathological differences in skeletal and cardiac muscles compared to control from 3 to 127 weeks of age (Ozawa et al., 2006). The only noted differences observed: 1) rotarod test showed motor impairment deficit in the knockouts, and 2) electrocardiography showed mild prolongation of atrioventricular conduction time in emerin-lacking male mice older than 40 weeks of age (Ozawa et al., 2006). Another group also generated emerin null mice and also found lack of notable difference between the mice lacking emerin and WT (Melcon et al., 2006). They did, however, find that emerin null mice had deficits in muscle regeneration and highlighted the role of Rb and E2F (Melcon et al., 2006). The lack of obvious phenotype of emerin-null mice has left a gap in the understanding of laminopathies.

Mouse models of other nuclear lamina proteins

A lamin B1 deletion mice line was generated using gene trap technology (Vergnes et al., 2004). Homozygous *Lmnb1* gene-trap mice did not survive beyond a few minutes postnatal, which may have been caused by respiratory failure (Vergnes et al., 2004). Additionally the *Lmnb1*^{GT-/-} mice have defects in bone. The severe phenotype of these mice is in contrasts to the

Lmna knockouts which survive at least 2 weeks after birth, suggesting that lamin B1 has more broad tissue requirements.

A mouse line was generated allowing conditional knockout of LAP1 in striated muscle (Shin et al., 2013). Mice homozygous depletion of LAP1 in striated muscle had a median survival of 150 days post-natal with none surviving past 211 days. Skeletal muscle of these mice showed classic phenotypes of muscular dystrophy such as dystrophic myofibers and central myonuclei. These mice also had mild phenotypes in the heart with increased presence of interstitial fibrosis. However lethality is not due to the heart as a cardiomyocyte specific knockout of LAP1 had normal lifespan (Shin et al., 2014).

Gap in understanding

In mice, cardiac defects are often the cause of lethality of A-type lamin deletions or mutations, while deletions in other nuclear lamina proteins such as lamin B1 and LAP1 did not seem to negatively affect the heart as much as other tissues. This makes mice a great model organism to study the requirement of lamin A/C in the heart. Unfortunately, the lack of phenotypes in mice with emerin knockout suggests the mouse heart does not fully replicate the biomolecular conditions of cardiomyopathy. The mice may have compensatory factors that protect its heart from cardiac disruptions caused by loss of emerin, possibly a larger amount of the interacting protein LAP1 in striated muscle (Shin et al., 2013).

Mouse models that existed at the commencement of this study were observing the net effect of knocking down A-type lamins in all cell types. While death was often attributed to cardiac deficits, is it not clear at which step of mouse cardiomyogenesis lamin A/C is most consequential. Given the role of lamin A/C in differentiation, and the nuclear lamina involvement in signaling, transcription, and chromatin regulation, it is important to understand the details of lamin A/C involvement in the heart.

Mouse cardiomyogenesis

The basic anatomical features of the postnatal heart in humans and mice are very similar at comparable developmental stages (Krishnan et al., 2014; Wessels and Sedmera, 2003). Mouse cardiac development has been comprehensively characterized (Krishnan et al., 2014; Vuillemin and Pexieder, 1989a; Vuillemin and Pexieder, 1989b). The first major morphogenic event in cardiac development occurs around embryonic day 9, when the cardiac loop is formed (Krishnan et al., 2014). Prior to the formation of the cardiac loop, cardiac progenitors originated from the splanchnic mesoderm differentiate into cardiomyocytes by assembling the contractile machinery of the sarcomeres at around embryonic day 7 (Tyser et al., 2016). These cardiomyocytes are in a linear tube-like structure, which later folds to form the cardiac loop, where the first heartbeat is observed. However, contracting cardiomyocytes with regular calcium transients are found before the formation of the linear heart tube, although these calcium-dependent contractions are not synchronized (Tyser et al., 2016). By embryonic day 15, all major cardiac structures are formed with subsequent development dedicated to myocardial compaction and valve refinement (Krishnan et al., 2014).

At birth, expansion of the lung leads to dramatic changes in circulation and blood pressure resulting in increased cardiac workload and an altered metabolic environment (Talman et al., 2018). Maternal milk supplies crucial lipids that provides the condition for the alteration in metabolism, where the heart switches from anaerobic glycolysis, the main source of energy in the embryonic heart, to mitochondrial fatty acid β -oxidation (Lopaschuk and Jaswal, 2010; Paredes et al., 2023). The significant shifts in cardiomyocyte energy metabolism are linked to mitochondrial changes. Fetal-type mitochondria undergo mitophagy and are substituted with mature adult-type mitochondria through a Parkin-dependent process, enabling an enhanced ATP production (Gong et al., 2015). This heightened oxidative metabolism leads to increased production of ROS, triggering a DNA damage response that is thought to contribute to

cardiomyocyte cell cycle arrest (Lopaschuk and Jaswal, 2010; Puente et al., 2014). This shift from carbohydrates to fatty acids as the main source of ATP is reflected in the proteome of the heart; key proteins that regulate anaerobic metabolism were downregulated after birth and key proteins related to fatty acid metabolism and oxidative phosphorylation were upregulated (Talman et al., 2018).

Postnatal maturation of the mouse heart is divided into three stages: hyperplasia until postnatal day 4, rapid hypertrophy between days 5 and 15, and slow hypertrophy after day 15 (Leu et al., 2001). During hyperplasia, the mass of the heart increases from replicating cardiomyocytes, while the volume of the cardiomyocytes remains relatively constant. Subsequently, in hypertrophy, the growth of the heart is contributed by the increase in the cardiomyocyte cell volume (Leu et al., 2001). It has been found that the neonatal mouse's heart has the capacity to regenerate itself after injury until day 7 postnatal age (Porrello et al., 2011). This regenerative capacity was shown after resection of the heart apex in newborn mice, as well as in a model of myocardial infarction (Haubner et al., 2012; Porrello et al., 2011). This occurs through the proliferation of existing cardiomyocytes with minimal hypertrophy or fibrosis, and normal systolic function (Porrello et al., 2011).

Results

Lamin A/C knockout in striated muscle highlights heart

Given all the functions of A-type lamins in the cell, and nuclear lamina, and the various requirement of those functions during cardiomyogenesis, it is important to dissect the specific functions of A-type lamins. A mature cardiomyocyte will have different requirements for the nuclear lamina than a rapidly dividing cardiomyocyte precursor. To investigate the role of lamin A/C in striated muscles, I first examined the effect of A-type lamin deletion in cardiomyocytes.

I crossed the *Lmna*^{flox/flox} mouse line to an MCK-Cre mouse line. The expression of Cre recombinase is driven by the muscle creatine kinase promoter (MCK), which is normally expressed at the later stages of skeletal and cardiac myocyte differentiation and detectable by embryonic day 17 (Beedle et al., 2012; Brüning et al., 1998). However, MCK expression can be detected as early as embryonic day 9, in the midst of cardiac morphogenesis (Han et al., 2015). At the P0 cross to generated F1 mice that will have the genotype MCK-Cre+; *Lmna*^{flox/flox}, death occurred in the litter starting at 3 weeks. Upon genotyping, it became apparent that the mice with the genotype MCK-Cre +; *Lmna*^{flox/flox} were dying starting at day 23 postnatal, with none surviving past day 35 (Figure 3.1A). There were no differences between male and female mouse survival rates (Figure 3.1B). Closer tracking of the weaning mice showed that the homozygous mice were at similar bodyweights at 2 weeks postnatal, however at 3 weeks their body weights were trending lower than their littermates (Figure 3.1C).

Mouse hearts were collected at 3 weeks postnatal age for histological analysis. Histology of hearts of MCK-Cre+; *Lmna*^{flox/flox} mice shows thinning of the ventricular wall, and enlargement of the ventricular chamber (Figure 3.2). At the cardiomyocyte level, cardiac myofibers are thinner (Figure 3.2). Slight increase in interstitial fibrosis is seen in trichrome staining (Figure 3.3). MCK also drives expression in skeletal muscle. Histology of the skeletal muscle (tibialis anterior) does not exhibit any clear morphological differences between knockdown and control (Figure 3.4).

All mice were confirmed to have correct recombination at the intended flox site with primers from original paper that generated the *Lmna* floxed mice (Kim and Zheng, 2013). Despite the clear phenotype, no significant protein decrease can be detected at 3 weeks postnatal. There was no detectable protein reduction on immunoblotting of heart or muscle despite at the point of failure and significant increase in fibrosis (Figure 3.5A). These samples contained not only cardiomyocytes or skeletal myocytes but also many other cell types.

However, when I analyzed another mouse line using the identical MCK-Cre, but with the alleles encoding LAP1 floxed. This mouse was previously characterized by Dr. Ji-Yeon Shin in 2014 (Shin et al., 2014). MCK-Cre; *Lap1*^{flox/flox} mice exhibited significant increase in cardiac fibrosis and clear protein reduction was detected from whole heart lysates (Figure 3.5B). Therefore, despite lack or a dramatic detectable reduction in protein levels, genetic knockdown of A-type lamins in striated muscles caused death, likely due to dilated cardiomyopathy and heart failure.

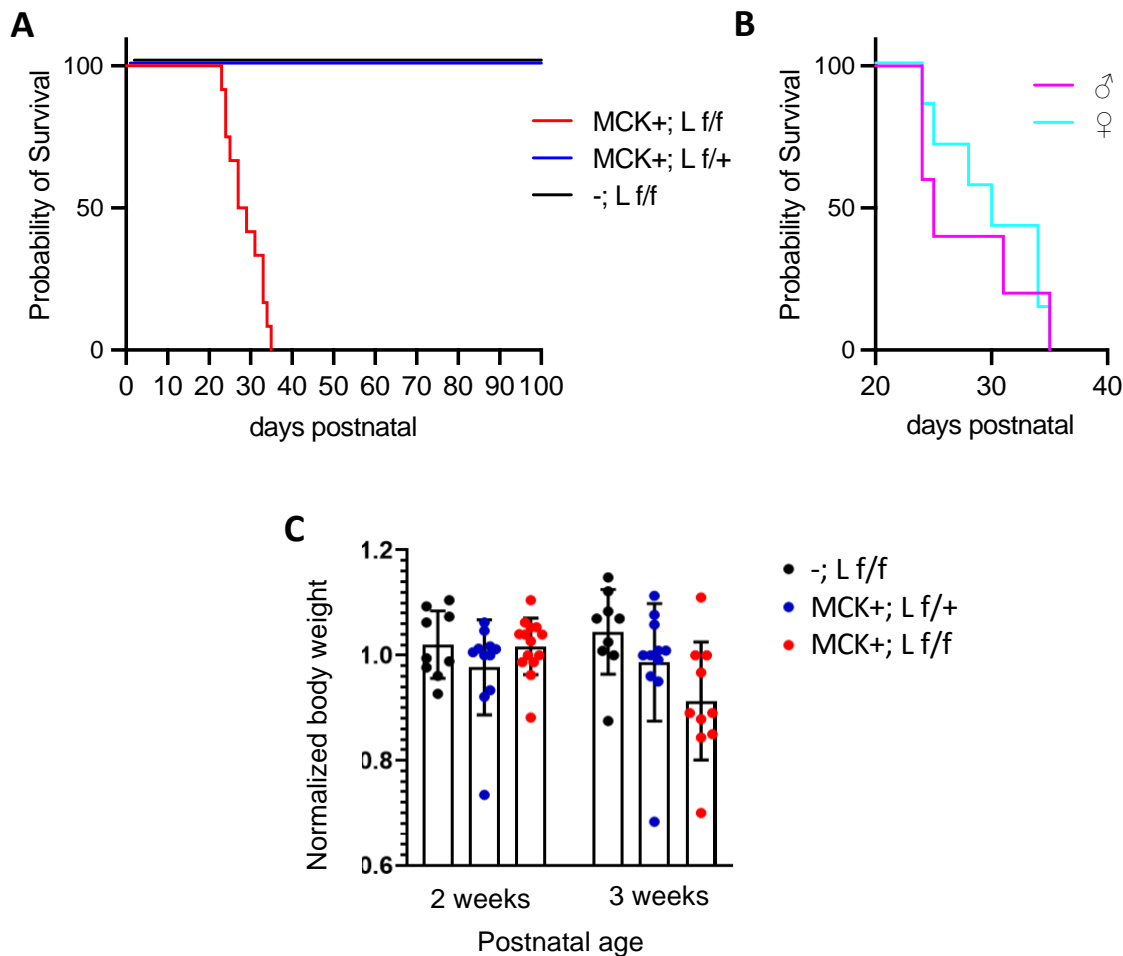


Figure 3.1: MCK-Cre; *Lmna*^{flox/flox} has normal development but deteriorates rapidly and dies 3-4 weeks postnatal. (A) Kaplan-Meier survival curves for MCK-Cre; *Lmna*^{flox/flox} (“MCK+; L f/f”; n=12), littermate control *Lmna*^{flox/flox} (“-; L f/f”; n=10), heterozygous knockout MCK+; *Lmna*^{flox/flox} as Cre+ control (“MCK+; L f/+”; n=12). For MCK-Cre; *Lmna*^{flox/flox}, first death occurred at 23 days post-natal, none survived past 31 days postnatal, Median survival for is 28 days post-natal. (B) Male and female mice have the same survival curves. (C) No significant difference in body weight between 3 groups, Mean body weight ± SD, body weight normalized between each litter.

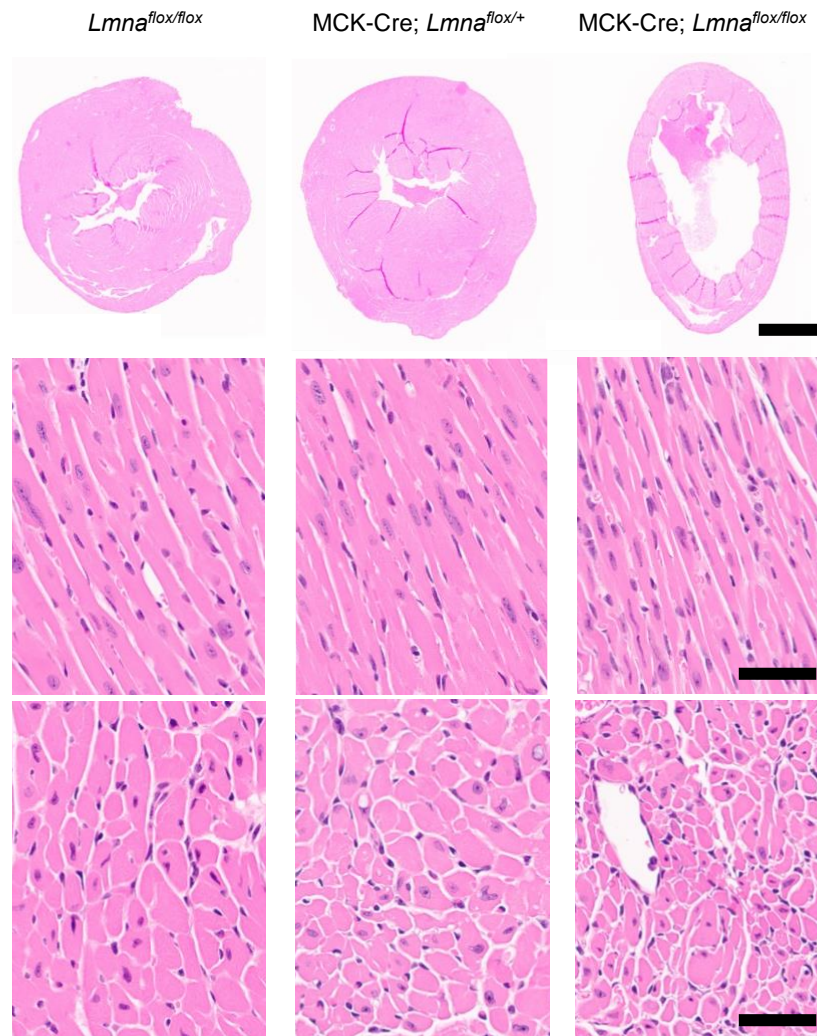


Figure 3.2: MCK-Cre; *Lmna*^{flox/flox} heart exhibit ventricular dilation and dystrophic cardiac myocytes. (top row) Representative hematoxylin and eosin stained heart cross sections from 2.5 week old MCK-Cre; *Lmna*^{flox/flox} mouse shows thinning of the ventricle walls and dilatation of the ventricle chamber compared with littermate control *Lmna*^{flox/flox} and heterozygous knockdown MCK-Cre; *Lmna*^{flox/+} as Cre+ control. 4 mice of each genotype were analyzed. Scale bar: 1 mm. B) Zoomed in area of longitudinal fibers. Scale bar: 50 μ M. (bottom row) zoomed in area of transverse fibers. Scale bar: 50 μ M.

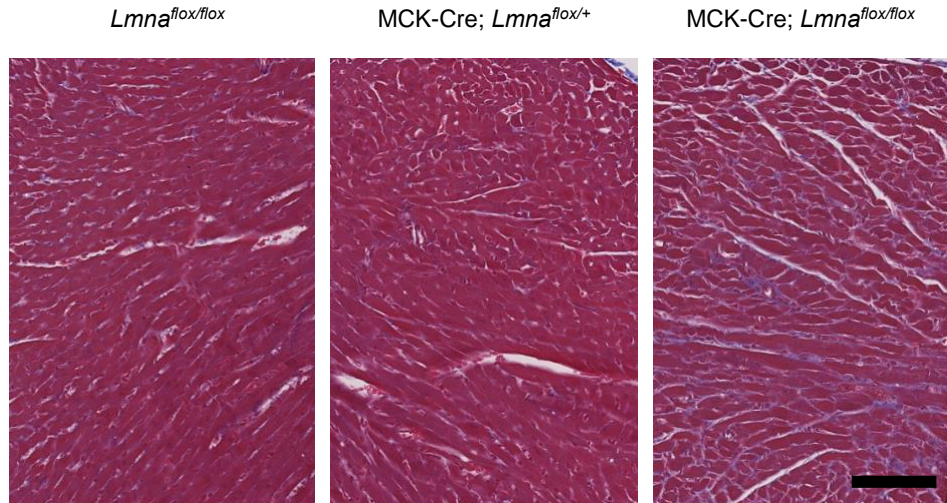


Figure 3.3: increased interstitial fibrosis in MCK-Cre; *Lmna*^{flox/flox} mice. Representative trichrome stained sections of heart from 2.5 week old mice. MCK-Cre; *Lmna*^{flox/flox} mice presents increased fibrosis (blue stain) between the cardiac myofibers, compared to littermate control *Lmna*^{flox/flox}, and heterozygous knockout MCK-Cre; *Lmna*^{flox/+} as Cre positive control. 4 mice were analyzed per genotype. Scale bar: 100 μ M.

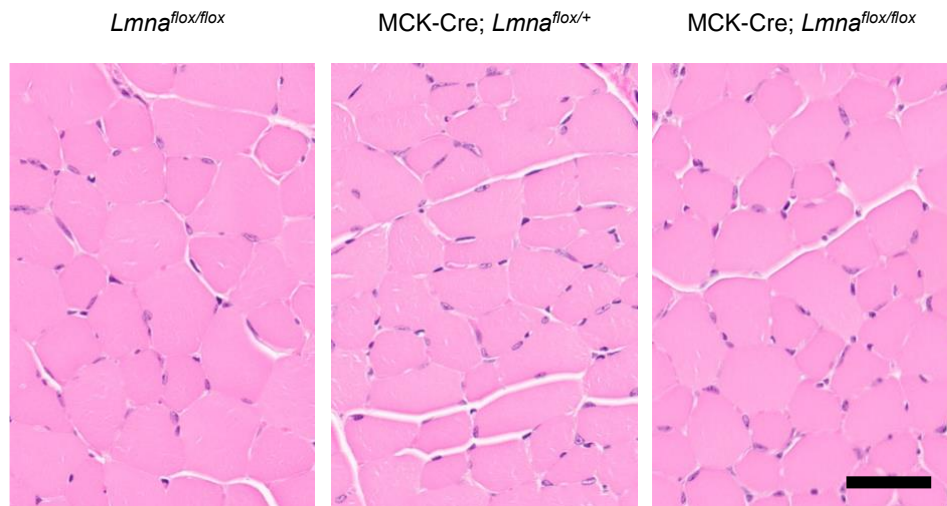


Figure 3.4: MCK-Cre; *LMNA*^{flox/flox} mice exhibit no differences in skeletal muscle fiber morphology. Representative hematoxylin and eosin stained tibialis anterior cross sections from 2.5 week old MCK-Cre; *Lmna*^{flox/flox} mice shows no observable differences compared to littermate control *Lmna*^{flox/flox} mouse and heterozygous knockdown MCK-Cre; *Lmna*^{flox/+} mice as Cre+ control. 4 mice of each genotype were analyzed. Scale bar: 50 μ M.

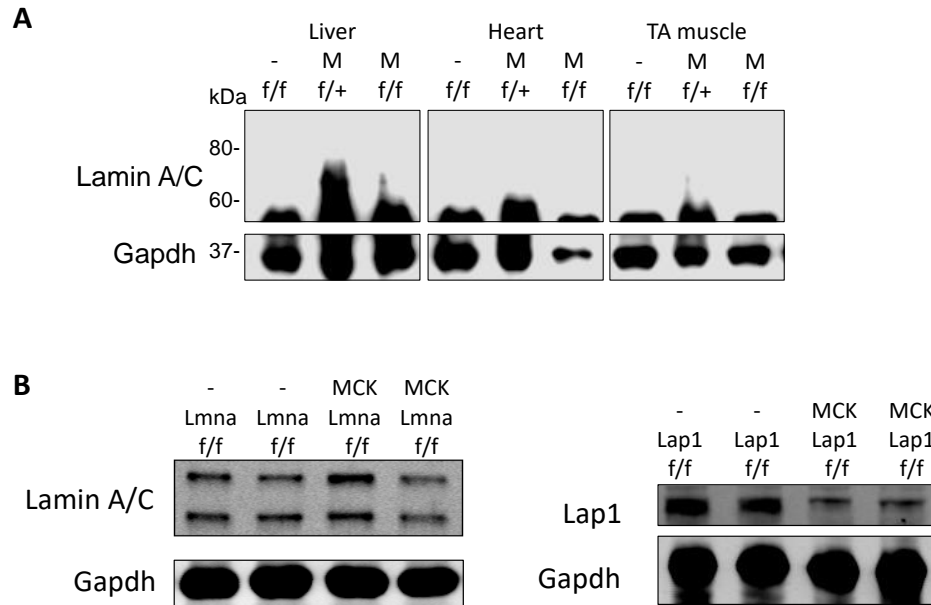


Figure 3.5: Undetectable reduction in Lamin A/C protein in skeletal and cardiac muscle. (A) Protein extracts from liver, heart and tibialis anterior muscle from 2.5 week old MCK-Cre; *Lmna*^{flox/flox} (M, f/f) and littermate control *Lmna*^{flox/flox} (-, f/f) and heterozygous knockdown MCK-Cre; *Lmna*^{flox/+} (M, f/+) as Cre+ control were separated by SDS-polyacrylamide gel electrophoresis and immunoblotted for lamin A/C and Gapdh. 8 animals were analyzed. (B) MCK-Cre induced knockdown is detectable on immunoblot of heart tissue lysate as seen with MCK-Cre; *Lap1*^{flox/flox} (MCK Lap1 f/f), however it is not obviously detectable with MCK-Cre; *Lmna*^{flox/flox}.

Induction of Lamin A/C knockdown in adult cardiac muscle causes immediate fibrotic change and death 3 weeks post induction

While the MCK driven knockout of *Lmna* induced genetic recombination and knockout at differentiated cardiomyocytes, embryonic and early postnatal mice heart have specific developmental requirements and properties. To investigate the requirement of A-type lamins in mature adult heart, I used an inducible MerCreMer (MCM) driven by the alpha myosin heavy chain (MHC) promoter which will express only in mature cardiomyocytes. Injection of tamoxifen will lead to recombination of the *Lmna* gene leading to its knockdown with temporal control.

MHC-MCM; *Lmna*^{flox/+} mice were obtained by crossing homozygous MHC-MCM mice with *LMNA*^{flox/flox} mice. MHC-MCM; *Lmna*^{flox/+} mice were then crossed with *Lmna*^{flox/flox} to generate

all experimental and control mice in the same litter. Genomic recombination was induced by tamoxifen injection, which led to recombination in all cells that express MHC-MCM, namely cardiomyocytes. Ten-week old mice were injected with tamoxifen to induce cardiomyocyte-specific knockdown of *Lmna*.

Administration of tamoxifen for 5 consecutive days at 100 mg/kg to induce the homozygous knockout of *Lmna* in MHC-MCM; *Lmna*^{flox/flox} mice caused lethality starting from day 21 post induction, with no mice surviving past 37 days post induction (Figure 3.6). Both groups of littermate controls, *Lmna*^{flox/flox} and MHC-MCM; *Lmna*^{flox/+} mice that were treated with tamoxifen were not affected. Mice heart collected at 2.5 weeks post tamoxifen administration for histological analysis. Histology of hearts of MHC-MCM; *Lmna*^{flox/flox} mice shows thinning of the ventricle wall, and enlargement of the ventricular chamber (Figure 3.7). At the cardiomyocyte level, cardiac myofibers are thinner (Figure 3.7). Increase in interstitial fibrosis seen in trichrome staining (Figure 3.8).

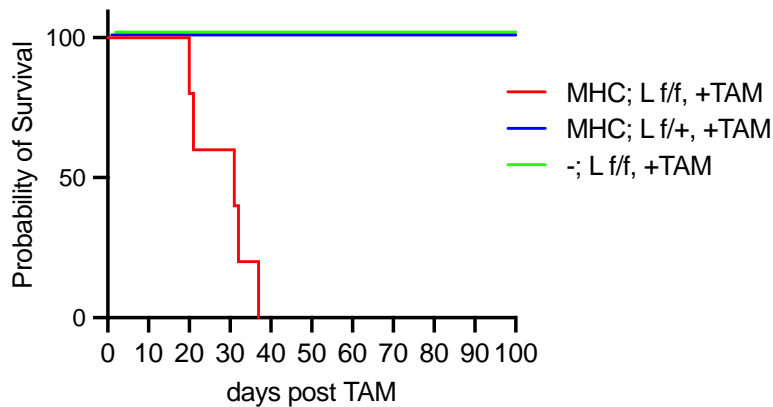


Figure 3.6: induction of cardiomyocyte specific knockout of *Lmna* in adult mice lead to lethality. Kaplan-Meier survival curves for MHC-MCM; *Lmna*^{flox/flox} x mice given tamoxifen (TAM) (“MHC; L f/f, +TAM”; n=8), littermate control *Lmna*^{flox/flox} mice given tamoxifen (“-; L f/f, +TAM”; n=8), and heterozygous knockout MHC-MCM; *Lmna*^{flox/flox} mice given tamoxifen as Cre+ control (“MHC; L f/+, +TAM”; n=10). Tamoxifen was administered to 10 week old adult mice. For MHC-MCM; *Lmna*^{flox/flox} mice given tamoxifen, the first death occurred at 21 days post administration; none survived past 37 days post administration. Median survival for is 31 days post tamoxifen administration for MHC-MCM; *Lmna*^{flox/flox} mice given tamoxifen.

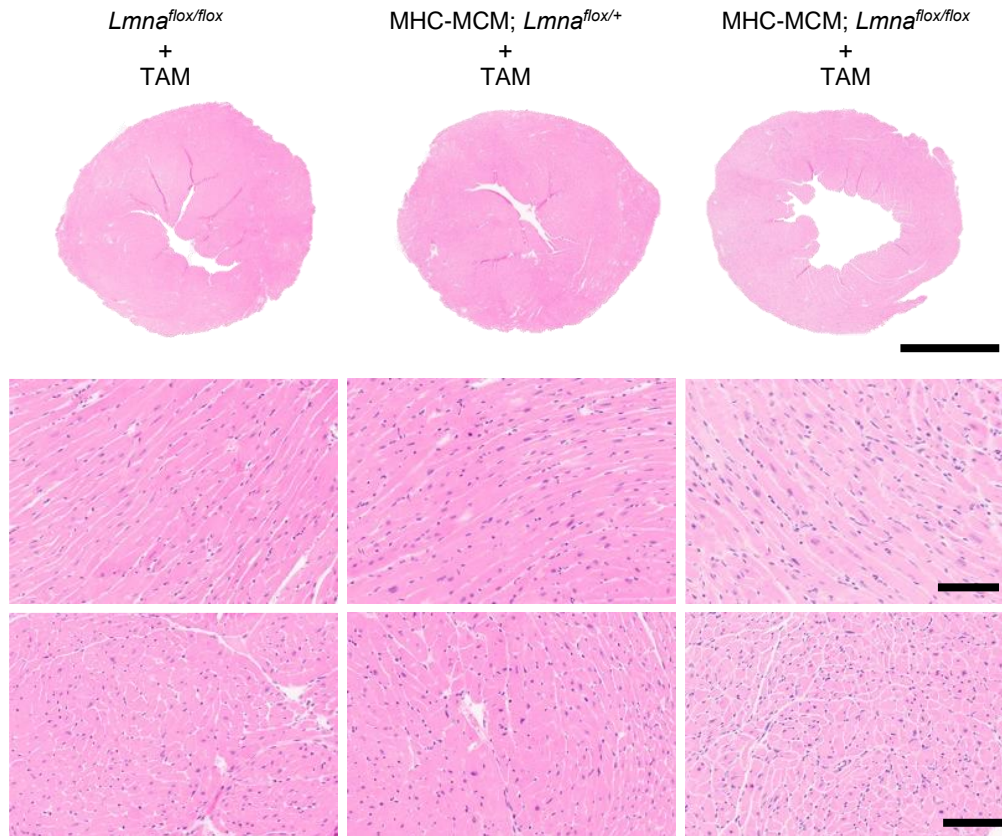


Figure 3.7: Hearts of MHC-MCM; *LMNA*^{flox/flox} mice treated with tamoxifen (TAM) exhibit ventricular dilation and hypotrophic cardiac myocytes. (top row) representative hematoxylin and eosin stained heart cross sections from MHC-MCM; *Lmna*^{flox/flox} and control mice 3 weeks post TAM treatment, treated at 8 weeks postnatal age. Hearts from MHC-MCM; *Lmna*^{flox/flox} +TAM mice shows thinning of the ventricle walls and dilatation of the ventricle chamber compared to littermate control *Lmna*^{flox/flox} treated with TAM and heterozygous knockdown MHC-MCM; *Lmna*^{flox/+} treated with TAM Cre+ control. 4 mice of each genotype were analyzed. Scale bar: 2mm. (middle row) zoomed in area of longitudinal fibers. Scale bar: 100 μ M. (bottom row) zoomed in area of transverse fibers. Scale bars: 100 μ M.

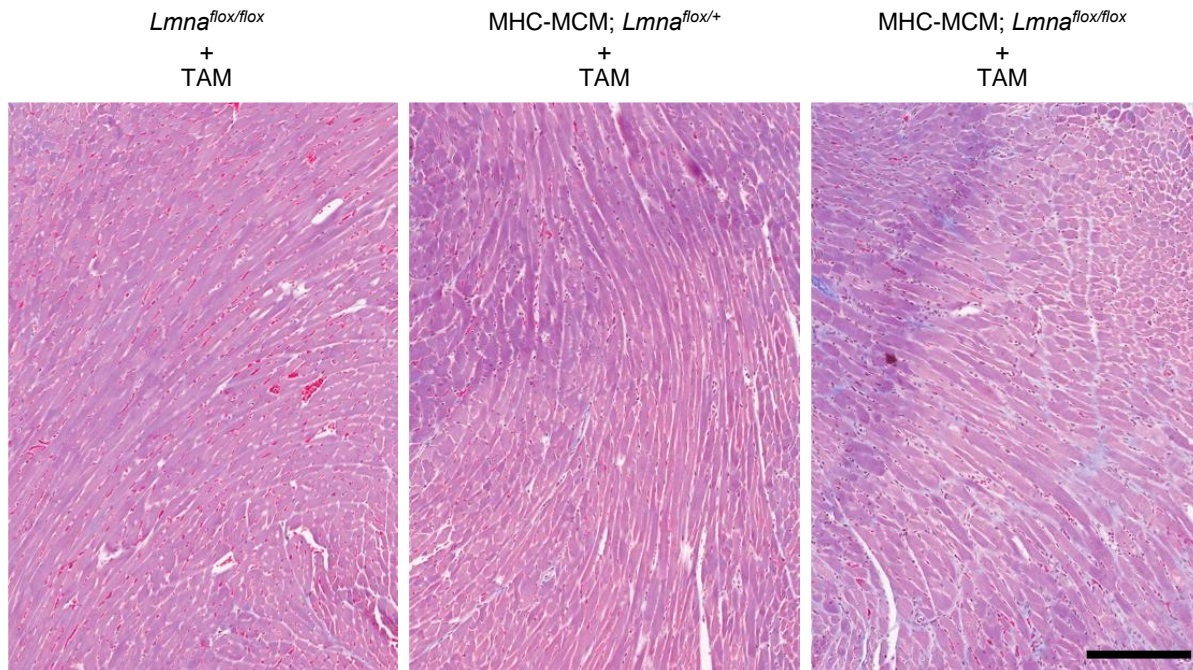


Figure 3.8: Increased interstitial fibrosis in MHC-MCM; *Lmna*^{flox/flox} mice treated with tamoxifen (TAM). Representative trichrome stained sections of hearts from mice 3 weeks post TAM injection. Hearts of MHC-MCM; *Lmna*^{flox/flox} mice treated with TAM have increased fibrosis (blue stain) between the cardiac myofibers, compared to littermate control *Lmna*^{flox/flox} mice treated with TAM, and heterozygous knockout MHC-MCM; *Lmna*^{flox/+} mice treated with TAM as Cre positive control. 4 mice were analyzed per genotype. Scale bar 200 μ M.

Discussion

Disruption of *Lmna* expression is detrimental to cardiomyocytes

Inducing knockout of *Lmna* in differentiated cardiomyocytes in the embryo led to severe thinning of the ventricular wall, dilation of the ventricle chamber, increase in fibrosis, and lethality with median survival of 27 days. Inducing knockout of *Lmna* in mature cardiomyocytes in an adult mice led to moderate thinning of the ventricular wall, moderate dilatation of the ventricle chamber, increase in fibrosis, and lethality with median survival of 31 days.

At the commencement of this study, the literature lacked data on cardiomyocytes specific knockdown of *Lmna* model mice. However, one study has been published since then that characterized the MHC-Cre induced *Lmna* knockout in adult, with a different floxed *Lmna*

mice at exon 11 (Chai et al., 2021). They found the median lifespan of mice was 27 days post tamoxifen injection, due to features of dilated cardiomyopathy, which corroborates my finding (Chai et al., 2021).

Therefore, the loss of lamin A/C expression after cardiomyogenesis is sufficient to induce dilated cardiomyopathy and lethality. Furthermore, I speculate that the pathologies of *Lmna*-induced cardiac lethality are independent of postnatal cardiac maturation. MCK-Cre is reported to be expressed at embryonic day 17, approximately 1 week before birth. Accounting for the duration of *Lmna* knockout before birth, MCK-Cre; *Lmna*^{flox/flox} mice died approximately 4-5 weeks post knockdown induction, which is comparable the time to lethality of MHC-MCM induced deletion of *Lmna*.

In the different strains of germline *Lmna* knockout mice, it has been noted that homozygous knockout mice are normal at birth, and during the first week of postnatal life, there are no differences in weight between homozygous knockout and control littermates (Kim and Zheng, 2013; Kubben et al., 2011). The growth of *Lmna* deficient mice deviates at after 1 week post-natal and they die between during the 3rd week. MCK-Cre mice die during the 4th-5th week of life, despite losing the ability to synthesize lamin A/C about 2 weeks later compared to homozygous germline knockout, albeit only in the heart. Furthermore, I found *Lmna* knockdown in adults also lead to lethality at 4th-6th week post induction.

MCK-*Lmna*^{flox/flox} mice also have induction of knockout at skeletal muscles. However skeletal muscles are overtly normal. A mouse line with skeletal muscle-specific conditional knockdown of *Lmna* has been published. Interestingly, the group that analyzed it turned their focus on the bone in one study and neuromuscular junction in the other (Gao et al., 2020a; Xiong et al., 2020). Our lab has unpublished data with an inducible *Lmna* knockout in skeletal muscles only with no phenotype 3 months post-induction. This can be due to many reasons. Skeletal muscle may take longer to show a phenotype. Additionally, the sedentary lifestyle of

the lab mice may cause underuse of their skeletal muscle, which may be a factor in the penetrance of any potential phenotype.

Potential long half-life of lamin A/C

My studies of lamin A/C knockdown in mice hearts produced a dramatic phenotype: rapid lethality. Despite that, my efforts to show a significant reduction of lamin A/C protein levels have been far from conclusive. I speculate this is due to the long half-life of A-type lamins. Numerous studies have suggested long half-lives of nuclear lamina proteins. Lamin B1 and B2 have been shown to have a long half-life; proteins were found in post-mitotic neurons and photoreceptors for 9 months despite its knockout being induced at embryonic specification (Razafsky et al. 2016). In a metabolic pulse-chase study in rats to identify long-lived proteins, the authors included many nuclear proteins, and they found ~25% of nuclear pore complex protein Nup205 persists after one year, a significant portion of a rat's life (Toyama et al. 2014). The same authors speculated that the lack of nuclear envelope breakdown and reassembly is likely the culprit of the long half-lives (Toyama and Hetzer, 2013). These findings suggest the high stability of nuclear proteins in post-mitotic cells. Furthermore, nuclear pore proteins have been found to last longer than one month in the short-lived *C. elegans*, hence persisting for the duration of the organism's life (D'Angelo et al. 2009). Therefore, lamin A/C may also have a long half-life, especially in post-mitotic cells such as cardiomyocytes.

Lamin A/C positive signal in the cell is dominant by the nuclear rim pattern (peripheral lamina) adjacent to the nuclear envelope. That is where lamin A/C is thought to form insoluble intermediate filament networks. The soluble pool of A-type lamins within the nucleoplasm is not polymerized, is highly mobile, and may play critical roles in gene expression, splicing, and DNA damage response (Dechat et al., 2010). It may be the first pool of lamin A/C to be affected by genetic knockdown.

Chapter 4: Discussions and Future Directions

Cardiomyocytes require the expression of A-type lamins for cardiac function

My study demonstrates that the knockdown of lamin A/C in mature cardiomyocytes at the prenatal or adult stage causes phenotypes consistent with dilated cardiomyopathy, is detrimental to whole heart function, and causes lethality. This study added two major findings about lamin A/C function in mouse heart.

First, A-type lamins have a different effect in cardiomyocyte precursors compared to cardiomyocytes. Both the *Lmna* gene-trap knockout mice and the *Lmna* floxed mice induced at germline have no macroscopic defects at first and through the first week of post-natal development (Kim and Zheng, 2013; Kubben et al., 2011). However, growth retardation is detected at the start of the second week of life; lethality for both null models occurred from day 16 to 18 (Kim and Zheng, 2013; Kubben et al., 2011). While MCK-Cre; *Lmna*^{flox/flox} mice exhibited lethality day 23 through to 35. MCK promoter expression has the potential range from as early as embryonic day 9 to the confirmed embryonic day 17 (Han et al., 2015; Trask and Billadello, 1990). Taking into consideration that MCK-Cre; *Lmna*^{flox/flox} mice loses expression of *Lmna* in striated muscle starting at embryonic day 9 at the earliest, the survival length of *Lmna*^{-/-} mice and MCK-Cre; *Lmna*^{flox/flox} mice from the time they lose *Lmna* expression are very similar. Therefore it can be inferred that lamin A/C is most critical for differentiated cardiomyocytes, and its absence in cardiomyocyte precursors is trivial.

Second, there is no significant difference between knocking out *Lmna* in differentiated cardiomyocytes at the embryonic stage versus adults. This also takes into account the potential range of MCK promoter expression from as early as embryonic day 9 to the confirmed embryonic day 17 (Han et al., 2015; Trask and Billadello, 1990). Lethality occurred 21-37 days post induction in adult MHC-MCM; *Lmna*^{flox/flox} mice. Meanwhile, MCK-Cre; *Lmna*^{flox/flox} mice

experienced lethality 23 to 35 days post-natal. Knockout of *Lmna* in adult cardiomyocytes and embryonic cardiomyocytes causes lethality in approximately the same window of time through the manifestation of similar pathogenic phenotypes of ventricle dilatation, hypertrophic cardiac muscle fibers, and fibrosis. Therefore, it is safe to conclude any defects in late embryonic and post-natal cardiac development do not contribute to the defect in *Lmna* genetic knockout in cardiomyocytes.

Why is the disruption of lamin A/C in cardiomyocytes so detrimental? A previous study showed decoupling the nuclear lamina from the LINC complex can partially rescue the cardiac phenotype and lethality in mice with cardiomyocyte-specific *Lmna* knockout, therefore supporting the involvement of mechanical stress in causing cardiac defects (Chai et al., 2021; Zhang et al., 2023). Clues from iPSC-CMs may offer further insights into the potential mechanisms. I propose metabolic disruptions could potentially be a reason behind the sensitivity to lamin A/C disruption in mature hearts. The metabolic maturation of cardiomyocytes that occurs during the first week of post-natal development could be the reason *Lmna* mutant mice are born normal and develop defects post-natal across many *Lmna* mutant mice models. Multi-omic studies of *Lmna* mutant mice hearts, or specific cell types within these hearts, at these early timepoints can offer clues.

It must be noted that my study demonstrated that knocking out *Lmna* is not associated with the complete or even significant loss of protein, which is controversial to the traditional understanding that phenotypes from homozygous genetic knockout of protein-coding genes are due to loss of the protein, even if it is haploinsufficient.

Long lived lamins and implications

Growing lines of indirect evidence suggest lamins are long-lived in cardiomyocytes. Very recently, a study showed through a novel method of determining protein half-life in different tissues that lamin A/C is among the longest-lasting protein in any given cell (Hasper et al.,

2023). Furthermore, it is even longer lasting in the heart compared to other organs like the liver, with a half-life of 28 days (Hasper et al., 2023). Another study with the exact same mouse model as I created and demonstrated via immunoblot of isolated cardiomyocytes only half lamin A/C reduction at 2 weeks post-induction (En et al., 2023). These two studies, in addition to my finding, are in direct conflict with previous study by Chai *et al.* which showed significant loss of lamin A/C in whole heart lysates from their mouse model (Chai et al., 2021).

Active lamin A/C synthesis may be required for the maintenance of cardiac function. Products of active synthesis include products of transcription, translation of prelamin A and lamin C, and byproducts of processing. Without adequate evidence, the absence of any of the mentioned products could be implicated in the deleterious effect of homozygous lamin A/C knockout in cardiomyocytes. I speculate that newly synthesized A-type lamins, whether processed or between processing steps, may participate in a pool of lamins with certain functions in the cell. After participating in this “newly synthesized pool” of A-type lamins, the proteins are eventually incorporated, through posttranslational modifications or natural kinetics, into the “traditional pool” of lamin A/C. Therefore, the cessation of synthesis can cause a phenotype, in the presence of adequate protein present. It is suggested that a pool of lamin A/C is soluble and subjected to constant degradation while the ones incorporated into the insoluble mesh that is traditionally thought of as the nuclear lamina is stable and less degradable (Buchwalter, 2023). Furthermore, post-mitotic cells, which do not require nuclear envelope breakdown in mitosis, might have unique features of their nuclear lamina that make it more resistant to degradation compared to mitotic cells. There has yet to be studies that investigated the different lamin dynamics in mitotic versus post-mitotic cells.

To date, there are no human cell models of an inducible knockout of *LMNA* that can recreate the circumstance where the production of A-type lamins ceases in the presence of an already synthesized protein pool. Due to that absence, the importance of a “newly synthesized

pool” of A-type lamins cannot be tested in a human-relevant model. Without such a model, there is a possibility that the lethality in the absence of significant protein reduction could be a mouse-specific effect. It must be noted that mice lamin A/C deficiency is not a faithful model of cardiolaminopathies, despite having comparable cardiac phenotypes, due to the fact that all human patients have a functional copy of *LMNA*. Heterozygous *Lmna*-deficient mice that are normal enough to be indistinguishable from their WT littermates in my studies. Mice with emerin deficiency does not have obvious abnormal phenotype (Ozawa et al., 2006). Perhaps features of the mice make the cellular effects of lamin A/C haploinsufficiency and emerin deficiency less penetrant on an organism-wide level.

Lamin A/C deficient mouse models highlight the consequence of long-lived lamins, showing a possible new functional pool of A-type lamins and the possibility of weakening the paradigm that knockout phenotypes are due to complete protein loss. All these points are important for future investigations into the basic biology of A-type lamins, which can lead to a better understanding of laminopathies as a whole.

New understanding of lamin functions

While mice studies showed that the heart has a specific requirement of A-type lamins, the mechanism as to why their deficiency leads to organ failure is still unclear. My studies on iPSC-CMs have shown several things. Consistent with the “gene expression” hypothesis, also known as the chromatin hypothesis, lamin A/C haploinsufficient and emerin deficient iPSC-CMs have upregulated expression of genes associated with the nervous system, in agreement with previous report (Shah et al., 2021b). The direct consequence of this aberrant activation of alternative fate genes is unknown. These nervous system-associated genes, among them ones that encode for ion channels, have been hypothesized to be the cause of early conduction defects seen in patients with cardiolaminopathy (Bertero et al., 2019). Further inquiry is required

to understand the basic biological effect of the expression of nervous system genes in the cellular context of cardiomyocytes haploinsufficient for lamin A/C or lacking emerin.

As to the reason why nervous system related genes are upregulated in lamin A/C haploinsufficient and emerin deficient iPSC-CMs, one possibility is that the derepressed chromatin regions may have unique molecular features such as histone modification that allow them to be uniquely affected. Therefore, closer examination of the specific chromatin modifications that marks specific cell lineage genes is required. Currently, 3D genome organization and its alteration in development and disease is a rapidly advancing field, including in the context of the nervous system. Insight gained from research in chromatin organization in nervous system development and disease may aid in the understanding what the aberrant activation of nervous system genes in iPSC-CMs cardiomyocytes haploinsufficient for lamin A/C or lacking emerin.

The gene expression hypothesis has not implicated alterations in RNA splicing as contributors to the pathogenesis of disease. However, I found significant enrichment of proteins involved in splicing in the downregulated proteins of both lamin A/C haploinsufficient and emerin deficient iPSC-CMs. Nuclear envelope proteins might aid in the maintenance of nucleoplasmic proteins, such as splicing factors. Furthermore, I serendipitously discovered that lamin A/C haploinsufficient and emerin deficient iPSC-CMs expressed a smaller cardiac troponin protein variant (Figure 2.4). Additional structural proteins may be prone to aberrant splicing in these mutant iPSC-CMs. With alternate forms of important structural proteins added to the mix in cardiomyocytes, mis-regulation and degeneration of force generation may occur and may add another dimension to the “structural hypothesis”. More work is required to understand the implications of mis-regulation of splicing factors, and how alternate or aberrant splicing of RNAs of certain structural proteins may affect cardiomyocyte function.

Alterations in metabolism are a possible underlying feature of cardiolaminopathy

I found lamin A/C-haploinsufficient and emerin-deficient iPSC-CMs have dysregulated expression of genes associated with metabolism, in particular, ones involved in mitochondria cellular respiration and lipid metabolism. *LDHB* is reduced at the transcript and protein levels, and its metabolite lactate is also reduced in the cells. Pathogenic *LMNA* mutations are thought to disrupt metabolic pathways in other laminopathies including lipodystrophic laminopathies (Peng et al., 2022). This result opens the possibility that the role of lamin A/C in metabolism is not exclusive to laminopathies with dominant metabolic features and may also underly cardiolaminopathy.

Mechanisms behind the changes in metabolic components are unknown. They could be altered at the gene expression level, via disrupted interactions between the nuclear lamina and transcription factors, or through altered interactions with chromatin. One class of transcription factors, the nuclear receptor class, are particularly notable as a potentially being involved in the mechanism that link metabolic alterations with the disruption of nuclear lamina by lamin A/C haploinsufficiency or emerin deficiency. The nuclear receptors identified in this study, FXR, LXR, and PXR, presents compelling grounds for future study.

I found that ER and mitochondrial cellular components were disrupted in lamin A/C haploinsufficient and emerin deficient iPSC-CMs. Mutations in lamin A/C have been linked to ER stress (Carmosino et al., 2016; Vidak et al., 2023; West et al., 2016). Although not well understood, ER stress is a key feature of metabolic disorders (Lemmer et al., 2021). Furthermore, there is extensive contact and cross-talk between ER and mitochondria, which has implications in metabolic pathways such as glucose homeostasis (Rieusset, 2018). In the understanding of metabolic features in cardiolaminopathy, ER and mitochondrial cross-talk invite closer scrutiny.

The downregulation of *LDHB* raises the question of the mechanism behind sensitivity to hypoxia reported in past iPSC-CM models of cardiomyopathy (Shah et al., 2019). Although my study captured the reduction of lactate in lamin A/C haploinsufficient and emerin deficient iPSC-CMs, future studies could investigate the dynamic changes in lactate levels, using newly improved fluorescent intracellular sensors under different physiological conditions such as hypoxia (Bekdash et al., 2021). *LDHB* and lactate reduction may be just a result of the greater metabolic disarray caused by an emerin deficiency or lamin A/C haploinsufficiency, which includes alterations in lipid synthesis pathways, glycosylation pathways, and nuclear receptor pathways, including retinoic acid receptors.

Two studies by Muchir *et al.* showed enrichment in transcripts associated with metabolism-related GO terms in the hearts of either *Emd*^{-/-} mice and *Lmna*^{H222P/H222P} mice (Muchir et al., 2007a; Muchir et al., 2007b). These terms include “phospholipid metabolism”, “ribonucleotide metabolism”, “vitamin metabolism”, “fatty acid biosynthesis”, and “sphingolipid metabolism”. (Muchir et al., 2007a; Muchir et al., 2007b). Another study showed that the cardiac transcriptome of *Lmna*^{-/-} mice was enriched in differences associated with “oxidative phosphorylation,” “TCA cycle,” and “fatty acid-oxidation” (Pradas et al., 2020). Alterations in these specific categories of genes were rescued upon re-expression of lamin A/C. In the study where the first *Lmna* knockout mice were generated, transcriptomic alterations in fatty acid oxidation and electron transport chain related genes were found from mRNA isolated from ventricle cardiac tissue (Kubben et al., 2011). Metabolic pathways have also been found to be dysregulated in hearts of human subjects with cardiomyopathy caused by *LMNA* mutations (Cheedipudi et al., 2019; Topriceanu et al., 2023)

Alterations in metabolism as a mechanism of laminopathy can fit under the two existing hypothesis of laminopathy. Changes in gene expression may cause metabolic alterations; however, many differentially expressed metabolic genes and their encoded proteins

demonstrated opposite changes in both *Lmna*^{-/+} and *EMD*^{-/-} iPSC-CMs. Transcriptional changes may however be responding secondarily to metabolic alterations. Changes in nuclear structure do not have clear connection to alterations in metabolism, but they could indirectly affect the metabolic demands of the cell. There are enough independent lines of evidence that would support a third hypothesis of laminopathies, the “metabolic hypothesis.”

The metabolic hypothesis of laminopathy and emerinopathy

There is a strong link between laminopathies and metabolic syndrome (Carboni et al., 2013). Laminopathies affect metabolically active organs that are composed significantly of post-mitotic cells. An exception is the brain, but it may be spared because neurons have little to no lamin A expression (Jung et al., 2012). LMNA mutations have been found to cause striated muscle disorders as well as lipodystrophy, suggesting the two phenotypes may have underlying molecular commonalties (Garg et al., 2002; van der Kooi et al., 2002). A group of individuals with metabolic syndrome were found to harbor novel mutations in *LMNA* that were predicted to be damaging suggesting that patients with metabolic syndrome are more likely to have laminopathies than the general population (Dutour et al., 2011).

Mature cardiomyocytes have different metabolisms compared to embryonic or early postnatal versions. My mouse study showed that induced knockout of *Lmna* in cardiomyocytes has similar effect as embryonic conditional knockout of *Lmna* in striated muscles. Furthermore, as previously noted in this chapter, full *Lmna* knockout mice do not exhibit growth retardation and cardiac phenotypes until the second week after birth. I hypothesize that it is due to the alteration of cardiac metabolism that occurs in the first week of postnatal growth that leads to the phenotypes in mice and the eventual lethality.

The core metabolic pathways of glycolysis, TCA cycle, and β -oxidation are affected in both emerin deficient and lamin A/C haploinsufficient iPSC-CMs based on their transcriptomic, proteomic, and metabolomic profiles. Pathways associated with “Mature Onset Diabetes of the

Young (MODY)” implicate the process of glycolysis and its potential dysregulation. There is also enrichment in mitochondria-associated differentially expressed proteins in both mutant cells. Lipid metabolism and other closely associated genes are also enriched in transcriptomic and proteomic differences between the mutant and WT cells. Lastly, the lactate metabolic pathway, seen through multi-omic changes, is also altered in by both *LMNA* and *EMD* mutation. Alterations in these core metabolic pathways could have consequences in a high metabolic organ such as the heart.

There are many additional metabolic pathways interconnected with the core metabolic pathways. Two notable ones that I hypothesize are important for the pathogenesis of EDMD are membrane lipid metabolism and protein glycosylation. Many proteins associated with membrane lipid synthesis were found to be dysregulated proteome in both lamin A/C haploinsufficient and emerin deficient iPSC-CMs. AGPAT1 and 4 are mis-regulated and they are important in converting lysophosphatidic acid (LPA) to phosphatidic acid (PA), a key step in lipid synthesis. Both LPA and PA are directly involved in phospholipid synthesis. Several enzymes directly involved in phospholipid synthesis are mis-regulated in the proteome of both lamin A/C haploinsufficient and emerin deficient iPSC-CMs, including CDS2, PTPMT1, PTDSS2, and LPGAT1. Many of these proteins are located in the ER and mitochondria membrane (Fagone and Jackowski, 2009). Additionally, ER and mitochondrial membranes are cellular components that were highly enriched in the transcriptome of lamin A/C haploinsufficient and emerin deficient iPSC-CMs. This is particularly relevant as membrane lipids are transferred between the ER and mitochondria at specific sites called MAMs, which has particular relevance of cardiomyopathies (Flis and Daum, 2013; Gao et al., 2020b). All these lines of reasoning offer compelling motivation to investigate the effect of EDMD-associated *LMNA* and *EMD* mutations on membrane lipid metabolism.

Another candidate metabolic pathway that may be involved in the pathogenesis of EDMD is protein glycosylation. Glycosylation involves the addition of a sugar residue to proteins and has been implicated in cardiovascular disease (Loeza-Reyes et al., 2021). There are nine nucleotide sugars that act as glycosyl donors in glycosylation reactions, catalyzed by glycotransferases (Mikkola, 2020). Four of the nine nucleotide sugars, uridine diphosphate-N-acetylgalactosamine (UDP-GalNAc), uridine diphosphate-N-acetylglucosamine (UDP-GlcNAc), uridine diphosphate galactose (UDP-Gal) and uridine diphosphate glucose (UDP-Glc), I found to be significantly more abundant in emerin deficient iPSC-CMs. Furthermore, GMPPA and GMPPB, which catalyze the reaction that converts mannose-1-phosphate and GTP to GDP-mannose (GDP-Man), are significantly upregulated in the proteome of both lamin A/C haploinsufficient and emerin deficient iPSC-CMs. CMAS, which catalyzes the activation of Neu5Ac to cytidine 5-prime-monophosphate N-acetylneuraminic acid (CMP-Neu5Ac), is upregulated in both the transcriptome and proteome of both lamin A/C haploinsufficient and emerin deficient iPSC-CMs. All these lines of evidence implicate six out of the nine nucleotide sugars and suggest possible mis-regulation of the cellular glycosylation pathways.

Glycomics and glycoproteomics are emerging fields and has the potential to offer a revolutionary understanding of biology, as glycosylation is capable of providing huge proteome diversity (Čaval et al., 2021). Protein glycosylation is initiated in the ER, which can offer a potential mechanistic explanation to how lamin A/C and emerin in the directly connected nuclear envelope could directly affect these processes (Schoberer et al., 2018). Furthermore, despite participating in the transfer reaction to make a nucleotide sugar required throughout the cell, CMAS is specifically localized to the nucleus (Kean et al., 2004). There is no explanation as to why CMAS is localized to the nucleus. It's possible interaction with other nuclear residents such as proteins of the nuclear lamina could be worthy of future investigation.

While membrane lipid metabolism and protein glycosylation are processes worthy of future investigation in studies of the pathogenesis of EDMD, they are intricately linked to the core metabolic pathways and are more likely than not a result of metabolic disturbances. I would like to propose a possible mechanism that has the potential to be upstream of all the metabolic changes. Pathway analysis showed enrichment of processes associated with LXR/RXR, PXR/RXR, FXR/RXR. Additional pathways that are enriched can be attributed to nuclear receptors, such as “xenobiotic metabolism” and pathways associated with coagulation (Shih et al., 2004; Timsit and Negishi, 2007). HNF1A tops the list of upstream regulators and is regulated by the nuclear receptor HNF4A, which happens to be the next on the list (Kuo et al., 1992). Specific nuclear receptors are differentially expressed in both lamin A/C haploinsufficient and emerin deficient iPSC-CMs, including NR0B1, NR0B2, NR1H4, NR1I2, NR2F1, etc.

Many nuclear receptors sense metabolic conditions in the cell and enter the nucleus to regulate gene expression that affects metabolic processes (Scholtes and Giguère, 2022). Through their mechanisms there is the potential for direct interactions of nuclear receptors with lamin A/C and emerin inside the nucleus. There is preliminary evidence that shows nuclear lamins interact with the nuclear receptor PPARG (Lowe et al., 2014). The nuclear lamina may help stabilize nuclear receptors, which help regulate metabolism.

Overlapping effects of lamin A/C haploinsufficiency and emerin deficiency.

Using isogenic iPSC lines of human origin, I found that iPSC-CMs with emerin deficiency have overlapping transcriptomic, proteomic, and metabolomic changes with iPSC-CMs with lamin A/C haploinsufficiency. This validates the idea that the original clinical observations of AD-EDMD sharing the same features as X-linked EDMD is due to similar biological mechanisms. In terms of cellular biology, it is worth investigating why emerin deficiency has similar effect as lamin A/C haploinsufficiency. While both emerin and lamin A/C are part of the nuclear lamina and are involved in many interactions with their fellow nuclear lamina constituents, the overlap

in phenotype of lamin A/C haploinsufficiency and emerin deficiency highlight their unique interplay.

Additionally, it is unknown if the interaction between lamin A/C and emerin is uniquely important in cardiomyocytes. It would appear so on the basis that emerin deficiency in human subjects only causes cardiac skeletal muscle phenotypes, whereas *LMNA* mutations can affect various tissues. The isogenic iPSCs I generated can also be differentiated into other cell types such as hepatocytes and adipocytes, to see if lamin A/C haploinsufficiency and emerin deficiency have the same effects in other cells. I hypothesize that the overlap in their effects is a unique characteristic of cardiomyocytes. A similar study by Shah and colleagues that found differences in chromosome arrangements in iPSC with *LMNA* mutations differentiated into cardiomyocytes, hepatocytes, and adipocytes (Shah et al., 2021b).

How does emerin loss have the same cellular effects as lamin A/C haploinsufficiency?

My proteomics data showed that loss of emerin led to a loss of lamin A/C (approximately 50% of WT levels), although not to the degree of lamin A/C haploinsufficiency cells (approximately 25% of WT levels), suggesting emerin has a role in stabilizing lamin A/C levels. There is the possibility that the resultant level of nuclear lamina destabilization from either lamin A/C haploinsufficiency or emerin deficiency is similar enough to cause similar phenotypes. On the other hand, it is also possible lamin A/C and emerin complex with additional factors that assist in their functions, and a loss of either of the two will cause significant disruption of the unknown and consequential lamin A/C and emerin interactor. This interactor may regulate gene expression by binding to LADs, or affect metabolism by binding to upstream regulators of metabolism. Another possibility is that emerin contributes to nuclear architecture in a different but equally important way as lamin A/C. Emerin has been found to regulate actin polymerization and contributes to the formation of an actin network on the INM (Holaska et al., 2004). I found significant loss of ACTB in the proteome of emerin deficient iPSC-CMs,

supporting emerin's role in stabilizing actin networks. The destabilization of the nuclear actin network may cause a similar detrimental effect as loss of over half of lamin A/C. Furthermore, emerin has been found to oligomerize, and its oligomeric state might confer stability to the nucleus (Fernandez et al., 2022). Despite all these possibilities, we are still very much in the dark on how loss of emerin, an integral INM protein, can have the same phenotype as partial loss of a lamin A/C, an nuclear intermediate filament.

Final Word

This study further demonstrates the extensive involvement and influences of the nuclear envelope proteins lamin A/C and emerin in the cell. Six decades after Dr. Emery and Dr. Dreifuss characterized the first case of EDMD, and almost three decades after the discovery of their genetic cause, the link between these proteins and disease phenotypes is still elusive. Findings from this study offers avenues of focus for future investigation to uncover the mysteries that surround these proteins and their impact on basic cellular processes and the pathobiology of diseases.

Chapter 5: Material and Methods

Basic methods

Immunofluorescence staining and microscopy

Primary antibodies used are listed in Table 5.1. Cells were fixed with 4% paraformaldehyde for 15 minutes. Permeabilization and blocking was performed in PBS with 5% BSA and 0.5% Triton X-100. Primary and secondary antibodies incubation were performed in PBS with 1% BSA and 0.5% Tween 20 for 1-2 hrs at room temperature or overnight at 4°C. All washes after primary and secondary antibody incubation were done with PBS. After the final wash was completed, coverlips were mounted with VECTASHIELD® Antifade Mounting Medium containing DAPI and sealed with nail polish. Confocal imaging was performed with Nikon A1 scanning confocal microscope at the Columbia Confocal and Specialized Microscopy Shared Resource.

Immunoblotting

Primary antibodies used are listed in Table 5.1. Equal volume of 2x SDS sample buffer was added to tissue samples homogenized in lysis buffer or cell pellet. SDS-PAGE was performed with Invitrogen precast bis-tris gels in MOPS running buffer and the separated proteins were transferred onto nitrocellulose membrane. Membranes were blocked with blocking buffer (PBS with 5% milk and 0.05% Tween 20) for 30 minutes. Primary antibody incubation was performed in blocking buffer overnight at 4°C, washed with PBS with 0.05% Tween 20, and incubated with secondary antibody in blocking buffer for 1 hour at room temperature. Membranes were imaged using an Odyssey Infrared Imager (Model 9120, LI-COR Biosciences). Protein intensity was measured using the 'Gels' function in ImageJ.

Table 5.1: List of antibodies

target	species raised	company	note
LDHB	Rabbit	Proteintech 14824-1-AP	WB 1:5000
lamin A/C	Mouse	Santa Cruz sc-376248	WB 1:1000; IF 1:500
emerin	Rabbit	Abcam ab40688	WB 1:5000; IF 1:500
emerin	Rabbit	Abcam ab156871	WB 1:1000
emerin	Mouse	Leica NCL-emerin	WB 1:500; IF 1:50
emerin	Mouse	Santa Cruz sc-25284	WB 1:500
emerin	Mouse	sigma AMAB90562	WB 1:1000
cTnT 13-11	Mouse	Thermo Fisher MA5-12960	WB 1:5000
cTNT	Goat	Abcam ab56357	IF 1:500
H3K9me3	Rabbit	Abcam 8898	IF: 1:500
histone H3	Rabbit	Biomatik	WB 1:5000
GAPDH	Mouse	Invotrogen AM4300	WB 1:5000
LBR	Mouse	Abcam ab232731	IF 1:500

Mice

Mouse husbandry

List of mouse lines and PCR primers used for genotyping are provided in Table 5.2. The genetic background of all mice in this study was a combination of C57BL/6J and 129SvEv. All mice were fertile and produced at the expected Mendelian frequencies. Mice were housed in a climate-controlled room with a 12-hour light/12-hour dark cycle and fed a regular chow diet (Purina Mills, 5053). The Institutional Animal Care and Use Committee of Columbia University Medical Center approved all protocols.

Tamoxifen was dissolved in corn oil at 20 mg/ml and administered mice via intraperitoneal injection at 100mg/kg (0.1ml for a 20g mice).

Table 5.2: List of mouse lines.

genotype	JAX ID	Genotyping primers
<i>Lmna</i> ^{flox/flox}	026284	F: 5'-AACCCAGCCTCAGAACTGGTGGATG-3' R: 5'-GACAGCTCTCCTCTGAAGTGCTTGGA-3'
MCK-Cre	006405	F: 5'-GTGAAACAGCATTGCTGTCACT-3' R: 5'-TAAGTCTGAACCCGGTCTGC-3'
MHC-MerCreMer	005657	F common: 5'-TCT ATT GCA CAC AGC AAT CCA-3' R wildtype: 5'-CCA ACT CTT GTG AGA GGA GCA-3' R mutant: 5'-CCA GCA TTG TGA GAA CAA GG-3'

Histology

Mice were euthanized, and the heart and tibialis anterior muscle were immediately excised and blotted dry. Tissue samples were fixed in 4% formaldehyde for 48 hours, embedded in paraffin, sectioned at 5 μ M, and stained with hemotoxylin and eosin, or trichrome.

IPSCs

IPSC maintenance

The iPS-DF19-9-11T line was purchased from WiCell. All iPSCs were maintained in a feeder-free system on Matrigel (Corning 354230) coated plates with mTESR plus media (Stem Cell Tech 100-0276). iPSCs were passaged at approximately 80% confluency or no longer than 5 days since previous passage. iPSCs were detached with 5 min incubation in 0.5mn EDTA in PBS at 37°C then removed, followed by addition of mTESR plus media to physically dislodge the cells. iPSCs were replated at 1:6 dilution onto new Matrigel coated wells. ROCK inhibitor (Stem Cell Tech 72304) was added to newly plated iPSCs and removed after 24 hours by changing the media.

CRISPR

CRISPR guide sequences were designed using the Synthego online CRISPR design tool. Sequences are given in Table 5.2. CRISPR sgRNA and Cas9 were purchased from Synthego. For electroporation, the P3 Primary cell 4D-Nucleofector X kit S (Lonza V4XP-3032) was used per the manufacturer's instructions. For each electroporation, 20 pmol of Cas9 was

mixed with 180 pmol sgRNA to assemble the ribonucleoprotein complex in a 25 μ L volume of nucleofector solution. One hundred thousand iPSCs in 5 μ L of nucleofector solution were added to each reaction. The now 30 μ L mix was added to the nucleofector strip and placed in the Lonza 4D-X unit set to program CM130. After run completion, cells were recovered with mTESR plus media immediately and moved to 24 well plates coated with Matrigel. Ten percent ClonR (StemCell Tech) was added to the media to improve cell survival for 3 days. When the cells in each well reached confluence, the cells in the well were passaged with enzymatic dissociation to create single cell suspension, then 1/5 of the cell suspension was replated onto 10-cm plates coated with Matrigel in mTESR and 10% ClonR. The remaining cell suspension was used for DNA extraction and Sanger sequencing to detect the efficacy of the CRISPR reaction. Primers used are provided in in Table 5.4. CRISPR efficacy was determined by uploading the Sanger sequencing chromatograph file onto Synthego online ICE CRISPR analysis tool. If the CRISPR reaction worked and genomic edits at the intended site was detected, clonal selection was performed on the corresponding 10-cm plate. Individual clones were picked using a p200 pipette tip under a light microscope in a sterile cell culture hood. Each separate colony was transferred into a 96-well plate coated with Matrigel in mTESR plus media with 10% ClonR. After a few days, each well was dissociated and the cell suspension split between 2 new plates for additional expansion. One plate was then used for DNA extraction for each clonal candidate and sequenced. Candidates were selected based on sequence, then expanded further. The final selected CRISPR edited lines were submitted for whole genome sequencing at Praxis Genomics LLC to verify that no significant off-target edits occurred.

Table 5.3: sgRNA sequences for CRISPR.

Gene targeted	sgRNA sequence
<i>LMNA</i>	#1: 5'-CUUUAGCAAUACCAAGAAGGAGG-3' #2: 5'-GGCUCUGCUGAACUCCAAGGAGG-3' #3: 5'-UCUGCGGGGCCAGGUGGCCAAGG-3'
<i>EMD</i>	#1: 5'-UCCGGCCAGGAUCAACUCGUAGG-3' #2: 5'-UCUUCGAGUACGAGACCCAGAGG-3'

#3: 5'-CCUCCUCUUAUAGCUUCUCUGG-3'

Table 5.4: PCR and sequencing primers for confirmation of CRISPR edits.

	PCR primers	Sequencing primer
<i>LMNA</i>	F: 5'-GGGGCTCAGATCGAGAAGTG-3' R: 5'-GGACAGGTGAATGGCTCTGA-3'	5'-GAAAGAATGGGAGGAGAGAGAG-3'
<i>EMD</i>	F: 5'-TTTCGGATACCGAGCTGACC-3' R: 5'-GTACCCAAGTACAGGACGCC-3'	5'-GTAGCTCTCTTCATAGTAGTCGTC-3'

Cardiomyocyte differentiation

iPSCs were grown to 90% confluence, then differentiated using a 30 day protocol (Gifure 5.1). At the start of differentiation, the media was changed to basal differentiation media (RPMI 1640 with B27 minus insulin supplement) with 9 μ M CHIR-99021 (Tocris 4423) for 24 hours of incubation. The media was then changed to just basal media for 24 hours. Subsequently, the media was changed to basal differentiation media with 5 μ M IWP2 (Tocris 3533) for 48 hours. Then the cells were maintained in basal differentiation media, with media changes every two days. Around day 7, spontaneous contracting cells were observed. Ten days after the start of differentiation, media was switched to maintenance media (RPMI 1640 with B27 Supplement). Purification media (RPMI 1640 no glucose with B27 supplement) was added one day later for a duration of 3 days, after which maintenance media was replaced back for one day. Then purification media was added for another 3 days, after which the cells were maintained in maturation media, with media changes every 3 days. Optional replating was done on day 14 and 18. Cells were used at day 30.

Maturation media was composed in DMEM without glucose (Thermo Fisher Scientific, 11966025) supplemented with 3 mM glucose (Sigma Aldrich, G7021), 10 mM L-lactate (Sigma Aldrich, 71718), 5 μ g/ml vitamin B12 (Sigma Aldrich, V6629), 0.82 μ M biotin (Sigma Aldrich, B4639), 5 mM creatine monohydrate (Sigma Aldrich, C3630), 2 mM taurine (Sigma Aldrich, T0625), 2 mM L-carnitine (Sigma Aldrich, C0283), 0.5 mM ascorbic acid (Sigma Aldrich,

A8960), 1x NEAA (Thermo Fisher Scientific, 11140), 0.5% (w/v) Albumax (Thermo Fisher Scientific, 11020021), 1x B27 and 1% KOSR (Thermo Fisher Scientific, 10828028).

0	1	2	3	4	5	6	7	8	9	10	11	12	13	14	Cont.
RPMI										RPMI no glucose					
B27 minus insulin										B27					
CHIR 9uM		IWP2 5uM													

15	16	17	18	19	20	21	22	23	24	25	26	27	28	29	30
RPMI no glucose			Maturation media												
B27															

Figure 5.1: Timeline of protocol for differentiation of iPSCs to cardiomyocytes. On day 0, media is changed to RPMI 1640 (RPMI) with B27 minus insulin and 9 μ M CHIR99021. Twenty-four hours later on day 1, media is changed to RPMI with B27 minus insulin. On day 2, media is changed to RPMI with B27 minus insulin and 5 μ M IWP2. On day 4, media is changed to RPMI with B27 minus insulin, and maintained until day 10, with media change every 2 days. On day 10 media is changed to RPMI with B27. The media is changed to RPMI no glucose with B27 on day 11 for 3 days, then changed back to RPMI with B27. On day 15 the media is changed RPMI no glucose with B27 for another 3 days. Afterwards on day 18, media is changed to maturation media, which the iPSC-CMs are maintained in until usage. Maturation media is changed every 3 days.

Proximity ligation assay

Proximity ligation assay was performed using Duolink In Situ Red Starter Kit Mouse/Rabbit (Sigma DUO92101) according to the manufacturer's instructions. Fixation, blocking, permeabilization, and primary antibody incubation were performed identically as in the immunofluorescence protocol. Following the last after primary antibody incubation, mice PLUS PLA probe and rabbit MINUS PLA probe diluted in the supplied antibody dilutant was added to the coverslip and incubated at 37°C for 1 hour. The sample was then washed twice for 5 minutes each with the supplied wash buffer A. Then diluted ligation mix with ligase is added to the sample and incubated at 37°C for 30 minutes. The sample was then washed twice for 5 minutes each with wash buffer A. Finally, the amplification mix with polymerase was added to the sample and incubated at 37°C for 100 minutes. the sample was washed with the supplied

wash buffer B twice for 10 minutes each, then once with 0.01X wash buffer B. The sample is then mounted with DUOLINK In Situ Mounting Medium with DAPI (Sigma DUO82040).

RNA sequencing

RNA isolation, and sequencing. RNA was extracted from iPSC and cardiomyocyte cells using the QIAGEN miRNeasy Mini Kit (Qiagen, 217004) as advised by the manufacturers. Next generation sequencing (NGS) libraries were created using the Illumina Stranded Total RNA Prep with Ribo-Zero Plus (Illumina, 20040525) kit. Sequencing was performed on an Illumina NovaSeq 6000 instrument at Praxis Genomics LLC. Alignment of FASTQ files was performed against the GRCh38 reference by HISAT2 (v2.2.1). Accurate reconstruction of all transcript isoforms was performed by StringTie (v2.2.0), with gene read count abundance determined by featureCounts (v2.0.1). Differential expression analysis was performed by DESeq2 for library size normalization and statistical significance calculations. Differentially expressed genes were selected with the threshold of $|\log_2FC| > 1$ and $FDR < 0.00005$. GO enrichment analysis was performed with Panther. Pathway analysis performed by Qiagen IPA.

Proteomic analysis

Three samples of each genotype of iPSC-CMs were detached with 1x TrypLE select enzyme (Gibco 12563011) and pelleted in 1.5ml microcentrifuge tubes. The cell pellet was washed 3x with PBS. After the last wash, the cell pellet was flash frozen in liquid nitrogen. The samples were submitted to the Columbia Proteomics and Macromolecular Crystallography Shared Resource at the Herbert Irving Comprehensive Cancer Center for global quantitative proteomic analysis. Significantly changed protein abundance was determined by un-paired t-test with a threshold for significance of $p < 0.05$ (permutation-based FDR correction) and 0.58 \log_2FC . Enrichment analysis was performed with Panther.

Metabolomic Analysis

Adherent iPSC-CMs on a 6 well plate were washed 2x with ice cold PBS. After the last wash is removed, the cells are flash frozen by placing the entire plate onto a dried ice slurry. 1ml of 80% (v/v) methanol (pre-chilled in a dry ice slurry) was added to each well. The cells were detached using a rubber-tipped cell scraper and the cell suspension is transferred into precooled (dry ice) Eppendorf tube. The samples are submitted to the Columbia Quantitative Proteomics and Metabolomics Center for untargeted metabolomics. Three samples of each genotype was submitted. Cell number was used as normalization. Cell number for each treatment was obtained by counting a 4th well that was plated at the exact same density as the other 3 wells harvested. Overrepresentation analysis was performed using Metaboanalyst.

References

- Aaronson, R.P., and G. Blobel. 1974. On the attachment of the nuclear pore complex. *J Cell Biol.* 62:746-754.
- Abdalla, S., X. Fu, S.S. Elzahwy, K. Klaetschke, T. Streichert, and U. Quitterer. 2011. Up-regulation of the cardiac lipid metabolism at the onset of heart failure. *Cardiovasc Hematol Agents Med Chem.* 9:190-206.
- Agarwal, A.K., J.P. Fryns, R.J. Auchus, and A. Garg. 2003. Zinc metalloproteinase, ZMPSTE24, is mutated in mandibuloacral dysplasia. *Hum Mol Genet.* 12:1995-2001.
- Ahmed, K., H. Dehghani, P. Rugg-Gunn, E. Fussner, J. Rossant, and D.P. Bazett-Jones. 2010. Global Chromatin Architecture Reflects Pluripotency and Lineage Commitment in the Early Mouse Embryo. *Plos One.* 5.
- Arbustini, E., A. Pilotto, A. Repetto, M. Grasso, A. Negri, M. Diegoli, C. Campana, L. Scelsi, E. Baldini, and A. Gavazzi. 2002. Autosomal dominant dilated cardiomyopathy with atrioventricular block: a lamin A/C defect-related disease. *Journal of the American College of Cardiology.* 39:981-990.
- Arimura, T., A. Helbling-Leclerc, C. Massart, S. Varnous, F. Niel, E. Lacène, Y. Fromes, M. Toussaint, A.M. Mura, D.I. Keller, H. Amthor, R. Isnard, M. Malissen, K. Schwartz, and G. Bonne. 2005. Mouse model carrying H222P-Lmna mutation develops muscular dystrophy and dilated cardiomyopathy similar to human striated muscle laminopathies. *Hum Mol Genet.* 14:155-169.
- Astejada, M.N., K. Goto, A. Nagano, S. Ura, S. Noguchi, I. Nonaka, I. Nishino, and Y.K. Hayashi. 2007. Emerinopathy and laminopathy clinical, pathological and molecular features of muscular dystrophy with nuclear envelopathy in Japan. *Acta Myol.* 26:159-164.
- Augustus, A.S., J. Buchanan, T.S. Park, K. Hirata, H.L. Noh, J. Sun, S. Homma, J. D'Armiento, E.D. Abel, and I.J. Goldberg. 2006. Loss of lipoprotein lipase-derived fatty acids leads to increased cardiac glucose metabolism and heart dysfunction. *J Biol Chem.* 281:8716-8723.
- Beck, L.A., T.J. Hosick, and M. Sinensky. 1990. Isoprenylation Is Required for the Processing of the Lamin-a Precursor. *J Cell Biol.* 110:1489-1499.
- Beedle, A.M., A.J. Turner, Y. Saito, J.D. Lueck, S.J. Foltz, M.J. Fortunato, P.M. Nienaber, and K.P. Campbell. 2012. Mouse fukutin deletion impairs dystroglycan processing and recapitulates muscular dystrophy. *J Clin Invest.* 122:3330-3342.
- Bekdash, R., J.R. Quejada, S. Ueno, F. Kawano, K. Morikawa, A.D. Klein, K. Matsumoto, T.C. Lee, K. Nakanishi, A. Chalan, T.M. Lee, R. Liu, S. Homma, C.S. Lin, M.V. Yelshanskaya, A.I. Sobolevsky, K. Goda, and M. Yazawa. 2021. GEM-IL: A highly responsive fluorescent lactate indicator. *Cell Rep Methods.* 1:100092.
- Benedetti, S., E. Bertini, S. Iannaccone, C. Angelini, M. Trisciani, D. Toniolo, B. Sferrazza, P. Carrera, G. Comi, M. Ferrari, A. Quattrini, and S.C. Previtali. 2005. Dominant LMNA mutations can cause combined muscular dystrophy and peripheral neuropathy. *J Neurol Neurosurg Psychiatry.* 76:1019-1021.
- Berk, J.M., S. Maitra, A.W. Dawdy, J. Shabanowitz, D.F. Hunt, and K.L. Wilson. 2013. O-Linked β -N-acetylglucosamine (O-GlcNAc) regulates emerin binding to barrier to autointegration factor (BAF) in a chromatin- and lamin B-enriched "niche". *J Biol Chem.* 288:30192-30209.
- Bertacchini, J., F. Beretti, V. Cenni, M. Guida, F. Gibellini, L. Mediani, O. Marin, N.M. Maraldi, A. de Pol, G. Lattanzi, L. Cocco, and S. Marmioli. 2013. The protein kinase Akt/PKB regulates both prelamin A degradation and Lmna gene expression. *Faseb j.* 27:2145-2155.

- Bertero, A., P.A. Fields, A.S.T. Smith, A. Leonard, K. Beussman, N.J. Sniadecki, D.H. Kim, H.F. Tse, L. Pabon, J. Shendure, W.S. Noble, and C.E. Murry. 2019. Chromatin compartment dynamics in a haploinsufficient model of cardiac laminopathy. *J Cell Biol.* 218:2919-2944.
- Bertrand, A.T., L. Renou, A. Papadopoulos, M. Beuvin, E. Lacene, C. Massart, C. Ottolenghi, V. Decostre, S. Maron, and S. Schlossarek. 2012. DelK32-lamin A/C has abnormal location and induces incomplete tissue maturation and severe metabolic defects leading to premature death. *Hum Mol Genet.* 21:1037-1048.
- Biamonti, G., M. Giacca, G. Perini, G. Contreas, L. Zentilin, F. Weighardt, M. Guerra, G. Della Valle, S. Saccone, S. Riva, and et al. 1992. The gene for a novel human lamin maps at a highly transcribed locus of chromosome 19 which replicates at the onset of S-phase. *Mol Cell Biol.* 12:3499-3506.
- Bione, S., E. Maestrini, S. Rivella, M. Mancini, S. Regis, G. Romeo, and D. Toniolo. 1994. Identification of a Novel X-Linked Gene Responsible for Emery-Dreifuss Muscular-Dystrophy. *Nature Genetics.* 8:323-327.
- Bonne, G., M.R. Di Barletta, S. Varnous, H.M. Becane, E.H. Hammouda, L. Merlini, F. Muntoni, C.R. Greenberg, F. Gary, J.A. Urtizbera, D. Duboc, M. Fardeau, D. Toniolo, and K. Schwartz. 1999. Mutations in the gene encoding lamin A/C cause autosomal dominant Emery-Dreifuss muscular dystrophy. *Nature Genetics.* 21:285-288.
- Bonne, G., E. Mercuri, A. Muchir, A. Urtizbera, H.M. Bécane, D. Recan, L. Merlini, M. Wehnert, R. Boor, U. Reuner, M. Vorgerd, E.M. Wicklein, B. Eymard, D. Duboc, I. Penisson-Besnier, J.M. Cuisset, X. Ferrer, I. Desguerre, D. Lacombe, K. Bushby, C. Pollitt, D. Toniolo, M. Fardeau, K. Schwartz, and F. Muntoni. 2000. Clinical and molecular genetic spectrum of autosomal dominant Emery-Dreifuss muscular dystrophy due to mutations of the lamin A/C gene. *Ann Neurol.* 48:170-180.
- Bonne, G., and S. Quijano-Roy. 2013. Emery-Dreifuss muscular dystrophy, laminopathies, and other nuclear envelopathies. *Handb Clin Neurol.* 113:1367-1376.
- Boren, J., M. Veniant, and S. Young. 1998. Apo B100-containing lipoproteins are secreted by the heart. *The Journal of clinical investigation.* 101:1197-1202.
- Boriani, G., E. Biagini, M. Ziacchi, V.L. Malavasi, M. Vitolo, M. Talarico, E. Mauro, G. Gorlato, and G. Lattanzi. 2018. Cardiolaminopathies from bench to bedside: challenges in clinical decision-making with focus on arrhythmia-related outcomes. *Nucleus-Phila.* 9:442-459.
- Boschmann, M., S. Engeli, C. Moro, A. Luedtke, F. Adams, K. Gorzelniak, G. Rahn, A. Mähler, K. Dobberstein, A. Krüger, S. Schmidt, S. Spuler, F.C. Luft, S.R. Smith, H.H. Schmidt, and J. Jordan. 2010. LMNA mutations, skeletal muscle lipid metabolism, and insulin resistance. *J Clin Endocrinol Metab.* 95:1634-1643.
- Bourgeois, B., B. Gilquin, C. Tellier-Lebègue, C. Östlund, W. Wu, J. Pérez, P. El Hage, F. Lallemand, H.J. Worman, and S. Zinn-Justin. 2013. Inhibition of TGF- β signaling at the nuclear envelope: characterization of interactions between MAN1, Smad2 and Smad3, and PPM1A. *Sci Signal.* 6:ra49.
- Brady, G.F., R. Kwan, P.J. Ulintz, P. Nguyen, S. Bassirian, V. Basrur, A.I. Nesvizhskii, R. Looma, and M.B. Omary. 2018. Nuclear lamina genetic variants, including a truncated LAP2, in twins and siblings with nonalcoholic fatty liver disease. *Hepatology.* 67:1710-1725.
- Brodsky, G.L., F. Muntoni, S. Miocic, G. Sinagra, C. Sewry, and L. Mestroni. 2000. Lamin A/C gene mutation associated with dilated cardiomyopathy with variable skeletal muscle involvement. *Circulation.* 101:473-476.
- Broers, J.L.V., and F.C.S. Ramaekers. 2014. The Role of the Nuclear Lamina in Cancer and Apoptosis. *In Cancer Biology and the Nuclear Envelope: Recent Advances May Elucidate Past Paradoxes.* E.C. Schirmer and J.I. de las Heras, editors. Springer New York, New York, NY. 27-48.

- Brown, C.A., J. Scharner, K. Felice, M.N. Meriggioli, M. Tarnopolsky, M. Bower, P.S. Zammit, J.R. Mendell, and J.A. Ellis. 2011. Novel and recurrent EMD mutations in patients with Emery-Dreifuss muscular dystrophy, identify exon 2 as a mutation hot spot. *J Hum Genet.* 56:589-594.
- Brüning, J.C., M.D. Michael, J.N. Winnay, T. Hayashi, D. Hörsch, D. Accili, L.J. Goodyear, and C.R. Kahn. 1998. A muscle-specific insulin receptor knockout exhibits features of the metabolic syndrome of NIDDM without altering glucose tolerance. *Mol Cell.* 2:559-569.
- Buchwalter, A. 2023. Intermediate, but not average: The unusual lives of the nuclear lamin proteins. *Curr Opin Cell Biol.* 84:102220.
- Butin-Israeli, V., S.A. Adam, A.E. Goldman, and R.D. Goldman. 2012. Nuclear lamin functions and disease. *Trends Genet.* 28:464-471.
- Cai, M., Y. Huang, R. Ghirlando, K.L. Wilson, R. Craigie, and G.M. Clore. 2001. Solution structure of the constant region of nuclear envelope protein LAP2 reveals two LEM-domain structures: one binds BAF and the other binds DNA. *The EMBO journal.* 20:4399-4407.
- Cao, H., and R.A. Hegele. 2000. Nuclear lamin A/C R482Q mutation in Canadian kindreds with Dunnigan-type familial partial lipodystrophy. *Hum Mol Genet.* 9:109-112.
- Capanni, C., E. Mattioli, M. Columbaro, E. Lucarelli, V.K. Parnaik, G. Novelli, M. Wehnert, V. Cenni, N.M. Maraldi, S. Squarzone, and G. Lattanzi. 2005. Altered pre-lamin A processing is a common mechanism leading to lipodystrophy. *Hum Mol Genet.* 14:1489-1502.
- Carboni, N., L. Politano, M. Floris, A. Mateddu, E. Solla, S. Olla, L. Maggi, M. Antonietta Maioli, R. Piras, E. Cocco, G. Marrosu, and M. Giovanna Marrosu. 2013. Overlapping syndromes in laminopathies: a meta-analysis of the reported literature. *Acta Myol.* 32:7-17.
- Carmosino, M., A. Gerbino, G. Schena, G. Procino, R. Miglionico, C. Forleo, S. Favale, and M. Svelto. 2016. The expression of Lamin A mutant R321X leads to endoplasmic reticulum stress with aberrant Ca(2+) handling. *J Cell Mol Med.* 20:2194-2207.
- Caux, F., E. Dubosclard, O. Lascols, B. Buendia, O. Chazouillères, A. Cohen, J.C. Courvalin, L. Laroche, J. Capeau, C. Vigouroux, and S. Christin-Maitre. 2003. A new clinical condition linked to a novel mutation in lamins A and C with generalized lipoatrophy, insulin-resistant diabetes, disseminated leukomelanodermic papules, liver steatosis, and cardiomyopathy. *J Clin Endocrinol Metab.* 88:1006-1013.
- Čaval, T., A.J.R. Heck, and K.R. Reiding. 2021. Meta-heterogeneity: Evaluating and Describing the Diversity in Glycosylation Between Sites on the Same Glycoprotein. *Mol Cell Proteomics.* 20:100010.
- Cestan, R., and P. Lejonne. 1902. Une myopathie avec retractions familiales. *Nouv Iconograph Salpetriere.* 15:38-52.
- Chai, R.J., H. Werner, P.Y. Li, Y.L. Lee, K.T. Nyein, I. Solovei, T.D.A. Luu, B. Sharma, R. Navasankari, M. Maric, L.Y.E. Sim, Y.J. Loh, E. Aliwarga, J.W.L. Cheong, A. Chojnowski, M.I. Autio, Y. Haiyang, K.K. Boon Tan, C.T. Keng, S.L. Ng, W.L. Chew, M. Ferenczi, B. Burke, R.S.Y. Foo, and C.L. Stewart. 2021. Disrupting the LINC complex by AAV mediated gene transduction prevents progression of Lamin induced cardiomyopathy. *Nat Commun.* 12:4722.
- Chandran, S., V.S. Rajadurai, W.H. Hoi, S.E. Flanagan, K. Hussain, and F. Yap. 2020. A Novel HNF4A Mutation Causing Three Phenotypic Forms of Glucose Dysregulation in a Family. *Frontiers in Pediatrics.* 8.
- Chatham, J.C., Z.-P. Gao, A. Bonen, and J.R. Forder. 1999. Preferential inhibition of lactate oxidation relative to glucose oxidation in the rat heart following diabetes. *Cardiovascular research.* 43:96-106.

- Chaturvedi, P., and V.K. Parnaik. 2010. Lamin A rod domain mutants target heterochromatin protein 1alpha and beta for proteasomal degradation by activation of F-box protein, FBXW10. *Plos One*. 5:e10620.
- Chawla, A., J.J. Repa, R.M. Evans, and D.J. Mangelsdorf. 2001. Nuclear receptors and lipid physiology: opening the X-files. *Science*. 294:1866-1870.
- Cheedipudi, S.M., S.J. Matkovich, C. Coarfa, X. Hu, M.J. Robertson, M. Sweet, M. Taylor, L. Mestroni, J. Cleveland, J.T. Willerson, P. Gurha, and A.J. Marian. 2019. Genomic Reorganization of Lamin-Associated Domains in Cardiac Myocytes Is Associated With Differential Gene Expression and DNA Methylation in Human Dilated Cardiomyopathy. *Circ Res*. 124:1198-1213.
- Chen, H.Y., X.B. Zheng, and Y.X. Zheng. 2014. Age-Associated Loss of Lamin-B Leads to Systemic Inflammation and Gut Hyperplasia. *Cell*. 159:829-843.
- Chen, L., L. Lee, B.A. Kudlow, H.G. Dos Santos, O. Sletvold, Y. Shafeghati, E.G. Botha, A. Garg, N.B. Hanson, G.M. Martin, I.S. Mian, B.K. Kennedy, and J. Oshima. 2003. LMNA mutations in atypical Werner's syndrome. *Lancet*. 362:440-445.
- Chen, L., S. Luo, A. Dupre, R.P. Vasoya, A. Parthasarathy, R. Aita, R. Malhotra, J. Hur, N.H. Toke, E. Chiles, M. Yang, W.H. Cao, J. Flores, C.E. Ellison, N. Gao, A. Sahota, X.Y. Su, E.M. Bonder, and M.P. Verzi. 2021. The nuclear receptor HNF4 drives a brush border gene program conserved across murine intestine, kidney, and embryonic yolk sac. *Nat Commun*. 12.
- Choi, J.C., W. Wu, A. Muchir, S. Iwata, S. Homma, and H.J. Worman. 2012. Dual specificity phosphatase 4 mediates cardiomyopathy caused by lamin A/C (LMNA) gene mutation. *J Biol Chem*. 287:40513-40524.
- Cobb, A.M., T.V. Murray, D.T. Warren, Y. Liu, and C.M. Shanahan. 2016. Disruption of PCNA-lamins A/C interactions by prelamin A induces DNA replication fork stalling. *Nucleus-Phila*. 7:498-511.
- Coffeen, C.M., C.E. McKenna, A.H. Koeppen, N.M. Plaster, N. Maragakis, J. Mihalopoulos, J.D. Schwankhaus, K.M. Flanigan, R.G. Gregg, L.J. Ptacek, and Y.H. Fu. 2000. Genetic localization of an autosomal dominant leukodystrophy mimicking chronic progressive multiple sclerosis to chromosome 5q31. *Hum Mol Genet*. 9:787-793.
- Coffinier, C., H.-J. Jung, Z. Li, C. Nobumori, U.J. Yun, E.A. Farber, B.S. Davies, M.M. Weinstein, S.H. Yang, and J. Lammerding. 2010. Direct synthesis of lamin A, bypassing prelamin A processing, causes misshapen nuclei in fibroblasts but no detectable pathology in mice. *J Biol Chem*. 285:20818-20826.
- Columbaro, M., E. Mattioli, G. Lattanzi, C. Rutigliano, A. Ognibene, N.M. Maraldi, and S. Squarzone. 2001. Staurosporine treatment and serum starvation promote the cleavage of emerin in cultured mouse myoblasts: involvement of a caspase-dependent mechanism. *Febs Lett*. 509:423-429.
- Constantinescu, D., H.L. Gray, P.J. Sammak, G.P. Schatten, and A.B. Csoka. 2006. Lamin A/C expression is a marker of mouse and human embryonic stem cell differentiation. *Stem Cells*. 24:177-185.
- Crasto, S., I. My, and E. Di Pasquale. 2020. The Broad Spectrum of LMNA Cardiac Diseases: From Molecular Mechanisms to Clinical Phenotype. *Front Physiol*. 11:761.
- Crisp, M., Q. Liu, K. Roux, J.B. Rattner, C. Shanahan, B. Burke, P.D. Stahl, and D. Hodzic. 2006. Coupling of the nucleus and cytoplasm: role of the LINC complex. *J Cell Biol*. 172:41-53.
- Cristofoli, F., T. Moss, H.W. Moore, K. Devriendt, H. Flanagan-Steet, M. May, J. Jones, F. Roelens, C. Fons, A. Fernandez, L. Martorell, A. Selicorni, S. Maitz, G. Vitiello, G. Van der Hoeven, S.A. Skinner, M. Bollen, J.R. Vermeesch, R. Steet, and H. Van Esch. 2020. De Novo Variants in LMNB1 Cause Pronounced Syndromic Microcephaly and Disruption of Nuclear Envelope Integrity. *Am J Hum Genet*. 107:753-762.

- D'Angelo, M.A., and M.W. Hetzer. 2006. The role of the nuclear envelope in cellular organization. *Cell Mol Life Sci.* 63:316-332.
- Dauer, W.T., and H.J. Worman. 2009. The nuclear envelope as a signaling node in development and disease. *Dev Cell.* 17:626-638.
- Davies, B.S., R.H. Barnes, Y. Tu, S. Ren, D.A. Andres, H.P. Spielmann, J. Lammerding, Y. Wang, S.G. Young, and L.G. Fong. 2010. An accumulation of non-farnesylated prelamin A causes cardiomyopathy but not progeria. *Hum Mol Genet.* 19:2682-2694.
- De Sandre-Giovannoli, A., R. Bernard, P. Cau, C. Navarro, J. Amiel, I. Boccaccio, S. Lyonnet, C.L. Stewart, A. Munnich, M. Le Merrer, and N. Lévy. 2003. Lamin a truncation in Hutchinson-Gilford progeria. *Science.* 300:2055.
- De Sandre-Giovannoli, A., M. Chaouch, S. Kozlov, J.M. Vallat, M. Tazir, N. Kassouri, P. Szepietowski, T. Hammadouche, A. Vandenberghe, C.L. Stewart, D. Grid, and N. Lévy. 2002. Homozygous defects in LMNA, encoding lamin A/C nuclear-envelope proteins, cause autosomal recessive axonal neuropathy in human (Charcot-Marie-Tooth disorder type 2) and mouse. *Am J Hum Genet.* 70:726-736.
- De Vos, W.H., F. Houben, R.A. Hoebe, R. Hennekam, B. van Engelen, E.M. Manders, F.C. Ramaekers, J.L. Broers, and P. Van Oostveldt. 2010. Increased plasticity of the nuclear envelope and hypermobility of telomeres due to the loss of A-type lamins. *Biochim Biophys Acta.* 1800:448-458.
- DeBusk, F.L. 1972. The Hutchinson-Gilford progeria syndrome. Report of 4 cases and review of the literature. *J Pediatr.* 80:697-724.
- Dechat, T., K. Gesson, and R. Foisner. 2010. Lamina-independent lamins in the nuclear interior serve important functions. *Cold Spring Harb Symp Quant Biol.* 75:533-543.
- Demmerle, J., A.J. Koch, and J.M. Holaska. 2012. The nuclear envelope protein emerin binds directly to histone deacetylase 3 (HDAC3) and activates HDAC3 activity. *J Biol Chem.* 287:22080-22088.
- Dhe-Paganon, S., E.D. Werner, Y.-I. Chi, and S.E. Shoelson. 2002. Structure of the globular tail of nuclear lamin. *J Biol Chem.* 277:17381-17384.
- Ding, J.H., X. Xu, D. Yang, P.H. Chu, N.D. Dalton, Z. Ye, J.M. Yeakley, H. Cheng, R.P. Xiao, J. Ross, J. Chen, and X.D. Fu. 2004. Dilated cardiomyopathy caused by tissue-specific ablation of SC35 in the heart. *Embo j.* 23:885-896.
- Dittmer, T.A., and T. Misteli. 2011. The lamin protein family. *Genome Biol.* 12:222.
- Dong, S., L. Qian, Z. Cheng, C. Chen, K. Wang, S. Hu, X. Zhang, and T. Wu. 2021a. Lactate and Myocardial Energy Metabolism. *Frontiers in Physiology.* 12.
- Dong, S., L. Qian, Z. Cheng, C. Chen, K. Wang, S. Hu, X. Zhang, and T. Wu. 2021b. Lactate and Myocardial Energy Metabolism. *Front Physiol.* 12:715081.
- Dreger, M., L. Bengtsson, T. Schoneberg, H. Otto, and F. Hucho. 2001. Nuclear envelope proteomics: Novel integral membrane proteins of the inner nuclear membrane. *P Natl Acad Sci USA.* 98:11943-11948.
- Dreifuss, F.E., and G.R. Hogan. 1961. Survival in X-Chromosomal Muscular Dystrophy. *Neurology.* 11:734-&.
- Duband-Goulet, I., J.C. Courvalin, and B. Buendia. 1998. LBR, a chromatin and lamin binding protein from the inner nuclear membrane, is proteolyzed at late stages of apoptosis. *J Cell Sci.* 111:1441-1451.
- Dutour, A., P. Roll, B. Gaborit, S. Courrier, M.-C. Alessi, D.-A. Tregouet, F. Angelis, A. Robaglia-Schlupp, N. Lesavre, P. Cau, N. Lévy, C. Badens, and P.-E. Morange. 2011. High prevalence of laminopathies among patients with metabolic syndrome. *Hum Mol Genet.* 20:3779-3786.
- Earle, A.J., T.J. Kirby, G.R. Fedorchak, P. Isermann, J. Patel, S. Iruvanti, S.A. Moore, G. Bonne, L.L. Wallrath, and J. Lammerding. 2020. Mutant lamins cause nuclear envelope rupture and DNA damage in skeletal muscle cells. *Nature Materials.* 19:464-473.

- Eckersley-Maslin, M.A., J.H. Bergmann, Z. Lazar, and D.L. Spector. 2013. Lamin A/C is expressed in pluripotent mouse embryonic stem cells. *Nucleus-Phila.* 4:53-60.
- Ellis, J.A., M. Craxton, J.R. Yates, and J. Kendrick-Jones. 1998. Aberrant intracellular targeting and cell cycle-dependent phosphorylation of emerin contribute to the Emery-Dreifuss muscular dystrophy phenotype. *J Cell Sci.* 111 (Pt 6):781-792.
- Emery, A.E. 2002. The muscular dystrophies. *Lancet.* 359:687-695.
- Emery, A.E., and F.E. Dreifuss. 1966. Unusual type of benign x-linked muscular dystrophy. *J Neurol Neurosurg Psychiatry.* 29:338-342.
- En, A., H. Bogireddi, B. Thomas, A. Stutzman, S. Ikegami, B. LaForest, O. Almakki, P. Pytel, I.P. Moskowitz, and K. Ikegami. 2023. The cGAS-STING pathway is dispensable in a mouse model of LMNA-cardiomyopathy despite nuclear envelope rupture. *bioRxiv:2023.2008.2028.555134.*
- Eriksson, M., W.T. Brown, L.B. Gordon, M.W. Glynn, J. Singer, L. Scott, M.R. Erdos, C.M. Robbins, T.Y. Moses, P. Berglund, A. Dutra, E. Pak, S. Durkin, A.B. Csoka, M. Boehnke, T.W. Glover, and F.S. Collins. 2003. Recurrent de novo point mutations in lamin A cause Hutchinson-Gilford progeria syndrome. *Nature.* 423:293-298.
- Fagone, P., and S. Jackowski. 2009. Membrane phospholipid synthesis and endoplasmic reticulum function. *J Lipid Res.* 50 Suppl:S311-316.
- Fatkin, D., C. MacRae, T. Sasaki, M.R. Wolff, M. Porcu, M. Frenneaux, J. Atherton, H.J. Vidaillet, S. Spudich, U. De Girolami, J.G. Seidman, C.E. Seidman, F. Muntoni, G. Muehle, W. Johnson, and B. McDonough. 1999. Missense mutations in the rod domain of the lamin A/C gene as causes of dilated cardiomyopathy and conduction-system disease. *New Engl J Med.* 341:1715-1724.
- Fernandez, A., M. Bautista, L. Wu, and F. Pinaud. 2022. Emerin self-assembly and nucleoskeletal coupling regulate nuclear envelope mechanics against stress. *J Cell Sci.* 135.
- Feyen, D.A.M., W.L. McKeithan, A.A.N. Bruyneel, S. Spiering, L. Hörmann, B. Ulmer, H. Zhang, F. Briganti, M. Schweizer, B. Hegyi, Z. Liao, R.P. Pölönen, K.S. Ginsburg, C.K. Lam, R. Serrano, C. Wahlquist, A. Kreymerman, M. Vu, P.L. Amatya, C.S. Behrens, S. Ranjbarvaziri, R.G.C. Maas, M. Greenhaw, D. Bernstein, J.C. Wu, D.M. Bers, T. Eschenhagen, C.M. Metallo, and M. Mercola. 2020. Metabolic Maturation Media Improve Physiological Function of Human iPSC-Derived Cardiomyocytes. *Cell Rep.* 32:107925.
- Fisher, D.Z., N. Chaudhary, and G. Blobel. 1986. cDNA sequencing of nuclear lamins A and C reveals primary and secondary structural homology to intermediate filament proteins. *Proc Natl Acad Sci U S A.* 83:6450-6454.
- Flis, V.V., and G. Daum. 2013. Lipid transport between the endoplasmic reticulum and mitochondria. *Cold Spring Harb Perspect Biol.* 5.
- Fong, L.G., J.K. Ng, J. Lammerding, T.A. Vickers, M. Meta, N. Coté, B. Gavino, X. Qiao, S.Y. Chang, and S.R. Young. 2006. Prelamin A and lamin A appear to be dispensable in the nuclear lamina. *The Journal of clinical investigation.* 116:743-752.
- Fu, S.N., S.M. Watkins, and G.S. Hotamisligil. 2012. The Role of Endoplasmic Reticulum in Hepatic Lipid Homeostasis and Stress Signaling. *Cell Metab.* 15:623-634.
- Furukawa, K. 1999. LAP2 binding protein 1 (L2BP1/BAF) is a candidate mediator of LAP2-chromatin interaction. *J Cell Sci.* 112:2485-2492.
- Gabriel-Costa, D., T.F. da Cunha, L.R.G. Bechara, R.S. Fortunato, L.H.M. Bozi, M.d.A. Coelho, M.L. Barreto-Chaves, and P.C. Brum. 2015. Lactate Up-Regulates the Expression of Lactate Oxidation Complex-Related Genes in Left Ventricular Cardiac Tissue of Rats. *Plos One.* 10:e0127843.
- Galassi, G., M.G. Modena, A. Benassi, R. Nemni, M. Gibertoni, G. Volpi, and A. Colombo. 1986. Autosomal-dominant dystrophy with humeroperoneal weakness and cardiopathy: a genetic variant of Emery-Dreifuss disease? *Ital J Neurol Sci.* 7:125-132.

- Galganski, L., M.O. Urbanek, and W.J. Krzyzosiak. 2017. Nuclear speckles: molecular organization, biological function and role in disease. *Nucleic Acids Res.* 45:10350-10368.
- Gao, N., K. Zhao, Y. Cao, X. Ren, H. Jing, G. Xing, W.C. Xiong, and L. Mei. 2020a. A Role of Lamin A/C in Preventing Neuromuscular Junction Decline in Mice. *J Neurosci.* 40:7203-7215.
- Gao, P., Z. Yan, and Z. Zhu. 2020b. Mitochondria-Associated Endoplasmic Reticulum Membranes in Cardiovascular Diseases. *Frontiers in Cell and Developmental Biology.* 8.
- Garg, A., R.A. Speckman, and A.M. Bowcock. 2002. Multisystem dystrophy syndrome due to novel missense mutations in the amino-terminal head and alpha-helical rod domains of the lamin A/C gene. *Am J Med.* 112:549-555.
- Geiss-Friedlander, R., and F. Melchior. 2007. Concepts in sumoylation: a decade on. *Nat Rev Mol Cell Biol.* 8:947-956.
- Gerace, L., and G. Blobel. 1980. The nuclear envelope lamina is reversibly depolymerized during mitosis. *Cell.* 19:277-287.
- Gerace, L., A. Blum, and G. Blobel. 1978. Immunocytochemical localization of the major polypeptides of the nuclear pore complex-lamina fraction. Interphase and mitotic distribution. *J Cell Biol.* 79:546-566.
- Gerace, L., and M.D. Huber. 2012. Nuclear lamina at the crossroads of the cytoplasm and nucleus. *J Struct Biol.* 177:24-31.
- Gesson, K., P. Rescheneder, M.P. Skoruppa, A. von Haeseler, T. Dechat, and R. Foisner. 2016. A-type lamins bind both hetero- and euchromatin, the latter being regulated by lamina-associated polypeptide 2 alpha. *Genome Res.* 26:462-473.
- Gigante, C.M., M. Dibattista, F.N. Dong, X.B. Zheng, S.B.A. Yue, S.G. Young, J. Reisert, Y.X. Zheng, and H.Q. Zhao. 2017. Lamin B1 is required for mature neuron-specific gene expression during olfactory sensory neuron differentiation. *Nat Commun.* 8.
- Gigli, M., R.L. Begay, G. Morea, S.L. Graw, G. Sinagra, M.R. Taylor, H. Granzier, and L. Mestroni. 2016. A review of the giant protein titin in clinical molecular diagnostics of cardiomyopathies. *Frontiers in cardiovascular medicine.* 3:21.
- Goizet, C., R.B. Yaou, L. Demay, P. Richard, S. Bouillot, M. Rouanet, E. Hermosilla, G. Le Masson, A. Lagueny, G. Bonne, and X. Ferrer. 2004. A new mutation of the lamin A/C gene leading to autosomal dominant axonal neuropathy, muscular dystrophy, cardiac disease, and leuconychia. *J Med Genet.* 41:e29.
- Goldman, R.D., Y. Gruenbaum, R.D. Moir, D.K. Shumaker, and T.P. Spann. 2002. Nuclear lamins: building blocks of nuclear architecture. *Genes Dev.* 16:533-547.
- Gong, G., M. Song, G. Csordas, D.P. Kelly, S.J. Matkovich, and G.W. Dorn, 2nd. 2015. Parkin-mediated mitophagy directs perinatal cardiac metabolic maturation in mice. *Science.* 350:aad2459.
- González, J.M., A. Navarro-Puche, B. Casar, P. Crespo, and V. Andrés. 2008. Fast regulation of AP-1 activity through interaction of lamin A/C, ERK1/2, and c-Fos at the nuclear envelope. *J Cell Biol.* 183:653-666.
- Gotic, I., M. Leschnik, U. Kolm, M. Markovic, B.J. Haubner, K. Biadasiewicz, B. Metzler, C.L. Stewart, and R. Foisner. 2010a. Lamina-associated polypeptide 2alpha loss impairs heart function and stress response in mice. *Circ Res.* 106:346-353.
- Gotic, I., W.M. Schmidt, K. Biadasiewicz, M. Leschnik, R. Spilka, J. Braun, C.L. Stewart, and R. Foisner. 2010b. Loss of LAP2 alpha delays satellite cell differentiation and affects postnatal fiber-type determination. *Stem Cells.* 28:480-488.
- Gruenbaum, Y., and R. Foisner. 2015. Lamins: Nuclear Intermediate Filament Proteins with Fundamental Functions in Nuclear Mechanics and Genome Regulation. *Annual Review of Biochemistry.* 84:131-164.

- Guelen, L., L. Pagie, E. Brasset, W. Meuleman, M.B. Faza, W. Talhout, B.H. Eussen, A. de Klein, L. Wessels, W. de Laat, and B. van Steensel. 2008. Domain organization of human chromosomes revealed by mapping of nuclear lamina interactions. *Nature*. 453:948-951.
- Gueneau, L., A.T. Bertrand, J.P. Jais, M.A. Salih, T. Stojkovic, M. Wehnert, M. Hoeltzenbein, S. Spuler, S. Saitoh, A. Verschueren, C. Tranchant, M. Beuvin, E. Lacene, N.B. Romero, S. Heath, D. Zelenika, T. Voit, B. Eymard, R. Ben Yaou, and G. Bonne. 2009. Mutations of the FHL1 gene cause Emery-Dreifuss muscular dystrophy. *Am J Hum Genet*. 85:338-353.
- Guillín-Amarelle, C., A. Fernández-Pombo, S. Sánchez-Iglesias, and D. Araújo-Vilar. 2018. Lipodystrophic laminopathies: Diagnostic clues. *Nucleus-Phila*. 9:249-260.
- Guo, W., S. Schafer, M.L. Greaser, M.H. Radke, M. Liss, T. Govindarajan, H. Maatz, H. Schulz, S. Li, and A.M. Parrish. 2012. RBM20, a gene for hereditary cardiomyopathy, regulates titin splicing. *Nature medicine*. 18:766-773.
- Han, Y.C., J.A. Vidigal, P. Mu, E. Yao, I. Singh, A.J. González, C.P. Concepcion, C. Bonetti, P. Ogradowski, B. Carver, L. Selleri, D. Betel, C. Leslie, and A. Ventura. 2015. An allelic series of miR-17 ~ 92-mutant mice uncovers functional specialization and cooperation among members of a microRNA polycistron. *Nat Genet*. 47:766-775.
- Haque, F., D.J. Lloyd, D.T. Smallwood, C.L. Dent, C.M. Shanahan, A.M. Fry, R.C. Trembath, and S. Shackleton. 2006. SUN1 interacts with nuclear lamin A and cytoplasmic nesprins to provide a physical connection between the nuclear lamina and the cytoskeleton. *Molecular and cellular biology*. 26:3738-3751.
- Haque, F., D. Mazzeo, J.T. Patel, D.T. Smallwood, J.A. Ellis, C.M. Shanahan, and S. Shackleton. 2010. Mammalian SUN protein interaction networks at the inner nuclear membrane and their role in laminopathy disease processes. *J Biol Chem*. 285:3487-3498.
- Harada, T., J. Swift, J. Irianto, J.W. Shin, K.R. Spinler, A. Athirasala, R. Diegmiller, P.C. Dingal, I.L. Ivanovska, and D.E. Discher. 2014. Nuclear lamin stiffness is a barrier to 3D migration, but softness can limit survival. *J Cell Biol*. 204:669-682.
- Haraguchi, T., J.M. Holaska, M. Yamane, T. Koujin, N. Hashiguchi, C. Mori, K.L. Wilson, and Y. Hiraoka. 2004. Emerin binding to Btf, a death-promoting transcriptional repressor, is disrupted by a missense mutation that causes Emery-Dreifuss muscular dystrophy. *Eur J Biochem*. 271:1035-1045.
- Hart, G.W., C. Slawson, G. Ramirez-Correa, and O. Lagerlof. 2011. Cross talk between O-GlcNAcylation and phosphorylation: roles in signaling, transcription, and chronic disease. *Annu Rev Biochem*. 80:825-858.
- Hasper, J., K. Welle, K. Swovick, J. Hryhorenko, S. Ghaemmaghami, and A. Buchwalter. 2023. Long lifetime and tissue-specific accumulation of lamin A/C in Hutchinson–Gilford progeria syndrome. *J Cell Biol*. 223.
- Hasselberg, N.E., T. Edvardsen, H. Petri, K.E. Berge, T.P. Leren, H. Bundgaard, and K.H. Haugaa. 2014. Risk prediction of ventricular arrhythmias and myocardial function in Lamin A/C mutation positive subjects. *Europace*. 16:563-571.
- Haubner, B.J., M. Adamowicz-Brice, S. Khadayate, V. Tiefenthaler, B. Metzler, T. Aitman, and J.M. Penninger. 2012. Complete cardiac regeneration in a mouse model of myocardial infarction. *Aging (Albany NY)*. 4:966-977.
- Heald, R., and F. McKeon. 1990. Mutations of phosphorylation sites in lamin A that prevent nuclear lamina disassembly in mitosis. *Cell*. 61:579-589.
- Hegele, R. 2005. LMNA mutation position predicts organ system involvement in laminopathies. *Clin Genet*. 68:31-34.

- Hegele, R.A., H. Cao, D.M. Liu, G.A. Costain, V. Charlton-Menys, N.W. Rodger, and P.N. Durrington. 2006. Sequencing of the reannotated LMNB2 gene reveals novel mutations in patients with acquired partial lipodystrophy. *Am J Hum Genet.* 79:383-389.
- Helbling-Leclerc, A., G. Bonne, and K. Schwartz. 2002. Emery-Dreifuss muscular dystrophy. *Eur J Hum Genet.* 10:157-161.
- Hellemans, J., O. Preobrazhenska, A. Willaert, P. Debeer, P.C.M. Verdonk, T. Costa, K. Janssens, B. Menten, N. Van Roy, S.J.T. Vermeulen, R. Savarirayan, W. Van Hul, F. Vanhoenacker, D. Huylebroeck, A. De Paepe, J.M. Naeyaert, J. Vandesompele, F. Speleman, K. Verschueren, P.J. Coucke, and G.R. Mortier. 2004. Loss-of-function mutations in LEMD3 result in osteopoikilosis, Buschke-Ollendorff syndrome and melorheostosis. *Nature Genetics.* 36:1213-1218.
- Hershberger, R.E., and J.D. Siegfried. 2011. Update 2011: Clinical and Genetic Issues in Familial Dilated Cardiomyopathy. *Journal of the American College of Cardiology.* 57:1641-1649.
- Holaska, J.M., A.K. Kowalski, and K.L. Wilson. 2004. Emerin caps the pointed end of actin filaments: evidence for an actin cortical network at the nuclear inner membrane. *PLoS Biol.* 2:E231.
- Holaska, J.M., K.K. Lee, A.K. Kowalski, and K.L. Wilson. 2003. Transcriptional repressor germ cell-less (GCL) and barrier to autointegration factor (BAF) compete for binding to emerin in vitro. *J Biol Chem.* 278:6969-6975.
- Holaska, J.M., S. Rais-Bahrami, and K.L. Wilson. 2006. Lmo7 is an emerin-binding protein that regulates the transcription of emerin and many other muscle-relevant genes. *Hum Mol Genet.* 15:3459-3472.
- Holaska, J.M., and K.L. Wilson. 2007. An emerin "proteome": purification of distinct emerin-containing complexes from HeLa cells suggests molecular basis for diverse roles including gene regulation, mRNA splicing, signaling, mechanosensing, and nuclear architecture. *Biochemistry.* 46:8897-8908.
- Hozák, P., A.M. Sasseville, Y. Raymond, and P.R. Cook. 1995. Lamin proteins form an internal nucleoskeleton as well as a peripheral lamina in human cells. *J Cell Sci.* 108 (Pt 2):635-644.
- Ikegami, K., S. Secchia, O. Almakki, J.D. Lieb, and I.P. Moskowitz. 2020. Phosphorylated Lamin A/C in the Nuclear Interior Binds Active Enhancers Associated with Abnormal Transcription in Progeria. *Dev Cell.* 52:699-713.e611.
- Im, S.S., L.E. Hammond, L. Yousef, C. Nugas-Selby, D.J. Shin, Y.K. Seo, L.G. Fong, S.G. Young, and T.F. Osborne. 2009. Sterol regulatory element binding protein 1a regulates hepatic fatty acid partitioning by activating acetyl coenzyme A carboxylase 2. *Mol Cell Biol.* 29:4864-4872.
- Ishikawa, T., H. Mishima, J. Barc, M.P. Takahashi, K. Hirono, S. Terada, S. Kowase, T. Sato, Y. Mukai, Y. Yui, K. Ohkubo, H. Kimoto, H. Watanabe, Y. Hata, T. Aiba, S. Ohno, A. Chishaki, W. Shimizu, M. Horie, F. Ichida, A. Nogami, K.I. Yoshiura, J.J. Schott, and N. Makita. 2020. Cardiac Emerinopathy A Nonsyndromic Nuclear Envelopathy With Increased Risk of Thromboembolic Stroke Due to Progressive Atrial Standstill and Left Ventricular Noncompaction. *Circ-Arrhythmia Elec.* 13:1165-1174.
- Ivorra, C., M. Kubicek, J.M. Gonzalez, S.M. Sanz-Gonzalez, A. Alvarez-Barrientos, J.E. O'Connor, B. Burke, and V. Andres. 2006. A mechanism of AP-1 suppression through interaction of c-Fos with lamin A/C (vol 20, pg 307, 2006). *Gene Dev.* 20:747-747.
- Jagatheesan, G., S. Thanumalayan, B. Muralikrishna, N. Rangaraj, A.A. Karande, and V.K. Parnaik. 1999. Colocalization of intranuclear lamin foci with RNA splicing factors. *J Cell Sci.* 112 (Pt 24):4651-4661.
- Johnson, B.R., R.T. Nitta, R.L. Frock, L. Mounkes, D.A. Barbie, C.L. Stewart, E. Harlow, and B.K. Kennedy. 2004. A-type lamins regulate retinoblastoma protein function by

- promoting subnuclear localization and preventing proteasomal degradation. *Proc Natl Acad Sci U S A*. 101:9677-9682.
- Kayman-Kurekci, G., B. Talim, P. Korkusuz, N. Sayar, T. Sarioglu, I. Oncel, P. Sharafi, H. Gundesli, B. Balci-Hayta, and N. Purali. 2014. Mutation in TOR1AIP1 encoding LAP1B in a form of muscular dystrophy: a novel gene related to nuclear envelopathies. *Neuromuscular Disorders*. 24:624-633.
- Kayvanpour, E., F. Sedaghat-Hamedani, A. Amr, A. Lai, J. Haas, D.B. Holzer, K.S. Frese, A. Keller, K. Jensen, and H.A. Katus. 2017. Genotype-phenotype associations in dilated cardiomyopathy: meta-analysis on more than 8000 individuals. *Clinical Research in Cardiology*. 106:127-139.
- Kean, E.L., A.K. Münster-Kühnel, and R. Gerardy-Schahn. 2004. CMP-sialic acid synthetase of the nucleus. *Biochim Biophys Acta*. 1673:56-65.
- Keith Chenault, H., and G.M. Whitesides. 1989. Lactate dehydrogenase-catalyzed regeneration of NAD from NADH for use in enzyme-catalyzed synthesis. *Bioorganic Chemistry*. 17:400-409.
- Keller, H., C. Dreyer, J. Medin, A. Mahfoudi, K. Ozato, and W. Wahli. 1993. Fatty acids and retinoids control lipid metabolism through activation of peroxisome proliferator-activated receptor-retinoid X receptor heterodimers. *Proc Natl Acad Sci U S A*. 90:2160-2164.
- Kim, Y., A.A. Sharov, K. McDole, M. Cheng, H. Hao, C.M. Fan, N. Gaiano, M.S. Ko, and Y. Zheng. 2011. Mouse B-type lamins are required for proper organogenesis but not by embryonic stem cells. *Science*. 334:1706-1710.
- Kim, Y., and Y. Zheng. 2013. Generation and characterization of a conditional deletion allele for *Lmna* in mice. *Biochem Biophys Res Commun*. 440:8-13.
- Klevstig, M., M. Arif, M. Mannila, S. Svedlund, I. Mardani, M. Ståhlman, L. Andersson, M. Lindbom, A. Miljanovic, A. Franco-Cereceda, P. Eriksson, A. Jeppsson, L.M. Gan, M. Levin, A. Mardinoglu, E. Ehrenborg, and J. Borén. 2019. Cardiac expression of the microsomal triglyceride transport protein protects the heart function during ischemia. *J Mol Cell Cardiol*. 137:1-8.
- Koch, A.J., and J.M. Holaska. 2012. Loss of emerin alters myogenic signaling and miRNA expression in mouse myogenic progenitors. *Plos One*. 7:e37262.
- Koch, A.J., and J.M. Holaska. 2014. Emerin in health and disease. *Seminars in Cell & Developmental Biology*. 29:95-106.
- Kochin, V., T. Shimi, E. Torvaldson, S.A. Adam, A. Goldman, C.G. Pack, J. Melo-Cardenas, S.Y. Imanishi, R.D. Goldman, and J.E. Eriksson. 2014. Interphase phosphorylation of lamin A. *J Cell Sci*. 127:2683-2696.
- Kolb, T., K. Maass, M. Hergt, U. Aebi, and H. Herrmann. 2011. Lamin A and lamin C form homodimers and coexist in higher complex forms both in the nucleoplasmic fraction and in the lamina of cultured human cells. *Nucleus-Phila*. 2:425-433.
- Kovalchuk, T., E. Yakovleva, S. Fetisova, T. Vershinina, V. Lebedeva, T. Lyubimtseva, D. Lebedev, L. Mitrofanova, A. Ryzhkov, P. Sokolnikova, Y. Fomicheva, A. Kozyreva, S. Zhuk, N. Smolina, A. Zlotina, T. Pervunina, A. Kostareva, and E. Vasichkina. 2021. Case Reports: Emery-Dreifuss Muscular Dystrophy Presenting as a Heart Rhythm Disorders in Children. *Front Cardiovasc Med*. 8:668231.
- Krimm, I., C. Östlund, B. Gilquin, J. Couprie, P. Hossenlopp, J.-P. Mornon, G. Bonne, J.-C. Courvalin, H.J. Worman, and S. Zinn-Justin. 2002. The Ig-like structure of the C-terminal domain of lamin A/C, mutated in muscular dystrophies, cardiomyopathy, and partial lipodystrophy. *Structure*. 10:811-823.
- Krishnan, A., R. Samtani, P. Dhanantwari, E. Lee, S. Yamada, K. Shiota, M.T. Donofrio, L. Leatherbury, and C.W. Lo. 2014. A detailed comparison of mouse and human cardiac development. *Pediatr Res*. 76:500-507.

- Kubben, N., J.W. Voncken, G. Konings, M. van Weeghel, M.M.G. van den Hoogenhof, M. Gijbels, A. van Erk, K. Schoonderwoerd, B. van den Bosch, V. Dahlmans, C. Calis, S.M. Houten, T. Misteli, and Y.M. Pinto. 2011. Post-natal myogenic and adipogenic developmental Defects and metabolic impairment upon loss of A-type lamins. *Nucleus-Phila.* 2:195-207.
- Kumar, S., S.H. Baldinger, E. Gandjbakhch, P. Maury, J.M. Sellal, A.F.A. Androulakis, X. Waintraub, P. Charron, A. Rollin, P. Richard, W.G. Stevenson, C.J. Macintyre, C.Y. Ho, T. Thompson, J.K. Vohra, J.M. Kalman, K. Zeppenfeld, F. Sacher, U.B. Tedrow, and N.K. Lakdawala. 2016. Long-Term Arrhythmic and Nonarrhythmic Outcomes of Lamin A/C Mutation Carriers. *Journal of the American College of Cardiology.* 68:2299-2307.
- Kumaran, R.I., B. Muralikrishna, and V.K. Parnaik. 2002. Lamin A/C speckles mediate spatial organization of splicing factor compartments and RNA polymerase II transcription. *J Cell Biol.* 159:783-793.
- Kuo, C.J., P.B. Conley, L. Chen, F.M. Sladek, J.E. Darnell, Jr., and G.R. Crabtree. 1992. A transcriptional hierarchy involved in mammalian cell-type specification. *Nature.* 355:457-461.
- Kwan, R., G.F. Brady, M. Brzozowski, S.V. Weerasinghe, H. Martin, M.J. Park, M.J. Brunt, R.K. Menon, X. Tong, L. Yin, C.L. Stewart, and M.B. Omary. 2017. Hepatocyte-Specific Deletion of Mouse Lamin A/C Leads to Male-Selective Steatohepatitis. *Cell Mol Gastroenter.* 4:365-383.
- Lammerding, J., L.G. Fong, J.Y. Ji, K. Reue, C.L. Stewart, S.G. Young, and R.T. Lee. 2006. Lamins A and C but not lamin B1 regulate nuclear mechanics. *J Biol Chem.* 281:25768-25780.
- Lammerding, J., J. Hsiao, P.C. Schulze, S. Kozlov, C.L. Stewart, and R.T. Lee. 2005. Abnormal nuclear shape and impaired mechanotransduction in emerin-deficient cells. *J Cell Biol.* 170:781-791.
- Lammerding, J., P.C. Schulze, T. Takahashi, S. Kozlov, T. Sullivan, R.D. Kamm, C.L. Stewart, and R.T. Lee. 2004. Lamin A/C deficiency causes defective nuclear mechanics and mechanotransduction. *J Clin Invest.* 113:370-378.
- Lattanzi, G., V. Cenni, S. Marmiroli, C. Capanni, E. Mattioli, L. Merlini, S. Squarzone, and N.M. Maraldi. 2003. Association of emerin with nuclear and cytoplasmic actin is regulated in differentiating myoblasts. *Biochem Biophys Res Commun.* 303:764-770.
- Lazarte, J., S.J. Jurgens, S.H. Choi, S. Khurshid, V.N. Morrill, L.C. Weng, V. Nauffal, J.P. Pirruccello, J.L. Halford, R.A. Hegele, P.T. Ellinor, K.L. Lunetta, and S.A. Lubitz. 2022. LMNA Variants and Risk of Adult-Onset Cardiac Disease. *J Am Coll Cardiol.* 80:50-59.
- Lazebnik, Y.A., A. Takahashi, G.G. Poirier, S.H. Kaufmann, and W.C. Earnshaw. 1995. Characterization of the execution phase of apoptosis in vitro using extracts from condemned-phase cells. *J Cell Sci Suppl.* 19:41-49.
- Lebel, S., C. Lampron, A. Royal, and Y. Raymond. 1987. Lamins A and C appear during retinoic acid-induced differentiation of mouse embryonal carcinoma cells. *J Cell Biol.* 105:1099-1104.
- Lee, J., V. Termglinchan, S. Diecke, I. Itzhaki, C.K. Lam, P. Garg, E. Lau, M. Greenhaw, T. Seeger, H. Wu, J.Z. Zhang, X. Chen, I.P. Gil, M. Ameen, K. Sallam, J.W. Rhee, J.M. Churko, R. Chaudhary, T. Chour, P.J. Wang, M.P. Snyder, H.Y. Chang, I. Karakikes, and J.C. Wu. 2019. Activation of PDGF pathway links LMNA mutation to dilated cardiomyopathy. *Nature.* 572:335-340.
- Lee, K.K., T. Haraguchi, R.S. Lee, T. Koujin, Y. Hiraoka, and K.L. Wilson. 2001. Distinct functional domains in emerin bind lamin A and DNA-bridging protein BAF. *J Cell Sci.* 114:4567-4573.

- Lee, Y.K., Y.M. Lau, Z.J. Cai, W.H. Lai, L.Y. Wong, H.F. Tse, K.M. Ng, and C.W. Siu. 2017. Modeling Treatment Response for Lamin A/C Related Dilated Cardiomyopathy in Human Induced Pluripotent Stem Cells. *J Am Heart Assoc.* 6.
- Lemaître, C., A. Grabarz, K. Tsouroula, L. Andronov, A. Furst, T. Pankotai, V. Heyer, M. Rogier, K.M. Attwood, P. Kessler, G. Dellaire, B. Klaholz, B. Reina-San-Martin, and E. Soutoglou. 2014. Nuclear position dictates DNA repair pathway choice. *Genes Dev.* 28:2450-2463.
- Lemmer, I.L., N. Willemsen, N. Hilal, and A. Bartelt. 2021. A guide to understanding endoplasmic reticulum stress in metabolic disorders. *Mol Metab.* 47:101169.
- Leu, M., E. Ehler, and J.C. Perriard. 2001. Characterisation of postnatal growth of the murine heart. *Anat Embryol (Berl).* 204:217-224.
- Li, D., A. Morales, J. Gonzalez-Quintana, N. Norton, J.D. Siegfried, M. Hofmeyer, and R.E. Hershberger. 2010. Identification of novel mutations in RBM20 in patients with dilated cardiomyopathy. *Clinical and translational science.* 3:90-97.
- Lian, X., J. Zhang, S.M. Azarin, K. Zhu, L.B. Hazeltine, X. Bao, C. Hsiao, T.J. Kamp, and S.P. Palecek. 2013. Directed cardiomyocyte differentiation from human pluripotent stem cells by modulating Wnt/ β -catenin signaling under fully defined conditions. *Nat Protoc.* 8:162-175.
- Lin, F., D.L. Blake, I. Callebaut, I.S. Skerjanc, L. Holmer, M.W. McBurney, M. Paulin-Levasseur, and H.J. Worman. 2000. MAN1, an inner nuclear membrane protein that shares the LEM domain with lamina-associated polypeptide 2 and emerlin. *J Biol Chem.* 275:4840-4847.
- Lin, F., J.M. Morrison, W. Wu, and H.J. Worman. 2005. MAN1, an integral protein of the inner nuclear membrane, binds Smad2 and Smad3 and antagonizes transforming growth factor-beta signaling. *Hum Mol Genet.* 14:437-445.
- Lin, F., and H.J. Worman. 1993. Structural organization of the human gene encoding nuclear lamin A and nuclear lamin C. *J Biol Chem.* 268:16321-16326.
- Lin, F., and H.J. Worman. 1995. Structural organization of the human gene (LMNB1) encoding nuclear lamin B1. *Genomics.* 27:230-236.
- Lin, Y., Y. Wang, and P.-f. Li. 2022. Mutual regulation of lactate dehydrogenase and redox robustness. *Frontiers in Physiology.* 13.
- Lindenboim, L., H. Zohar, H.J. Worman, and R. Stein. 2020. The nuclear envelope: target and mediator of the apoptotic process. *Cell Death Discov.* 6.
- Lloyd, D.J., R.C. Trembath, and S. Shackleton. 2002. A novel interaction between lamin A and SREBP1: implications for partial lipodystrophy and other laminopathies. *Hum Mol Genet.* 11:769-777.
- Loaeza-Reyes, K.J., E. Zenteno, A. Moreno-Rodríguez, R. Torres-Rosas, L. Argueta-Figueroa, R. Salinas-Marín, L.M. Castillo-Real, S. Pina-Canseco, and Y.P. Cervera. 2021. An Overview of Glycosylation and its Impact on Cardiovascular Health and Disease. *Frontiers in Molecular Biosciences.* 8.
- Loewinger, L., and F. McKeon. 1988. Mutations in the nuclear lamin proteins resulting in their aberrant assembly in the cytoplasm. *The EMBO journal.* 7:2301-2309.
- Lopaschuk, G.D., and J.S. Jaswal. 2010. Energy metabolic phenotype of the cardiomyocyte during development, differentiation, and postnatal maturation. *J Cardiovasc Pharmacol.* 56:130-140.
- Lopez-Soler, R.I., R.D. Moir, T.P. Spann, R. Stick, and R.D. Goldman. 2001. A role for nuclear lamins in nuclear envelope assembly. *J Cell Biol.* 154:61-70.
- Lowe, N., J.S. Rees, J. Roote, E. Ryder, I.M. Armean, G. Johnson, E. Drummond, H. Spriggs, J. Drummond, J.P. Magbanua, H. Naylor, B. Sanson, R. Bastock, S. Huelsmann, V. Trovisco, M. Landgraf, S. Knowles-Barley, J.D. Armstrong, H. White-Cooper, C. Hansen, R.G. Phillips, K.S. Lilley, S. Russell, and D. St Johnston. 2014. Analysis of the

- expression patterns, subcellular localisations and interaction partners of Drosophila proteins using a pigP protein trap library. *Development*. 141:3994-4005.
- Lund, E.G., I. Duband-Goulet, A. Oldenburg, B. Buendia, and P. Collas. 2015. Distinct features of lamin A-interacting chromatin domains mapped by ChIP-sequencing from sonicated or micrococcal nuclease-digested chromatin. *Nucleus-Phila*. 6:30-39.
- Malhas, A., C.F. Lee, R. Sanders, N.J. Saunders, and D.J. Vaux. 2007. Defects in lamin B1 expression or processing affect interphase chromosome position and gene expression. *J Cell Biol*. 176:593-603.
- Manilal, S., T.M. Nguyen, C.A. Sewry, and G.E. Morris. 1996. The Emery-Dreifuss muscular dystrophy protein, emerin, is a nuclear membrane protein. *Hum Mol Genet*. 5:801-808.
- Mansharamani, M., and K.L. Wilson. 2005. Direct binding of nuclear membrane protein MAN1 to emerin in vitro and two modes of binding to barrier-to-autointegration factor. *J Biol Chem*. 280:13863-13870.
- Marcelot, A., H.J. Worman, and S. Zinn-Justin. 2021. Protein structural and mechanistic basis of progeroid laminopathies. *Febs j*. 288:2757-2772.
- Margalit, A., A. Brachner, J. Gotzmann, R. Foisner, and Y. Gruenbaum. 2007. Barrier-to-autointegration factor--a BAFfling little protein. *Trends Cell Biol*. 17:202-208.
- Markiewicz, E., K. Tilgner, N. Barker, M. van de Wetering, H. Clevers, M. Dorobek, I. Hausmanowa-Petrusewicz, F.C. Ramaekers, J.L. Broers, W.M. Blankesteyn, G. Salpingidou, R.G. Wilson, J.A. Ellis, and C.J. Hutchison. 2006. The inner nuclear membrane protein emerin regulates beta-catenin activity by restricting its accumulation in the nucleus. *Embo j*. 25:3275-3285.
- Maynard, S., G. Keijzers, M. Akbari, M.B. Ezra, A. Hall, M. Morevati, M. Scheibye-Knudsen, S. Gonzalo, J. Bartek, and V.A. Bohr. 2019. Lamin A/C promotes DNA base excision repair. *Nucleic Acids Res*. 47:11709-11728.
- McKeon, F.D., M.W. Kirschner, and D. Caput. 1986. Homologies in both primary and secondary structure between nuclear envelope and intermediate filament proteins. *Nature*. 319:463-468.
- McNally, E.M., and L. Mestroni. 2017. Dilated Cardiomyopathy Genetic Determinants and Mechanisms. *Circ Res*. 121:731-748.
- Meaburn, K.J., E. Cabuy, G. Bonne, N. Levy, G.E. Morris, G. Novelli, I.R. Kill, and J.M. Bridger. 2007. Primary laminopathy fibroblasts display altered genome organization and apoptosis. *Aging Cell*. 6:139-153.
- Meister, P., S.E. Mango, and S.M. Gasser. 2011. Locking the genome: nuclear organization and cell fate. *Curr Opin Genet Dev*. 21:167-174.
- Melcon, G., S. Kozlov, D.A. Cutler, T. Sullivan, L. Hernandez, P. Zhao, S. Mitchell, G. Nader, M. Bakay, J.N. Rottman, E.P. Hoffman, and C.L. Stewart. 2006. Loss of emerin at the nuclear envelope disrupts the Rb1/E2F and MyoD pathways during muscle regeneration. *Hum Mol Genet*. 15:637-651.
- Mikkola, S. 2020. Nucleotide Sugars in Chemistry and Biology. *Molecules*. 25.
- Miller, R.G., R.B. Layzer, M.A. Mellenthin, M. Golabi, R.A. Francoz, and J.C. Mall. 1985. Emery-Dreifuss muscular dystrophy with autosomal dominant transmission. *Neurology*. 35:1230-1233.
- Moir, R.D., M. Montag-Lowy, and R.D. Goldman. 1994. Dynamic properties of nuclear lamins: lamin B is associated with sites of DNA replication. *J Cell Biol*. 125:1201-1212.
- Moir, R.D., M. Yoon, S. Khuon, and R.D. Goldman. 2000. Nuclear lamins A and B1: different pathways of assembly during nuclear envelope formation in living cells. *J Cell Biol*. 151:1155-1168.
- Molloy, A., O. Cotter, R. van Spaendonk, E. Sistermans, and B. Sweeney. 2012. A patient with a rare leukodystrophy related to lamin B1 duplication. *Ir Med J*. 105:186-187.

- Moulson, C.L., G. Go, J.M. Gardner, A.C. van der Wal, J.H. Smitt, J.M. van Hagen, and J.H. Miner. 2005. Homozygous and compound heterozygous mutations in ZMPSTE24 cause the laminopathy restrictive dermopathy. *J Invest Dermatol.* 125:913-919.
- Mounkes, L.C., S.V. Kozlov, J.N. Rottman, and C.L. Stewart. 2005. Expression of an LMNA-N195K variant of A-type lamins results in cardiac conduction defects and death in mice. *Hum Mol Genet.* 14:2167-2180.
- Muchir, A., G. Bonne, A.J. van der Kool, M. van Meegen, F. Baas, P.A. Bolhuis, M. de Visser, and K. Schwartz. 2000. Identification of mutations in the gene encoding lamins A/C in autosomal dominant limb girdle muscular dystrophy with atrioventricular conduction disturbances (LGMD1B). *Hum Mol Genet.* 9:1453-1459.
- Muchir, A., P. Pavlidis, G. Bonne, Y.K. Hayashi, and H.J. Worman. 2007a. Activation of MAPK in hearts of EMD null mice: similarities between mouse models of X-linked and autosomal dominant Emery–Dreifuss muscular dystrophy. *Hum Mol Genet.* 16:1884-1895.
- Muchir, A., P. Pavlidis, V. Decostre, A.J. Herron, T. Arimura, G. Bonne, and H.J. Worman. 2007b. Activation of MAPK pathways links LMNA mutations to cardiomyopathy in Emery-Dreifuss muscular dystrophy. *J Clin Invest.* 117:1282-1293.
- Muchir, A., and H.J. Worman. 2016. Targeting Mitogen-Activated Protein Kinase Signaling in Mouse Models of Cardiomyopathy Caused by Lamin A/C Gene Mutations. *Methods Enzymol.* 568:557-580.
- Murase, Y., K. Yagi, Y. Katsuda, A. Asano, J. Koizumi, and H. Mabuchi. 2002. An LMNA variant is associated with dyslipidemia and insulin resistance in the Japanese. *Metabolism.* 51:1017-1021.
- Murray-Nerger, L.A., J.L. Justice, P. Rekapalli, J.E. Hutton, and I.M. Cristea. 2021. Lamin B1 acetylation slows the G1 to S cell cycle transition through inhibition of DNA repair. *Nucleic Acids Res.* 49:2044-2064.
- Naetar, N., B. Korbei, S. Kozlov, M.A. Kerenyi, D. Dorner, R. Kral, I. Gotic, P. Fuchs, T.V. Cohen, R. Bittner, C.L. Stewart, and R. Foisner. 2008. Loss of nucleoplasmic LAP2alpha-lamin A complexes causes erythroid and epidermal progenitor hyperproliferation. *Nat Cell Biol.* 10:1341-1348.
- Nagano, A., R. Koga, M. Ogawa, Y. Kurano, J. Kawada, R. Okada, Y.K. Hayashi, T. Tsukahara, and K. Arahata. 1996. Emerin deficiency at the nuclear membrane in patients with Emery-Dreifuss muscular dystrophy. *Nat Genet.* 12:254-259.
- Navarro, C.L., A. De Sandre-Giovannoli, R. Bernard, I. Boccaccio, A. Boyer, D. Geneviève, S. Hadj-Rabia, C. Gaudy-Marqueste, H.S. Smitt, P. Vabres, L. Faivre, A. Verloes, T. Van Essen, E. Flori, R. Hennekam, F.A. Beemer, N. Laurent, M. Le Merrer, P. Cau, and N. Lévy. 2004. Lamin A and ZMPSTE24 (FACE-1) defects cause nuclear disorganization and identify restrictive dermopathy as a lethal neonatal laminopathy. *Hum Mol Genet.* 13:2493-2503.
- Nielsen, L.B., M. Véniant, J. Borén, M. Raabe, J.S. Wong, C. Tam, L. Flynn, T. Vanni-Reyes, M.D. Gunn, and I.J. Goldberg. 1998. Genes for apolipoprotein B and microsomal triglyceride transfer protein are expressed in the heart: evidence that the heart has the capacity to synthesize and secrete lipoproteins. *Circulation.* 98:13-16.
- Nishiuchi, S., T. Makiyama, T. Aiba, K. Nakajima, S. Hirose, H. Kohjitani, Y. Yamamoto, T. Harita, M. Hayano, Y. Wuriyanghai, J.R. Chen, K. Sasaki, N. Yagihara, T. Ishikawa, K. Onoue, N. Murakoshi, I. Watanabe, K. Ohkubo, H. Watanabe, S. Ohno, T. Doi, S. Shizuta, T. Minamino, Y. Saito, Y. Oginosawa, A. Nogami, K. Aonuma, K. Kusano, N. Makita, W. Shimizu, M. Horie, and T. Kimura. 2017. Gene-Based Risk Stratification for Cardiac Disorders in LMNA Mutation Carriers. *Circ-Cardiovasc Gene.* 10.

- Norwood, F.L., C. Harling, P.F. Chinnery, M. Eagle, K. Bushby, and V. Straub. 2009. Prevalence of genetic muscle disease in Northern England: in-depth analysis of a muscle clinic population. *Brain*. 132:3175-3186.
- Novelli, G., A. Muchir, F. Sangiuolo, A. Helbling-Leclerc, M.R. D'Apice, C. Massart, F. Capon, P. Sbraccia, M. Federici, R. Lauro, C. Tudisco, R. Pallotta, G. Scarano, B. Dallapiccola, L. Merlini, and G. Bonne. 2002. Mandibuloacral dysplasia is caused by a mutation in LMNA-encoding lamin A/C. *Am J Hum Genet*. 71:426-431.
- Ognibene, A., P. Sabatelli, S. Petrini, S. Squarzoni, M. Riccio, S. Santi, M. Villanova, S. Palmeri, L. Merlini, and N.M. Maraldi. 1999. Nuclear changes in a case of X-linked Emery-Dreifuss muscular dystrophy. *Muscle Nerve*. 22:864-869.
- Okumura, K., K. Nakamachi, Y. Hosoe, and N. Nakajima. 2000. Identification of a novel retinoic acid-responsive element within the lamin A/C promoter. *Biochem Bioph Res Co*. 269:197-202.
- Ostlund, C., J. Ellenberg, E. Hallberg, J. Lippincott-Schwartz, and H.J. Worman. 1999. Intracellular trafficking of emerin, the Emery-Dreifuss muscular dystrophy protein. *J Cell Sci*. 112 (Pt 11):1709-1719.
- Ostlund, C., T. Sullivan, C.L. Stewart, and H.J. Worman. 2006. Dependence of diffusional mobility of integral inner nuclear membrane proteins on A-type lamins. *Biochemistry*. 45:1374-1382.
- Ozawa, R., Y.K. Hayashi, M. Ogawa, R. Kurokawa, H. Matsumoto, S. Noguchi, I. Nonaka, and I. Nishino. 2006. Emerin-lacking mice show minimal motor and cardiac dysfunctions with nuclear-associated vacuoles. *Am J Pathol*. 168:907-917.
- Padiath, Q.S., and Y.H. Fu. 2010. Autosomal dominant leukodystrophy caused by lamin B1 duplications a clinical and molecular case study of altered nuclear function and disease. *Methods Cell Biol*. 98:337-357.
- Padiath, Q.S., K. Saigoh, R. Schiffmann, H. Asahara, T. Yamada, A. Koeppen, K. Hogan, L.J. Ptacek, and Y.H. Fu. 2006. Lamin B1 duplications cause autosomal dominant leukodystrophy. *Nature Genetics*. 38:1114-1123.
- Padmakumar, V., T. Libotte, W. Lu, H. Zaim, S. Abraham, A.A. Noegel, J. Gotzmann, R. Foisner, and I. Karakesisoglou. 2005. The inner nuclear membrane protein Sun1 mediates the anchorage of Nesprin-2 to the nuclear envelope. *J Cell Sci*. 118:3419-3430.
- Paredes, A., R. Justo-Méndez, D. Jiménez-Blasco, V. Núñez, I. Calero, M. Villalba-Orero, A. Alegre-Martí, T. Fischer, A. Gradillas, V.A.R. Sant'Anna, F. Were, Z. Huang, P. Hernansanz-Agustín, C. Contreras, F. Martínez, E. Camafeita, J. Vázquez, J. Ruiz-Cabello, E. Area-Gómez, F. Sánchez-Cabo, E. Treuter, J.P. Bolaños, E. Estébanez-Perpiñá, F.J. Rupérez, C. Barbas, J.A. Enríquez, and M. Ricote. 2023. γ -Linolenic acid in maternal milk drives cardiac metabolic maturation. *Nature*. 618:365-373.
- Park, Y.-E., Y.K. Hayashi, K. Goto, H. Komaki, Y. Hayashi, T. Inuzuka, S. Noguchi, I. Nonaka, and I. Nishino. 2009. Nuclear changes in skeletal muscle extend to satellite cells in autosomal dominant Emery-Dreifuss muscular dystrophy/limb-girdle muscular dystrophy 1B. *Neuromuscular Disorders*. 19:29-36.
- Parry, D.A., J.F. Conway, and P.M. Steinert. 1986. Structural studies on lamin. Similarities and differences between lamin and intermediate-filament proteins. *Biochem J*. 238:305-308.
- Pellegrini, C., M. Columbaro, C. Capanni, M.R. D'Apice, C. Cavallo, M. Murdocca, G. Lattanzi, and S. Squarzoni. 2015. All-trans retinoic acid and rapamycin normalize Hutchinson Gilford progeria fibroblast phenotype. *Oncotarget*. 6:29914-29928.
- Peng, Y., Q. Tang, F. Xiao, and N. Fu. 2022. Regulation of Lipid Metabolism by Lamin in Mutation-Related Diseases. *Front Pharmacol*. 13:820857.
- Peter, M., E. Heitlinger, M. Häner, U. Aebi, and E.A. Nigg. 1991. Disassembly of in vitro formed lamin head-to-tail polymers by CDC2 kinase. *Embo j*. 10:1535-1544.

- Peter, M., J. Nakagawa, M. Dorée, J.C. Labbé, and E.A. Nigg. 1990. In vitro disassembly of the nuclear lamina and M phase-specific phosphorylation of lamins by cdc2 kinase. *Cell*. 61:591-602.
- Phair, R.D., and T. Misteli. 2000. High mobility of proteins in the mammalian cell nucleus. *Nature*. 404:604-609.
- Porrello, E.R., A.I. Mahmoud, E. Simpson, J.A. Hill, J.A. Richardson, E.N. Olson, and H.A. Sadek. 2011. Transient regenerative potential of the neonatal mouse heart. *Science*. 331:1078-1080.
- Pradas, J.C., G. Auguste, S.J. Matkovich, R. Lombardi, S.N. Chen, T. Garnett, K. Chamberlain, J.M. Riyad, T. Weber, S.K. Singh, M.J. Robertson, C. Coarfa, A.J. Marian, and P. Gurha. 2020. Identification of Genes and Pathways Regulated by Lamin A in Heart. *Journal of the American Heart Association*. 9:e015690.
- Puckelwartz, M.J., F.F. Depreux, and E.M. McNally. 2011. Gene expression, chromosome position and lamin A/C mutations. *Nucleus-Phila*. 2:162-167.
- Puckett, S.W., and W.J. Reddy. 1979. A decrease in the malate-aspartate shuttle and glutamate translocase activity in heart mitochondria from alloxan-diabetic rats. *Journal of molecular and cellular cardiology*. 11:173-187.
- Puente, B.N., W. Kimura, S.A. Muralidhar, J. Moon, J.F. Amatruda, K.L. Phelps, D. Grinsfelder, B.A. Rothermel, R. Chen, J.A. Garcia, C.X. Santos, S. Thet, E. Mori, M.T. Kinter, P.M. Rindler, S. Zacchigna, S. Mukherjee, D.J. Chen, A.I. Mahmoud, M. Giacca, P.S. Rabinovitch, A. Aroumougame, A.M. Shah, L.I. Szweda, and H.A. Sadek. 2014. The oxygen-rich postnatal environment induces cardiomyocyte cell-cycle arrest through DNA damage response. *Cell*. 157:565-579.
- Raffaele Di Barletta, M., E. Ricci, G. Galluzzi, P. Tonali, M. Mora, L. Morandi, A. Romorini, T. Voit, K.H. Orstavik, L. Merlini, C. Trevisan, V. Biancalana, I. Housmanowa-Petrusewicz, S. Bione, R. Ricotti, K. Schwartz, G. Bonne, and D. Toniolo. 2000. Different mutations in the LMNA gene cause autosomal dominant and autosomal recessive Emery-Dreifuss muscular dystrophy. *Am J Hum Genet*. 66:1407-1412.
- Ramos, F.J., S.C. Chen, M.G. Garelick, D.F. Dai, C.Y. Liao, K.H. Schreiber, V.L. MacKay, E.H. An, R. Strong, W.C. Ladiges, P.S. Rabinovitch, M. Kaerberlein, and B.K. Kennedy. 2012. Rapamycin reverses elevated mTORC1 signaling in lamin A/C-deficient mice, rescues cardiac and skeletal muscle function, and extends survival. *Sci Transl Med*. 4:144ra103.
- Ranuncolo, S.M., S. Ghosh, J.A. Hanover, G.W. Hart, and B.A. Lewis. 2012. Evidence of the involvement of O-GlcNAc-modified human RNA polymerase II CTD in transcription in vitro and in vivo. *J Biol Chem*. 287:23549-23561.
- Rao, L., D. Perez, and E. White. 1996. Lamin proteolysis facilitates nuclear events during apoptosis. *J Cell Biol*. 135:1441-1455.
- Read, J.A., V.J. Winter, C.M. Eszes, R.B. Sessions, and R.L. Brady. 2001. Structural basis for altered activity of M- and H-isozyme forms of human lactate dehydrogenase. *Proteins*. 43:175-185.
- Refaat, M.M., S.A. Lubitz, S. Makino, Z. Islam, J.M. Frangiskakis, H. Mehdi, R. Gutmann, M.L. Zhang, H.L. Bloom, and C.A. MacRae. 2012. Genetic variation in the alternative splicing regulator RBM20 is associated with dilated cardiomyopathy. *Heart Rhythm*. 9:390-396.
- Rieusset, J. 2018. The role of endoplasmic reticulum-mitochondria contact sites in the control of glucose homeostasis: an update. *Cell Death & Disease*. 9:388.
- Ritterhoff, J., and R. Tian. 2017. Metabolism in cardiomyopathy: every substrate matters. *Cardiovasc Res*. 113:411-421.
- Robson, M.I., J.I. De Las Heras, R. Czapiewski, P.L. Thanh, D.G. Booth, D.A. Kelly, S. Webb, A.R.W. Kerr, and E.C. Schirmer. 2016. Tissue-Specific Gene Repositioning by Muscle Nuclear Membrane Proteins Enhances Repression of Critical Developmental Genes during Myogenesis. *Mol Cell*. 62:834-847.

- Rodríguez, J., F. Calvo, J.M. González, B. Casar, V. Andrés, and P. Crespo. 2010. ERK1/2 MAP kinases promote cell cycle entry by rapid, kinase-independent disruption of retinoblastoma-lamin A complexes. *J Cell Biol.* 191:967-979.
- Rowat, A.C., J. Lammerding, and J.H. Ipsen. 2006. Mechanical properties of the cell nucleus and the effect of emerin deficiency. *Biophys J.* 91:4649-4664.
- Rowland, L.P., M. Fetell, M. Olarte, A. Hays, N. Singh, and F.E. Wanat. 1979. Emery-Dreifuss Muscular-Dystrophy. *Ann Neurol.* 5:111-117.
- Rusiñol, A.E., and M.S. Sinensky. 2006. Farnesylated lamins, progeroid syndromes and farnesyl transferase inhibitors. *J Cell Sci.* 119:3265-3272.
- Saitoh, N., C.S. Spahr, S.D. Patterson, P. Bubulya, A.F. Neuwald, and D.L. Spector. 2004. Proteomic analysis of interchromatin granule clusters. *Mol Biol Cell.* 15:3876-3890.
- Sakabe, K., Z. Wang, and G.W. Hart. 2010. Beta-N-acetylglucosamine (O-GlcNAc) is part of the histone code. *Proc Natl Acad Sci U S A.* 107:19915-19920.
- Salvarani, N., S. Crasto, M. Miragoli, A. Bertero, M. Paulis, P. Kunderfranco, S. Serio, A. Forni, C. Lucarelli, M. Dal Ferro, V. Larcher, G. Sinagra, P. Vezzoni, C.E. Murry, G. Faggian, G. Condorelli, and E. Di Pasquale. 2019. The K219T-Lamin mutation induces conduction defects through epigenetic inhibition of SCN5A in human cardiac laminopathy. *Nat Commun.* 10:2267.
- Sambandam, N., G.D. Lopaschuk, R.W. Brownsey, and M.F. Allard. 2002. Energy metabolism in the hypertrophied heart. *Heart Failure Reviews.* 7:161-173.
- Schirmer, E.C., L. Florens, T. Guan, J.R. Yates, 3rd, and L. Gerace. 2003. Nuclear membrane proteins with potential disease links found by subtractive proteomics. *Science.* 301:1380-1382.
- Schoberer, J., Y.J. Shin, U. Vavra, C. Veit, and R. Strasser. 2018. Analysis of Protein Glycosylation in the ER. *Methods Mol Biol.* 1691:205-222.
- Scholtes, C., and V. Giguère. 2022. Transcriptional control of energy metabolism by nuclear receptors. *Nature Reviews Molecular Cell Biology.* 23:750-770.
- Schwankhaus, J.D., D.A. Katz, R. Eldridge, S. Schlesinger, and H. Mcfarland. 1994. Clinical and Pathological Features of an Autosomal-Dominant, Adult-Onset Leukodystrophy Simulating Chronic Progressive Multiple-Sclerosis. *Arch Neurol-Chicago.* 51:757-766.
- Segura-Totten, M., A.K. Kowalski, R. Craigie, and K.L. Wilson. 2002. Barrier-to-autointegration factor: major roles in chromatin decondensation and nuclear assembly. *J Cell Biol.* 158:475-485.
- Shackleton, S., D.J. Lloyd, S.N.J. Jackson, R. Evans, M.F. Niermeijer, B.M. Singh, H. Schmidt, G. Brabant, S. Kumar, P.N. Durrington, S. Gregory, S. O'Rahilly, and R.C. Trembath. 2000. LMNA, encoding lamin A/C, is mutated in partial lipodystrophy. *Nature Genetics.* 24:153-156.
- Shackleton, S., D.T. Smallwood, P. Clayton, L.C. Wilson, A.K. Agarwal, A. Garg, and R.C. Trembath. 2005. Compound heterozygous ZMPSTE24 mutations reduce prelamin A processing and result in a severe progeroid phenotype. *J Med Genet.* 42:e36.
- Shah, D., L. Virtanen, C. Prajapati, M. Kiamehr, J. Gullmets, G. West, J. Kreutzer, M. Pekkanen-Mattila, T. Heliö, P. Kallio, P. Taimen, and K. Aalto-Setälä. 2019. Modeling of LMNA-Related Dilated Cardiomyopathy Using Human Induced Pluripotent Stem Cells. *Cells.* 8.
- Shah, P., C.M. Hobson, S. Cheng, M.J. Colville, M.J. Paszek, R. Superfine, and J. Lammerding. 2021a. Nuclear Deformation Causes DNA Damage by Increasing Replication Stress. *Current Biology.* 31:753-765.e756.
- Shah, P.P., W. Lv, J.H. Rhoades, A. Poleshko, D. Abbey, M.A. Caporizzo, R. Linares-Saldana, J.G. Heffler, N. Sayed, D. Thomas, Q. Wang, L.J. Stanton, K. Bedi, M.P. Morley, T.P. Cappola, A.T. Owens, K.B. Margulies, D.B. Frank, J.C. Wu, D.J. Rader, W. Yang, B.L. Prosser, K. Musunuru, and R. Jain. 2021b. Pathogenic LMNA variants disrupt cardiac

- lamina-chromatin interactions and de-repress alternative fate genes. *Cell Stem Cell*. 28:938-954.e939.
- Sharma, A., G. Li, K. Rajarajan, R. Hamaguchi, P.W. BurrIDGE, and S.M. Wu. 2015. Derivation of highly purified cardiomyocytes from human induced pluripotent stem cells using small molecule-modulated differentiation and subsequent glucose starvation. *J Vis Exp*.
- Shih, C.-h., S.-L. Chen, C.-C. Yen, Y.-H. Huang, C.-d. Chen, Y.-S. Lee, and K.-h. Lin. 2004. Thyroid Hormone Receptor-Dependent Transcriptional Regulation of Fibrinogen and Coagulation Proteins. *Endocrinology*. 145:2804-2814.
- Shimajima, M., S. Yuasa, C. Motoda, G. Yozu, T. Nagai, S. Ito, M. Lachmann, S. Kashimura, M. Takei, D. Kusumoto, A. Kunitomi, N. Hayashiji, T. Seki, S. Tohyama, H. Hashimoto, M. Kodaira, T. Egashira, K. Hayashi, C. Nakanishi, K. Sakata, M. Yamagishi, and K. Fukuda. 2017. Emerin plays a crucial role in nuclear invagination and in the nuclear calcium transient. *Scientific Reports*. 7:44312.
- Shin, J.Y., A. Hernandez-Ono, T. Fedotova, C. Östlund, M.J. Lee, S.B. Gibeley, C.C. Liang, W.T. Dauer, H.N. Ginsberg, and H.J. Worman. 2019. Nuclear envelope-localized torsinA-LAP1 complex regulates hepatic VLDL secretion and steatosis. *J Clin Invest*. 129:4885-4900.
- Shin, J.Y., C. Le Dour, F. Sera, S. Iwata, S. Homma, L.C. Joseph, J.P. Morrow, W.T. Dauer, and H.J. Worman. 2014. Depletion of lamina-associated polypeptide 1 from cardiomyocytes causes cardiac dysfunction in mice. *Nucleus-Phila*. 5:260-459.
- Shin, J.Y., I. Méndez-López, Y. Wang, A.P. Hays, K. Tanji, J.H. Lefkowitz, P.C. Schulze, H.J. Worman, and W.T. Dauer. 2013. Lamina-associated polypeptide-1 interacts with the muscular dystrophy protein emerin and is essential for skeletal muscle maintenance. *Dev Cell*. 26:591-603.
- Shumaker, D.K., L. Solimando, K. Sengupta, T. Shimi, S.A. Adam, A. Grunwald, S.V. Strelkov, U. Aebi, M.C. Cardoso, and R.D. Goldman. 2008. The highly conserved nuclear lamin Ig-fold binds to PCNA: its role in DNA replication. *J Cell Biol*. 181:269-280.
- Simon, D.N., and K.L. Wilson. 2013. Partners and post-translational modifications of nuclear lamins. *Chromosoma*. 122:13-31.
- Sinensky, M., K. Fantle, M. Trujillo, T. McLain, A. Kupfer, and M. Dalton. 1994. The processing pathway of prelamin A. *J Cell Sci*. 107 (Pt 1):61-67.
- Singh, M., C.R. Hunt, R.K. Pandita, R. Kumar, C.-R. Yang, N. Horikoshi, R. Bachoo, S. Serag, M.D. Story, J.W. Shay, S.N. Powell, A. Gupta, J. Jeffery, S. Pandita, B.P.C. Chen, D. Deckbar, M. Löbrich, Q. Yang, K.K. Khanna, H.J. Worman, and T.K. Pandita. 2013. Lamin A/C depletion enhances DNA damage-induced stalled replication fork arrest. *Molecular and cellular biology*. 33:1210-1222.
- Siu, C.W., Y.K. Lee, J.C. Ho, W.H. Lai, Y.C. Chan, K.M. Ng, L.Y. Wong, K.W. Au, Y.M. Lau, J. Zhang, K.W. Lay, A. Colman, and H.F. Tse. 2012. Modeling of lamin A/C mutation premature cardiac aging using patient-specific induced pluripotent stem cells. *Aging (Albany NY)*. 4:803-822.
- Solovei, I., M. Kreysing, C. Lanctot, S. Kosem, L. Peichl, T. Cremer, J. Guck, and B. Joffe. 2009. Nuclear Architecture of Rod Photoreceptor Cells Adapts to Vision in Mammalian Evolution. *Cell*. 137:356-368.
- Solovei, I., A.S. Wang, K. Thanisch, C.S. Schmidt, S. Krebs, M. Zwerger, T.V. Cohen, D. Devys, R. Foisner, L. Peichl, H. Herrmann, H. Blum, D. Engelkamp, C.L. Stewart, H. Leonhardt, and B. Joffe. 2013. LBR and lamin A/C sequentially tether peripheral heterochromatin and inversely regulate differentiation. *Cell*. 152:584-598.
- Soullam, B., and H.J. Worman. 1995. Signals and structural features involved in integral membrane protein targeting to the inner nuclear membrane. *J Cell Biol*. 130:15-27.

- Spann, T.P., A.E. Goldman, C. Wang, S. Huang, and R.D. Goldman. 2002. Alteration of nuclear lamin organization inhibits RNA polymerase II-dependent transcription. *J Cell Biol.* 156:603-608.
- Speckman, R.A., A. Garg, F.H. Du, L. Bennett, R. Veile, E. Arioglu, S.I. Taylor, M. Lovett, and A.M. Bowcock. 2000. Mutational and haplotype analyses of families with familial partial lipodystrophy (Dunnigan variety) reveal recurrent missense mutations in the globular C-terminal domain of lamin A/C. *Am J Hum Genet.* 66:1192-1198.
- Spector, D.L., X.D. Fu, and T. Maniatis. 1991. Associations between distinct pre-mRNA splicing components and the cell nucleus. *Embo j.* 10:3467-3481.
- Spector, D.L., W.H. Schrier, and H. Busch. 1983. Immunoelectron microscopic localization of snRNPs. *Biol Cell.* 49:1-10.
- Stanley, W.C., G.D. Lopaschuk, J.L. Hall, and J.G. McCormack. 1997. Regulation of myocardial carbohydrate metabolism under normal and ischaemic conditions. Potential for pharmacological interventions. *Cardiovascular Research.* 33:243-257.
- Stewart, C., and B. Burke. 1987. Teratocarcinoma stem cells and early mouse embryos contain only a single major lamin polypeptide closely resembling lamin B. *Cell.* 51:383-392.
- Stiekema, M., M. van Zandvoort, F.C.S. Ramaekers, and J.L.V. Broers. 2020. Structural and Mechanical Aberrations of the Nuclear Lamina in Disease. *Cells.* 9.
- Stierlé, V., J. Couprie, C. Ostlund, I. Krimm, S. Zinn-Justin, P. Hossenlopp, H.J. Worman, J.C. Courvalin, and I. Duband-Goulet. 2003. The carboxyl-terminal region common to lamins A and C contains a DNA binding domain. *Biochemistry.* 42:4819-4828.
- Sullivan, T., D. Escalante-Alcalde, H. Bhatt, M. Anver, N. Bhat, K. Nagashima, C.L. Stewart, and B. Burke. 1999. Loss of A-type lamin expression compromises nuclear envelope integrity leading to muscular dystrophy. *J Cell Biol.* 147:913-920.
- Swift, J., I.L. Ivanovska, A. Buxboim, T. Harada, P.C. Dingal, J. Pinter, J.D. Pajeroski, K.R. Spinler, J.W. Shin, M. Tewari, F. Rehfeldt, D.W. Speicher, and D.E. Discher. 2013. Nuclear lamin-A scales with tissue stiffness and enhances matrix-directed differentiation. *Science.* 341:1240104.
- Takahashi, K., K. Tanabe, M. Ohnuki, M. Narita, T. Ichisaka, K. Tomoda, and S. Yamanaka. 2007. Induction of pluripotent stem cells from adult human fibroblasts by defined factors. *Cell.* 131:861-872.
- Takahashi, K., and S. Yamanaka. 2006. Induction of pluripotent stem cells from mouse embryonic and adult fibroblast cultures by defined factors. *Cell.* 126:663-676.
- Talman, V., J. Teppo, P. Pöhö, P. Movahedi, A. Vaikkinen, S.T. Karhu, K. Trošt, T. Suviavaal, J. Heikkonen, T. Pahikkala, T. Kotiaho, R. Kostianen, M. Varjosalo, and H. Ruskoaho. 2018. Molecular Atlas of Postnatal Mouse Heart Development. *Journal of the American Heart Association.* 7:e010378.
- Taniura, H., C. Glass, and L. Gerace. 1995. A chromatin binding site in the tail domain of nuclear lamins that interacts with core histones. *J Cell Biol.* 131:33-44.
- Tauffmanberger, A., H. Fiumelli, S. Almustafa, and P.J. Magistretti. 2019. Lactate and pyruvate promote oxidative stress resistance through hormetic ROS signaling. *Cell Death Dis.* 10:653.
- Taylor, M.R.G., P.R. Fain, G. Sinagra, M.L. Robinson, A.D. Robertson, E. Carniel, A.D. Lenarda, T.J. Bohlmeier, D.A. Ferguson, G.L. Brodsky, M.M. Boucek, J. Lascor, A.C. Moss, W.-L.P. Li, G.L. Stetler, F. Muntoni, M.R. Bristow, and L. Mestroni. 2003. Natural history of dilated cardiomyopathy due to lamin A/C gene mutations. *Journal of the American College of Cardiology.* 41:771-780.
- Tesson, F., M. Saj, M.M. Uvaize, H. Nicolas, R. Ploski, and Z. Bilinska. 2014. Lamin A/C mutations in dilated cardiomyopathy. *Cardiol J.* 21:331-342.

- Thomas, J.D., J. Sznajder Ł., O. Bardhi, F.N. Aslam, Z.P. Anastasiadis, M.M. Scotti, I. Nishino, M. Nakamori, E.T. Wang, and M.S. Swanson. 2017. Disrupted prenatal RNA processing and myogenesis in congenital myotonic dystrophy. *Genes Dev.* 31:1122-1133.
- Thompson, L.J., M. Bollen, and A.P. Fields. 1997. Identification of protein phosphatase 1 as a mitotic lamin phosphatase. *J Biol Chem.* 272:29693-29697.
- Tifft, K.E., K.A. Bradbury, and K.L. Wilson. 2009. Tyrosine phosphorylation of nuclear-membrane protein emerlin by Src, Abl and other kinases. *J Cell Sci.* 122:3780-3790.
- Timsit, Y.E., and M. Negishi. 2007. CAR and PXR: the xenobiotic-sensing receptors. *Steroids.* 72:231-246.
- Topriceanu, C.C., M. Alfarih, A.D. Hughes, H. Shiwani, F. Chan, S.A. Mohiddin, W. Moody, R.P. Steeds, B. O'Brien, J. Vowinckel, P. Syrris, C. Coats, S. Pettit, E. Arbustini, J.C. Moon, and G. Captur. 2023. The atrial and ventricular myocardial proteome of end-stage lamin heart disease. *Acta Myol.* 42:43-52.
- Trask, R.V., and J.J. Billadello. 1990. Tissue-specific distribution and developmental regulation of M and B creatine kinase mRNAs. *Biochim Biophys Acta.* 1049:182-188.
- Tsai, P.L., C.G. Zhao, E. Turner, and C. Schlieker. 2016. The Lamin B receptor is essential for cholesterol synthesis and perturbed by disease-causing mutations. *Elife.* 5.
- Turgay, Y., M. Eibauer, A.E. Goldman, T. Shimi, M. Khayat, K. Ben-Harush, A. Dubrovsky-Gaupp, K.T. Sapra, R.D. Goldman, and O. Medalia. 2017. The molecular architecture of lamins in somatic cells. *Nature.* 543:261-264.
- Turgay, Y., and O. Medalia. 2017. The structure of lamin filaments in somatic cells as revealed by cryo-electron tomography. *Nucleus-Phila.* 8:475-481.
- Tyser, R.C., A.M. Miranda, C.M. Chen, S.M. Davidson, S. Srinivas, and P.R. Riley. 2016. Calcium handling precedes cardiac differentiation to initiate the first heartbeat. *Elife.* 5.
- Ugarte, F., R. Sousa, B. Cinquin, E.W. Martin, J. Krietsch, G. Sanchez, M. Inman, H. Tsang, M. Warr, E. Passegue, C.A. Larabell, and E.C. Forsberg. 2015. Progressive Chromatin Condensation and H3K9 Methylation Regulate the Differentiation of Embryonic and Hematopoietic Stem Cells. *Stem Cell Rep.* 5:728-740.
- Ulianov, S.V., S.A. Doronin, E.E. Khrameeva, P.I. Kos, A.V. Luzhin, S.S. Starikov, A.A. Galitsyna, V.V. Nenasheva, A.A. Ilyin, I.M. Flyamer, E.A. Mikhaleva, M.D. Logacheva, M.S. Gelfand, A.V. Chertovich, A.A. Gavrilov, S.V. Razin, and Y.Y. Shevelyov. 2019. Nuclear lamina integrity is required for proper spatial organization of chromatin in *Drosophila*. *Nat Commun.* 10.
- Van Berlo, J.H., J.W. Voncken, N. Kubben, J.L. Broers, R. Duisters, R.E. van Leeuwen, H.J. Crijns, F.C. Ramaekers, C.J. Hutchison, and Y.M. Pinto. 2005. A-type lamins are essential for TGF-beta1 induced PP2A to dephosphorylate transcription factors. *Hum Mol Genet.* 14:2839-2849.
- van der Kooi, A.J., G. Bonne, B. Eymard, D. Duboc, B. Talim, M. Van der Valk, P. Reiss, P. Richard, L. Demay, L. Merlini, K. Schwartz, H.F. Busch, and M. de Visser. 2002. Lamin A/C mutations with lipodystrophy, cardiac abnormalities, and muscular dystrophy. *Neurology.* 59:620-623.
- van Engelen, B.G., A. Muchir, C.J. Hutchison, A.J. van der Kooi, G. Bonne, and M. Lammens. 2005. The lethal phenotype of a homozygous nonsense mutation in the lamin A/C gene. *Neurology.* 64:374-376.
- van Rijsingen, I.A.W., E. Arbustini, P.M. Elliott, J. Mogensen, J.F. Hermans-van Ast, A.J. van der Kooi, J.P. van Tintelen, M.P. van den Berg, A. Pilotto, M. Pasotti, S. Jenkins, C. Rowland, U. Aslam, A.A.M. Wilde, A. Perrot, S. Pankuweit, A.H. Zwinderman, P. Charron, and Y.M. Pinto. 2012. Risk Factors for Malignant Ventricular Arrhythmias in Lamin A/C Mutation Carriers A European Cohort Study. *Journal of the American College of Cardiology.* 59:493-500.

- van Steensel, B., and A.S. Belmont. 2017. Lamina-Associated Domains: Links with Chromosome Architecture, Heterochromatin, and Gene Repression. *Cell*. 169:780-791.
- Vergnes, L., M. Peterfy, M.O. Bergo, S.G. Young, and K. Reue. 2004. Lamin B1 is required for mouse development and nuclear integrity. *P Natl Acad Sci USA*. 101:10428-10433.
- Vidak, S., L.A. Serebryanny, G. Pegoraro, and T. Misteli. 2023. Activation of endoplasmic reticulum stress in premature aging via the inner nuclear membrane protein SUN2. *Cell Rep*. 42:112534.
- Vignier, N., M. Chatzifrangkeskou, B. Morales Rodriguez, M. Mericskay, N. Mougnot, K. Wahbi, G. Bonne, and A. Muchir. 2018. Rescue of biosynthesis of nicotinamide adenine dinucleotide protects the heart in cardiomyopathy caused by lamin A/C gene mutation. *Hum Mol Genet*. 27:3870-3880.
- Vivante, A., I. Shoval, and Y. Garini. 2021. The Dynamics of Lamin a During the Cell Cycle. *Front Mol Biosci*. 8:705595.
- Vuillemin, M., and T. Pexieder. 1989a. Normal stages of cardiac organogenesis in the mouse: I. Development of the external shape of the heart. *Am J Anat*. 184:101-113.
- Vuillemin, M., and T. Pexieder. 1989b. Normal stages of cardiac organogenesis in the mouse: II. Development of the internal relief of the heart. *Am J Anat*. 184:114-128.
- Walter, M.C., T.N. Witt, B.S. Weigel, P. Reilich, P. Richard, D. Pongratz, G. Bonne, M.S. Wehnert, and H. Lochmüller. 2005. Deletion of the LMNA initiator codon leading to a neurogenic variant of autosomal dominant Emery-Dreifuss muscular dystrophy. *Neuromuscul Disord*. 15:40-44.
- Wang, E. 1985. Rapid Disappearance of Statin, a Nonproliferating and Senescent Cell-Specific Protein, Upon Reentering the Process of Cell Cycling. *J Cell Biol*. 101:1695-1701.
- Wang, E.T., N.A. Cody, S. Jog, M. Biancolella, T.T. Wang, D.J. Treacy, S. Luo, G.P. Schroth, D.E. Housman, S. Reddy, E. Lécuycer, and C.B. Burge. 2012. Transcriptome-wide regulation of pre-mRNA splicing and mRNA localization by muscleblind proteins. *Cell*. 150:710-724.
- Waterham, H.R., J. Koster, P. Mooyer, G. van Noort, R.I. Kelley, W.R. Wilcox, R.J.A. Wanders, R.C.M. Hennekam, and J.C. Oosterwijk. 2003. Autosomal recessive HEM/greenberg skeletal dysplasia is caused by 3 beta-hydroxysterol Delta(14)-reductase deficiency due to mutations in the lamin B receptor gene. *Am J Hum Genet*. 72:1013-1017.
- Wegner, L., G. Andersen, T. Sparsø, N. Grarup, C. Glümer, K. Borch-Johnsen, T. Jørgensen, T. Hansen, and O. Pedersen. 2007. Common variation in LMNA increases susceptibility to type 2 diabetes and associates with elevated fasting glycemia and estimates of body fat and height in the general population: studies of 7,495 Danish whites. *Diabetes*. 56:694-698.
- Wen, B., H. Wu, Y. Shinkai, R.A. Irizarry, and A.P. Feinberg. 2009. Large histone H3 lysine 9 dimethylated chromatin blocks distinguish differentiated from embryonic stem cells. *Nat Genet*. 41:246-250.
- Wessels, A., and D. Sedmera. 2003. Developmental anatomy of the heart: a tale of mice and man. *Physiological Genomics*. 15:165-176.
- West, G., J. Gullmets, L. Virtanen, S.P. Li, A. Keinänen, T. Shimi, M. Mauermann, T. Heliö, M. Kaartinen, L. Ollila, J. Kuusisto, J.E. Eriksson, R.D. Goldman, H. Herrmann, and P. Taimen. 2016. Deleterious assembly of the lamin A/C mutant p.S143P causes ER stress in familial dilated cardiomyopathy. *J Cell Sci*. 129:2732-2743.
- Wheeler, M.A., J.D. Davies, Q. Zhang, L.J. Emerson, J. Hunt, C.M. Shanahan, and J.A. Ellis. 2007. Distinct functional domains in nesprin-1alpha and nesprin-2beta bind directly to emerin and both interactions are disrupted in X-linked Emery-Dreifuss muscular dystrophy. *Exp Cell Res*. 313:2845-2857.

- Wilkinson, F.L., J.M. Holaska, Z. Zhang, A. Sharma, S. Manilal, I. Holt, S. Stamm, K.L. Wilson, and G.E. Morris. 2003. Emerin interacts in vitro with the splicing-associated factor, YT521-B. *Eur J Biochem.* 270:2459-2466.
- Wilkinson, K.A., and J.M. Henley. 2010. Mechanisms, regulation and consequences of protein SUMOylation. *Biochem J.* 428:133-145.
- Wolf, C.M., L. Wang, R. Alcalai, A. Pizard, P.G. Burgon, F. Ahmad, M. Sherwood, D.M. Branco, H. Wakimoto, G.I. Fishman, V. See, C.L. Stewart, D.A. Conner, C.I. Berul, C.E. Seidman, and J.G. Seidman. 2008. Lamin A/C haploinsufficiency causes dilated cardiomyopathy and apoptosis-triggered cardiac conduction system disease. *J Mol Cell Cardiol.* 44:293-303.
- Worman, H.J., and G. Bonne. 2007. "Laminopathies": A wide spectrum of human diseases. *Exp Cell Res.* 313:2121-2133.
- Worman, H.J., C.D. Evans, and G. Blobel. 1990. The lamin B receptor of the nuclear envelope inner membrane: a polytopic protein with eight potential transmembrane domains. *J Cell Biol.* 111:1535-1542.
- Worman, H.J., J. Yuan, G. Blobel, and S.D. Georgatos. 1988. A lamin B receptor in the nuclear envelope. *Proc Natl Acad Sci U S A.* 85:8531-8534.
- Xiong, L., K. Zhao, Y. Cao, H.H. Guo, J.X. Pan, X. Yang, X. Ren, L. Mei, and W.C. Xiong. 2020. Linking skeletal muscle aging with osteoporosis by lamin A/C deficiency. *PLoS Biol.* 18:e3000731.
- Yagyu, H., G. Chen, M. Yokoyama, K. Hirata, A. Augustus, Y. Kako, T. Seo, Y. Hu, E.P. Lutz, M. Merkel, A. Bensadoun, S. Homma, and I.J. Goldberg. 2003. Lipoprotein lipase (LpL) on the surface of cardiomyocytes increases lipid uptake and produces a cardiomyopathy. *J Clin Invest.* 111:419-426.
- Yates, J.R., J. Bagshaw, V.M. Aksmanovic, E. Coomber, R. McMahon, J.L. Whittaker, P.J. Morrison, J. Kendrick-Jones, and J.A. Ellis. 1999. Genotype-phenotype analysis in X-linked Emery-Dreifuss muscular dystrophy and identification of a missense mutation associated with a milder phenotype. *Neuromuscul Disord.* 9:159-165.
- Ye, Q., and H.J. Worman. 1996. Interaction between an integral protein of the nuclear envelope inner membrane and human chromodomain proteins homologous to Drosophila HP1. *J Biol Chem.* 271:14653-14656.
- Young, J., L. Morbois-Trabut, B. Couzinet, O. Lascols, E. Dion, V. Béréziat, B. Fève, I. Richard, J. Capeau, P. Chanson, and C. Vigouroux. 2005a. Type A insulin resistance syndrome revealing a novel lamin A mutation. *Diabetes.* 54:1873-1878.
- Young, S.G., L.G. Fong, and S. Michaelis. 2005b. Prelamin A, Zmpste24, misshapen cell nuclei, and progeria--new evidence suggesting that protein farnesylation could be important for disease pathogenesis. *J Lipid Res.* 46:2531-2558.
- Yu, J., K. Hu, K. Smuga-Otto, S. Tian, R. Stewart, Slukvin, II, and J.A. Thomson. 2009. Human induced pluripotent stem cells free of vector and transgene sequences. *Science.* 324:797-801.
- Yu, J., M.A. Vodyanik, K. Smuga-Otto, J. Antosiewicz-Bourget, J.L. Frane, S. Tian, J. Nie, G.A. Jonsdottir, V. Ruotti, R. Stewart, Slukvin, II, and J.A. Thomson. 2007. Induced pluripotent stem cell lines derived from human somatic cells. *Science.* 318:1917-1920.
- Yu, Z., J. Zhu, H. Wang, H. Li, and X. Jin. 2022. Function of BCLAF1 in human disease. *Oncol Lett.* 23:58.
- Zachara, N.E., H. Molina, K.Y. Wong, A. Pandey, and G.W. Hart. 2011. The dynamic stress-induced "O-GlcNAc-ome" highlights functions for O-GlcNAc in regulating DNA damage/repair and other cellular pathways. *Amino Acids.* 40:793-808.
- Zachara, N.E., N. O'Donnell, W.D. Cheung, J.J. Mercer, J.D. Marth, and G.W. Hart. 2004. Dynamic O-GlcNAc modification of nucleocytoplasmic proteins in response to stress. A survival response of mammalian cells. *J Biol Chem.* 279:30133-30142.

- Zhang, W., X.H. Liu, J.T. Zhou, C. Cheng, J. Xu, J. Yu, and X. Li. 2023. Apolipoprotein A-IV restrains fat accumulation in skeletal and myocardial muscles by inhibiting lipogenesis and activating PI3K-AKT signalling. *Arch Physiol Biochem*:1-11.
- Zhang, Y.Q., and K.D. Sarge. 2008. Sumoylation regulates lamin A function and is lost in lamin A mutants associated with familial cardiomyopathies. *J Cell Biol.* 182:35-39.
- Zheng, X.B., J.B. Hu, S.B. Yue, L. Kristiani, M. Kim, M. Sauria, J. Taylor, Y. Kim, and Y.X. Zheng. 2018. Lamins Organize the Global Three-Dimensional Genome from the Nuclear Periphery. *Mol Cell.* 71:802-+.
- Zhu, J., M. Adli, J.Y. Zou, G. Verstappen, M. Coyne, X.L. Zhang, T. Durham, M. Miri, V. Deshpande, P.L. De Jager, D.A. Bennett, J.A. Houmard, D.M. Muoio, T.T. Onder, R. Camahort, C.A. Cowan, A. Meissner, C.B. Epstein, N. Shores, and B.E. Bernstein. 2013. Genome-wide Chromatin State Transitions Associated with Developmental and Environmental Cues. *Cell.* 152:642-654.
- Zuleger, N., S. Boyle, D.A. Kelly, J.I. de las Heras, V. Lazou, N. Korfali, D.G. Batrakou, K.N. Randles, G.E. Morris, D.J. Harrison, W.A. Bickmore, and E.C. Schirmer. 2013. Specific nuclear envelope transmembrane proteins can promote the location of chromosomes to and from the nuclear periphery. *Genome Biol.* 14.

Appendix A

Table AA: Differentially expressed RNA transcripts. DOWN – downregulated in comparison; UP upregulated in comparison; NS – not significant in comparison.

Gene ID	Gene name	LMNA ^{+/-} vs WT	EMD ^{-/-} vs WT
ENSG00000023839	ABCC2	DOWN	DOWN
ENSG000000256340	ABCC6P1	DOWN	DOWN
ENSG000000160179	ABCG1	DOWN	DOWN
ENSG000000197142	ACSL5	DOWN	DOWN
ENSG000000106526	ACTR3C	DOWN	DOWN
ENSG000000123612	ACVR1C	DOWN	DOWN
ENSG000000132744	ACY3	DOWN	DOWN
ENSG00000042980	ADAM28	DOWN	DOWN
ENSG000000151651	ADAM8	DOWN	DOWN
ENSG000000164393	ADGRF2	DOWN	DOWN
ENSG000000205336	ADGRG1	DOWN	DOWN
ENSG000000144820	ADGRG7	DOWN	DOWN
ENSG000000116771	AGMAT	DOWN	DOWN
ENSG000000026652	AGPAT4	DOWN	DOWN
ENSG000000106541	AGR2	DOWN	DOWN
ENSG000000173467	AGR3	DOWN	DOWN
ENSG000000144891	AGTR1	DOWN	DOWN
ENSG000000113492	AGXT2	DOWN	DOWN
ENSG000000122787	AKR1D1	DOWN	DOWN
ENSG000000144908	ALDH1L1	DOWN	DOWN
ENSG000000175548	ALG10B	DOWN	DOWN
ENSG000000163295	ALPI	DOWN	DOWN
ENSG000000166126	AMN	DOWN	DOWN
ENSG000000132855	ANGPTL3	DOWN	DOWN
ENSG000000130812	ANGPTL6	DOWN	DOWN
ENSG000000175311	ANKS4B	DOWN	DOWN
ENSG000000131620	ANO1	DOWN	DOWN
ENSG000000104537	ANXA13	DOWN	DOWN
ENSG000000136250	AOAH	DOWN	DOWN
ENSG000000002726	AOC1	DOWN	DOWN
ENSG000000107282	APBA1	UP	UP
ENSG000000077420	APBB1IP	DOWN	DOWN
ENSG000000118137	APOA1	DOWN	DOWN
ENSG000000084674	APOB	DOWN	DOWN
ENSG000000109321	AREG	DOWN	DOWN
ENSG000000163947	ARHGEF3	DOWN	DOWN
ENSG000000161944	ASGR2	DOWN	DOWN
ENSG000000127249	ATP13A4	DOWN	DOWN
ENSG000000064270	ATP2C2	DOWN	DOWN
ENSG000000284138	ATP6V0CP4	DOWN	DOWN
ENSG000000006453	BAIAP2L1	DOWN	DOWN
ENSG000000153064	BANK1	DOWN	DOWN
ENSG000000060982	BCAT1	DOWN	DOWN
ENSG000000121380	BCL2L14	DOWN	DOWN

ENSG00000197580	BCO2	DOWN	DOWN
ENSG00000169668	BCRP2	DOWN	DOWN
ENSG00000215544	BCRP7	DOWN	DOWN
ENSG00000182492	BGN	UP	UP
ENSG00000162069	BICDL2	DOWN	DOWN
ENSG00000116985	BMP8B	DOWN	DOWN
ENSG00000138696	BMPR1B	DOWN	DOWN
ENSG00000182795	C1orf116	DOWN	DOWN
ENSG00000253313	C1orf210	DOWN	DOWN
ENSG00000165985	C1QL3	DOWN	DOWN
ENSG00000204128	C2orf72	DOWN	DOWN
ENSG00000171860	C3AR1	DOWN	DOWN
ENSG00000241224	C3orf85	DOWN	DOWN
ENSG00000123843	C4BPB	DOWN	DOWN
ENSG00000154274	C4orf19	DOWN	DOWN
ENSG00000164241	C5orf63	DOWN	DOWN
ENSG00000165118	C9orf64	DOWN	DOWN
ENSG00000104267	CA2	DOWN	DOWN
ENSG00000178538	CA8	DOWN	DOWN
ENSG00000198216	CACNA1E	UP	UP
ENSG00000182472	CAPN12	DOWN	DOWN
ENSG00000162949	CAPN13	DOWN	DOWN
ENSG00000257859	CASC18	UP	UP
ENSG00000183323	CCDC125	UP	UP
ENSG00000203799	CCDC162P	DOWN	DOWN
ENSG00000100557	CCDC198	DOWN	DOWN
ENSG00000161973	CCDC42	DOWN	DOWN
ENSG00000166510	CCDC68	DOWN	DOWN
ENSG00000151882	CCL28	DOWN	DOWN
ENSG00000118971	CCND2	DOWN	DOWN
ENSG00000182632	CCNYL2	DOWN	DOWN
ENSG00000167851	CD300A	DOWN	DOWN
ENSG00000160654	CD3G	DOWN	DOWN
ENSG00000079112	CDH17	DOWN	DOWN
ENSG00000099834	CDHR5	DOWN	DOWN
ENSG00000165556	CDX2	DOWN	DOWN
ENSG00000245848	CEBPA	DOWN	DOWN
ENSG00000089199	CHGB	DOWN	DOWN
ENSG00000180767	CHST13	DOWN	DOWN
ENSG00000187288	CIDEC	DOWN	DOWN
ENSG00000164007	CLDN19	DOWN	DOWN
ENSG00000165376	CLDN2	DOWN	DOWN
ENSG00000253958	CLDN23	DOWN	DOWN
ENSG00000165215	CLDN3	DOWN	DOWN
ENSG00000189143	CLDN4	DOWN	DOWN
ENSG00000181885	CLDN7	DOWN	DOWN
ENSG00000110852	CLEC2B	DOWN	DOWN
ENSG00000159212	CLIC6	DOWN	DOWN
ENSG00000180745	CLRN3	DOWN	DOWN
ENSG00000079101	CLUL1	UP	UP
ENSG00000198515	CNGA1	DOWN	DOWN

ENSG00000142675	CNKSR1	DOWN	DOWN
ENSG00000119946	CNNM1	DOWN	DOWN
ENSG00000119865	CNRIP1	UP	UP
ENSG00000122756	CNTFR	UP	UP
ENSG00000169031	COL4A3	DOWN	DOWN
ENSG00000081052	COL4A4	DOWN	DOWN
ENSG00000184374	COLEC10	DOWN	DOWN
ENSG00000198756	COLGALT2	UP	UP
ENSG00000047457	CP	DOWN	DOWN
ENSG00000158516	CPA2	DOWN	DOWN
ENSG00000139117	CPNE8	DOWN	DOWN
ENSG00000169169	CPT1C	UP	UP
ENSG00000060566	CREB3L3	DOWN	DOWN
ENSG00000112297	CRYBG1	DOWN	DOWN
ENSG00000176092	CRYBG2	DOWN	DOWN
ENSG00000182578	CSF1R	DOWN	DOWN
ENSG00000119535	CSF3R	DOWN	DOWN
ENSG00000066032	CTNNA2	UP	UP
ENSG00000103811	CTSH	DOWN	DOWN
ENSG00000107611	CUBN	DOWN	DOWN
ENSG00000161921	CXCL16	DOWN	DOWN
ENSG00000256612	CYP2B7P	DOWN	DOWN
ENSG00000073067	CYP2W1	DOWN	DOWN
ENSG00000146038	DCDC2	DOWN	DOWN
ENSG00000133083	DCLK1	UP	UP
ENSG00000077279	DCX	UP	UP
ENSG00000132437	DDC	DOWN	DOWN
ENSG00000162777	DENND2D	DOWN	DOWN
ENSG00000165325	DEUP1	DOWN	DOWN
ENSG00000211452	DIO1	DOWN	DOWN
ENSG00000197406	DIO3	DOWN	DOWN
ENSG00000187908	DMBT1	DOWN	DOWN
ENSG00000162643	DNAI3	DOWN	DOWN
ENSG00000147459	DOCK5	DOWN	DOWN
ENSG00000197635	DPP4	DOWN	DOWN
ENSG00000137857	DUOX1	DOWN	DOWN
ENSG00000140254	DUOXA1	DOWN	DOWN
ENSG00000140274	DUOXA2	DOWN	DOWN
ENSG00000130829	DUSP9	DOWN	DOWN
ENSG00000221818	EBF2	UP	UP
ENSG00000136160	EDNRB	DOWN	DOWN
ENSG00000198759	EGFL6	DOWN	DOWN
ENSG00000164318	EGFLAM	DOWN	DOWN
ENSG00000135373	EHF	DOWN	DOWN
ENSG00000049540	ELN	UP	UP
ENSG00000182156	ENPP7	DOWN	DOWN
ENSG00000095203	EPB41L4B	DOWN	DOWN
ENSG00000119888	EPCAM	DOWN	DOWN
ENSG00000198758	EPS8L3	DOWN	DOWN
ENSG00000065361	ERBB3	DOWN	DOWN
ENSG00000244476	ERVFRD-1	DOWN	DOWN

ENSG00000187017	ESPN	DOWN	DOWN
ENSG00000124491	F13A1	DOWN	DOWN
ENSG00000180210	F2	DOWN	DOWN
ENSG00000164251	F2RL1	DOWN	DOWN
ENSG00000117525	F3	DOWN	DOWN
ENSG00000163586	FABP1	DOWN	DOWN
ENSG00000172782	FADS6	DOWN	DOWN
ENSG00000162391	FAM151A	DOWN	DOWN
ENSG00000182103	FAM181B	UP	UP
ENSG00000179813	FAM216B	DOWN	DOWN
ENSG00000213185	FAM24B	DOWN	DOWN
ENSG00000230368	FAM41C	DOWN	DOWN
ENSG00000105523	FAM83E	DOWN	DOWN
ENSG00000133477	FAM83F	DOWN	DOWN
ENSG00000182366	FAM87A	DOWN	DOWN
ENSG00000165323	FAT3	UP	UP
ENSG00000165140	FBP1	DOWN	DOWN
ENSG00000141665	FBXO15	DOWN	DOWN
ENSG00000268388	FENDRR	DOWN	DOWN
ENSG00000139132	FGD4	DOWN	DOWN
ENSG00000156427	FGF18	DOWN	DOWN
ENSG00000160867	FGFR4	DOWN	DOWN
ENSG00000171557	FGG	DOWN	DOWN
ENSG00000231426	FILNC1	DOWN	DOWN
ENSG00000129514	FOXA1	DOWN	DOWN
ENSG00000125798	FOXA2	DOWN	DOWN
ENSG00000170608	FOXA3	DOWN	DOWN
ENSG00000054598	FOXC1	UP	UP
ENSG00000176692	FOXC2	UP	UP
ENSG00000103241	FOXF1	DOWN	DOWN
ENSG00000137273	FOXF2	DOWN	DOWN
ENSG00000164379	FOXQ1	DOWN	DOWN
ENSG00000111816	FRK	DOWN	DOWN
ENSG00000168843	FSTL5	DOWN	DOWN
ENSG00000176920	FUT2	DOWN	DOWN
ENSG00000187889	FYB2	DOWN	DOWN
ENSG00000139112	GABARAPL1	DOWN	DOWN
ENSG00000115339	GALNT3	DOWN	DOWN
ENSG00000244300	GATA2-AS1	UP	UP
ENSG00000249948	GBA3	DOWN	DOWN
ENSG00000111846	GCNT2	DOWN	DOWN
ENSG00000140297	GCNT3	DOWN	DOWN
ENSG00000119125	GDA	DOWN	DOWN
ENSG00000168621	GDNF	DOWN	DOWN
ENSG00000137960	GIPC2	DOWN	DOWN
ENSG00000169562	GJB1	DOWN	DOWN
ENSG00000169605	GKN1	DOWN	DOWN
ENSG00000178445	GLDC	DOWN	DOWN
ENSG00000182327	GLTPD2	DOWN	DOWN
ENSG00000267265	GP6-AS1	DOWN	DOWN
ENSG00000165370	GPR101	DOWN	DOWN

ENSG00000173890	GPR160	DOWN	DOWN
ENSG00000176153	GPX2	DOWN	DOWN
ENSG00000141449	GREB1L	DOWN	DOWN
ENSG00000083307	GRHL2	DOWN	DOWN
ENSG00000116032	GRIN3B	DOWN	DOWN
ENSG00000126010	GRPR	DOWN	DOWN
ENSG00000243955	GSTA1	DOWN	DOWN
ENSG00000244067	GSTA2	DOWN	DOWN
ENSG00000070019	GUCY2C	DOWN	DOWN
ENSG00000181218	H2AW	DOWN	DOWN
ENSG00000196890	H2BU1	DOWN	DOWN
ENSG00000113196	HAND1	DOWN	DOWN
ENSG00000113249	HAVCR1	DOWN	DOWN
ENSG00000182782	HCAR2	DOWN	DOWN
ENSG00000255398	HCAR3	DOWN	DOWN
ENSG00000206337	HCP5	DOWN	DOWN
ENSG00000138646	HERC5	DOWN	DOWN
ENSG00000138642	HERC6	DOWN	DOWN
ENSG00000113924	HGD	DOWN	DOWN
ENSG00000114455	HHLA2	DOWN	DOWN
ENSG00000179344	HLA-DQB1	DOWN	DOWN
ENSG00000204642	HLA-F	DOWN	DOWN
ENSG00000181126	HLA-V	DOWN	DOWN
ENSG00000108924	HLF	UP	UP
ENSG00000100292	HMOX1	DOWN	DOWN
ENSG00000135100	HNF1A	DOWN	DOWN
ENSG00000241388	HNF1A-AS1	DOWN	DOWN
ENSG00000275410	HNF1B	DOWN	DOWN
ENSG00000101076	HNF4A	DOWN	DOWN
ENSG00000254369	HOXA-AS3	UP	UP
ENSG00000253293	HOXA10	DOWN	DOWN
ENSG00000005073	HOXA11	DOWN	DOWN
ENSG00000106004	HOXA5	UP	UP
ENSG00000078399	HOXA9	DOWN	DOWN
ENSG00000164120	HPGD	DOWN	DOWN
ENSG00000105707	HPN	DOWN	DOWN
ENSG00000110169	HPX	DOWN	DOWN
ENSG00000168453	HR	UP	UP
ENSG00000185352	HS6ST3	UP	UP
ENSG00000086696	HSD17B2	DOWN	DOWN
ENSG00000203857	HSD3B1	DOWN	DOWN
ENSG00000163395	IGFN1	UP	UP
ENSG00000147255	IGSF1	DOWN	DOWN
ENSG00000163501	IHH	DOWN	DOWN
ENSG00000163701	IL17RE	DOWN	DOWN
ENSG00000103522	IL21R	UP	UP
ENSG00000163083	INHBB	DOWN	DOWN
ENSG00000168918	INPP5D	DOWN	DOWN
ENSG00000161896	IP6K3	DOWN	DOWN
ENSG00000117595	IRF6	DOWN	DOWN
ENSG00000115221	ITGB6	DOWN	DOWN

ENSG00000123243	ITIH5	DOWN	DOWN
ENSG00000176049	JAKMIP2	UP	UP
ENSG00000154721	JAM2	UP	UP
ENSG00000160593	JAML	DOWN	DOWN
ENSG00000177301	KCNA2	UP	UP
ENSG00000153822	KCNJ16	DOWN	DOWN
ENSG00000082482	KCNK2	UP	UP
ENSG00000075043	KCNQ2	UP	UP
ENSG00000185760	KCNQ5	DOWN	DOWN
ENSG00000183775	KCTD16	DOWN	DOWN
ENSG00000136883	KIF12	DOWN	DOWN
ENSG00000272666	KLHDC7B-DT	DOWN	DOWN
ENSG00000186832	KRT16	DOWN	DOWN
ENSG00000214822	KRT16P3	DOWN	DOWN
ENSG00000229028	KRT223P	DOWN	DOWN
ENSG00000135480	KRT7	DOWN	DOWN
ENSG00000115919	KYNU	DOWN	DOWN
ENSG00000177984	LCN15	DOWN	DOWN
ENSG00000115850	LCT	DOWN	DOWN
ENSG00000131981	LGALS3	DOWN	DOWN
ENSG00000145685	LHFPL2	UP	UP
ENSG00000106689	LHX2	UP	UP
ENSG00000225298	LINC00113	DOWN	DOWN
ENSG00000231535	LINC00278	DOWN	DOWN
ENSG00000235665	LINC00298	DOWN	DOWN
ENSG00000233237	LINC00472	DOWN	DOWN
ENSG00000250682	LINC00491	DOWN	DOWN
ENSG00000185904	LINC00839	DOWN	DOWN
ENSG00000249267	LINC00939	DOWN	DOWN
ENSG00000226673	LINC01108	DOWN	DOWN
ENSG00000257582	LINC01475	DOWN	DOWN
ENSG00000233008	LINC01725	DOWN	DOWN
ENSG00000232002	LINC01880	UP	UP
ENSG00000229155	LINC02038	DOWN	DOWN
ENSG00000214043	LINC02347	DOWN	DOWN
ENSG00000226453	LINC02542	DOWN	DOWN
ENSG00000255666	LINC02700	DOWN	DOWN
ENSG00000254416	LINC02732	DOWN	DOWN
ENSG00000255774	LINC02747	DOWN	DOWN
ENSG00000236039	LINC02889	DOWN	DOWN
ENSG00000177335	LINC02904	UP	UP
ENSG00000259666	LINGO1-AS1	DOWN	DOWN
ENSG00000101670	LIPG	DOWN	DOWN
ENSG00000254815	LMNTD2-AS1	DOWN	DOWN
ENSG00000087253	LPCAT2	DOWN	DOWN
ENSG00000162981	LRATD1	DOWN	DOWN
ENSG00000184434	LRRC19	DOWN	DOWN
ENSG00000175489	LRRC25	DOWN	DOWN
ENSG00000127399	LRRC61	DOWN	DOWN
ENSG00000188906	LRRK2	DOWN	DOWN
ENSG00000090382	LYZ	DOWN	DOWN

ENSG00000172478	MAB21L4	DOWN	DOWN
ENSG00000183742	MACC1	DOWN	DOWN
ENSG00000181751	MACIR	DOWN	DOWN
ENSG00000204740	MALRD1	DOWN	DOWN
ENSG00000069535	MAOB	DOWN	DOWN
ENSG00000165471	MBL2	DOWN	DOWN
ENSG00000229111	MED4-AS1	UP	UP
ENSG00000112818	MEP1A	DOWN	DOWN
ENSG00000229719	MIR194-2HG	DOWN	DOWN
ENSG00000230937	MIR205HG	DOWN	DOWN
ENSG00000257612	MIR4307HG	DOWN	DOWN
ENSG00000247516	MIR4458HG	DOWN	DOWN
ENSG00000100427	MLC1	DOWN	DOWN
ENSG00000115648	MLPH	DOWN	DOWN
ENSG00000009950	MLXIPL	DOWN	DOWN
ENSG00000106384	MOGAT3	DOWN	DOWN
ENSG00000149573	MPZL2	DOWN	DOWN
ENSG00000183695	MRGPRX2	DOWN	DOWN
ENSG00000003987	MTMR7	DOWN	DOWN
ENSG00000138823	MTTP	DOWN	DOWN
ENSG00000173702	MUC13	DOWN	DOWN
ENSG00000205592	MUC19	DOWN	DOWN
ENSG00000169894	MUC3A	DOWN	DOWN
ENSG00000030304	MUSK	DOWN	DOWN
ENSG00000187616	MYMK	DOWN	DOWN
ENSG00000145555	MYO10	DOWN	DOWN
ENSG00000166866	MYO1A	DOWN	DOWN
ENSG00000169994	MYO7B	DOWN	DOWN
ENSG00000154654	NCAM2	DOWN	DOWN
ENSG00000226953	NCKAP5-AS2	DOWN	DOWN
ENSG00000173376	NDNF	DOWN	DOWN
ENSG00000104419	NDRG1	DOWN	DOWN
ENSG00000242242	NECTIN3-AS1	UP	UP
ENSG00000237928	NFIA-AS2	UP	UP
ENSG00000066248	NGEF	UP	UP
ENSG00000119919	NKX2-3	DOWN	DOWN
ENSG00000089250	NOS1	UP	UP
ENSG00000015520	NPC1L1	DOWN	DOWN
ENSG00000056291	NPFFR2	DOWN	DOWN
ENSG00000131910	NR0B2	DOWN	DOWN
ENSG00000144852	NR1I2	DOWN	DOWN
ENSG00000175745	NR2F1	UP	UP
ENSG00000153234	NR4A2	UP	UP
ENSG00000116833	NR5A2	DOWN	DOWN
ENSG00000133636	NTS	DOWN	DOWN
ENSG00000173391	OLR1	DOWN	DOWN
ENSG00000180785	OR51E1	DOWN	DOWN
ENSG00000036473	OTC	DOWN	DOWN
ENSG00000188162	OTOG	DOWN	DOWN
ENSG00000172818	OVOL1	DOWN	DOWN
ENSG00000180914	OXTR	UP	UP

ENSG00000250103	PANCR	DOWN	DOWN
ENSG00000258376	PAPLN-AS1	DOWN	DOWN
ENSG00000137819	PAQR5	DOWN	DOWN
ENSG00000113209	PCDHB5	DOWN	DOWN
ENSG00000081853	PCDHGA2	DOWN	DOWN
ENSG00000099139	PCSK5	DOWN	DOWN
ENSG00000140479	PCSK6	DOWN	DOWN
ENSG00000132915	PDE6A	DOWN	DOWN
ENSG00000174827	PDZK1	DOWN	DOWN
ENSG00000261371	PECAM1	DOWN	DOWN
ENSG00000119630	PGF	DOWN	DOWN
ENSG00000139144	PIK3C2G	DOWN	DOWN
ENSG00000170927	PKHD1	DOWN	DOWN
ENSG00000138308	PLA2G12B	DOWN	DOWN
ENSG00000188257	PLA2G2A	DOWN	DOWN
ENSG00000145287	PLAC8	DOWN	DOWN
ENSG00000163803	PLB1	DOWN	DOWN
ENSG00000137841	PLCB2	DOWN	DOWN
ENSG00000008323	PLEKHG6	DOWN	DOWN
ENSG00000054690	PLEKHH1	DOWN	DOWN
ENSG00000161381	PLXDC1	UP	UP
ENSG00000277531	PNMA8C	UP	UP
ENSG00000114631	PODXL2	UP	UP
ENSG00000124429	POF1B	DOWN	DOWN
ENSG00000233854	POU6F2-AS2	DOWN	DOWN
ENSG00000057657	PRDM1	DOWN	DOWN
ENSG00000113494	PRLR	DOWN	DOWN
ENSG00000100033	PRODH	DOWN	DOWN
ENSG00000007062	PROM1	DOWN	DOWN
ENSG00000167183	PRR15L	DOWN	DOWN
ENSG00000135378	PRRG4	DOWN	DOWN
ENSG00000204314	PRRT1	UP	UP
ENSG00000275896	PRSS2	DOWN	DOWN
ENSG00000005001	PRSS22	DOWN	DOWN
ENSG0000010438	PRSS3	DOWN	DOWN
ENSG00000132698	RAB25	DOWN	DOWN
ENSG00000131831	RAI2	UP	UP
ENSG00000184672	RALYL	DOWN	DOWN
ENSG00000136237	RAPGEF5	DOWN	DOWN
ENSG00000189431	RASSF10	DOWN	DOWN
ENSG00000169435	RASSF6	DOWN	DOWN
ENSG00000130701	RBBP8NL	DOWN	DOWN
ENSG00000114113	RBP2	DOWN	DOWN
ENSG00000265203	RBP3	DOWN	DOWN
ENSG00000138207	RBP4	DOWN	DOWN
ENSG00000205517	RGL3	DOWN	DOWN
ENSG00000185304	RGPD2	DOWN	DOWN
ENSG00000090104	RGS1	DOWN	DOWN
ENSG00000186479	RGS7BP	UP	UP
ENSG00000132677	RHBG	DOWN	DOWN
ENSG00000126785	RHOJ	UP	UP

ENSG00000234493	RHOXF1P1	DOWN	DOWN
ENSG00000183421	RIPK4	DOWN	DOWN
ENSG00000239553	RN7SL12P	DOWN	DOWN
ENSG00000026297	RNASET2	DOWN	DOWN
ENSG00000133135	RNF128	DOWN	DOWN
ENSG00000134321	RSAD2	DOWN	DOWN
ENSG00000101115	SALL4	DOWN	DOWN
ENSG00000164764	SBSPON	UP	UP
ENSG00000006747	SCIN	DOWN	DOWN
ENSG00000170786	SDR16C5	DOWN	DOWN
ENSG00000197249	SERPINA1	DOWN	DOWN
ENSG00000188488	SERPINA5	DOWN	DOWN
ENSG00000170542	SERPINB9	DOWN	DOWN
ENSG00000099937	SERPIND1	DOWN	DOWN
ENSG00000253309	SERPINE3	DOWN	DOWN
ENSG00000167711	SERPINF2	DOWN	DOWN
ENSG00000100095	SEZ6L	UP	UP
ENSG00000104332	SFRP1	UP	UP
ENSG00000225383	SFTA1P	DOWN	DOWN
ENSG00000162105	SHANK2	DOWN	DOWN
ENSG00000164690	SHH	DOWN	DOWN
ENSG00000090402	SI	DOWN	DOWN
ENSG00000117090	SLAMF1	DOWN	DOWN
ENSG00000070915	SLC12A3	DOWN	DOWN
ENSG00000141485	SLC13A5	DOWN	DOWN
ENSG00000088386	SLC15A1	DOWN	DOWN
ENSG00000036565	SLC18A1	DOWN	DOWN
ENSG00000165646	SLC18A2	DOWN	DOWN
ENSG00000170482	SLC23A1	DOWN	DOWN
ENSG00000145217	SLC26A1	DOWN	DOWN
ENSG00000091138	SLC26A3	DOWN	DOWN
ENSG00000140284	SLC27A2	DOWN	DOWN
ENSG00000117394	SLC2A1	DOWN	DOWN
ENSG00000163581	SLC2A2	DOWN	DOWN
ENSG00000169507	SLC38A11	DOWN	DOWN
ENSG00000139540	SLC39A5	DOWN	DOWN
ENSG00000204385	SLC44A4	DOWN	DOWN
ENSG00000186198	SLC51B	DOWN	DOWN
ENSG00000148942	SLC5A12	DOWN	DOWN
ENSG00000103546	SLC6A2	DOWN	DOWN
ENSG00000003989	SLC7A2	DOWN	DOWN
ENSG00000279903	SLC7A2-IT1	DOWN	DOWN
ENSG00000099960	SLC7A4	DOWN	DOWN
ENSG00000021488	SLC7A9	DOWN	DOWN
ENSG00000084453	SLCO1A2	DOWN	DOWN
ENSG00000137491	SLCO2B1	DOWN	DOWN
ENSG00000256235	SMIM3	DOWN	DOWN
ENSG00000259120	SMIM6	DOWN	DOWN
ENSG00000256162	SMLR1	DOWN	DOWN
ENSG00000167780	SOAT2	DOWN	DOWN
ENSG00000198944	SOWAHA	DOWN	DOWN

ENSG00000186212	SOWAHB	DOWN	DOWN
ENSG00000187808	SOWAHD	DOWN	DOWN
ENSG00000164651	SP8	DOWN	DOWN
ENSG00000164266	SPINK1	DOWN	DOWN
ENSG00000173898	SPTBN2	DOWN	DOWN
ENSG00000149418	ST14	DOWN	DOWN
ENSG00000115107	STEAP3	DOWN	DOWN
ENSG00000145087	STXBP5L	UP	UP
ENSG00000198203	SULT1C2	DOWN	DOWN
ENSG00000109193	SULT1E1	UP	UP
ENSG00000105398	SULT2A1	DOWN	DOWN
ENSG00000099994	SUSD2	DOWN	DOWN
ENSG00000165025	SYK	DOWN	DOWN
ENSG00000271848	SYNPO2L-AS1	UP	UP
ENSG00000095383	TBC1D2	DOWN	DOWN
ENSG00000092607	TBX15	UP	UP
ENSG00000267280	TBX2-AS1	UP	UP
ENSG00000177822	TENM3-AS1	UP	UP
ENSG00000112773	TENT5A	DOWN	DOWN
ENSG00000091513	TF	DOWN	DOWN
ENSG00000105967	TFEC	DOWN	DOWN
ENSG00000160182	TFF1	DOWN	DOWN
ENSG00000160181	TFF2	DOWN	DOWN
ENSG00000160180	TFF3	DOWN	DOWN
ENSG00000072274	TFRC	DOWN	DOWN
ENSG00000069702	TGFBR3	DOWN	DOWN
ENSG00000228828	TLK2P2	DOWN	DOWN
ENSG00000163762	TM4SF18	DOWN	DOWN
ENSG00000168955	TM4SF20	DOWN	DOWN
ENSG00000142484	TM4SF5	DOWN	DOWN
ENSG00000167608	TMC4	DOWN	DOWN
ENSG00000146859	TMEM140	DOWN	DOWN
ENSG00000164180	TMEM161B	DOWN	DOWN
ENSG00000226287	TMEM191A	DOWN	DOWN
ENSG00000198398	TMEM207	DOWN	DOWN
ENSG00000198133	TMEM229B	DOWN	DOWN
ENSG00000182107	TMEM30B	DOWN	DOWN
ENSG00000151715	TMEM45B	DOWN	DOWN
ENSG00000165685	TMEM52B	DOWN	DOWN
ENSG00000184012	TMPRSS2	DOWN	DOWN
ENSG00000187045	TMPRSS6	DOWN	DOWN
ENSG00000239697	TNFSF12	UP	UP
ENSG00000181634	TNFSF15	DOWN	DOWN
ENSG00000117586	TNFSF4	DOWN	DOWN
ENSG00000241874	TOMM22P6	DOWN	DOWN
ENSG00000176058	TPRN	DOWN	DOWN
ENSG00000215506	TPTE2P4	DOWN	DOWN
ENSG00000100181	TPTEP1	DOWN	DOWN
ENSG00000269113	TRABD2B	UP	UP
ENSG00000118094	TREH	DOWN	DOWN
ENSG00000124731	TREM1	DOWN	DOWN

ENSG00000137699	TRIM29	DOWN	DOWN
ENSG00000142185	TRPM2	DOWN	DOWN
ENSG00000119121	TRPM6	DOWN	DOWN
ENSG00000182612	TSPAN10	DOWN	DOWN
ENSG00000099282	TSPAN15	DOWN	DOWN
ENSG00000127324	TSPAN8	DOWN	DOWN
ENSG00000223756	TSSC2	UP	UP
ENSG00000006555	TTC22	DOWN	DOWN
ENSG00000139865	TTC6	DOWN	DOWN
ENSG00000184470	TXNRD2	DOWN	UP
ENSG00000154127	UBASH3B	DOWN	DOWN
ENSG00000171234	UGT2B7	DOWN	DOWN
ENSG00000174607	UGT8	DOWN	DOWN
ENSG00000271474	UNC5C-AS1	UP	UP
ENSG00000112494	UNC93A	DOWN	DOWN
ENSG00000100373	UPK3A	DOWN	DOWN
ENSG00000183463	URAD	DOWN	DOWN
ENSG00000006611	USH1C	DOWN	DOWN
ENSG00000150630	VEGFC	DOWN	DOWN
ENSG00000127831	VIL1	DOWN	DOWN
ENSG00000109072	VTN	DOWN	DOWN
ENSG00000165816	VWA2	DOWN	DOWN
ENSG00000158125	XDH	DOWN	DOWN
ENSG00000188707	ZBED6CL	DOWN	DOWN
ENSG00000166707	ZCCHC18	UP	UP
ENSG00000174992	ZG16	DOWN	DOWN
ENSG00000141497	ZMYND15	DOWN	DOWN
ENSG00000198105	ZNF248	DOWN	DOWN
ENSG00000225192	ZNF33BP1	DOWN	DOWN
ENSG00000227124	ZNF717	DOWN	DOWN
ENSG00000234444	ZNF736	DOWN	DOWN
ENSG00000250284	-	DOWN	DOWN
ENSG00000287460	-	DOWN	DOWN
ENSG00000249803	-	DOWN	DOWN
ENSG00000279932	-	DOWN	DOWN
ENSG00000255595	-	DOWN	DOWN
ENSG00000229628	-	DOWN	DOWN
ENSG00000280453	-	DOWN	DOWN
ENSG00000258932	-	DOWN	DOWN
ENSG00000259098	-	DOWN	DOWN
ENSG00000240086	-	DOWN	DOWN
ENSG00000272070	-	DOWN	DOWN
ENSG00000250546	-	DOWN	DOWN
ENSG00000258732	-	DOWN	DOWN
ENSG00000279289	-	DOWN	DOWN
ENSG00000237713	-	DOWN	DOWN
ENSG00000267327	-	DOWN	DOWN
ENSG00000272163	-	DOWN	DOWN
ENSG00000236283	-	DOWN	DOWN
ENSG00000189229	-	DOWN	DOWN
ENSG00000286358	-	DOWN	DOWN

ENSG00000216802	-	DOWN	DOWN
ENSG00000249605	-	DOWN	DOWN
ENSG00000250511	-	DOWN	DOWN
ENSG00000244062	-	DOWN	DOWN
ENSG00000286912	-	DOWN	DOWN
ENSG00000237356	-	DOWN	DOWN
ENSG00000289349	-	DOWN	DOWN
ENSG00000257855	-	DOWN	DOWN
ENSG00000287248	-	DOWN	DOWN
ENSG00000232524	-	DOWN	DOWN
ENSG00000287385	-	DOWN	DOWN
ENSG00000289262	-	DOWN	DOWN
ENSG00000257680	-	DOWN	DOWN
ENSG00000261468	-	DOWN	DOWN
ENSG00000237250	.	DOWN	DOWN
ENSG00000237471	.	DOWN	DOWN
ENSG00000232896	.	DOWN	DOWN
ENSG00000254290	.	DOWN	DOWN
ENSG00000248763	.	DOWN	DOWN
ENSG00000286062	.	UP	UP
ENSG00000259280	.	UP	UP
ENSG00000175899	A2M	DOWN	NS
ENSG00000144452	ABCA12	UP	NS
ENSG00000154258	ABCA9	UP	NS
ENSG00000108846	ABCC3	DOWN	NS
ENSG00000261143	ADAMTS7P3	DOWN	NS
ENSG00000150594	ADRA2A	UP	NS
ENSG00000135439	AGAP2	UP	NS
ENSG00000118514	ALDH8A1	UP	NS
ENSG00000133805	AMPD3	DOWN	NS
ENSG00000237276	ANO7L1	DOWN	NS
ENSG00000152056	AP1S3	DOWN	NS
ENSG00000248329	APELA	UP	NS
ENSG00000134817	APLNR	UP	NS
ENSG00000100336	APOL4	UP	NS
ENSG00000171885	AQP4	DOWN	NS
ENSG00000103569	AQP9	UP	NS
ENSG00000232332	ARL5AP5	UP	NS
ENSG00000167311	ART5	DOWN	NS
ENSG00000188611	ASAH2	DOWN	NS
ENSG00000152092	ASTN1	UP	NS
ENSG00000118322	ATP10B	DOWN	NS
ENSG00000166148	AVPR1A	DOWN	NS
ENSG00000167080	B4GALNT2	DOWN	NS
ENSG00000064787	BCAS1	DOWN	NS
ENSG00000166546	BEAN1	UP	NS
ENSG00000122870	BICC1	UP	NS
ENSG00000095585	BLNK	DOWN	NS
ENSG00000183682	BMP8A	DOWN	NS
ENSG00000198797	BRINP2	UP	NS
ENSG00000166920	C15orf48	DOWN	NS

ENSG00000187699	C2orf88	UP	NS
ENSG00000142408	CACNG8	UP	NS
ENSG00000104327	CALB1	UP	NS
ENSG00000172137	CALB2	UP	NS
ENSG00000008118	CAMK1G	UP	NS
ENSG00000168497	CAVIN2	UP	NS
ENSG00000236830	CBR3-AS1	DOWN	NS
ENSG00000158485	CD1B	UP	NS
ENSG00000135218	CD36	DOWN	NS
ENSG00000167286	CD3D	DOWN	NS
ENSG0000013725	CD6	UP	NS
ENSG00000153283	CD96	UP	NS
ENSG00000074276	CDHR2	DOWN	NS
ENSG00000163624	CDS1	DOWN	NS
ENSG00000086548	CEACAM6	DOWN	NS
ENSG00000154227	CERS3	UP	NS
ENSG00000182022	CHST15	UP	NS
ENSG00000166165	CKB	DOWN	NS
ENSG00000170289	CNGB3	UP	NS
ENSG00000118432	CNR1	DOWN	NS
ENSG00000184144	CNTN2	UP	NS
ENSG00000144619	CNTN4	DOWN	NS
ENSG00000084636	COL16A1	UP	NS
ENSG00000065618	COL17A1	DOWN	NS
ENSG00000093010	COMT	DOWN	NS
ENSG00000153002	CPB1	DOWN	NS
ENSG00000178772	CPN2	DOWN	NS
ENSG00000196872	CRACDL	UP	NS
ENSG00000213145	CRIP1	UP	NS
ENSG00000006016	CRLF1	DOWN	NS
ENSG00000223518	CSNK1A1P1	UP	NS
ENSG00000178531	CTXN1	UP	NS
ENSG00000145824	CXCL14	DOWN	NS
ENSG00000121966	CXCR4	DOWN	NS
ENSG00000240194	CYMP	DOWN	NS
ENSG00000148795	CYP17A1	UP	NS
ENSG00000140465	CYP1A1	DOWN	NS
ENSG00000186684	CYP27C1	UP	NS
ENSG00000197408	CYP2B6	DOWN	NS
ENSG00000146122	DAAM2	UP	NS
ENSG00000187323	DCC	DOWN	NS
ENSG00000146966	DENND2A	UP	NS
ENSG00000258498	DIO3OS	DOWN	NS
ENSG00000187773	DIPK1C	UP	NS
ENSG00000185559	DLK1	DOWN	NS
ENSG00000105880	DLX5	DOWN	NS
ENSG00000158856	DMTN	DOWN	NS
ENSG00000197959	DNM3	UP	NS
ENSG00000230630	DNM3OS	UP	NS
ENSG00000107099	DOCK8	DOWN	NS
ENSG00000149295	DRD2	DOWN	NS

ENSG00000158050	DUSP2	UP	NS
ENSG00000163435	ELF3	DOWN	NS
ENSG00000234678	ELF3-AS1	DOWN	NS
ENSG00000229847	EMX2OS	UP	NS
ENSG00000183317	EPHA10	DOWN	NS
ENSG00000154928	EPHB1	DOWN	NS
ENSG00000177106	EPS8L2	DOWN	NS
ENSG00000124882	EREG	DOWN	NS
ENSG00000164220	F2RL2	UP	NS
ENSG00000103089	FA2H	DOWN	NS
ENSG00000145384	FABP2	DOWN	NS
ENSG00000150510	FAM124A	DOWN	NS
ENSG00000112214	FHL5	UP	NS
ENSG00000179431	FJX1	UP	NS
ENSG00000275620	FLJ16779	DOWN	NS
ENSG00000244161	FLNB-AS1	UP	NS
ENSG00000267121	FMNL1-DT	DOWN	NS
ENSG00000160097	FNDC5	UP	NS
ENSG00000251493	FOXD1	DOWN	NS
ENSG00000178919	FOXE1	DOWN	NS
ENSG00000128573	FOXP2	UP	NS
ENSG00000179772	FOXS1	UP	NS
ENSG00000175229	GAL3ST3	UP	NS
ENSG00000205318	GCNT2P1	DOWN	NS
ENSG00000176928	GCNT4	DOWN	NS
ENSG00000248587	GDNF-AS1	DOWN	NS
ENSG00000204136	GGTA1	UP	NS
ENSG00000188910	GJB3	DOWN	NS
ENSG00000248590	GLDCP1	DOWN	NS
ENSG00000065325	GLP2R	DOWN	NS
ENSG00000166073	GPR176	UP	NS
ENSG00000155269	GPR78	DOWN	NS
ENSG00000138271	GPR87	DOWN	NS
ENSG00000180875	GREM2	DOWN	NS
ENSG00000120251	GRIA2	UP	NS
ENSG00000105737	GRIK5	UP	NS
ENSG00000232729	GTF2I-AS1	DOWN	NS
ENSG00000145681	HAPLN1	DOWN	NS
ENSG00000228789	HCG22	UP	NS
ENSG00000188175	HEPACAM2	DOWN	NS
ENSG00000069812	HES2	DOWN	NS
ENSG00000226088	HHLA3-AS1	UP	NS
ENSG00000177374	HIC1	UP	NS
ENSG00000204252	HLA-DOA	UP	NS
ENSG00000134240	HMGCS2	DOWN	NS
ENSG00000105996	HOXA2	UP	NS
ENSG00000105997	HOXA3	UP	NS
ENSG00000237380	HOXD-AS2	UP	NS
ENSG00000175879	HOXD8	UP	NS
ENSG00000257017	HP	UP	NS
ENSG00000198857	HSD3BP5	DOWN	NS

ENSG00000102878	HSF4	DOWN	NS
ENSG00000179546	HTR1D	DOWN	NS
ENSG00000148680	HTR7	DOWN	NS
ENSG00000117318	ID3	UP	NS
ENSG00000137965	IFI44	UP	NS
ENSG00000137959	IFI44L	UP	NS
ENSG00000152580	IGSF10	UP	NS
ENSG00000161405	IKZF3	DOWN	NS
ENSG00000115604	IL18R1	DOWN	NS
ENSG00000164509	IL31RA	DOWN	NS
ENSG00000157368	IL34	UP	NS
ENSG00000163362	INAVA	DOWN	NS
ENSG00000205363	INSYN1	UP	NS
ENSG00000188916	INSYN2A	UP	NS
ENSG00000090376	IRAK3	UP	NS
ENSG00000105855	ITGB8	UP	NS
ENSG00000179914	ITLN1	UP	NS
ENSG00000123104	ITPR2	DOWN	NS
ENSG00000009765	IYD	DOWN	NS
ENSG00000092051	JPH4	UP	NS
ENSG00000158445	KCNB1	UP	NS
ENSG00000115041	KCNIP3	UP	NS
ENSG00000121361	KCNJ8	DOWN	NS
ENSG00000197584	KCNMB2	UP	NS
ENSG00000143603	KCNN3	UP	NS
ENSG00000250423	KIAA1210	UP	NS
ENSG00000179023	KLHDC7A	DOWN	NS
ENSG00000162873	KLHDC8A	UP	NS
ENSG00000102271	KLHL4	UP	NS
ENSG00000134539	KLRD1	DOWN	NS
ENSG00000205420	KRT6A	DOWN	NS
ENSG00000220378	KRT8P42	UP	NS
ENSG00000058085	LAMC2	DOWN	NS
ENSG00000050555	LAMC3	DOWN	NS
ENSG00000106003	LFNG	UP	NS
ENSG00000143355	LHX9	UP	NS
ENSG00000215533	LINC00189	UP	NS
ENSG00000229246	LINC00377	UP	NS
ENSG00000235621	LINC00494	DOWN	NS
ENSG00000227036	LINC00511	DOWN	NS
ENSG00000235770	LINC00607	UP	NS
ENSG00000258548	LINC00645	UP	NS
ENSG00000251209	LINC00923	DOWN	NS
ENSG00000251442	LINC01094	DOWN	NS
ENSG00000204588	LINC01123	DOWN	NS
ENSG00000224259	LINC01133	UP	NS
ENSG00000281404	LINC01176	DOWN	NS
ENSG00000229981	LINC01435	DOWN	NS
ENSG00000228065	LINC01515	DOWN	NS
ENSG00000225328	LINC01594	DOWN	NS
ENSG00000253414	LINC01605	UP	NS

ENSG00000236532	LINC01695	UP	NS
ENSG00000227947	LINC01738	UP	NS
ENSG00000250891	LINC02208	DOWN	NS
ENSG00000226791	LINC02611	UP	NS
ENSG00000236908	LINC02827	DOWN	NS
ENSG00000163898	LIPH	DOWN	NS
ENSG00000147145	LPAR4	UP	NS
ENSG00000128606	LRRC17	UP	NS
ENSG00000162494	LRRC38	DOWN	NS
ENSG00000183908	LRRC55	UP	NS
ENSG00000154237	LRRK1	DOWN	NS
ENSG00000054219	LY75	DOWN	NS
ENSG00000135525	MAP7	DOWN	NS
ENSG00000153898	MCOLN2	DOWN	NS
ENSG00000175471	MCTP1	DOWN	NS
ENSG00000102802	MEDAG	UP	NS
ENSG00000183496	MEX3B	UP	NS
ENSG00000225783	MIAT	UP	NS
ENSG00000125462	MIR9-1HG	DOWN	NS
ENSG00000099953	MMP11	UP	NS
ENSG00000233217	MROH3P	DOWN	NS
ENSG00000038945	MSR1	DOWN	NS
ENSG00000181143	MUC16	UP	NS
ENSG00000157601	MX1	DOWN	NS
ENSG00000133020	MYH8	UP	NS
ENSG00000137474	MYO7A	DOWN	NS
ENSG00000102452	NALCN	DOWN	NS
ENSG00000250290	NCAPGP1	DOWN	NS
ENSG00000124479	NDP	DOWN	NS
ENSG00000100285	NEFH	UP	NS
ENSG00000104722	NEFM	DOWN	NS
ENSG00000162599	NFIA	UP	NS
ENSG00000101198	NKAIN4	DOWN	NS
ENSG00000169760	NLGN1	DOWN	NS
ENSG00000007171	NOS2	DOWN	NS
ENSG00000007952	NOX1	UP	NS
ENSG00000151322	NPAS3	UP	NS
ENSG00000122585	NPY	DOWN	NS
ENSG0000012504	NR1H4	UP	NS
ENSG00000237187	NR2F1-AS1	UP	NS
ENSG00000135318	NT5E	DOWN	NS
ENSG00000144460	NYAP2	DOWN	NS
ENSG00000089127	OAS1	DOWN	NS
ENSG00000104044	OCA2	DOWN	NS
ENSG00000162745	OLFML2B	UP	NS
ENSG00000225101	OR52K3P	DOWN	NS
ENSG00000109991	P2RX3	UP	NS
ENSG00000273129	PACERR	UP	NS
ENSG00000075891	PAX2	UP	NS
ENSG00000136099	PCDH8	UP	NS
ENSG00000254245	PCDHGA3	DOWN	NS

ENSG00000163710	PCOLCE2	UP	NS
ENSG00000188389	PDCD1	UP	NS
ENSG00000128655	PDE11A	UP	NS
ENSG00000134853	PDGFRA	UP	NS
ENSG00000162366	PDZK1IP1	UP	NS
ENSG00000165966	PDZRN4	DOWN	NS
ENSG00000163218	PGLYRP4	UP	NS
ENSG00000154864	PIEZO2	UP	NS
ENSG00000234465	PINLYP	UP	NS
ENSG00000171033	PKIA	DOWN	NS
ENSG00000145632	PLK2	UP	NS
ENSG00000148123	PLPPR1	UP	NS
ENSG00000185664	PMEL	DOWN	NS
ENSG00000152192	POU4F1	DOWN	NS
ENSG00000224086	PPM1F-AS1	UP	NS
ENSG00000046889	PREX2	UP	NS
ENSG00000176532	PRR15	DOWN	NS
ENSG00000204983	PRSS1	DOWN	NS
ENSG00000204264	PSMB8	DOWN	NS
ENSG00000240065	PSMB9	DOWN	NS
ENSG00000165186	PTCHD1	UP	NS
ENSG00000144407	PTH2R	UP	NS
ENSG00000087494	PTHLH	DOWN	NS
ENSG00000105894	PTN	UP	NS
ENSG00000106278	PTPRZ1	UP	NS
ENSG00000163661	PTX3	DOWN	NS
ENSG00000101265	RASSF2	UP	NS
ENSG00000114115	RBP1	UP	NS
ENSG00000115255	REEP6	DOWN	NS
ENSG00000143954	REG3G	UP	NS
ENSG00000088320	REM1	UP	NS
ENSG00000162944	RFTN2	UP	NS
ENSG00000252982	RN7SKP234	DOWN	NS
ENSG00000254656	RTL1	DOWN	NS
ENSG00000168077	SCARA3	UP	NS
ENSG00000166257	SCN3B	UP	NS
ENSG00000136546	SCN7A	UP	NS
ENSG00000250722	SELENOP	DOWN	NS
ENSG00000063015	SEZ6	UP	NS
ENSG00000170624	SGCD	UP	NS
ENSG00000118515	SGK1	UP	NS
ENSG00000105492	SIGLEC6	DOWN	NS
ENSG00000147100	SLC16A2	UP	NS
ENSG00000141526	SLC16A3	DOWN	NS
ENSG00000168679	SLC16A4	DOWN	NS
ENSG00000179520	SLC17A8	UP	NS
ENSG00000147606	SLC26A7	DOWN	NS
ENSG00000227533	SLC2A1-AS1	DOWN	NS
ENSG00000173262	SLC2A14	DOWN	NS
ENSG00000059804	SLC2A3	DOWN	NS
ENSG00000142583	SLC2A5	DOWN	NS

ENSG00000197106	SLC6A17	DOWN	NS
ENSG00000163817	SLC6A20	DOWN	NS
ENSG00000130876	SLC7A10	DOWN	NS
ENSG00000173930	SLCO4C1	DOWN	NS
ENSG00000198732	SMOC1	UP	NS
ENSG00000236577	SNRPGP14	DOWN	NS
ENSG00000147481	SNTG1	UP	NS
ENSG00000181449	SOX2	DOWN	NS
ENSG00000152583	SPARCL1	UP	NS
ENSG00000144057	ST6GAL2	UP	NS
ENSG00000070731	ST6GALNAC2	DOWN	NS
ENSG00000148488	ST8SIA6	DOWN	NS
ENSG00000113739	STC2	DOWN	NS
ENSG00000152953	STK32B	DOWN	NS
ENSG00000104435	STMN2	DOWN	NS
ENSG00000137573	SULF1	UP	NS
ENSG00000196562	SULF2	UP	NS
ENSG00000277013	SUNO1	DOWN	NS
ENSG00000165124	SVEP1	DOWN	NS
ENSG00000181392	SYNE4	DOWN	NS
ENSG00000143469	SYT14	DOWN	NS
ENSG00000149043	SYT8	DOWN	NS
ENSG00000102362	SYTL4	UP	NS
ENSG00000184292	TACSTD2	DOWN	NS
ENSG00000121068	TBX2	UP	NS
ENSG00000176907	TCIM	DOWN	NS
ENSG00000149256	TENM4	UP	NS
ENSG00000087510	TFAP2C	DOWN	NS
ENSG00000170537	TMC7	DOWN	NS
ENSG00000167895	TMC8	DOWN	NS
ENSG00000166292	TMEM100	UP	NS
ENSG00000144868	TMEM108	UP	NS
ENSG00000151952	TMEM132D	DOWN	NS
ENSG00000188760	TMEM198	DOWN	NS
ENSG00000188133	TMEM215	UP	NS
ENSG00000196932	TMEM26	UP	NS
ENSG00000167105	TMEM92	DOWN	NS
ENSG00000164761	TNFRSF11B	DOWN	NS
ENSG00000157873	TNFRSF14	DOWN	NS
ENSG00000120949	TNFRSF8	UP	NS
ENSG00000121858	TNFSF10	DOWN	NS
ENSG00000120332	TNN	UP	NS
ENSG00000187688	TRPV2	DOWN	NS
ENSG00000182463	TSHZ2	UP	NS
ENSG00000122691	TWIST1	UP	NS
ENSG00000107165	TYRP1	DOWN	NS
ENSG00000199856	U3	DOWN	NS
ENSG00000213886	UBD	DOWN	NS
ENSG00000135220	UGT2A3	DOWN	NS
ENSG00000124602	UNC5CL	DOWN	NS
ENSG00000143494	VASH2	UP	NS

ENSG00000170162	VGLL2	DOWN	NS
ENSG00000112299	VNN1	UP	NS
ENSG00000187260	WDR86	UP	NS
ENSG00000182931	WFDC10B	DOWN	NS
ENSG00000124116	WFDC3	DOWN	NS
ENSG00000162552	WNT4	UP	NS
ENSG00000154764	WNT7A	DOWN	NS
ENSG00000241743	XACT	DOWN	NS
ENSG00000275591	XKR5	UP	NS
ENSG00000122121	XPNPEP2	DOWN	NS
ENSG00000102383	ZDHHC15	UP	NS
ENSG00000183779	ZNF703	UP	NS
ENSG00000203995	ZYG11A	DOWN	NS
ENSG00000289069	-	UP	NS
ENSG00000284640	-	UP	NS
ENSG00000289561	-	UP	NS
ENSG00000275888	-	DOWN	NS
ENSG00000287281	-	UP	NS
ENSG00000230615	-	UP	NS
ENSG00000275266	-	DOWN	NS
ENSG00000256616	-	UP	NS
ENSG00000288808	-	UP	NS
ENSG00000269553	-	UP	NS
ENSG00000277247	-	DOWN	NS
ENSG00000286633	-	UP	NS
ENSG00000278351	-	DOWN	NS
ENSG00000273368	-	DOWN	NS
ENSG00000274840	-	DOWN	NS
ENSG00000233005	-	UP	NS
ENSG00000267287	-	UP	NS
ENSG00000288897	-	DOWN	NS
ENSG00000232110	-	DOWN	NS
ENSG00000283973	-	DOWN	NS
ENSG00000273162	-	UP	NS
ENSG00000284695	-	UP	NS
ENSG00000237645	-	DOWN	NS
ENSG00000289417	-	DOWN	NS
ENSG00000283999	-	DOWN	NS
ENSG00000231204	-	UP	NS
ENSG00000225177	-	DOWN	NS
ENSG00000287712	-	DOWN	NS
ENSG00000266602	-	UP	NS
ENSG00000231440	-	DOWN	NS
ENSG00000275216	-	DOWN	NS
ENSG00000256995	-	DOWN	NS
ENSG00000238178	-	DOWN	NS
ENSG00000287661	-	UP	NS
ENSG00000275850	-	DOWN	NS
ENSG00000289615	-	UP	NS
ENSG00000230910	-	UP	NS
ENSG00000259290	-	UP	NS

ENSG00000223665	.	UP	NS
ENSG00000253123	.	UP	NS
ENSG00000287171	.	UP	NS
ENSG00000274444	.	UP	NS
ENSG00000289621	.	DOWN	NS
ENSG00000287550	.	UP	NS
ENSG00000226043	.	UP	NS
ENSG00000236393	.	DOWN	NS
ENSG00000289454	.	UP	NS
ENSG00000251244	.	UP	NS
ENSG00000289522	.	DOWN	NS
ENSG00000272626	.	DOWN	NS
ENSG00000257890	.	UP	NS
ENSG00000273301	.	DOWN	NS
ENSG00000250501	.	UP	NS
ENSG00000148584	A1CF	NS	DOWN
ENSG00000114771	AADAC	NS	DOWN
ENSG00000142513	ACP4	NS	DOWN
ENSG00000069206	ADAM7	NS	DOWN
ENSG00000248144	ADH1C	NS	DOWN
ENSG00000169129	AFAP1L2	NS	DOWN
ENSG00000079557	AFM	NS	DOWN
ENSG00000081051	AFP	NS	DOWN
ENSG00000145192	AHSG	NS	DOWN
ENSG00000163631	ALB	NS	DOWN
ENSG00000136872	ALDOB	NS	DOWN
ENSG00000179593	ALOX15B	NS	DOWN
ENSG00000012779	ALOX5	NS	DOWN
ENSG00000106927	AMBP	NS	DOWN
ENSG00000233273	AMMECR1LP1	NS	UP
ENSG00000171819	ANGPTL7	NS	DOWN
ENSG00000215559	ANKRD20A11P	NS	DOWN
ENSG00000198483	ANKRD35	NS	DOWN
ENSG00000188399	ANKRD36P1	NS	DOWN
ENSG00000158874	APOA2	NS	DOWN
ENSG00000110244	APOA4	NS	DOWN
ENSG00000110245	APOC3	NS	DOWN
ENSG00000091583	APOH	NS	DOWN
ENSG00000236699	ARHGEF38	NS	DOWN
ENSG00000108381	ASPA	NS	DOWN
ENSG00000168874	ATOH8	NS	UP
ENSG00000112309	B3GAT2	NS	DOWN
ENSG00000168903	BTNL3	NS	DOWN
ENSG00000173715	C11orf80	NS	DOWN
ENSG00000185742	C11orf87	NS	UP
ENSG00000278505	C17orf78	NS	DOWN
ENSG00000205929	C21orf62	NS	DOWN
ENSG00000187068	C3orf70	NS	UP
ENSG00000186493	C5orf38	NS	UP
ENSG00000164879	CA3	NS	DOWN
ENSG00000167434	CA4	NS	DOWN

ENSG00000162545	CAMK2N1	NS	DOWN
ENSG00000254166	CASC19	NS	DOWN
ENSG00000233766	CAVIN2-AS1	NS	UP
ENSG00000213213	CCDC183	NS	DOWN
ENSG00000162592	CCDC27	NS	DOWN
ENSG00000205089	CCNI2	NS	DOWN
ENSG00000039068	CDH1	NS	DOWN
ENSG00000136305	CIDEB	NS	DOWN
ENSG00000165959	CLMN	NS	DOWN
ENSG00000134115	CNTN6	NS	DOWN
ENSG00000106789	CORO2A	NS	DOWN
ENSG00000103316	CRYM	NS	UP
ENSG00000249201	CTD-3080P12.3	NS	DOWN
ENSG00000161544	CYGB	NS	DOWN
ENSG00000138109	CYP2C9	NS	DOWN
ENSG00000228314	CYP4F29P	NS	DOWN
ENSG00000070190	DAPP1	NS	UP
ENSG00000170959	DCDC1	NS	UP
ENSG00000164825	DEFB1	NS	DOWN
ENSG00000102385	DRP2	NS	UP
ENSG00000134760	DSG1	NS	DOWN
ENSG00000143507	DUSP10	NS	DOWN
ENSG00000164035	EMCN	NS	UP
ENSG00000249082	EPIST	NS	DOWN
ENSG00000214860	EVPLL	NS	DOWN
ENSG00000197245	FAM110D	NS	UP
ENSG00000196990	FAM163B	NS	DOWN
ENSG00000183844	FAM3B	NS	DOWN
ENSG00000147378	FATE1	NS	DOWN
ENSG00000116661	FBXO2	NS	DOWN
ENSG00000171560	FGA	NS	DOWN
ENSG00000171564	FGB	NS	DOWN
ENSG00000118972	FGF23	NS	DOWN
ENSG00000122025	FLT3	NS	DOWN
ENSG00000186564	FOXD2	NS	UP
ENSG00000176678	FOXL1	NS	UP
ENSG00000258537	FRMD6-AS2	NS	DOWN
ENSG00000162998	FRZB	NS	DOWN
ENSG00000179348	GATA2	NS	UP
ENSG00000187210	GCNT1	NS	DOWN
ENSG00000166840	GLYATL1	NS	DOWN
ENSG00000111664	GNB3	NS	DOWN
ENSG00000125787	GNRH2	NS	DOWN
ENSG00000174567	GOLT1A	NS	DOWN
ENSG00000183840	GPR39	NS	DOWN
ENSG00000198785	GRIN3A	NS	UP
ENSG00000148702	HABP2	NS	DOWN
ENSG00000051108	HERPUD1	NS	DOWN
ENSG00000229005	HNF4A-AS1	NS	DOWN
ENSG00000164749	HNF4G	NS	DOWN
ENSG00000180818	HOXC10	NS	DOWN

ENSG00000186603	HPDL	NS	DOWN
ENSG00000203855	HSD3BP4	NS	DOWN
ENSG00000196684	HSH2D	NS	DOWN
ENSG00000211597	IGKJ1	NS	DOWN
ENSG00000137033	IL33	NS	UP
ENSG00000104951	IL411	NS	UP
ENSG00000170561	IRX2	NS	UP
ENSG00000175329	ISX	NS	DOWN
ENSG00000055957	ITIH1	NS	DOWN
ENSG00000115474	KCNJ13	NS	DOWN
ENSG00000285844	KCNQ5-DT	NS	DOWN
ENSG00000112232	KHDRBS2	NS	DOWN
ENSG00000149633	KIAA1755	NS	UP
ENSG00000133116	KL	NS	DOWN
ENSG00000134962	KLB	NS	DOWN
ENSG00000167749	KLK4	NS	DOWN
ENSG00000113889	KNG1	NS	DOWN
ENSG00000214856	KRT16P1	NS	DOWN
ENSG00000125869	LAMP5	NS	UP
ENSG00000225329	LHFPL3-AS2	NS	DOWN
ENSG00000131914	LIN28A	NS	DOWN
ENSG00000231776	LINC01611	NS	UP
ENSG00000259485	LINC02253	NS	DOWN
ENSG00000257345	LINC02413	NS	DOWN
ENSG00000248740	LINC02428	NS	DOWN
ENSG00000251688	LINC02507	NS	UP
ENSG00000235142	LINC02532	NS	DOWN
ENSG00000233593	LINC02609	NS	DOWN
ENSG00000231680	LINC02723	NS	DOWN
ENSG00000166035	LIPC	NS	DOWN
ENSG00000204022	LIPJ	NS	DOWN
ENSG00000135363	LMO2	NS	UP
ENSG00000167419	LPO	NS	DOWN
ENSG00000156265	MAP3K7CL	NS	UP
ENSG00000144583	MARCHF4	NS	UP
ENSG00000055732	MCOLN3	NS	DOWN
ENSG00000257335	MGAM	NS	DOWN
ENSG00000224141	MIR548XHG	NS	DOWN
ENSG00000172689	MS4A10	NS	DOWN
ENSG00000166961	MS4A15	NS	DOWN
ENSG00000166959	MS4A8	NS	DOWN
ENSG00000178860	MSC	NS	UP
ENSG00000120279	MYCT1	NS	UP
ENSG00000133392	MYH11	NS	UP
ENSG00000091536	MYO15A	NS	DOWN
ENSG00000184454	NCMAP	NS	DOWN
ENSG00000104967	NOVA2	NS	UP
ENSG00000185823	NPAP1	NS	DOWN
ENSG00000197085	NPSR1-AS1	NS	DOWN
ENSG00000171246	NPTX1	NS	DOWN
ENSG00000169297	NR0B1	NS	UP

ENSG00000124785	NRN1	NS	DOWN
ENSG00000119900	OGFRL1	NS	DOWN
ENSG00000130558	OLFM1	NS	UP
ENSG00000119547	ONECUT2	NS	DOWN
ENSG00000221836	OR2A5	NS	DOWN
ENSG00000229314	ORM1	NS	DOWN
ENSG00000174740	PABPC5	NS	DOWN
ENSG00000171759	PAH	NS	DOWN
ENSG00000099260	PALMD	NS	UP
ENSG00000204956	PCDHGA1	NS	DOWN
ENSG00000220515	PGAM1P10	NS	DOWN
ENSG00000162896	PIGR	NS	DOWN
ENSG00000069011	PITX1	NS	DOWN
ENSG00000224186	PITX1-AS1	NS	DOWN
ENSG00000184363	PKP3	NS	DOWN
ENSG00000149527	PLCH2	NS	DOWN
ENSG00000122194	PLG	NS	DOWN
ENSG00000107317	PTGDS	NS	DOWN
ENSG00000204179	PTPN20	NS	DOWN
ENSG00000259905	PWRN1	NS	DOWN
ENSG00000100302	RASD2	NS	DOWN
ENSG00000185272	RBM11	NS	DOWN
ENSG00000185002	RFX6	NS	DOWN
ENSG00000182732	RGS6	NS	UP
ENSG00000141314	RHBDL3	NS	UP
ENSG00000239794	RN7SL653P	NS	DOWN
ENSG00000267128	RNF157-AS1	NS	DOWN
ENSG00000124813	RUNX2	NS	DOWN
ENSG00000189334	S100A14	NS	DOWN
ENSG00000177098	SCN4B	NS	DOWN
ENSG00000140093	SERPINA10	NS	DOWN
ENSG00000100665	SERPINA4	NS	DOWN
ENSG00000170099	SERPINA6	NS	DOWN
ENSG00000123561	SERPINA7	NS	DOWN
ENSG00000260802	SERTM2	NS	DOWN
ENSG00000106483	SFRP4	NS	UP
ENSG00000107295	SH3GL2	NS	DOWN
ENSG00000168779	SHOX2	NS	UP
ENSG00000161640	SIGLEC11	NS	DOWN
ENSG00000146039	SLC17A4	NS	DOWN
ENSG00000259803	SLC22A31	NS	DOWN
ENSG00000137204	SLC22A7	NS	DOWN
ENSG00000165794	SLC39A2	NS	DOWN
ENSG00000138449	SLC40A1	NS	DOWN
ENSG00000004939	SLC4A1	NS	DOWN
ENSG00000115665	SLC5A7	NS	UP
ENSG00000254042	SLIT3-AS2	NS	UP
ENSG00000172594	SMPDL3A	NS	DOWN
ENSG00000122862	SRGN	NS	UP
ENSG00000159167	STC1	NS	DOWN
ENSG00000241316	SUCLG2-AS1	NS	DOWN

ENSG00000198829	SUCNR1	NS	UP
ENSG00000166863	TAC3	NS	DOWN
ENSG00000121075	TBX4	NS	DOWN
ENSG00000176769	TCERG1L	NS	DOWN
ENSG00000241186	TDGF1	NS	DOWN
ENSG00000133863	TEX15	NS	DOWN
ENSG00000113296	THBS4	NS	UP
ENSG00000169903	TM4SF4	NS	DOWN
ENSG00000144339	TMEFF2	NS	UP
ENSG00000162460	TMEM82	NS	DOWN
ENSG00000137747	TMPRSS13	NS	DOWN
ENSG00000137648	TMPRSS4	NS	DOWN
ENSG00000103460	TOX3	NS	DOWN
ENSG00000211772	TRBC2	NS	DOWN
ENSG00000204616	TRIM31	NS	DOWN
ENSG00000119283	TRIM67	NS	UP
ENSG00000170703	TTLL6	NS	DOWN
ENSG00000118271	TTR	NS	DOWN
ENSG00000178462	TUBAL3	NS	DOWN
ENSG00000109181	UGT2B10	NS	DOWN
ENSG00000213759	UGT2B11	NS	DOWN
ENSG00000145626	UGT3A1	NS	DOWN
ENSG00000230266	XXYL1-AS2	NS	DOWN
ENSG00000115085	ZAP70	NS	DOWN
ENSG00000174460	ZCCHC12	NS	UP
ENSG00000287232	-	NS	UP
ENSG00000256552	-	NS	DOWN
ENSG00000288253	-	NS	DOWN
ENSG00000279433	-	NS	DOWN
ENSG00000261786	-	NS	DOWN
ENSG00000286895	-	NS	DOWN
ENSG00000256101	-	NS	DOWN
ENSG00000217801	-	NS	DOWN
ENSG00000248752	-	NS	DOWN
ENSG00000283914	-	NS	DOWN
ENSG00000243081	-	NS	DOWN
ENSG00000273443	-	NS	DOWN
ENSG00000253872	-	NS	DOWN
ENSG00000256969	-	NS	DOWN
ENSG00000256654	-	NS	UP
ENSG00000278962	-	NS	UP
ENSG00000228944	-	NS	DOWN
ENSG00000256417	-	NS	DOWN
ENSG00000277619	-	NS	DOWN
ENSG00000286073	-	NS	DOWN
ENSG00000286123	-	NS	DOWN
ENSG00000226014	-	NS	DOWN
ENSG00000255983	-	NS	DOWN
ENSG00000250421	-	NS	DOWN
ENSG00000273258	-	NS	DOWN
ENSG00000271857	-	NS	DOWN

ENSG00000273066	-	NS	DOWN
ENSG00000230552	-	NS	UP
ENSG00000259275	.	NS	UP
ENSG00000254293	.	NS	DOWN
ENSG00000261222	.	NS	DOWN
ENSG00000280323	.	NS	UP
ENSG00000218274	.	NS	DOWN
ENSG00000277047	.	NS	DOWN
ENSG00000250376	.	NS	DOWN
ENSG00000236543	.	NS	DOWN
ENSG00000285960	.	NS	DOWN
ENSG00000229498	.	NS	UP
ENSG00000224935	.	NS	DOWN

Appendix B

Table AB: Differentially expressed proteins. DOWN – downregulated in comparison; UP upregulated in comparison; NS – not significant in comparison.

Protein	LMNA ^{+/-} vs WT	EMD ^{-/-} vs WT
AAGAB	DOWN	DOWN
ABCB8	UP	DOWN
ABCD1	UP	DOWN
ABHD13	UP	DOWN
ACACB	UP	DOWN
ACAD11	UP	DOWN
ACAD9	UP	DOWN
ACSL3	UP	DOWN
ACTB	DOWN	DOWN
ACTR5	DOWN	DOWN
ACYP2	DOWN	DOWN
ADAMTS3	DOWN	DOWN
ADCK5	UP	DOWN
ADCY5	UP	DOWN
ADO	DOWN	DOWN
ADPRHL1	UP	DOWN
AGT	DOWN	DOWN
AHNAK	DOWN	DOWN
AK5	DOWN	DOWN
AKR1B15	DOWN	DOWN
ALDH1A1	DOWN	DOWN
ALG11	UP	DOWN
ALYREF	DOWN	DOWN
ANKRD20A4P	DOWN	DOWN
ANKRD63	DOWN	DOWN
ANO6	UP	DOWN
ANP32A	DOWN	DOWN
ANP32B	DOWN	DOWN
ANXA11	DOWN	DOWN
ANXA5	DOWN	DOWN
AP5B1	UP	DOWN
APIP	DOWN	DOWN
ARAF	UP	DOWN
ARFGEF2	UP	DOWN
ARHGAP1	UP	DOWN
ARHGAP45	UP	DOWN
ARHGEF9	UP	DOWN
ARL1	UP	DOWN
ARL6IP1	UP	DOWN
ARMCX1	UP	DOWN
ARMCX3	UP	DOWN
ARMH3	UP	DOWN
ARSA	DOWN	DOWN

ATF7IP	DOWN	DOWN
ATP5PF	UP	DOWN
B3GALT6	UP	DOWN
BASP1	UP	DOWN
BICD1	DOWN	DOWN
BMP10	UP	DOWN
BMP2	UP	DOWN
BMP4	DOWN	DOWN
BNIP2	UP	DOWN
BOD1L1	DOWN	DOWN
BRAT1	UP	DOWN
BRD3	DOWN	DOWN
C1orf174	UP	DOWN
C2CD5	DOWN	DOWN
CADPS	UP	DOWN
CALM1	DOWN	DOWN
CAND2	UP	DOWN
CAPN3	UP	DOWN
CARS1	UP	DOWN
CASP7	DOWN	DOWN
CASQ2	DOWN	DOWN
CAVIN1	DOWN	DOWN
CAVIN3	DOWN	DOWN
CBLL1	DOWN	DOWN
CBX3	DOWN	DOWN
CCDC115	DOWN	DOWN
CCDC127	UP	DOWN
CCDC134	DOWN	DOWN
CCDC150	UP	DOWN
CCDC59	UP	DOWN
CCDC90B	UP	DOWN
CCDC90B	UP	DOWN
CCPG1	UP	DOWN
CCS	DOWN	DOWN
CCSMST1	UP	DOWN
CD81	UP	DOWN
CD99	UP	DOWN
CDKN1B	DOWN	DOWN
CDKN2AIPNL	DOWN	DOWN
CDS2	UP	DOWN
CEND1	UP	DOWN
CENPB	UP	DOWN
CENPH	DOWN	DOWN
CERS1	UP	DOWN
CFDP1	DOWN	DOWN
CHMP1A	DOWN	DOWN
CHMP1B	DOWN	DOWN
CHMP2A	DOWN	DOWN
CIAO2B	UP	DOWN
CLN6	UP	DOWN

CLPTM1	UP	DOWN
CLU	DOWN	DOWN
CMBL	DOWN	DOWN
CNRIP1	DOWN	DOWN
COBL	DOWN	DOWN
COG4	UP	DOWN
COPZ1	DOWN	DOWN
COX18	UP	DOWN
COX7A1	DOWN	DOWN
COX7C	UP	DOWN
COX8A	UP	DOWN
CPNE6	DOWN	DOWN
CPQ	DOWN	DOWN
CPT1A	UP	DOWN
CRABP1	DOWN	DOWN
CREB1	DOWN	DOWN
CREG1	DOWN	DOWN
CTCF	DOWN	DOWN
CYB5R2	DOWN	DOWN
CYP51A1	UP	DOWN
DBI	DOWN	DOWN
DCUN1D1	DOWN	DOWN
DCXR	UP	DOWN
DENND6A	UP	DOWN
DHCR7	UP	DOWN
DHFR	DOWN	DOWN
DHRS7B	UP	DOWN
DHX32	UP	DOWN
DMXL1	UP	DOWN
DNAJA4	UP	DOWN
DNAJB9	UP	DOWN
DNASE2	DOWN	DOWN
DPCD	DOWN	DOWN
DPH1	UP	DOWN
DPH6	DOWN	DOWN
DPY30	UP	DOWN
DSG1	DOWN	DOWN
DTD1	DOWN	DOWN
DYNLRB1	DOWN	DOWN
EAPP	DOWN	DOWN
EBP	UP	DOWN
ECD	UP	DOWN
EDRF1	UP	DOWN
EGLN3	DOWN	DOWN
EIF1AX	DOWN	DOWN
ELF1	DOWN	DOWN
ELOVL1	UP	DOWN
EMC3	UP	DOWN
EPB41L1	DOWN	DOWN
EPDR1	DOWN	DOWN

EPHA2	UP	DOWN
ESRP1	UP	DOWN
ESRRA	UP	DOWN
EXTL3	UP	DOWN
FADD	UP	DOWN
FAM210A	UP	DOWN
FAM50B	DOWN	DOWN
FAU	DOWN	DOWN
FBXL12	UP	DOWN
FERMT1	UP	DOWN
FGF8	DOWN	DOWN
FKBP10	DOWN	DOWN
FMOD	DOWN	DOWN
FNDC3B	UP	DOWN
FXD1	UP	DOWN
FXD6	UP	DOWN
GABBR1	UP	DOWN
GAN	UP	DOWN
GCLM	DOWN	DOWN
GDF15	UP	DOWN
GDPD1	UP	DOWN
GGH	DOWN	DOWN
GGNBP2	UP	DOWN
GIN5	DOWN	DOWN
GLO1	DOWN	DOWN
GLRX	UP	DOWN
GLUD2	DOWN	DOWN
GMFB	DOWN	DOWN
GMPPA	UP	DOWN
GMPPB	UP	DOWN
GNAO1	UP	DOWN
GNG10	UP	DOWN
GNPDA1	UP	DOWN
GOLT1B	DOWN	DOWN
GPD1	UP	DOWN
GPD1L	UP	DOWN
GPN2	UP	DOWN
GSTA2	DOWN	DOWN
GSTP1	DOWN	DOWN
GTF2E1	DOWN	DOWN
GYS1	UP	DOWN
H1-0	UP	DOWN
H1-4	DOWN	DOWN
H2AX	DOWN	DOWN
H2BC20P	DOWN	DOWN
H3-2	DOWN	DOWN
H3C15	UP	DOWN
HACD2	UP	DOWN
HBE1	DOWN	DOWN
HDAC3	DOWN	DOWN

HEBP2	DOWN	DOWN
HECTD1	UP	DOWN
HERC2	UP	DOWN
HERPUD1	UP	DOWN
HEXB	DOWN	DOWN
HHATL	UP	DOWN
HIF1AN	DOWN	DOWN
HK2	UP	DOWN
HMGCS2	DOWN	DOWN
HMGN1	DOWN	DOWN
HMGN5	DOWN	DOWN
HNRNPAB	DOWN	DOWN
HNRNPDL	DOWN	DOWN
HNRNPDL	DOWN	DOWN
HRC	UP	DOWN
HSD17B12	UP	DOWN
HSD17B7	UP	DOWN
HSDL1	UP	DOWN
HSP90AB2P	DOWN	DOWN
HSP90AB4P	DOWN	DOWN
HSPB6	DOWN	DOWN
IFRD1	UP	DOWN
IK	DOWN	DOWN
ILVBL	UP	DOWN
ING1	DOWN	DOWN
INIP	DOWN	DOWN
INPP4B	UP	DOWN
INTS5	UP	DOWN
INTS8	UP	DOWN
IPO11	UP	DOWN
ISY1	DOWN	DOWN
ISYNA1	UP	DOWN
ITGA2	UP	DOWN
ITGA9	DOWN	DOWN
ITIH2	UP	DOWN
ITM2C	UP	DOWN
KATNAL1	UP	DOWN
KDM5B	UP	DOWN
KIF15	DOWN	DOWN
KIF1A	UP	DOWN
KRT10	DOWN	DOWN
KRT2	DOWN	DOWN
KRT6A	DOWN	DOWN
KRTCAP2	UP	DOWN
LAGE3	UP	DOWN
LEPROT	UP	DOWN
LGALS3	DOWN	DOWN
LIAS	UP	DOWN
LIMD1	DOWN	DOWN
LIMS1	DOWN	DOWN

LIPE	UP	DOWN
LMAN1	UP	DOWN
LMF1	UP	DOWN
LMNA	DOWN	DOWN
LPGAT1	UP	DOWN
LRP6	DOWN	DOWN
LRRC69	DOWN	DOWN
LSM3	DOWN	DOWN
LSM6	DOWN	DOWN
LSM8	DOWN	DOWN
LTV1	DOWN	DOWN
LUC7L2	DOWN	DOWN
LYRM1	UP	DOWN
LYRM2	DOWN	DOWN
MAGED4	UP	DOWN
MALSU1	UP	DOWN
MAPKAPK3	UP	DOWN
MARCKS	DOWN	DOWN
MAZ	DOWN	DOWN
MDP1	DOWN	DOWN
MED15	DOWN	DOWN
MEF2A	DOWN	DOWN
METTL2B	UP	DOWN
MFSD10	UP	DOWN
MGST3	UP	DOWN
MIEN1	DOWN	DOWN
MIGA2	UP	DOWN
MLF2	DOWN	DOWN
MMGT1	UP	DOWN
MMS19	UP	DOWN
MPC1	UP	DOWN
MPV17	UP	DOWN
MRPL52	DOWN	DOWN
MRPS16	UP	DOWN
MRPS24	UP	DOWN
MRPS30	UP	DOWN
MRS2	UP	DOWN
MRTFB	DOWN	DOWN
MSMO1	UP	DOWN
MT-CO3	UP	DOWN
MT-ND4	UP	DOWN
MTCH2	UP	DOWN
MTFP1	UP	DOWN
MTTP	DOWN	DOWN
MTX2	UP	DOWN
MYH4	UP	DOWN
N4BP3	UP	DOWN
NCEH1	UP	DOWN
NDNF	UP	DOWN
NDRG2	UP	DOWN

NDUFA9	UP	DOWN
NDUFAF6	UP	DOWN
NDUFB8	UP	DOWN
NDUFC1	UP	DOWN
NEDD4L	DOWN	DOWN
NEDD8	DOWN	DOWN
NFXL1	UP	DOWN
NFYC	DOWN	DOWN
NIBAN1	UP	DOWN
NIBAN3	UP	DOWN
NID1	DOWN	DOWN
NME6	UP	DOWN
NOB1	DOWN	DOWN
NOMO3	UP	DOWN
NPM1	DOWN	DOWN
NRP2	UP	DOWN
NSL1	DOWN	DOWN
NUDT4B	DOWN	DOWN
ODR4	UP	DOWN
ORMDL2	UP	DOWN
OSTC	UP	DOWN
PAAF1	DOWN	DOWN
PBK	DOWN	DOWN
PCDHGA5	UP	DOWN
PCIF1	UP	DOWN
PCNA	DOWN	DOWN
PCOLCE	DOWN	DOWN
PCSK5	UP	DOWN
PDK1	UP	DOWN
PDZD11	DOWN	DOWN
PEX16	UP	DOWN
PFDN2	DOWN	DOWN
PFKFB2	UP	DOWN
PGPEP1	UP	DOWN
PHC1	DOWN	DOWN
PIGT	UP	DOWN
PIH1D1	DOWN	DOWN
PIN4	DOWN	DOWN
PIP4P2	DOWN	DOWN
PIP5K1A	UP	DOWN
PISD	UP	DOWN
PITPNM1	UP	DOWN
PKP2	DOWN	DOWN
PLEKHA2	UP	DOWN
PLEKHA5	DOWN	DOWN
PLEKHA6	DOWN	DOWN
PMEL	UP	DOWN
POGK	UP	DOWN
POLE3	DOWN	DOWN
POLR1E	UP	DOWN

POLR2L	DOWN	DOWN
POLR3B	UP	DOWN
POP4	UP	DOWN
PPFIBP1	DOWN	DOWN
PPIE	DOWN	DOWN
PQBP1	DOWN	DOWN
PREB	UP	DOWN
PRKCE	UP	DOWN
PROX1	DOWN	DOWN
PRPSAP1	UP	DOWN
PRSS23	UP	DOWN
PRSS35	DOWN	DOWN
PSMA6	DOWN	DOWN
PSMF1	DOWN	DOWN
PTDSS2	UP	DOWN
PTMS	DOWN	DOWN
PTPMT1	UP	DOWN
PUF60	DOWN	DOWN
PUSL1	UP	DOWN
RAB23	DOWN	DOWN
RAB3GAP2	UP	DOWN
RAB8B	UP	DOWN
RAD9A	UP	DOWN
RAP1A	DOWN	DOWN
RAPH1	UP	DOWN
RBBP4	DOWN	DOWN
RBBP9	UP	DOWN
RBM24	DOWN	DOWN
RBMXL1	DOWN	DOWN
RBX1	DOWN	DOWN
RCHY1	UP	DOWN
RDH11	UP	DOWN
REEP6	UP	DOWN
RFTN1	UP	DOWN
RHOA	UP	DOWN
RNASET2	DOWN	DOWN
RNF170	UP	DOWN
ROBO1	DOWN	DOWN
ROMO1	UP	DOWN
RPL32	DOWN	DOWN
RPL35	DOWN	DOWN
RPL38	DOWN	DOWN
RPS13	DOWN	DOWN
RPS18	DOWN	DOWN
RPS28	DOWN	DOWN
RRP12	UP	DOWN
RRP8	UP	DOWN
RTF2	DOWN	DOWN
RTN2	UP	DOWN
RUSF1	UP	DOWN

RWDD1	DOWN	DOWN
S100A13	DOWN	DOWN
S100A4	DOWN	DOWN
SAA4	DOWN	DOWN
SAP18	DOWN	DOWN
SARNP	DOWN	DOWN
SCAMP1	UP	DOWN
SCD	UP	DOWN
SDC1	DOWN	DOWN
SDC4	DOWN	DOWN
SDHC	UP	DOWN
SDHD	UP	DOWN
SELENOH	DOWN	DOWN
SELENOI	UP	DOWN
SELENON	DOWN	DOWN
SELENOT	UP	DOWN
SEPHS1	DOWN	DOWN
SERINC1	UP	DOWN
SERPINE1	UP	DOWN
SESN2	UP	DOWN
SESTD1	UP	DOWN
SF3B6	DOWN	DOWN
SFRP5	DOWN	DOWN
SFSWAP	DOWN	DOWN
SFXN4	UP	DOWN
SH3BGRL	DOWN	DOWN
SLC12A2	DOWN	DOWN
SLC25A1	UP	DOWN
SLC27A3	UP	DOWN
SLC29A2	UP	DOWN
SLC2A1	UP	DOWN
SLC2A4	UP	DOWN
SLC30A3	UP	DOWN
SLC30A9	UP	DOWN
SLC35A1	UP	DOWN
SLC35E1	UP	DOWN
SLC38A1	UP	DOWN
SLC38A10	UP	DOWN
SLC38A2	UP	DOWN
SLC4A4	DOWN	DOWN
SLC9A3R1	DOWN	DOWN
SMC6	DOWN	DOWN
SMG6	UP	DOWN
SMIM13	UP	DOWN
SMPDL3B	DOWN	DOWN
SMPX	DOWN	DOWN
SNRPB	DOWN	DOWN
SNRPC	DOWN	DOWN
SNRPD3	DOWN	DOWN
SNRPE	DOWN	DOWN

SNX8	UP	DOWN
SORBS1	DOWN	DOWN
SP3	DOWN	DOWN
SPOCK2	DOWN	DOWN
SPON1	DOWN	DOWN
SQLE	UP	DOWN
SQSTM1	UP	DOWN
SRSF1	DOWN	DOWN
SRSF2	DOWN	DOWN
SRSF9	DOWN	DOWN
SSR1	DOWN	DOWN
STAT2	UP	DOWN
STAT3	UP	DOWN
STEEP1	DOWN	DOWN
STING1	UP	DOWN
STK25	UP	DOWN
STMN1	DOWN	DOWN
SULT1A1	DOWN	DOWN
SUMO1	DOWN	DOWN
SUPT4H1	DOWN	DOWN
TAF7	DOWN	DOWN
TAF8	DOWN	DOWN
TBPL1	UP	DOWN
TBRG4	UP	DOWN
TCF25	UP	DOWN
TECRL	UP	DOWN
TEX2	UP	DOWN
TFB1M	UP	DOWN
TFB2M	UP	DOWN
TGFBRAP1	UP	DOWN
THAP11	DOWN	DOWN
TIGAR	DOWN	DOWN
TIMM22	UP	DOWN
TM9SF2	UP	DOWN
TMA16	DOWN	DOWN
TMCO1	UP	DOWN
TMEM165	UP	DOWN
TMEM205	UP	DOWN
TMEM222	UP	DOWN
TMEM223	UP	DOWN
TMEM30A	UP	DOWN
TMEM41B	UP	DOWN
TNPO1	UP	DOWN
TOMM20	UP	DOWN
TOMM7	UP	DOWN
TPD52L2	DOWN	DOWN
TPI1	DOWN	DOWN
TRAM1	UP	DOWN
TRAPPC11	UP	DOWN
TRAPPC12	UP	DOWN

TRAPPC3	DOWN	DOWN
TRIR	DOWN	DOWN
TSC22D3	UP	DOWN
TSPAN14	DOWN	DOWN
TTC17	UP	DOWN
TTC33	DOWN	DOWN
TTR	DOWN	DOWN
TUBG1	UP	DOWN
TUT4	DOWN	DOWN
UBE2A	DOWN	DOWN
UBE2S	DOWN	DOWN
UCHL1	UP	DOWN
UFM1	DOWN	DOWN
UNC119B	DOWN	DOWN
UNC45B	UP	DOWN
UQCC3	UP	DOWN
USP5	DOWN	DOWN
UTP14A	DOWN	DOWN
VAT1	UP	DOWN
VIPAS39	UP	DOWN
VMP1	UP	DOWN
VPS35L	UP	DOWN
VPS53	UP	DOWN
VWA1	DOWN	DOWN
WARS1	UP	DOWN
WASHC4	UP	DOWN
WASHC5	UP	DOWN
WBP11	DOWN	DOWN
WDR45B	UP	DOWN
WFS1	UP	DOWN
WIP11	UP	DOWN
WLS	UP	DOWN
XPO4	UP	DOWN
XPOT	UP	DOWN
XPR1	UP	DOWN
YAF2	UP	DOWN
YBX3	DOWN	DOWN
ZBED1	DOWN	DOWN
ZFPM2	DOWN	DOWN
ZMAT2	DOWN	DOWN
ZNF143	DOWN	DOWN
ZNF281	DOWN	DOWN
ZNF330	DOWN	DOWN
ZNF740	UP	DOWN
AAMDC	DOWN	NS
ABHD14B	DOWN	NS
ABLIM3	UP	NS
ACYP1	DOWN	NS
ADAM23	UP	NS
ADAMTS7	DOWN	NS

AGRN	DOWN	NS
ALPL	DOWN	NS
ANXA1	UP	NS
ANXA4	DOWN	NS
ARG2	UP	NS
ARHGDIB	DOWN	NS
ARL14EP	DOWN	NS
ARMCX2	UP	NS
ARPIN	DOWN	NS
ARSL	DOWN	NS
ASNS	UP	NS
ATAT1	DOWN	NS
ATG4A	DOWN	NS
ATOX1	DOWN	NS
ATP1A3	UP	NS
ATP2A2	UP	NS
B9D1	DOWN	NS
BNIP3	UP	NS
BRD4	DOWN	NS
BUD13	DOWN	NS
BVES	UP	NS
CASC3	DOWN	NS
CBR1	DOWN	NS
CBX2	DOWN	NS
CCDC6	DOWN	NS
CD200	DOWN	NS
CD2AP	DOWN	NS
CD2BP2	DOWN	NS
CDH1	DOWN	NS
CDK2AP1	DOWN	NS
CECR2	DOWN	NS
CHAF1B	DOWN	NS
CHCHD6	UP	NS
CHD1L	DOWN	NS
CHRAC1	DOWN	NS
CKAP2	DOWN	NS
CKS1B	DOWN	NS
CNN1	UP	NS
COA4	UP	NS
COL11A2	DOWN	NS
COL12A1	UP	NS
COL2A1	UP	NS
COQ10A	UP	NS
COX5A	UP	NS
COX6C	UP	NS
COX7B	UP	NS
CPA5	UP	NS
CRABP2	DOWN	NS
CRTC1	DOWN	NS
CRTC3	DOWN	NS

CTSF	DOWN	NS
CUEDC2	DOWN	NS
CWC27	DOWN	NS
CXCL12	UP	NS
CYB5R1	UP	NS
CYP2J2	UP	NS
DAP	DOWN	NS
DDX28	UP	NS
DES	UP	NS
DHPS	DOWN	NS
DLC1	UP	NS
DNAJC8	DOWN	NS
DPYSL5	DOWN	NS
DUS3L	DOWN	NS
DYSF	UP	NS
ERBB4	DOWN	NS
EXOSC4	DOWN	NS
FAHD1	UP	NS
FAM110B	DOWN	NS
FASTKD5	UP	NS
FBLN2	UP	NS
FDX2	UP	NS
FER1L6-AS2	UP	NS
FEZ2	DOWN	NS
FHL1	DOWN	NS
FKBP4	DOWN	NS
FTH1	UP	NS
GDF6	UP	NS
GEMIN7	DOWN	NS
GOLM1	DOWN	NS
GOLPH3L	DOWN	NS
GPAT3	UP	NS
GPC3	DOWN	NS
GPKOW	DOWN	NS
GPN1	DOWN	NS
GRK4	UP	NS
GRK5	UP	NS
H2AC21	DOWN	NS
HCN1	UP	NS
HDGF	DOWN	NS
HDGFL2	DOWN	NS
HID1	UP	NS
HIRIP3	DOWN	NS
HMGA1	DOWN	NS
HSPB11	DOWN	NS
HSPB3	UP	NS
IAH1	DOWN	NS
IFI30	UP	NS
IGFBP5	DOWN	NS
IL6ST	UP	NS

ING2	DOWN	NS
ING4	DOWN	NS
INHBE	UP	NS
ITGB3	UP	NS
ITM2B	DOWN	NS
KCTD2	DOWN	NS
KDM5A	DOWN	NS
KIAA1109	UP	NS
KIAA1841	DOWN	NS
KIF14	UP	NS
KIF4A	DOWN	NS
KRT17	DOWN	NS
KRT7	UP	NS
LDHB	DOWN	NS
LMO4	DOWN	NS
LPIN3	DOWN	NS
LRRC14B	UP	NS
MCM2	DOWN	NS
MCM3	DOWN	NS
MCM4	DOWN	NS
MCM5	DOWN	NS
MCM6	DOWN	NS
MCM7	DOWN	NS
MIB2	DOWN	NS
MLYCD	UP	NS
MORC2	DOWN	NS
MRPS11	UP	NS
MRPS21	UP	NS
MTAP	DOWN	NS
MVB12A	DOWN	NS
MVP	DOWN	NS
MZT2B	DOWN	NS
NASP	DOWN	NS
NCALD	DOWN	NS
NDE1	DOWN	NS
NDUFA1	UP	NS
NDUFC2	UP	NS
NEB	UP	NS
NEO1	DOWN	NS
NFATC2IP	DOWN	NS
NFYB	DOWN	NS
NISCH	DOWN	NS
NKRF	DOWN	NS
NOP2	DOWN	NS
NUDCD2	DOWN	NS
OGDH	UP	NS
OGDHL	UP	NS
OTX2	DOWN	NS
P3H1	DOWN	NS
P3H3	DOWN	NS

PABIR2	DOWN	NS
PBX1	DOWN	NS
PBX2	DOWN	NS
PCK2	UP	NS
PDIA5	DOWN	NS
PDPN	UP	NS
PEG10	DOWN	NS
PHAX	DOWN	NS
PKN1	DOWN	NS
PLBD1	DOWN	NS
PLN	UP	NS
PODXL	DOWN	NS
POGLUT3	DOWN	NS
POM121C	UP	NS
POPDC2	UP	NS
PPP1R9B	DOWN	NS
PROS1	UP	NS
PTMA	DOWN	NS
PTN	DOWN	NS
PTP4A3	UP	NS
PTTG1IP	UP	NS
QSER1	DOWN	NS
RAB25	DOWN	NS
RABGAP1L	UP	NS
RBFOX2	DOWN	NS
RBM12	DOWN	NS
RBM4B	DOWN	NS
RCC2	DOWN	NS
RCN2	DOWN	NS
RCOR2	DOWN	NS
RELN	UP	NS
REST	DOWN	NS
RFX1	DOWN	NS
RNF126	DOWN	NS
RNF40	DOWN	NS
RPL35A	DOWN	NS
RPS21	DOWN	NS
S100A16	DOWN	NS
SALL2	DOWN	NS
SALL4	DOWN	NS
SAMHD1	DOWN	NS
SDF2L1	UP	NS
SELENBP1	DOWN	NS
SH3BGRL3	DOWN	NS
SH3PXD2B	DOWN	NS
SINHCAF	DOWN	NS
SLC20A2	UP	NS
SLC25A15	UP	NS
SLC25A4	UP	NS
SLC8A1	UP	NS

SMAD1	DOWN	NS
SMAD5	DOWN	NS
SMAP	DOWN	NS
SMG9	DOWN	NS
SNX15	DOWN	NS
SP100	DOWN	NS
SPAG7	DOWN	NS
SPART	DOWN	NS
SPC25	DOWN	NS
SSBP2	DOWN	NS
STC1	UP	NS
SUMO2	DOWN	NS
SUMO3	DOWN	NS
SUSD2	DOWN	NS
SYNC	DOWN	NS
TAF5	DOWN	NS
TAX1BP1	UP	NS
TCEAL4	DOWN	NS
TDRP	DOWN	NS
TFAP4	DOWN	NS
TGFBI	UP	NS
TIMM29	UP	NS
TMEM163	UP	NS
TMEM214	UP	NS
TMEM88	DOWN	NS
TMX2	UP	NS
TNC	UP	NS
TNFRSF10C	UP	NS
TNIP1	DOWN	NS
TNNC1	UP	NS
TNNI3	UP	NS
TPD52	DOWN	NS
TRH	UP	NS
TTI1	UP	NS
TUBB8	DOWN	NS
TXN	DOWN	NS
UBE2C	DOWN	NS
UBE2K	DOWN	NS
UBE2L3	DOWN	NS
UBR1	DOWN	NS
UHRF1	DOWN	NS
UIMC1	DOWN	NS
UQCRC2	UP	NS
UQCRQ	UP	NS
VANGL2	DOWN	NS
VIL1	DOWN	NS
VKORC1L1	UP	NS
VPS37B	DOWN	NS
WAC	DOWN	NS
WNK1	DOWN	NS

WNT11	UP	NS
YEATS2	DOWN	NS
YIF1A	UP	NS
YIPF5	UP	NS
ZC3H11A	DOWN	NS
ZFAND6	DOWN	NS
ZFYVE19	DOWN	NS
ZHX2	DOWN	NS
ZNF384	DOWN	NS
ZNF521	DOWN	NS
AAK1	NS	DOWN
AATF	NS	DOWN
ABCB7	NS	DOWN
ABCD3	NS	DOWN
ABHD6	NS	DOWN
ABI2	NS	DOWN
ABLIM1	NS	DOWN
ABR	NS	DOWN
ACAA1	NS	DOWN
ACADM	NS	DOWN
ACADS	NS	DOWN
ACAT1	NS	DOWN
ACBD6	NS	DOWN
ACLY	NS	DOWN
ACOT2	NS	DOWN
ACOT7	NS	DOWN
ACSF3	NS	DOWN
ACTN3	NS	DOWN
ADK	NS	DOWN
ADSL	NS	DOWN
ADSS1	NS	DOWN
AGL	NS	DOWN
AGO2	NS	DOWN
AGPAT1	NS	DOWN
AGPAT4	NS	DOWN
AGTRAP	NS	DOWN
AHCY	NS	DOWN
AHCYL1	NS	DOWN
AHDC1	NS	DOWN
AIFM1	NS	DOWN
AK3	NS	DOWN
AKAP8L	NS	DOWN
AKR1C1	NS	DOWN
AKT2	NS	DOWN
ALDH16A1	NS	DOWN
ALDH2	NS	DOWN
ALDOA	NS	DOWN
ALG1	NS	DOWN
ALG6	NS	DOWN
ALKBH7	NS	DOWN

AMPH	NS	DOWN
AMY2A	NS	DOWN
ANAPC2	NS	DOWN
ANAPC4	NS	DOWN
ANAPC7	NS	DOWN
ANKLE2	NS	DOWN
ANPEP	NS	DOWN
ANTXR1	NS	DOWN
AP1G1	NS	DOWN
AP3D1	NS	DOWN
AP3S1	NS	DOWN
APEX1	NS	DOWN
APOA1	NS	DOWN
APOE	NS	DOWN
APOH	NS	DOWN
APOL2	NS	DOWN
AQP1	NS	DOWN
ARAP1	NS	DOWN
ARFGAP2	NS	DOWN
ARFGEF1	NS	DOWN
ARHGAP12	NS	DOWN
ARHGAP5	NS	DOWN
ARHGEF10	NS	DOWN
ARID3B	NS	DOWN
ARIH1	NS	DOWN
ARL2	NS	DOWN
ARL6IP5	NS	DOWN
ARL8A	NS	DOWN
ARL8B	NS	DOWN
ARRB2	NS	DOWN
ARSB	NS	DOWN
ASAH1	NS	DOWN
ASCC3	NS	DOWN
ASMTL	NS	DOWN
ASS1	NS	DOWN
ATAD2B	NS	DOWN
ATG5	NS	DOWN
ATL3	NS	DOWN
ATM	NS	DOWN
ATP11A	NS	DOWN
ATP1A1	NS	DOWN
ATP1B2	NS	DOWN
ATP2C1	NS	DOWN
ATP5F1D	NS	DOWN
ATP5IF1	NS	DOWN
ATP5ME	NS	DOWN
ATP5PB	NS	DOWN
ATP5PD	NS	DOWN
ATP6AP2	NS	DOWN
ATP6V0D1	NS	DOWN

ATP6V1F	NS	DOWN
ATP6V1G1	NS	DOWN
ATP6V1G2	NS	DOWN
ATP6V1H	NS	DOWN
ATP7A	NS	DOWN
ATPAF1	NS	DOWN
ATRN	NS	DOWN
ATXN10	NS	DOWN
BAG5	NS	DOWN
BAG6	NS	DOWN
BAIAP2L1	NS	DOWN
BAP1	NS	DOWN
BAZ1A	NS	DOWN
BAZ2A	NS	DOWN
BCAS3	NS	DOWN
BCAT2	NS	DOWN
BCL2L13	NS	DOWN
BDH1	NS	DOWN
BIN3	NS	DOWN
BIRC3	NS	DOWN
BLOC1S1	NS	DOWN
BMPER	NS	DOWN
BNIP3L	NS	DOWN
BORCS5	NS	DOWN
BPGM	NS	DOWN
BPNT1	NS	DOWN
BRCC3	NS	DOWN
BSG	NS	DOWN
BST2	NS	DOWN
BTN2A1	NS	DOWN
BZW2	NS	DOWN
C11orf68	NS	DOWN
C1GALT1C1	NS	DOWN
C2CD2	NS	DOWN
C2orf49	NS	DOWN
C4A	NS	DOWN
C6orf120	NS	DOWN
C8orf33	NS	DOWN
CA14	NS	DOWN
CAB39L	NS	DOWN
CACNB2	NS	DOWN
CADM1	NS	DOWN
CADM4	NS	DOWN
CALCOCO2	NS	DOWN
CAMLG	NS	DOWN
CAMSAP1	NS	DOWN
CAND1	NS	DOWN
CANX	NS	DOWN
CAPG	NS	DOWN
CAPN2	NS	DOWN

CAPZB	NS	DOWN
CASP9	NS	DOWN
CASQ1	NS	DOWN
CAVIN4	NS	DOWN
CCDC124	NS	DOWN
CCDC47	NS	DOWN
CCDC83	NS	DOWN
CCNL1	NS	DOWN
CCNY	NS	DOWN
CCT2	NS	DOWN
CD151	NS	DOWN
CD46	NS	DOWN
CD47	NS	DOWN
CD59	NS	DOWN
CD63	NS	DOWN
CDAN1	NS	DOWN
CDC16	NS	DOWN
CDC27	NS	DOWN
CDIPT	NS	DOWN
CDK5	NS	DOWN
CDK9	NS	DOWN
CEBPZ	NS	DOWN
CEP41	NS	DOWN
CEP43	NS	DOWN
CERS6	NS	DOWN
CETN2	NS	DOWN
CFAP20	NS	DOWN
CFAP36	NS	DOWN
CFAP410	NS	DOWN
CFC1B	NS	DOWN
CFTR	NS	DOWN
CHCHD1	NS	DOWN
CHCHD5	NS	DOWN
CHCHD7	NS	DOWN
CHD2	NS	DOWN
CHFR	NS	DOWN
CHKB	NS	DOWN
CHMP4B	NS	DOWN
CHMP7	NS	DOWN
CHRM2	NS	DOWN
CHST12	NS	DOWN
CIRBP	NS	DOWN
CISD2	NS	DOWN
CIZ1	NS	DOWN
CLDN6	NS	DOWN
CLK2	NS	DOWN
CLNS1A	NS	DOWN
CLPX	NS	DOWN
CLTA	NS	DOWN
CLTB	NS	DOWN

CMC2	NS	DOWN
CMC4	NS	DOWN
CMSS1	NS	DOWN
CMTR1	NS	DOWN
CNIH4	NS	DOWN
CNOT7	NS	DOWN
CNPY2	NS	DOWN
COA6	NS	DOWN
COA7	NS	DOWN
COG1	NS	DOWN
COG3	NS	DOWN
COG7	NS	DOWN
COL18A1	NS	DOWN
COL1A1	NS	DOWN
COL1A2	NS	DOWN
COL26A1	NS	DOWN
COL4A1	NS	DOWN
COL4A6	NS	DOWN
COL6A2	NS	DOWN
COPB1	NS	DOWN
COPE	NS	DOWN
COPG1	NS	DOWN
COPS7B	NS	DOWN
CORO1A	NS	DOWN
COX19	NS	DOWN
COX7A2	NS	DOWN
COX7A2L	NS	DOWN
CPEB2	NS	DOWN
CPNE1	NS	DOWN
CPNE3	NS	DOWN
CPPED1	NS	DOWN
CRELD1	NS	DOWN
CSE1L	NS	DOWN
CSNK1A1	NS	DOWN
CSPG4	NS	DOWN
CTBS	NS	DOWN
CTF1	NS	DOWN
CTIF	NS	DOWN
CTNNA2	NS	DOWN
CTPS1	NS	DOWN
CTSD	NS	DOWN
CTSL	NS	DOWN
CTTN	NS	DOWN
CTTNBP2NL	NS	DOWN
CUL1	NS	DOWN
CUL3	NS	DOWN
CUL4B	NS	DOWN
CUL5	NS	DOWN
CUL7	NS	DOWN
CUX1	NS	DOWN

CWC15	NS	DOWN
CWC22	NS	DOWN
CYCS	NS	DOWN
CYFIP1	NS	DOWN
CYFIP2	NS	DOWN
CYP27A1	NS	DOWN
CZIB	NS	DOWN
DAD1	NS	DOWN
DAG1	NS	DOWN
DAGLB	NS	DOWN
DAP3	NS	DOWN
DBT	NS	DOWN
DCAF10	NS	DOWN
DCAF8	NS	DOWN
DCPS	NS	DOWN
DCTN3	NS	DOWN
DCUN1D5	NS	DOWN
DDOST	NS	DOWN
DDX10	NS	DOWN
DDX24	NS	DOWN
DDX27	NS	DOWN
DDX39B	NS	DOWN
DDX5	NS	DOWN
DDX52	NS	DOWN
DDX6	NS	DOWN
DECR2	NS	DOWN
DENND5B	NS	DOWN
DGAT1	NS	DOWN
DHCR24	NS	DOWN
DHX40	NS	DOWN
DIABLO	NS	DOWN
DIAPH1	NS	DOWN
DICER1	NS	DOWN
DIP2C	NS	DOWN
DIS3L2	NS	DOWN
DKC1	NS	DOWN
DLG1	NS	DOWN
DLST	NS	DOWN
DMAC2	NS	DOWN
DNAJC10	NS	DOWN
DNAJC11	NS	DOWN
DNAJC13	NS	DOWN
DNAJC16	NS	DOWN
DNAJC19	NS	DOWN
DNAJC25	NS	DOWN
DNAJC5	NS	DOWN
DOCK5	NS	DOWN
DOCK7	NS	DOWN
DOHH	NS	DOWN
DOLPP1	NS	DOWN

DOP1A	NS	DOWN
DPH2	NS	DOWN
DPP3	NS	DOWN
DPY19L1	NS	DOWN
DPY19L3	NS	DOWN
DPYSL4	NS	DOWN
DR1	NS	DOWN
DSTN	NS	DOWN
DUT	NS	DOWN
DYNLL1	NS	DOWN
E2F4	NS	DOWN
ECHDC1	NS	DOWN
ECHDC2	NS	DOWN
ECHDC3	NS	DOWN
ECPAS	NS	DOWN
EEF1AKMT2	NS	DOWN
EEFSEC	NS	DOWN
EFHD2	NS	DOWN
EFL1	NS	DOWN
EGLN1	NS	DOWN
EHMT1	NS	DOWN
EI24	NS	DOWN
EIF1	NS	DOWN
EIF2B2	NS	DOWN
EIF2B4	NS	DOWN
EIF3C	NS	DOWN
EIF3L	NS	DOWN
EIF4A2	NS	DOWN
EIF4G2	NS	DOWN
ELAC2	NS	DOWN
ELOVL5	NS	DOWN
EMC2	NS	DOWN
EMC8	NS	DOWN
EML2	NS	DOWN
ENPP1	NS	DOWN
ENPP4	NS	DOWN
EPHA4	NS	DOWN
EPHB2	NS	DOWN
EPHB3	NS	DOWN
EPHB4	NS	DOWN
EPHX1	NS	DOWN
ERBIN	NS	DOWN
ERC1	NS	DOWN
ERCC4	NS	DOWN
ERG28	NS	DOWN
ERGIC2	NS	DOWN
ERMP1	NS	DOWN
ESYT2	NS	DOWN
ETFB	NS	DOWN
ETFRF1	NS	DOWN

EXOC4	NS	DOWN
EXOC6B	NS	DOWN
EXOG	NS	DOWN
EXOSC5	NS	DOWN
EYA3	NS	DOWN
FABP3	NS	DOWN
FADS1	NS	DOWN
FAF1	NS	DOWN
FAM118A	NS	DOWN
FAM120A	NS	DOWN
FAM120B	NS	DOWN
FAM168A	NS	DOWN
FAM172A	NS	DOWN
FAM53C	NS	DOWN
FAM98A	NS	DOWN
FASN	NS	DOWN
FASTKD1	NS	DOWN
FAT2	NS	DOWN
FBN3	NS	DOWN
FBXO30	NS	DOWN
FBXW9	NS	DOWN
FDFT1	NS	DOWN
FERMT2	NS	DOWN
FGA	NS	DOWN
FGFBP3	NS	DOWN
FGG	NS	DOWN
FHIT	NS	DOWN
FIP1L1	NS	DOWN
FKBP5	NS	DOWN
FKBP7	NS	DOWN
FKBP9	NS	DOWN
FLG2	NS	DOWN
FLOT2	NS	DOWN
FLRT3	NS	DOWN
FN1	NS	DOWN
FNTB	NS	DOWN
FOCAD	NS	DOWN
FOXJ3	NS	DOWN
FOXO1	NS	DOWN
FOXO3	NS	DOWN
FREM2	NS	DOWN
FRMD3	NS	DOWN
FSD1	NS	DOWN
FSD2	NS	DOWN
FUCA1	NS	DOWN
FUNDC1	NS	DOWN
FUNDC2	NS	DOWN
FXR2	NS	DOWN
GADD45B	NS	DOWN
GALNT1	NS	DOWN

GAMT	NS	DOWN
GARRE1	NS	DOWN
GASK1B	NS	DOWN
GATB	NS	DOWN
GATC	NS	DOWN
GATM	NS	DOWN
GBA	NS	DOWN
GBA3	NS	DOWN
GBE1	NS	DOWN
GBF1	NS	DOWN
GCAT	NS	DOWN
GCN1	NS	DOWN
GDAP1	NS	DOWN
GDPGP1	NS	DOWN
GEMIN4	NS	DOWN
GGA2	NS	DOWN
GGACT	NS	DOWN
GGCX	NS	DOWN
GHITM	NS	DOWN
GJA1	NS	DOWN
GLE1	NS	DOWN
GLIPR2	NS	DOWN
GLMN	NS	DOWN
GLRX2	NS	DOWN
GLRX5	NS	DOWN
GLS	NS	DOWN
GLT8D1	NS	DOWN
GLTP	NS	DOWN
GM2A	NS	DOWN
GMDS	NS	DOWN
GNB2	NS	DOWN
GNE	NS	DOWN
GNPAT	NS	DOWN
GNS	NS	DOWN
GOLGA5	NS	DOWN
GOLIM4	NS	DOWN
GORASP1	NS	DOWN
GOT1	NS	DOWN
GPAA1	NS	DOWN
GPC1	NS	DOWN
GPHN	NS	DOWN
GPS1	NS	DOWN
GPX3	NS	DOWN
GPX7	NS	DOWN
GRAMD4	NS	DOWN
GRPEL1	NS	DOWN
GRWD1	NS	DOWN
GSPT2	NS	DOWN
GSTM3	NS	DOWN
GSTM4	NS	DOWN

GTF2H2	NS	DOWN
GTF2H3	NS	DOWN
GTF2H4	NS	DOWN
GTF3C1	NS	DOWN
GTF3C3	NS	DOWN
GTF3C5	NS	DOWN
GTPBP1	NS	DOWN
GTPBP3	NS	DOWN
GTPBP4	NS	DOWN
GXYLT1	NS	DOWN
GYG2	NS	DOWN
H1-2	NS	DOWN
H1-3	NS	DOWN
H1-5	NS	DOWN
H3-3A	NS	DOWN
H3C1	NS	DOWN
HACD1	NS	DOWN
HACE1	NS	DOWN
HADHA	NS	DOWN
HBB	NS	DOWN
HCFC2	NS	DOWN
HDAC6	NS	DOWN
HDHD2	NS	DOWN
HEATR1	NS	DOWN
HEATR3	NS	DOWN
HEATR5A	NS	DOWN
HEATR6	NS	DOWN
HEBP1	NS	DOWN
HECTD4	NS	DOWN
HERC1	NS	DOWN
HERC4	NS	DOWN
HEXA	NS	DOWN
HGH1	NS	DOWN
HGS	NS	DOWN
HIGD2A	NS	DOWN
HIKESHI	NS	DOWN
HINT2	NS	DOWN
HMGCS1	NS	DOWN
HNRNPC	NS	DOWN
HNRNPH2	NS	DOWN
HNRNPLL	NS	DOWN
HNRNPR	NS	DOWN
HSD17B11	NS	DOWN
HSD17B8	NS	DOWN
HSP90AB3P	NS	DOWN
HSPA13	NS	DOWN
HSPBP1	NS	DOWN
HSPE1	NS	DOWN
HTRA2	NS	DOWN
HTT	NS	DOWN

HUWE1	NS	DOWN
HYI	NS	DOWN
IARS2	NS	DOWN
IFI16	NS	DOWN
IFIT5	NS	DOWN
IFT74	NS	DOWN
IGF1R	NS	DOWN
IMPACT	NS	DOWN
INF2	NS	DOWN
INPP4A	NS	DOWN
INPPL1	NS	DOWN
INTS11	NS	DOWN
INTS2	NS	DOWN
INTS3	NS	DOWN
INTS4	NS	DOWN
INTS7	NS	DOWN
IPO4	NS	DOWN
IPO7	NS	DOWN
IPO8	NS	DOWN
IQCB1	NS	DOWN
IRGQ	NS	DOWN
IRX4	NS	DOWN
ITPR1	NS	DOWN
JPH1	NS	DOWN
JPT2	NS	DOWN
KANK2	NS	DOWN
KANSL1	NS	DOWN
KAT7	NS	DOWN
KAT8	NS	DOWN
KBTBD2	NS	DOWN
KCMF1	NS	DOWN
KCTD10	NS	DOWN
KDM4B	NS	DOWN
KDM5C	NS	DOWN
KDM6B	NS	DOWN
KDSR	NS	DOWN
KIF13B	NS	DOWN
KIF2A	NS	DOWN
KIFBP	NS	DOWN
KIFC1	NS	DOWN
KLC2	NS	DOWN
KLC4	NS	DOWN
KLHL4	NS	DOWN
KLHL41	NS	DOWN
KPNA1	NS	DOWN
KPNA2	NS	DOWN
KPNA4	NS	DOWN
KPNB1	NS	DOWN
KRT1	NS	DOWN
KRT16	NS	DOWN

KRT5	NS	DOWN
KTI12	NS	DOWN
KXD1	NS	DOWN
L1TD1	NS	DOWN
LAMP1	NS	DOWN
LAMTOR2	NS	DOWN
LAMTOR3	NS	DOWN
LAMTOR5	NS	DOWN
LANCL2	NS	DOWN
LARP6	NS	DOWN
LARS2	NS	DOWN
LASP1	NS	DOWN
LCLAT1	NS	DOWN
LCMT1	NS	DOWN
LDAH	NS	DOWN
LDHA	NS	DOWN
LDLR	NS	DOWN
LEFTY2	NS	DOWN
LEMD2	NS	DOWN
LEPROTL1	NS	DOWN
LGALS1	NS	DOWN
LGALS3BP	NS	DOWN
LHFPL2	NS	DOWN
LIN7C	NS	DOWN
LLGL1	NS	DOWN
LLPH	NS	DOWN
LMNB2	NS	DOWN
LMO7	NS	DOWN
LMOD1	NS	DOWN
LNPBK	NS	DOWN
LONP2	NS	DOWN
LPCAT1	NS	DOWN
LPL	NS	DOWN
LRBA	NS	DOWN
LRRC1	NS	DOWN
LRRC20	NS	DOWN
LRRC41	NS	DOWN
LRRC47	NS	DOWN
LRRC57	NS	DOWN
LRRFIP1	NS	DOWN
LRRFIP2	NS	DOWN
LSG1	NS	DOWN
LSM1	NS	DOWN
LSM5	NS	DOWN
LSM7	NS	DOWN
LTF	NS	DOWN
LTN1	NS	DOWN
LYPLA2	NS	DOWN
LYRM4	NS	DOWN
LYSMD3	NS	DOWN

MACROD2	NS	DOWN
MAD2L1	NS	DOWN
MAEA	NS	DOWN
MAN1A1	NS	DOWN
MAN2C1	NS	DOWN
MAOB	NS	DOWN
MAP1A	NS	DOWN
MAP2K1	NS	DOWN
MAP2K2	NS	DOWN
MAP2K3	NS	DOWN
MAP2K4	NS	DOWN
MAP2K7	NS	DOWN
MAP4K3	NS	DOWN
MAP4K5	NS	DOWN
MAPK1	NS	DOWN
MAPK12	NS	DOWN
MAPK3	NS	DOWN
MAPK8IP3	NS	DOWN
MAPK9	NS	DOWN
MARCKSL1	NS	DOWN
MAVS	NS	DOWN
MB	NS	DOWN
MBD2	NS	DOWN
MCM3AP	NS	DOWN
MCTS1	NS	DOWN
MCU	NS	DOWN
MDH2	NS	DOWN
MDN1	NS	DOWN
ME1	NS	DOWN
MEAK7	NS	DOWN
MED17	NS	DOWN
MED27	NS	DOWN
MED28	NS	DOWN
MED29	NS	DOWN
MED31	NS	DOWN
MEF2D	NS	DOWN
MEIS2	NS	DOWN
METTL1	NS	DOWN
METTL26	NS	DOWN
MFAP4	NS	DOWN
MGAT5	NS	DOWN
MGME1	NS	DOWN
MGST1	NS	DOWN
MGST2	NS	DOWN
MICOS10	NS	DOWN
MID1	NS	DOWN
MIEF1	NS	DOWN
MIF4GD	NS	DOWN
MIX23	NS	DOWN
MKRN2	NS	DOWN

MMP14	NS	DOWN
MMRN2	NS	DOWN
MMTAG2	NS	DOWN
MOCS1	NS	DOWN
MOCS3	NS	DOWN
MON2	NS	DOWN
MPC2	NS	DOWN
MPZL1	NS	DOWN
MRAS	NS	DOWN
MRM3	NS	DOWN
MRPL10	NS	DOWN
MRPL11	NS	DOWN
MRPL12	NS	DOWN
MRPL22	NS	DOWN
MRPL23	NS	DOWN
MRPL24	NS	DOWN
MRPL27	NS	DOWN
MRPL33	NS	DOWN
MRPL34	NS	DOWN
MRPL39	NS	DOWN
MRPL41	NS	DOWN
MRPL45	NS	DOWN
MRPL51	NS	DOWN
MRPL54	NS	DOWN
MRPS15	NS	DOWN
MRPS17	NS	DOWN
MRPS18C	NS	DOWN
MRPS28	NS	DOWN
MRPS33	NS	DOWN
MRPS9	NS	DOWN
MSRB2	NS	DOWN
MT-ATP6	NS	DOWN
MT-CYB	NS	DOWN
MT-ND3	NS	DOWN
MTMR10	NS	DOWN
MTMR2	NS	DOWN
MTO1	NS	DOWN
MTOR	NS	DOWN
MTPAP	NS	DOWN
MTPN	NS	DOWN
MTRES1	NS	DOWN
MTX1	NS	DOWN
MVK	NS	DOWN
MYADM	NS	DOWN
MYBBP1A	NS	DOWN
MYDGF	NS	DOWN
MYH6	NS	DOWN
MYL2	NS	DOWN
MYL3	NS	DOWN
MYL5	NS	DOWN

MYL6	NS	DOWN
MYLK3	NS	DOWN
MYO1D	NS	DOWN
MYO1E	NS	DOWN
MYO9B	NS	DOWN
MYOZ1	NS	DOWN
NAA15	NS	DOWN
NAA80	NS	DOWN
NAB2	NS	DOWN
NACA	NS	DOWN
NAPRT	NS	DOWN
NAT10	NS	DOWN
NCAPG	NS	DOWN
NCKIPSD	NS	DOWN
NCL	NS	DOWN
NCLN	NS	DOWN
NCOR2	NS	DOWN
NCSTN	NS	DOWN
NDRG1	NS	DOWN
NDUFA13	NS	DOWN
NDUFA3	NS	DOWN
NDUFA4	NS	DOWN
NDUFA7	NS	DOWN
NDUFAF2	NS	DOWN
NDUFAF3	NS	DOWN
NDUFB11	NS	DOWN
NDUFB3	NS	DOWN
NDUFS1	NS	DOWN
NDUFS5	NS	DOWN
NDUFS6	NS	DOWN
NEFL	NS	DOWN
NEK9	NS	DOWN
NELFB	NS	DOWN
NELFCD	NS	DOWN
NEU1	NS	DOWN
NEXN	NS	DOWN
NF1	NS	DOWN
NFIC	NS	DOWN
NFKB1	NS	DOWN
NFKB2	NS	DOWN
NFU1	NS	DOWN
NFX1	NS	DOWN
NHEJ1	NS	DOWN
NHLRC2	NS	DOWN
NIPBL	NS	DOWN
NIT1	NS	DOWN
NME1	NS	DOWN
NME7	NS	DOWN
NMT1	NS	DOWN
NOA1	NS	DOWN

NOC3L	NS	DOWN
NOL10	NS	DOWN
NOL6	NS	DOWN
NOL9	NS	DOWN
NOP10	NS	DOWN
NOP56	NS	DOWN
NOP58	NS	DOWN
NOTCH2	NS	DOWN
NPC1	NS	DOWN
NPM3	NS	DOWN
NPPB	NS	DOWN
NR3C1	NS	DOWN
NRAP	NS	DOWN
NRDC	NS	DOWN
NRF1	NS	DOWN
NT5C3B	NS	DOWN
NT5DC1	NS	DOWN
NT5DC2	NS	DOWN
NUB1	NS	DOWN
NUDCD1	NS	DOWN
NUDT12	NS	DOWN
NUDT15	NS	DOWN
NUDT4	NS	DOWN
NUDT9	NS	DOWN
NUP107	NS	DOWN
NUP155	NS	DOWN
NUP160	NS	DOWN
NUP188	NS	DOWN
NUP205	NS	DOWN
NUP42	NS	DOWN
NUP62	NS	DOWN
NUP85	NS	DOWN
NXN	NS	DOWN
OARD1	NS	DOWN
OCIAD1	NS	DOWN
ODF2	NS	DOWN
OFD1	NS	DOWN
OGFR	NS	DOWN
OPLAH	NS	DOWN
OR52P1P	NS	DOWN
ORC3	NS	DOWN
ORMDL3	NS	DOWN
OSBP	NS	DOWN
OSBPL1A	NS	DOWN
OSBPL3	NS	DOWN
OSBPL8	NS	DOWN
OSBPL9	NS	DOWN
OSGEP	NS	DOWN
OSGEPL1	NS	DOWN
OXA1L	NS	DOWN

OXR1	NS	DOWN
PABPC1	NS	DOWN
PABPC4	NS	DOWN
PABPN1	NS	DOWN
PALD1	NS	DOWN
PALM	NS	DOWN
PARN	NS	DOWN
PARP1	NS	DOWN
PARP16	NS	DOWN
PARP2	NS	DOWN
PARVB	NS	DOWN
PCBP4	NS	DOWN
PCID2	NS	DOWN
PCYOX1L	NS	DOWN
PDCD2	NS	DOWN
PDCD2L	NS	DOWN
PDCD6IP	NS	DOWN
PDK3	NS	DOWN
PDLIM1	NS	DOWN
PDS5B	NS	DOWN
PEDS1	NS	DOWN
PET100	NS	DOWN
PEX13	NS	DOWN
PEX19	NS	DOWN
PFAS	NS	DOWN
PFDN1	NS	DOWN
PFKL	NS	DOWN
PFKM	NS	DOWN
PFKP	NS	DOWN
PFN1	NS	DOWN
PFN3	NS	DOWN
PGAM1	NS	DOWN
PGAM2	NS	DOWN
PGD	NS	DOWN
PGK1	NS	DOWN
PHACTR2	NS	DOWN
PHB	NS	DOWN
PHB2	NS	DOWN
PHF3	NS	DOWN
PHF6	NS	DOWN
PHKB	NS	DOWN
PHLDB3	NS	DOWN
PHYHIP	NS	DOWN
PI4KA	NS	DOWN
PIAS1	NS	DOWN
PICK1	NS	DOWN
PIK3C2A	NS	DOWN
PIK3R1	NS	DOWN
PIK3R4	NS	DOWN
PIP4K2A	NS	DOWN

PIP4K2B	NS	DOWN
PIP4P1	NS	DOWN
PITHD1	NS	DOWN
PJA1	NS	DOWN
PKD1L3	NS	DOWN
PKLR	NS	DOWN
PLAA	NS	DOWN
PLCB4	NS	DOWN
PLD3	NS	DOWN
PLXNA2	NS	DOWN
PNISR	NS	DOWN
PNO1	NS	DOWN
PNPLA8	NS	DOWN
POLG2	NS	DOWN
POLI	NS	DOWN
POLR1A	NS	DOWN
POLR1B	NS	DOWN
POLR2C	NS	DOWN
POLR2J	NS	DOWN
POLR2M	NS	DOWN
POLR3A	NS	DOWN
POLR3C	NS	DOWN
POLR3F	NS	DOWN
POLRMT	NS	DOWN
POP1	NS	DOWN
PPCS	NS	DOWN
PPFIA2	NS	DOWN
PPIA	NS	DOWN
PPIB	NS	DOWN
PPIC	NS	DOWN
PPM1A	NS	DOWN
PPM1F	NS	DOWN
PPP1CC	NS	DOWN
PPP1R14B	NS	DOWN
PPP2R3A	NS	DOWN
PPP2R5E	NS	DOWN
PPP4C	NS	DOWN
PPP4R1	NS	DOWN
PPP4R3A	NS	DOWN
PPP4R3B	NS	DOWN
PPP6R3	NS	DOWN
PPT2	NS	DOWN
PRDX3	NS	DOWN
PREPL	NS	DOWN
PRKAA1	NS	DOWN
PRKAA2	NS	DOWN
PRKACA	NS	DOWN
PRKACB	NS	DOWN
PRKAG1	NS	DOWN
PRKAG2	NS	DOWN

PRKCSH	NS	DOWN
PRKD1	NS	DOWN
PRMT5	NS	DOWN
PRPF38A	NS	DOWN
PRPS1	NS	DOWN
PRSS1	NS	DOWN
PRUNE1	NS	DOWN
PRXL2B	NS	DOWN
PSD3	NS	DOWN
PSMA4	NS	DOWN
PSMA5	NS	DOWN
PSMB2	NS	DOWN
PSMD13	NS	DOWN
PSMD2	NS	DOWN
PSMD4	NS	DOWN
PSMD5	NS	DOWN
PSME4	NS	DOWN
PSMG2	NS	DOWN
PSMG4	NS	DOWN
PTGIS	NS	DOWN
PTPN12	NS	DOWN
PTPN2	NS	DOWN
PTPN23	NS	DOWN
PTPN9	NS	DOWN
PTRH2	NS	DOWN
PTRHD1	NS	DOWN
PUDP	NS	DOWN
PWP1	NS	DOWN
PXK	NS	DOWN
PYGB	NS	DOWN
PYGM	NS	DOWN
PYM1	NS	DOWN
PYROXD2	NS	DOWN
QKI	NS	DOWN
QPCTL	NS	DOWN
QTRT1	NS	DOWN
R3HDM2	NS	DOWN
RAB10	NS	DOWN
RAB11B	NS	DOWN
RAB18	NS	DOWN
RAB1B	NS	DOWN
RAB2B	NS	DOWN
RAB35	NS	DOWN
RAB3GAP1	NS	DOWN
RAB5B	NS	DOWN
RAB7A	NS	DOWN
RAB8A	NS	DOWN
RAB9B	NS	DOWN
RABEP2	NS	DOWN
RABGAP1	NS	DOWN

RABIF	NS	DOWN
RACGAP1	NS	DOWN
RADIL	NS	DOWN
RAF1	NS	DOWN
RALB	NS	DOWN
RALGAPA1	NS	DOWN
RALY	NS	DOWN
RALYL	NS	DOWN
RANBP6	NS	DOWN
RAP1GDS1	NS	DOWN
RAP2A	NS	DOWN
RARS1	NS	DOWN
RASA1	NS	DOWN
RB1	NS	DOWN
RBBP5	NS	DOWN
RBM17	NS	DOWN
RBM22	NS	DOWN
RBM28	NS	DOWN
RBM3	NS	DOWN
RBM38	NS	DOWN
RBM6	NS	DOWN
RBMS1	NS	DOWN
RBP4	NS	DOWN
RBPM52	NS	DOWN
RCOR3	NS	DOWN
REEP5	NS	DOWN
RELCH	NS	DOWN
REPIN1	NS	DOWN
RER1	NS	DOWN
RETREG3	NS	DOWN
REXO2	NS	DOWN
RFC3	NS	DOWN
RFC4	NS	DOWN
RFT1	NS	DOWN
RHBDD1	NS	DOWN
RHEB	NS	DOWN
RIC8A	NS	DOWN
RICTOR	NS	DOWN
RIDA	NS	DOWN
RINT1	NS	DOWN
RIOK3	NS	DOWN
RIT1	NS	DOWN
RLF	NS	DOWN
RMDN1	NS	DOWN
RMND5A	NS	DOWN
RNF114	NS	DOWN
RNF13	NS	DOWN
RNF14	NS	DOWN
RNF185	NS	DOWN
RNF25	NS	DOWN

RNPEP	NS	DOWN
RNPS1	NS	DOWN
RO60	NS	DOWN
ROR2	NS	DOWN
RPAP1	NS	DOWN
RPE	NS	DOWN
RPL10A	NS	DOWN
RPL13	NS	DOWN
RPL14	NS	DOWN
RPL18	NS	DOWN
RPL24	NS	DOWN
RPL26L1	NS	DOWN
RPL27A	NS	DOWN
RPL29	NS	DOWN
RPL31	NS	DOWN
RPL34	NS	DOWN
RPL36	NS	DOWN
RPL9	NS	DOWN
RPLP1	NS	DOWN
RPLP2	NS	DOWN
RPP25	NS	DOWN
RPP38	NS	DOWN
RPS12	NS	DOWN
RPS14	NS	DOWN
RPS15	NS	DOWN
RPS17	NS	DOWN
RPS19	NS	DOWN
RPS20	NS	DOWN
RPS23	NS	DOWN
RPS24	NS	DOWN
RPS25	NS	DOWN
RPS27	NS	DOWN
RPS27A	NS	DOWN
RPS6KB1	NS	DOWN
RPS9	NS	DOWN
RRAD	NS	DOWN
RRS1	NS	DOWN
RTCA	NS	DOWN
RTKN	NS	DOWN
RTN3	NS	DOWN
RUFY1	NS	DOWN
S100A11	NS	DOWN
SAFB	NS	DOWN
SAFB2	NS	DOWN
SALL1	NS	DOWN
SAMD1	NS	DOWN
SAP30BP	NS	DOWN
SAR1A	NS	DOWN
SAR1B	NS	DOWN
SART3	NS	DOWN

SBF1	NS	DOWN
SCAMP4	NS	DOWN
SCO2	NS	DOWN
SCRN3	NS	DOWN
SDAD1	NS	DOWN
SDF2	NS	DOWN
SDK2	NS	DOWN
SDSL	NS	DOWN
SEC23B	NS	DOWN
SEC24B	NS	DOWN
SEC24C	NS	DOWN
SEC31A	NS	DOWN
SEC61A1	NS	DOWN
SEC61G	NS	DOWN
SEC62	NS	DOWN
SELENOO	NS	DOWN
SELENOS	NS	DOWN
SEMA3A	NS	DOWN
SEMA4D	NS	DOWN
SENP3	NS	DOWN
SENP8	NS	DOWN
SEPTIN6	NS	DOWN
SERPINA10	NS	DOWN
SERPIND1	NS	DOWN
SET	NS	DOWN
SF3B4	NS	DOWN
SFT2D2	NS	DOWN
SFT2D3	NS	DOWN
SH3BGRL2	NS	DOWN
SHARPIN	NS	DOWN
SHBG	NS	DOWN
SIN3B	NS	DOWN
SIRT1	NS	DOWN
SLC16A1	NS	DOWN
SLC16A3	NS	DOWN
SLC25A10	NS	DOWN
SLC25A20	NS	DOWN
SLC25A22	NS	DOWN
SLC25A24	NS	DOWN
SLC25A46	NS	DOWN
SLC27A4	NS	DOWN
SLC29A1	NS	DOWN
SLC30A1	NS	DOWN
SLC34A2	NS	DOWN
SLC35A4	NS	DOWN
SLC39A6	NS	DOWN
SLC39A7	NS	DOWN
SLC41A3	NS	DOWN
SLC44A2	NS	DOWN
SLC7A6	NS	DOWN

SLC7A8	NS	DOWN
SMAD3	NS	DOWN
SMARCA2	NS	DOWN
SMARCC2	NS	DOWN
SMG1	NS	DOWN
SMIM26	NS	DOWN
SMPD4	NS	DOWN
SMYD3	NS	DOWN
SNAPIN	NS	DOWN
SNRPA	NS	DOWN
SNRPGP15	NS	DOWN
SNX29	NS	DOWN
SNX30	NS	DOWN
SOAT1	NS	DOWN
SOD3	NS	DOWN
SON	NS	DOWN
SORBS2	NS	DOWN
SORD	NS	DOWN
SP1	NS	DOWN
SP4	NS	DOWN
SPCS3	NS	DOWN
SPG21	NS	DOWN
SPOCK1	NS	DOWN
SPOUT1	NS	DOWN
SPPL2A	NS	DOWN
SPRING1	NS	DOWN
SRC	NS	DOWN
SRL	NS	DOWN
SRR	NS	DOWN
SRSF11	NS	DOWN
SRSF6	NS	DOWN
ST13	NS	DOWN
STAM	NS	DOWN
STARD3NL	NS	DOWN
STAT5B	NS	DOWN
STIM1	NS	DOWN
STK33	NS	DOWN
STK38	NS	DOWN
STKLD1	NS	DOWN
STOML3	NS	DOWN
STRIP1	NS	DOWN
STT3B	NS	DOWN
STX17	NS	DOWN
STX2	NS	DOWN
STX5	NS	DOWN
STX6	NS	DOWN
STX8	NS	DOWN
STXBP1	NS	DOWN
SUGP1	NS	DOWN
SWAP70	NS	DOWN

SYF2	NS	DOWN
TAF6	NS	DOWN
TAF9	NS	DOWN
TANC1	NS	DOWN
TANC2	NS	DOWN
TARBP2	NS	DOWN
TASOR2	NS	DOWN
TBC1D10B	NS	DOWN
TBC1D13	NS	DOWN
TBC1D17	NS	DOWN
TBC1D23	NS	DOWN
TBC1D4	NS	DOWN
TBCD	NS	DOWN
TBL2	NS	DOWN
TBX5	NS	DOWN
TECR	NS	DOWN
TELO2	NS	DOWN
TENT2	NS	DOWN
TEX10	NS	DOWN
TFDP1	NS	DOWN
THBS1	NS	DOWN
THY1	NS	DOWN
TIMELESS	NS	DOWN
TIMM13	NS	DOWN
TIMM50	NS	DOWN
TIMP3	NS	DOWN
TIPRL	NS	DOWN
TLCD4	NS	DOWN
TM9SF3	NS	DOWN
TMBIM6	NS	DOWN
TMEM109	NS	DOWN
TMEM201	NS	DOWN
TMEM245	NS	DOWN
TMEM256	NS	DOWN
TMEM33	NS	DOWN
TMEM38B	NS	DOWN
TMOD1	NS	DOWN
TMOD3	NS	DOWN
TMPPE	NS	DOWN
TMX1	NS	DOWN
TMX3	NS	DOWN
TNFAIP8	NS	DOWN
TNFAIP8L1	NS	DOWN
TNFRSF10B	NS	DOWN
TNNI3K	NS	DOWN
TNPO2	NS	DOWN
TNPO3	NS	DOWN
TNRC18	NS	DOWN
TNS3	NS	DOWN
TOE1	NS	DOWN

TOMM5	NS	DOWN
TPBG	NS	DOWN
TPM1	NS	DOWN
TPM2	NS	DOWN
TPM3	NS	DOWN
TPMT	NS	DOWN
TPPP	NS	DOWN
TPRG1L	NS	DOWN
TRA2B	NS	DOWN
TRAF2	NS	DOWN
TRAPPC1	NS	DOWN
TRAPPC8	NS	DOWN
TRIM25	NS	DOWN
TRIM26	NS	DOWN
TRIM3	NS	DOWN
TRIM56	NS	DOWN
TRIM71	NS	DOWN
TRIO	NS	DOWN
TRMT11	NS	DOWN
TRMT1L	NS	DOWN
TRPT1	NS	DOWN
TRUB1	NS	DOWN
TSC2	NS	DOWN
TSC22D1	NS	DOWN
TSPAN31	NS	DOWN
TSTD1	NS	DOWN
TTC23L	NS	DOWN
TTC37	NS	DOWN
TTC4	NS	DOWN
TTC5	NS	DOWN
TUBA1C	NS	DOWN
TUBA4A	NS	DOWN
TUBAL3	NS	DOWN
TUBGCP2	NS	DOWN
TUBGCP3	NS	DOWN
TUFM	NS	DOWN
TXLNGY	NS	DOWN
TXN2	NS	DOWN
TXNRD2	NS	DOWN
U2AF2	NS	DOWN
UBA6	NS	DOWN
UBAC1	NS	DOWN
UBE2Q1	NS	DOWN
UBE2T	NS	DOWN
UBE3C	NS	DOWN
UBE4B	NS	DOWN
UBR3	NS	DOWN
UBR4	NS	DOWN
UCHL3	NS	DOWN
UFC1	NS	DOWN

UHRF1BP1	NS	DOWN
UQCR11	NS	DOWN
URI1	NS	DOWN
USO1	NS	DOWN
USP13	NS	DOWN
USP19	NS	DOWN
USP22	NS	DOWN
USP24	NS	DOWN
USP25	NS	DOWN
USP28	NS	DOWN
USP48	NS	DOWN
USP9X	NS	DOWN
UTP20	NS	DOWN
UTP6	NS	DOWN
VAC14	NS	DOWN
VAPA	NS	DOWN
VAR51	NS	DOWN
VAV2	NS	DOWN
VCPIP1	NS	DOWN
VILL	NS	DOWN
VIRMA	NS	DOWN
VPS11	NS	DOWN
VPS13A	NS	DOWN
VPS18	NS	DOWN
VPS26C	NS	DOWN
VPS35	NS	DOWN
VPS37C	NS	DOWN
VPS50	NS	DOWN
VSNL1	NS	DOWN
VTA1	NS	DOWN
VTN	NS	DOWN
VWA5A	NS	DOWN
WASF1	NS	DOWN
WBP2	NS	DOWN
WDFY3	NS	DOWN
WDR12	NS	DOWN
WDR13	NS	DOWN
WDR18	NS	DOWN
WDR3	NS	DOWN
WDR36	NS	DOWN
WDR45	NS	DOWN
WDR7	NS	DOWN
WDR77	NS	DOWN
WDR91	NS	DOWN
WDTC1	NS	DOWN
WFDC13	NS	DOWN
WNK2	NS	DOWN
WRAP53	NS	DOWN
XAB2	NS	DOWN
XPO1	NS	DOWN

XPO5	NS	DOWN
XPO7	NS	DOWN
XRCC1	NS	DOWN
XRN1	NS	DOWN
YAP1	NS	DOWN
YWHAB	NS	DOWN
YWHAH	NS	DOWN
ZBTB8OS	NS	DOWN
ZC3H11B	NS	DOWN
ZC3HAV1L	NS	DOWN
ZC3HC1	NS	DOWN
ZCRB1	NS	DOWN
ZER1	NS	DOWN
ZFP36L1	NS	DOWN
ZHX1	NS	DOWN
ZKSCAN8	NS	DOWN
ZMPSTE24	NS	DOWN
ZMYM3	NS	DOWN
ZNF121	NS	DOWN
ZNF211	NS	DOWN
ZNF22	NS	DOWN
ZNF320	NS	DOWN
ZNF358	NS	DOWN
ZNF414	NS	DOWN
ZNF511	NS	DOWN
ZNF512	NS	DOWN
ZNF701	NS	DOWN
ZNF771	NS	DOWN
ZSCAN18	NS	DOWN

Appendix C

Table AC: Differentially abundant metabolites. DOWN – lower abundance in comparison; UP higher abundance in comparison; NS – not significant in comparison.

Metabolite	LMNA ^{+/-} vs WT	EMD ^{-ly} vs WT
2-Aminoheptanoate	UP	UP
2,4-Dihydroxypteridine	UP	UP
Allantoic Acid	UP	UP
Beta-Glycerophosphate	UP	UP
Beta-Hydroxypyruvic Acid	UP	UP
Coenzyme Q10	UP	UP
Cysteine-S-Sulfate	DOWN	DOWN
Erythronic Acid	UP	UP
Glycerate	UP	UP
Glycerol 3-Phosphate	UP	UP
Histidine	DOWN	DOWN
Hypoxanthine	UP	UP
L-Lactic Acid (Lactate)	DOWN	DOWN
Malonate	UP	UP
N-Acetyl-L-Aspartic Acid	UP	UP
N-Acetylaspartylglutamic Acid	UP	UP
N-Acetylputrescine	DOWN	DOWN
Phosphoenolpyruvate	UP	UP
Sphinganine	UP	UP
13-Methylmyristic Acid	DOWN	NS
4-Imidazoleacrylic Acid (Urocanate)	DOWN	NS
7-Methylguanine	DOWN	NS
Eicosapentaenoate (Eicosapentaenoic Acid)	DOWN	NS
Linoleate	DOWN	NS
Myristic Acid (Myristate)	DOWN	NS
Palmitoleic Acid	DOWN	NS
Palmitoylethanolamide	UP	NS
Sphingosine (C17)	DOWN	NS
Sphingosine (C18)	UP	NS
Uridine Monophosphate	UP	NS
2-Phosphoglycerate	NS	UP
3-Phosphoglycerate	NS	UP
Adenosine Diphosphoglucose	NS	UP
Alpha-D-Glucose	NS	UP
Galactose	NS	UP
Glucose	NS	UP
Guanosine 5-Triphosphate	NS	UP
Uridine Diphosphate Galactose	NS	UP
Uridine Diphosphate Glucose	NS	UP
Uridine Diphosphate-N-Acetylgalactosamine (UDP-GalNAc)	NS	UP
Uridine Diphosphate-N-Acetylglucosamine (UDP-GlcNAc)	NS	UP
1-Deoxy-D-Glucitol	NS	DOWN
2-Keto-3-Deoxy-Gluconate	NS	UP

2-Pyrrolidone-5-Carboxylic Acid (Oxoproline)	NS	DOWN
4-Hydroxy-3-Methoxyphenylglycol	NS	DOWN
Adenosine 3,5-Diphosphate	NS	UP
Adenosine 5-Diphosphate	NS	UP
Adenosine Triphosphate	NS	UP
Allose	NS	UP
Beta-Nicotinamide Adenine Dinucleotide	NS	UP
Choline	NS	UP
Cysteine	NS	DOWN
Cystine	NS	DOWN
Deoxyguanosine Triphosphate (DGTP)	NS	UP
Folate	NS	DOWN
Gluconolactone	NS	UP
Glycine	NS	DOWN
Guanosine Diphosphate Mannose	NS	UP
Indole	NS	DOWN
Lauric Acid (Laurate)	NS	DOWN
Lysine	NS	DOWN
Maltotetraose	NS	DOWN
Mannitol	NS	DOWN
O-Phosphoethanolamine	NS	UP
Oxalate	NS	UP
Oxidized Glutathione	NS	UP
P-Cresol Sulfate	NS	DOWN
Phenylalanine	NS	DOWN
Phosphocreatine	NS	UP
Purine	NS	UP
Pyroglutamic Acid	NS	DOWN
Stachyose	NS	DOWN
Trans-2-Hexadecenoyl-L-Carnitine	NS	DOWN
Tryptophan	NS	DOWN
Tyrosine	NS	DOWN
Xanthine	NS	DOWN